Characteristics of Curvilinear Flow Past Circular-Crested Weirs

Ngoc Diep Vo

A Thesis

in

The Department
of
Civil Engineering

Presented in Partial Fulfillment of the Requirements
for the Degree of Doctor of Philosophy at
Concordia University
Montreal, Quebec Canada

April, 1992

ISBN 0-315-80996-5

ABSTRACT

Characteristics of Curvilinear Flow Past Circular-Crested Weirs

Ngoc Diep Vo, Ph.D.

Concordia University, 1992

A program of study has been carried out to obtain the characteristics of curvilinear flow past circular-crested weirs. These weirs are used to measure and regulate the flow of water. The discharge coefficient of such weirs was obtained experimentally as a function of the dimensionless total head of the approaching flow. Effects of weir side slopes and nappe ventilation on the weir discharge coefficient are reported. The minimum pressure on the circular weir crest surface which indicates the cavitation potential of the weir and the crest pressure are also determined. The experimental data indicate that the circular-crested weir behaves like a sharp-crested weir when the dimensionless total head is extremely large. Some of the main characteristics of circular-crested weirs and standard spillways are qualitatively compared using an appropriate scale factor for the dimensionless approaching flow head.

Laser Doppler Velocimetry (LDV) measurements were obtained for a wide range of hydrodynamic and geometric variables characterising the curvilinear flow. The velocity profiles over the weir crest in the curvilinear region of the flow were obtained and integrated to get the weir discharge coefficient independently on the basis of a new semi empirical model. The weir coefficient obtained on the basis of this model agrees very well with the weir coefficient based on other proposed models. The test results were also used to confirm the basic assumption related to the irrotationality of the flow over the weir which is generally made in the theoretical analysis of weir flows.

The weir discharge coefficient was also determined on the basis of a simple momentum analysis and compared with results obtained from direct discharge measurements. Water surface profiles were obtained for the flow over the weir crest. These data, in turn enable one to determine the depth of flow over the crest and the radius of curvature of the surface streamline at the crest section. The latter is an important geometric parameter of the streamline pattern in the analysis of theoretical weir flow models.

Dressler Equations were used to analyse the curvilinear flow past circular-crested weirs. Specifically, the lower range of the flow depth over the weir crest was considered in the theoretical analysis, so that the shallow depth model could be adopted. The weir discharge coefficient based on this theoretical model was verified with the help of experimental data.

The measured velocity profile data in the curvilinear flow region over the weir crest were also used to get the flow pattern, the slope and the curvature of the streamlines. The results indicate that the theoretical assumptions of linearity related to both the streamline slope and the streamline curvature in the region above the weir crest appear to be quite valid, except in a narrow segment below the free-surface.

ACKNOWLEDGEMENT

The author wishes to thank Dr. A.S. Ramamurthy for suggesting the research topic. He also wishes to express his gratitude to the Dean and staff of the Faculty of Engineering and Computer Science and the Chairman and staff of the Department of Civil Engineering for the financial support received to complete this research program.

Thanks are due to Dr. Balachandar for his assistance during the course of the investigation. The assistance of the members of the machine shop is gratefully acknowledged. Finally, the author wishes to express his appreciation to his wife, Thi Duyen and the children for their patience and understanding.

TABLE OF CONTENTS

NOMENCLATURE

The following notations are used in the present thesis:

A^* = area, normalized velocity profile

B = width of channel

C_d = coefficient of discharge

C_{dTh} = coefficient of discharge based on theoretical model of Dressler

C_{dMom} = coefficient of discharge based on momentum balance model

C_{dVel} = coefficient of discharge based on velocity profile model

D = crest diameter (2R)

f( ) = function of

Fr = Froude number

g = acceleration due to gravity

h = piezometric head, flow depth above crest level

H = total head reckoned above crest level

k = curvature ($k = 1/r$)

K = coefficient for pressure

m = experimental parameter

n = normal distance from bed, coefficient

N = flow depth normal to bed

p = weir height

P = pressure

q = discharge per unit width

Q = flow discharge

r = radial distance, radius of curvature

r_y = radius of curvature parameter (Fig.2b)

R	=	weir crest radius
Re	=	Reynolds number
TEL	=	total energy line
s	=	distance along curved bed, s - direction
u	=	horizontal velocity component
U	=	reference velocity ($U = \sqrt{2gH_1}$)
U_1	=	maximum velocity at crest, ideal flow ($U_1 = \sqrt{2g\left(H_1 - (P/\gamma)_{cr}\right)}$)
v	=	vertical velocity component ($v = u \tan \phi$)
V	=	average velocity, tangential velocity , resultant velocity
We	=	Weber number
x	=	x - axis, horizontal distance
y	=	y - axis, vertical distance, depth from bed
Y	=	total flow depth
α	=	upstream slope angle
β'	=	momentum coefficient
β	=	downstream slope angle
δ	=	boundary layer thickness
γ	=	specific weight of water
ν	=	kinematic viscosity of water
σ	=	surface tension coefficient of water
θ	=	angular position, θ - direction
ϕ	=	inclination angle to horizontal, of streamline
ψ	=	streamline value
$\pi,\Phi,\Psi(\ )$	=	function of

Subscripts:

1	=	approach section 1, index
2	=	downstream section 2, index
cr	=	at weir crest
CW	=	circular-crested weir
D	=	design
max	=	maximum value
min	=	minimum value
m	=	point of minimum pressure
sep	=	separation of nappe
S	=	at free surface
SW	=	sharp-crested weir
w	=	wall
y	=	at depth y above weir crest
δ	=	at edge of the boundary layer ($y = \delta$)

Note: Additional notations are used in the tables and are defined as they appear .

LIST OF FIGURES

LIST OF TABLES

CHAPTER I

INTRODUCTION

CHAPTER I

CHARACTERISTICS OF CURVILINEAR FLOW PAST CIRCULAR-CRESTED WEIRS

INTRODUCTION

1.1 - General remarks: In hydraulic engineering, one comes across many situations where the flow is highly curvilinear. In the present study, the case of the flow past a circular-crested weir is considered to illustrate the characteristics of curvilinear flow. Measurement and control of flow form important aspects of the transportation and distribution of water. They contribute to the efficient management of water to meet the municipal, agricultural and industrial needs. To control water pollution, data related to water quantities and water qualities can be collected from measuring stations, which permit the monitoring of both quality and quantity of flow.

1.1.1- Classification of hydraulic structures: Weirs, flumes and orifices (Fig.1a and 1b) are among the common units of discharge measuring structures which have a known head-discharge relationship. Weirs are classified according to the shape of the crest in the flow direction and are further sub-divided according to the different cross-sections of the crest.

i) **Broad-crested weirs** (Fig.1a-i) have sufficient crest lengths L to allow straight and parallel streamlines at least over a short distance above the crest length.

ii) **Sharp-crest weirs** (Fig.1a-ii), also known as thin-plate weirs have a crest length of 1 to 2mm. The streamlines above the weir crests are strongly curved.

iii) **Short-crested weirs** (Fig.1a-iii,iv) possess characteristics of both the broad-crested weirs and the sharp-crested weirs. Over their crest surface, the streamlines are highly curved and the pressure across the flow nappe strongly deviates from hydrostatic conditions. Among these weir shapes, the circular-crested weir (Fig.1a-vi) is commonly used to measure and control open channel flows.

iv) **Flumes** (Fig.1b-i) have some functional resemblance with weirs, but are less restricted with respect to crest height (Parshall flume). Generally, their downstream section gradually diverge to regain energy.

v) **Orifices** (Fig.1b-ii) have some resemblance to weirs but possess closed perimeters.

vi) **Lateral weirs** (Fig.1b-iii) are mainly used to divert the flow and serve as flow control devices.

The above units of hydraulic structures, used for measurement and control of open channel flow, are designed to perform the following particular functions:

1) Discharge measuring structures measure the flow passing through the channel in which they are placed. There are no movable parts unless the structures are required to fulfil another function, such as varying water-level control.

2) Discharge regulating structures assist in maintaining an efficient distribution of flow. They are generally equipped with movable parts, such as weirs with movable crests. The regulating structures can also serve as flow measuring structures in some cases.

3) Flow dividers distribute the incoming flow into two or more channels. This can be easily achieved by a group of weirs with different control widths.

4) Flow totalizers measure the cumulative volume of water passing a particular section in a given period. They commonly include rotating parts and revolution counters.

1.1.2- Design and selection of structural units for flow measurement and regulation: In the design and selection of a suitable structure, the hydraulic performance is of fundamental importance. However, considerations should also be paid to other criteria such as construction costs, standardization and other non-technical demands. Thus, besides carrying out the functions of measuring and controlling flow, the hydraulic design should also be based on the following factors:

i) The hydraulic properties of the structure which includes the loss of head imposed by the structure, its measuring range, sensitivity and accuracy in measurement, flexibility due to change in distribution conditions, ability to transport solid material and giving passage to floating debris and also, the possibility to regulate the discharge or control water levels.

ii) The actual field conditions such as available head, range of discharge, water level in the stream, sediment loads, floating materials, pollutants and other topographic informations of the site.

iii) Other non-technical demands such as availability of construction materials, personnel and training, and importance of standardization for large number of construction projects in the system area.

1.1.3- Advantages and disadvantages of some typical hydraulic structures: Some of the main advantages and disadvantages of some of the hydraulic structures used for measurement and control of flow are summarized below:

-Flumes: The more commonly used critical flumes are the Parshall flumes. Since the data collected for these flumes do not belong to geometrically similar units, one has to use a large number of graphs and tables for their selection. Further, their construction is more complex. Throatless flumes, grouped generally with critical depth flumes, can be used to measure the discharge of open channel flow. Owing to their simple streamlined geometry and level bed, throatless flumes have very good capacity for passing floating materials and bottom sediments. They are easy to design and simple to construct (Keller, 1984; Ramamurthy, 1985; Ramamurthy,1987).

- **Broad-crested weirs** can be equipped for both measurement and control of flows. With a high vertical upstream face and a square edge, the weir will retain bottom sediment which may affect the weir characteristics. When floating debris are present, rounded-nose weirs are preferred.

-**Trapezoidal profile weirs** can operate as either the broad-crested or the short-crested weirs depending on the values of the crest breadth L and the approach flow head H_1. **Triangular profile weirs** are similar to trapezoidal shaped weirs where the crest breadth vanishes (L—>0).

-**Sharp-crested weirs** behave like orifices with a free water surface. In the air-filled area below the outflowing jet, atmospheric pressure should prevail to ensure flow stability.

-**Water Experimental Station (WES) Standard spillway crests** are shaped according to the lower surface of the nappe produced by the flow over a sharp-crested weir. It can be equipped with gates for flow regulation. However, while dealing with the safety aspects of the design of spillway for high dams, an uncontrolled overflow crest has always been recognized as the safest type (Cassidy and Elbert, 1984).

-**Circular-crested weirs** (Fig.1a-iv) are grouped generally with the short-crested weirs. The flow over their crest sections possesses curved streamlines and the pressure variation across the overflow nappe deviates largely from hydrostatic conditions. They are commonly constructed with a vertical upstream face tangential to a horizontal circular cylindrical crest of radius R which is perpendicular to the flow direction and, a downstream sloping face (β=45°). Using existing data from various sources, Bos (1978) related the weir discharge coefficient C_d with the dimensionless total head parameter H_1/R of the approaching flow. He found the maximum value of C_d to be 1.48 at H_1/R=5.0. The recommended limits of application for these weirs are as follows (Bos, 1978): i) The approach flow head h_1 (Fig.2) should be measured upstream from the weir face at a distance 2 to 3 times the maximum of h_1, and h_1 should be greater or equal to 0.06m. ii) To prevent water surface instability, p/h_1 should be greater than 0.33. Here p denotes the weir height. iii) To reduce side wall boundary layer effects, generally the dimensionless channel width parameter B/H_1 should be greater or equal to 2.0. iv) The ratio h_1/R should be limited to avoid the local minimum pressure head at crest to be not less than -4m water column. v) To prevent the tailwater channel bottom from influencing the flow pattern over the weir, the ratio p_2/H_1 should be greater or equal to unity. vi) The modular limit H_2/H_1 is 0.33. Here, p_2 and H_2 are the weir height and the total head in the section downstream of the weir.

Besides the above structures, under some circumstances, one also uses floor slots, branch channels and lateral weirs to control the flow in open channels.

1.2 - Objective of the present investigation: The objective of the present investigation is to study the characteristics of curvilinear flow past circular-crested weirs in detail, covering a wide range of geometric and hydrodynamic parameters. The following main weir characteristics are determined on the basis of theoretical and experimental studies:

A: i) Water surface profiles of curvilinear flow past circular-crested weirs, ii) The effect of ventilation and the effect of side slopes on the weir discharge coefficient, iii) Pressure at the crest and minimum pressure on the weir crest surface, iv) Velocity and pressure profiles for flow over the weir crest.

B: i) Weir discharge coefficient over a very wide range of hydraulic and geometric parameters based on a) direct discharge measurement, b) integrated velocity profile model and c) momentum balance model, ii) Behaviour of circular-crested weir as sharp-crested weirs when the head causing flow is relatively very large compared to the crest radius.

C: Discharge coefficient of the weir on the basis of Dressler theory which is applicable to curvilinear flow.

For the analysis of the flow over circular crested weirs, earlier theoretical models assumed that the flow is irrotational and that the radius of curvature and inclination of the streamlines varied linearly from the crest to the surface. This will be verified using limited amount of test data.

-**Motivation:** With increasing values of H_1/R, previous data for $H_1/R<10$ related to circular-crested weirs clearly indicate that C_d reaches a peak at or near $H_1/R=5.0$ and drops gradually to the value of C_d for sharp-crested weirs ($H_1/R \longrightarrow \infty$). This fact has been missed in the earlier studies. Data related to the effects of upstream slopes and nappe ventilation on the discharge coefficient of circular-crested weirs were not available (Bos, 1978). Correlation between the crest pressure with the weir discharge coefficient has not been explored in the past. Further, the location of minimum pressure on the circular weir crest surface which indicates the cavitation potential of the weir was not determined in previous studies. Previous studies were not successful in relating the characteristics of pressure at the crest for curvilinear flow over circular-crested weirs and standard spillway crests, using proper scale factors.

Application of the momentum equation to curvilinear flow situations is rendered not easy by the difficulty in determining the pressure distribution at the end sections considered. The non-intrusive LDV system can be used effectively to determine the velocity field at these sections. This in turn can be used to determine the pressure field at these sections where the flow is curvilinear, if the flow is irrotational. It was desirable to adopt this technique to solve the curvilinear flow past circular-crested weirs and thereby validate this procedure. Existing curvilinear flow theories such as Dressler's theory have not been used to obtain exact solutions of weir flow models. All these facts provided the motivation to pursue the present program of study.

CHAPTER II

REVIEW OF EXISTING LITERATURE

CHAPTER II

REVIEW OF EXISTING LITERATURE

2.1 - General remarks: This chapter deals with the review of existing literature devoted to the study of circular-crested weirs and the closely related topic of standard spillways. Discussions related to each study dealing with the determination of weir discharge coefficient based on a number of methods are also included.

2.2 - Flow past standard spillways and other related types of weir: Cassidy (1965) has presented approximate solutions (numerical) for flow past standard spillways. His numerical solutions have been slightly improved by Ali (1972). For standard spillways, the point of minimum pressure associated with incipient cavitation occurs at the point of maximum curvature (Cassidy-1965, 1984). A rational procedure to pass the maximum flood flow with a particular minimum crest pressure for these spillways was proposed by Cassidy (1970). Sinniger and Hager (1985) have also reported an interesting experimental study related to the characteristics of both gated and ungated standard spillways. Delgado et al (1984) used the finite element method to solve the problem of flow past a curvilinear leaf gate. Ackers et al (1978) have presented a comprehensive account of flow past weirs dealing with practical applications.

Using different forms of pitot tubes, Rajaratnam and Muralidhar (1971) have reported detailed static pressure and velocity distributions for the curvilinear flow over a sharp-crested weir. Following the same procedure, Udoyara (1986) used pitot spheres and static pitot tubes to obtain the pressure and velocity distribution in the nappe section of sharp-crested plate weirs to determine C_d using the momentum principle. It should be noted that there are no flow reversal (flow separation) in the curvilinear flow region over sharp-crested weirs.

2.3 - Flow past circular-crested weirs: Circular-crested weirs are used for flow measurement and have wide applications in hydraulic engineering, where they serve as overflow structures (Bos, 1978, Cassidy, 1990). They can be used to control the water level in farm ponds and reservoirs. Verwoera (1941) determined the effects of the various parameters such as h_1/R and p/R on C_d (Fig. 2a). Escande and Sananes (1959) showed that suction slots on the crest enhance the value of C_d. In the theoretical studies of Jaeger (1956) and Sananes (1957), the non-dimensional pressure head $(P/\gamma H_1)_{cr}$ at the crest C (Fig.2a) was taken as the minimum pressure head $(P/\gamma H_1)_{min}$ over the crest surface BCE. The latter can be expressed in terms of flow depth Y_2 at the crest, the total head H_1, the crest radius R and a parameter m related to the radius of curvature r_y of the streamlines. Accordingly (Bos, 1978),

$$\left(\frac{P}{\gamma H_1}\right)_{min} = 1 - \left(1 - \frac{Y_2}{H_1}\right)\left[1 + m\frac{Y_2}{R}\right]^{\frac{2}{m}} \text{ ----------- } (1)$$

Based on the measurements of Fawer (1937), Jaeger (1956) suggested a value of 2 for m in Eq. 1. In Fig. 2a, the radius of curvature parameter r_y along the vertical through the crest is defined as:

$$r_y = \frac{r}{\cos\phi} \text{ ------------------------------ } (2)$$

where, ϕ denotes the slope of the streamline at a height y above the crest C. The parameter r_y which depends on the streamline curvature is assumed to vary linearly (Jaeger, 1956) from the crest C to the free-surface A (Fig.2b). Hence, at $r_y = R$, $y = 0$ and for any depth y above the weir crest, one assumes the relation given by Eq. 3:

$$r_y = R + my \text{ ---------------------------- } (3)$$

Approximate variation of the radius r of the streamline can be obtained by graphical methods (flow net). Sananes (1957) used optical methods to determine the water surface profile for the weir flow. Using these data, he obtained the streamline parameters r, r_y and m for the flow over the weir crest. The studies of Jaeger (1956) and Sananes (1957), indicate that the parameter m is independent of H_1 and R. Eq. 4 was suggested (Bos, 1978) to relate m and the weir downstream slope β:

$$m = 1.6 + 0.35 \cot\beta \text{ ---------------------- } (4)$$

For flow over circular-crested weirs for which $H_1/R \leq 1.0$, Matthew (1963) outlined a simple theory which clearly explains the influence of surface tension, viscosity and the radius of curvature r of the streamline on C_d for flow over the weir crest. He assumed a linear variation of the streamline curvature 1/r from the crest to the free-surface.

Approximate solutions (numerical) have been obtained for some forms of circular-crested weirs (Cassidy, 1965). Circular-crested weirs and sharp-crested weirs were studied by Sarginson (1972) who determined the influence of surface tension on C_d using the theory of Jaeger (1956). Based on the experimental weir nappe profile data, he reported the value of the parameter m as 1.8 for circular-crested weir and 2.5 for sharp-crested weir. Seshadri et al (1981, 1984) experimentally studied the characteristics of circular-crested weirs, which had low weir heights.

2.4 - Discharge coefficient C_d of circular-crested weirs:

2.4.1- Discharge coefficient from direct discharge measurement: From direct measurement of the discharge passing over the weir model, the weir discharge coefficient C_d can be evaluated using Eq.5 (Bos, 1978):

$$q = C_d \frac{2}{3}\sqrt{\frac{2}{3}g}\, H_1^{1.5} \text{ ------------------------ (5)}$$

Here, q = the discharge / unit length of the weir crest, g = the acceleration due to gravity and H_1 = the total head of the approaching flow reckoned above the weir crest level.

Bos (1978) has analysed existing data in detail to present a relationship between C_d and H_1/R for circular-crested weirs for which $\beta = 45^o$. He showed that C_d based on test data increases continuously from a low value of 0.64 at $H_1/R = 0.05$ to a high value of 1.48 at $H_1/R = 5.50$ and that C_d remains unchanged for $5.50 < H_1/R \leq 9.50$. According to him, the crest pressure $(P/\gamma)_{cr}$ also denotes the minimum pressure $(P/\gamma)_{min}$ over the crest. Setting $Y_2 \approx 0.7\ H_1$ (Jaeger, 1956), and using the data of Escande and Sananes (1959), Bos (1978) related $(P/\gamma H_1)_{cr}$ with H_1/R. When the downstream slope of the weir $\beta = 45°$, and $H_1/R < 10$, this relation can be rewritten as,

$$\left(\frac{P}{\gamma H_1}\right)_{cr} = 1 - 0.3\left(1 + 1.365\ \frac{H_1}{R}\right)^{1.026} \text{ --------- (6)}$$

or,

$$\left(\frac{P}{\gamma H_1}\right)_{cr} \approx 0.71 - 0.44\left(\frac{H_1}{R}\right) \text{ ----------------- (7)}$$

2.4.2- Discharge coefficient from momentum models: Momentum principle was generally applied as a global approach to analyse the flow past sharp and broad-crested weirs (Chow, 1959; Henderson, 1956). In curvilinear flow fields such as the flow in the weir crest section, the pressure deviates from hydrostatic distribution. One can obtain experimentally the pressure and velocity data to determine the correction factors required to balance the momentum between the control section on the weir crest and an upstream section of the channel where the pressure is assumed to be hydrostatic. An expression for the discharge coefficient, namely C_{dMom} can be derived (Ramamurthy, 1980, 1986, 1988).

2.4.3- Discharge coefficient from theoretical flow models: Analysis of curvilinear flow fields is very much of interest to the hydraulic engineer. Such flow fields occur over weirs and spillways, which are used for measurement and control of water flow. Theoretical models have been developed to obtain the characteristics of flow past curvilinear boundary. Among them, the more common ones are (1) based on irrotational flow (Cassidy, 1965; Matthew, 1963; Sarginson, 1972), (2) shallow curvilinear flow theory (Jaeger, 1956; Dressler, 1978; Sivakumaran, 1981, 1983), and (3) the free-vortex model (Henderson, 1956; Morris and Wiggert, 1972; Featherstone and Nalluri, 1982).

Based on ideal flow theory, Dressler (1978) derived governing equations for shallow, two-dimensional flow over a curved channel floor of radius $r = 1/k$ for which the flow depth normal to the floor is N. His theory is applicable when the local shallowness parameter kN is in the range $-0.85 \leq kN \leq 0.50$. Negative values of kN refers to the convex profiles such as spillways. For flow over standard spillway crests, Sivakumaran et al (1981, 1983) stated that Dressler equations yield accurate crest pressure data in the range $-2.0 \leq kN \leq 0.54$. Dressler equations can be adapted to determine the weir char‌acteristics such as the velocity distribution at the crest section and the weir discharge coefficient, namely C_{dTh}.

2.4.4- Basic theoretical assumptions: For weirs flow with no end contraction, the theoretical models commonly assume the flow to be two-dimensional. Other basic assumptions can be cited as the following: - the weir flow is irrotational (Cassidy, 1965;

Matthew, 1963; Sarginson, 1972, ..), - the water surfaces can be expressed as cubics (Ali, 1972), - the flow depth Y_2 at weir crest is constant and approximates $0.7H_1$ for free flow (Bos, 1978), - the linear variation of the radius of curvature r or curvature 1/r, the radius of curvature parameter r_y (Eq.3) and the slope ϕ of streamlines, from their values at crest boundary to their values at the free surface (Jaeger, 1956; Sananes, 1957; Matthew, 1963; Sarginson,1972; ..). Also, the parameter m, rate of change of the radius of curvature r_y, was reported to be a constant (Jaeger, 1956; Sarginson, 1972), and independent of weir flow parameter H_1/R, but varying (Eq.4) with weir downstream slope β (Sananes, 1957; Bos, 1978).

2.5 - Thesis lay-out: Chapters 1 and 2 dealt with the introduction and survey of existing literature. Chapter 3 will deal with the weir discharge coefficient obtained from direct discharge measurement. Chapter 4 will deal with the weir coefficient obtained from direct velocity measurement. Chapters 5 will deal with the weir coefficient obtained from momentum principle. Chapter 6 will deal with the theoretical curvilinear flow model. Chapter 7 will summarize the results of the present study and Chapter 8, the scope for future investigation.

CHAPTER III

DISCHARGE COEFFICIENT OF CIRCULAR-CRESTED WEIRS FROM DIRECT DISCHARGE MEASUREMENT

CHAPTER III

DISCHARGE COEFFICIENT OF CIRCULAR-CRESTED WEIRS FROM DIRECT DISCHARGE MEASUREMENT

3.1 - General remarks: The discharge characteristics of circular-crested weirs are determined experimentally over a wide range of H_1/R. The dependence of the discharge coefficient C_d on the other parameters such as upstream, downstream side slopes and ventilation of the nappe are also determined. The range of H_1/R covered in the study is very large and enables one to determine the limiting value of C_d for $H_1/R \to \infty$. The weir crest pressure and the minimum pressure on the crest surface are determined as functions of H_1/R. The present data are compared with earlier experimental and theoretical results.

3.2 - Theoretical considerations: The following assumptions are made in the development of the model for the circular-crested weir (Figs. 2a and 2b):

1) The flow upstream of the weir is steady, two-dimensional and sub-critical.
2) The dimensionless weir height p/H_1 is large and its effect on the weir discharge is negligible ($p/H_1 \geq 3$).

The Froude number $Fr = V_1/\sqrt{g(h_1+p)}$, the Reynolds number $Re = 2R\sqrt{(2gH_1)}/\nu$ and the Weber number $We = \gamma H_1{}^2/\sigma$ for the approach flow. Here, ν, γ and σ, respectively denote the kinematic viscosity, specific weight and surface tension of water, while V_1, h_1, R and p, respectively, denote the velocity in the approach flow, the depth of the approach flow above the crest, the crest radius and the weir height. Letting f( ) denote a function, the relationship between the main variables can be expressed as,

$$C_d = \frac{q}{\frac{2}{3}\sqrt{\frac{2}{3}g}\; H_1^{\frac{3}{2}}} = f\left(\frac{H_1}{R}, \frac{p}{H_1}, \mathrm{Fr}, \mathrm{Re}, \mathrm{We}, \alpha, \beta\right) \text{------} (8)$$

Since $p/H_1 \geq 3$ in the present tests, the effect of velocity head in the approach flow related to p/H_1 is negligible ($h_1 \approx H_1$). The effects of surface tension and viscosity on C_d were eliminated to a large extent by keeping h_1 (Fig.2a) in the range $5\ \mathrm{cm} \leq h_1 \leq 18\ \mathrm{cm}$. Hence, Eq. 8 can be recast as follows:

$$C_d = \frac{q}{\frac{2}{3}\sqrt{\frac{2}{3}g}\; H_1^{\frac{3}{2}}} = \pi\left(\frac{H_1}{R}\right) \text{------------------} (9)$$

Here, π ( ) denotes a function. Similarly, the normalized pressure head at the crest $(P/\gamma H_1)_{cr}$ and the normalized minimum pressure head $(P/\gamma H_1)_{min}$ on the crest surface can be expressed as:

$$\left(\frac{P}{\gamma H_1}\right)_{cr} = \Phi\left(\frac{H_1}{R}\right) \text{------------------------} (10)$$

and

$$\left(\frac{P}{\gamma H_1}\right)_{min} = \Psi\left(\frac{H_1}{R}\right) \text{---------------------} (11)$$

Eqs. 9 to 11 represent the weir flow characteristics and Φ( ) and Ψ( ) denote functions.

3.3 - Experimental set-up and procedure: Machined plexiglass weir models were set in a smooth stainless steel flume (Fig.3). The radii of the weir models were 0.95 cm, 2.54 cm, 3.81 cm, 7.54 cm, 10.08 cm and 15.16 cm, and were true to the nearest 0.05 mm. The test section was 25.4 cm wide, 180 cm high and 250 cm long. The side walls were equipped with transparent windows for flow visualization. Sufficient stilling arrangements were provided to obtain smooth flow without large scale turbulence. To study the effects of weir slopes on C_d, tests were performed on weir models with combinations of upstream slopes α and downstream slopes β . The slopes were $\alpha = 90°$, $75°$ and $60°$ in combination with downstream slopes $\beta = 75°$, $60°$ and $45°$. For the weir with $\beta = 75°$, an intermediate upstream slope $\alpha = 85°$ was also used. For the weir without the downstream slope, a ventilation duct provided full aeration of the nappe. Tests were also conducted on sharp-crested weir models with an edge of 1.5 mm. These denoted the limiting case of a circular-crested weirs ($R/H_1 \rightarrow 0$).

All models were equipped with sufficient pressure taps of diameter 0.5 mm to record the pressure distribution along the centre line of the models. On the vertical upstream weir face, pressure taps were spaced at every 5 cm along the centre line. For models with $R \geq 2.54$ cm, pressure taps were spaced at 5 degree intervals on the weir crest. The pressure head was recorded to the nearest 0.5 mm. The water surface profiles over the weir crest and the flow depth upstream of the weir (Fig. 3) were measured by means of point gages to the nearest 0.3 mm. The flow rate was measured with the help of a standard 60^0 V-notch. The maximum error in the estimation of the discharge was 3%.
Besides the test equipment and test procedures described above, information related to additional equipment and procedures are provided in subsequent sections which are relevant to the tests carried out.

3.4 - Discussion of results:

Tables 1 to 21 contain data used to plot the results (Figs.4 to 40).

3.4.1- Variation of C_d with H_1/R: Fig.4a shows the experimentally determined relationship between C_d and H_1/R for circular-crested weirs for which $\alpha = 90°$ and $\beta = 45°$. The present test data agree very well with the previously published results for $H_1/R < 5.5$ (Fig.4a). For larger H_1/R, Bos (1978) used the data of Escande (1959) whose weir had a slot and shows that C_d attains an upper limiting value of 1.49 near $H_1/R = 5$ and remains unchanged for large H_1/R (Curve A, Fig.4a). The present data shows that C_d attains a maximum value of 1.50 as H_1/R is increased to 5.5 and then decreases with a further increase of H_1/R (Curve B, Fig.4a). This discrepancy may be traced in part to the effect of the slot on C_d in the tests of Escande (1959). Fig.4b denotes the expanded scale version of all the earlier data used by Bos (1978) to form the C_d - H_1/R relation. It indicates that, even in the earlier studies, C_d in fact, increases gradually with an increase in H_1/R, attains a maximum value and later decreases with a further increase in H_1/R. Fig.4c also includes the results of more recent studies (Seshadri, 1981), which confirm qualitatively the fact that C_d for a circular-crested weir increases from low values, attains a maximum as H_1/R increases and later decreases with a further increase in H_1/R. The present experimental values of C_d for the sharp-crested weirs ($\alpha = 90°$, $\beta = 45°$) are also included in Fig.4a to indicate that the circular-crested weirs behave like a sharp-crested weir when ($H_1/R \rightarrow \infty$).

The data of Sinniger and Hager (1985) shown in Fig.4c are related to standard spillway profiles. For these spillways, the crest pressure is atmospheric at $h_1/h_D = 1$. Here, h_D denotes the design head. For circular-crested weirs, the crest pressure will be shown to be atmospheric at $H_1/R = 1.5$ in a subsequent section. As such, a factor of 1.5 was used to relate the H_1/R scale with the h_1/h_D scale to compare the flow characteristics of the two weir profiles. It must be noted that a minor correction for the velocity head in the approach flow is also required to relate the parameters h_1/h_D and H_1/R, when the weir height parameter p/H_1 is small. Since a specific value of β cannot be attributed to the standard spillway, the results of Sinniger and Hager (1985) should be compared only qualitatively with the present data of the circular-crested weir for which $\beta = 45°$.

3.4.2- Effects of upstream weir slope α on C_d: Curves E, D and B in Figs.

5a, 5b and 5c, respectively, show the variation of C_d with H_1/R for weirs with fixed downstream slope β and varying upstream slope α. The data indicate that the variation of α does not significantly change C_d at fixed H_1/R and fixed β. For instance, the deviation in C_d is at most 2% (Fig.5c) when α is changed from 90° to 60° in the entire range of tests $(0.45 \leq H_1/R \leq 18.5)$ for the weir with a fixed downstream slope ($\beta = 45°$). This result compares favourably with the nearly constant value of the slope correction factor for C_d (Bos, 1978) reported for the Waterways Experimental Station (WES) spillways in which the upstream slope was changed ($\alpha = 90°$ to $\alpha = 45°$, $p/H_1 > 1.5$).

3.4.3- Effects of downstream weir slope β on C_d: For $0 < H_1/R \leq 3.5$ and $\alpha = 90°$, curves E, D and B of Fig.6 indicate that C_d does not vary with downstream slope ($45° < \beta < 75°$). For $H_1/R > 3.5$ and a fixed upstream slope $\alpha = 90°$, a steeper downstream slope increases C_d. The peak value of C_d occurs at a higher H_1/R value, as β increases gradually (Fig.6). Escande and Sananes (1959) too observed that a steeper downstream slope improves the weir performance. It should be noted that the flow at high H_1/R is less stable when β values are very large ($\beta > 60°$). The ideal flow model relating C_d and H_1/R given by Cassidy (1965) for circular-crested weir ($\alpha = 90°$ and $\beta = 60°$) is also shown in Fig.6 as a thick line. The small (< 5%) deviation between the numerical results based on ideal flow and the results of the present experiments can be traced in part to the presence of wall and crest boundary layers and the existence of flow separation in real flows. The data for two sharp-crested weirs which indicate the limiting case of the circular-crested weir ($H_1/R \rightarrow \infty$) are included in Fig.6.

3.4.4- Effect of nappe ventilation on C_d: Fig.7 shows the effect of nappe ventilation on the variation of C_d with H_1/R for the weirs with a vertical upstream face ($\alpha = 90°$) and without downstream slope. When the vent is shut, the overflow nappe clings to the weir crest surface and the streamlines are more curved. At higher H_1/R, very low crest pressures develop. These in turn accelerate the flow over the crest resulting in a higher C_d. However, instability of flow occurs at higher H_1/R, if ventilation is absent.

Direct visual observations showed that the under nappe separates from the weir surface easily when it is ventilated and the nappe separation point moves upstream gradually from $\theta \approx 170^o$ at $H_1/R = 0.7$ to $\theta \approx 65^o$ at $H_1/R = 18$. However, the flow remains stable when the nappe is fully ventilated. For a ventilated nappe, the pressure at the crest is nearly atmospheric and this reduces C_d. The effects of nappe ventilation are observed only after C_d reaches its peak value ($H_1/R \geq 2.5$, Fig.7). A decrease in C_d of about 4% is attributed to nappe ventilation. Fig.7 also includes C_d for a ventilated sharp-crested weir which indicates the limiting value for the corresponding circular-crested weir when $H_1/R \to \infty$.

3.4.5- Sharp-crested weir as the limiting case of a circular-crested weir ($H_1/R \to \infty$): For $R/H_1 \to 0$, the circular-crested weir resembles a sharp-crested weir. Tests were performed on sharp-crested weirs with various combinations of α and β. For $0.05 \leq h_1/p \leq 0.20$, the variation of C_d with h_1/p of sharp-crested weirs is insignificant (Curves 2 to 7, Fig.8). Even for ventilated vertical sharp-crested weirs, the variation of C_d with h_1/p is insignificant, when $0.05 \leq h_1/p \leq 0.20$. Figs.4, 5, 6 and 7 show that the limiting values of C_d at very large H_1/R for a circular-crested weir are the same as those for a sharp-crested weir when α, β and ventilation conditions are matched.

3.4.6- Pressure distribution: For circular-crested weirs with varying degrees of side slopes and $R \geq 2.54$ cm, the normalized minimum pressure head $(P/\gamma H_1)_{min}$ on the crest surface and the normalized crest pressure head $(P/\gamma H_1)_{cr}$ denoting the pressure at C,the highest point of the crest (Fig.2b) are both shown as functions of H_1/R in Figs.9a, 10a and 11a. Figs.9b, 10b and 11b indicate the weir surface locations at which the crest surface pressure was either minimum or atmospheric. The normalized minimum pressure head $(P/\gamma H_1)_{min}$ on the crest surface of the theoretical model of Cassidy (1965) are lower than that of the present case (Fig.11a). This can be attributed in part to the facts that the theoretical model weir crest heights were much smaller $(p/D = 3)$ and the theoretical minimum pressure on the crest surface was assumed to occur at the fixed downstream point of tangency. It may be added that Bos (1978) too assumed that the minimum pressure occurs at a fixed location of the weir crest. However, the present data (Figs.9b, 10b and 11b) indicate that the location of the minimum pressure on the crest surface moves upstream as H_1/R increases in the range $0 < H_1/R < 8$. This range of H_1/R also denotes the values encountered in practice (Bos, 1978).

As stated earlier, for standard spillways, the pressure on the weir surface is atmospheric when $h_1/h_D = 1$, while, for circular-crested weirs, the crest pressure is atmospheric when $H_1/R \approx 1.5$ (Figs.9b, 10b and 11b). For the standard spillways, when $h_1/h_D > 1$, the minimum pressure occurs at the section upstream of the crest, where the curvature is maximum (Fig.11c). For the circular-crested weirs, the curvature is constant on the crest surface and the minimum pressure occurs at a section downstream of the crest for low values of H_1/R and moves upstream towards the crest as H_1/R increases (Figs. 9b, 10b and 11b). In the context of cavitation potential of the weir, the pressure distribution on the crest of a standard spillway is clearly superior to the pressure distribution over the crest of a circular-crested weir (Fig.11c). Since circular-crested weirs are used as parts of small irrigation systems, cavitation potential of the weirs is not a major factor when H_1 is not very large. Further, it should be noted that circular-crested weirs are much simpler in design and easier to construct. These features render them useful devices to measure and control flow in small irrigation systems.

Figs.9a, 10a and 11a also show that the dependence of $(P/\gamma H_1)_{cr}$ with H_1/R agree well with the relation suggested by Bos (1978). The downstream slope is more influential than the upstream slope in affecting C_d and $(P/\gamma H_1)_{cr}$. Hence, existing experimental results of Seshadri (1981) related to the crest pressure over symmetric circular-crested weirs ($\alpha = \beta = 63.4°$) are also included in Fig.11a for purposes of comparison. His data compare well with the relation proposed by Bos (1978) and the present data for $\alpha = 90°$ and $\beta = 60°$. This further confirms the earlier statement that $(P/\gamma H_1)_{cr}$ and hence, C_d do not depend very much on α. The present crest pressure data (Fig.11a) also agree well with the results of the ideal flow model of Cassidy (1965).

For purposes of comparison, Fig.11a also includes previous experimental crest pressure data for standard spillways (Chow, 1959, $H_1/R \leq 2.0$; Henderson, 1966, $H_1/R < 4.5$). As before, the scale correction from h_1/h_D to H_1/R was applied and the comparison is quite good. However, the comparison should be viewed as qualitative since the precise equivalent downstream weir slope β cannot be prescribed to the standard spillways.

3.4.7- Correlation between C_d and $(P/\gamma H_1)_{cr}$: The boundary layer thickness δ on the crest is small ($\delta << H_1$) and the flow outside the boundary layer is assumed to be irrotational. Hence, the crest pressures $(P/\gamma H_1)_{cr}$ are expected to be related directly with the maximum theoretical velocity $U_1 \approx \sqrt{2g\left(H_1 - (P/\gamma)_{cr}\right)}$ at the edge of the boundary layer and influence the weir performance in terms of C_d. By allowing very low pressures to exist at the crest, Cassidy (1970) successfully proposed a rational method of underdesigning the spillway crest which ensures an economical and yet safe design to pass floods.

The insert of Fig.11a shows the variation of the crest pressure for circular-crested weirs with various types of side slopes. Curves b, d, e, f and g should be viewed with the corresponding curves B, D, E, F and G of Figs.6 and 7. Up to a value H_1/R close to 2.5, $(P/\gamma H_1)_{cr}$ and C_d are essentially the same for all the models tested. Further, they also indicate that for $H_1/R > 2.5$, variations in C_d values are directly correlated with the crest pressures attained at various H_1/R values. Lower crest pressures are associated with higher C_d values. One also notes that $(P/\gamma H_1)_{min}$ and $(P/\gamma H_1)_{cr}$ are nearly identical (Figs.9a, 10a and 11a) at H_1/R values which correspond to the maximum values of C_d (Fig.6) for the different weir types. For circular-crested weirs without the downstream slope and $\alpha = 90^o$, curves f and g of the insert of Fig.11a indicate that the crest pressure increases due to ventilation. This fact is also inferred from the corresponding curves F and G of Figs.6-7 in which C_d appears to decrease due to ventilation of the nappe.

3.5 - Summary: The following conclusions can be drawn:

1) In the range $0 < H_1/R \leq 5.5$, for weirs with $\alpha = 90^o$ and $\beta = 45^o$, the variation of C_d with H_1/R generally agrees very well with the results of previous studies. However, for $H_1/R > 5.5$, after attaining a maximum, C_d decreases and, for very large H_1/R, reaches the limiting value of C_d for a corresponding sharp-crested weir. A somewhat similar trend in the C_d - H_1/R relationship is noticed for weirs with other upstream and downstream slopes.

2) For a circular-crested weir without the downstream slope and $\alpha = 90^o$, a ventilated nappe reduces C_d slightly for $2 < H_1/R < 18$.

3) For a fixed downstream slope, the effect of upstream weir slope on C_d is marginal. For

a fixed upstream weir slope, for $3 < H_1/R$, C_d improves when the downstream slope is increased.

4) The minimum pressure on the crest surface occurs at a location downstream of the crest for low H_1/R values and moves upstream towards the crest as H_1/R increases. This minimum pressure generally occurs very near the crest when C_d attains its maximum value. The variation of the crest pressure with H_1/R agrees very well with previous theoretical and experimental data.

5) Using an appropriate scale factor for h_1/h_D and H_1/R, some of the main characteristics of circular-crested weirs and standard spillways can be qualitatively compared.

CHAPTER IV

WEIR COEFFICIENT FROM DIRECT VELOCITY MEASUREMENT

CHAPTER IV

WEIR COEFFICIENT FROM DIRECT VELOCITY MEASUREMENT

4.1 - General remarks: Curvilinear flow fields are associated with rapidly varied flows in open channel such as the flow over circular-crested weirs used for measurement of discharge and regulation of flow. Velocity profiles are easily obtained, using non-intrusive laser Doppler velocimetry (LDV) techniques in laboratory tests. A new semi-empirical approach is used to determine the discharge coefficient, namely C_{dVel}, of circular-crested weirs by integrating non-dimensional velocity profiles at the weir crest.

4.2 - Theoretical considerations: The following assumptions are made in the development of the model for flow over a circular-crested weir (Fig.2):

(1) The flow upstream of the weir is steady, two-dimensional and sub-critical;

(2) Compared to the total head H_1 reckoned above the weir crest, the height p of the crest C above the upstream horizontal channel bed is large ($p/H_1 > 3$);

(3) Frictional losses along boundaries of the approach channel and the weir surface are negligible;

(4) The crest boundary layer thickness δ (Fig.2c) is extremely small ($\delta/H_1 << 1$);

(5) At the crest, in the region above the boundary layer ($y \geq \delta$), the curvilinear flow is irrotational and the total head is constant.

Traditionally, the weir discharge coefficient C_d is evaluated from direct measurement of discharge (Eq. 5). The velocity profile data over the model weir crest C (Fig.2c) provides an alternate way of determining C_d, namely C_{dVel}, using Eq. 12 :

$$\int_0^{Y_2} u \, dy = q = C_d \frac{2}{3} \sqrt{\frac{2}{3} g} \, H_1^{1.5} \quad \text{--------------(12)}$$

where, u is the horizontal velocity component measured at a depth y above the crest (Fig.2c). Using the parameter $U = \sqrt{2g H_1}$ and the flow depth at crest Y_2 to normalize u and y, Eq. 12 can be reduced to the following form:

$$\frac{q}{Y_2 U} = \int_0^1 \frac{u}{U} \, d\left(\frac{y}{Y_2}\right) \quad \text{------------------------(13)}$$

The above integral represents the area of the dimensionless velocity profile. Denoting it as A* , one obtains Eqs. 14 and 15:

$$\frac{q}{Y_2 U} = A^* \quad \text{-------------------------------(14)}$$

$$C_{dVel} = \frac{3\sqrt{3}}{2} \left(\frac{Y_2}{H_1}\right) A^* \quad \text{--------------------(15)}$$

To verify this model, test data related to three different circular-crested weirs were obtained.

4.3 - Experimental set-up and procedure: The weir models and the setup used are the same as described previously (Ch.3). The accuracies in the measurement of water surface profiles, flow depths, pressure heads and flow discharges remain unchanged.

Laser velocimetry: The pitot tube is a sluggish instrument and is insensitive to changes in streamline orientation. The accuracy of velocity measurement with a pitot tube is quite limited. The pitot tube itself disturbs the flow when placed in the thin boundary layer on the crest, only LDV systems are emminently suited to determine the velocity profiles in curvilinear flow regions, without disturbing the flow field. As such, a Helium-Neon Laser Doppler Velocimeter (LDV) System [TSI 9100-3] was used to survey the horizontal velocity distribution in the curvilinear flow field above the weir crest. The velocity calibration data supplied by the LDV manufacturer (TSI) was verified (Balachandar, 1990) by determining the velocity in the potential core region of an axisymmetrical jet (12.50 mm diameter) set-up. The uncertainties in the velocity measurement were estimated to be close to 0.5%.

Two-dimensionality of the flow: To verify the two-dimensionality of the flow, the horizontal velocity distributions along the vertical cross-section were obtained on the crest C (Fig.2c) at span-wise locations 12.5 cm, 8.0 cm, 1.5 cm and 0.5 cm from the side wall for a fixed depth Y_2. These four velocity distributions indicated that the profiles were similar and the deviation in the average velocity was of the order of 1%.

4.4 - Discussion of results: Thirty profiles of the horizontal velocity component u were recorded at the crest section C (Fig.2c), covering the range $0.5 \leq H_1/R \leq 5.0$ for the three weir models:

(i) $\alpha = 90^o$, no downstream slope and nappe ventilated,

(ii) $\alpha = 90^o$, $\beta = 45^o$ and

(iii) $\alpha = 60^o$, $\beta = 45^o$.

4.4.1- Weir with $\alpha = 90^o$, no downstream slope and nappe ventilated: For a weir with $\alpha = 90^{o}$, no downstream slope and a ventilated nappe, Figs.12a, 12b and 12c show the dimensionless velocity profiles at the crest section C (Fig.2c). The insert of Fig. 12b shows the variations of the non-dimensional crest pressure $(P/\gamma H_1)_{cr}$ and the non-dimensional minimum pressure $(P/\gamma H_1)_{min}$ on the crest surface with H_1/R. The non-dimensional minimum pressure $(P/\gamma H_1)_{min}$ for this weir decreases from -0.4 to -1.3, as H_1/R increases from 0.55 to 1.38. For $H_1/R \geq 1.38$, $(P/\gamma H_1)_{min}$ increases rapidly till $H_1/R \geq 2.2$. For $H_1/R > 2.2$, $(P/\gamma H_1)_{min}$ increases gradually to the atmospheric pressure. These variations are shown as curve abcd in the insert of Fig.12b.

For $0.5 \leq H_1/R \leq 5.0$, $(P/\gamma H_1)_{cr}$ drops from a high value of 0.5 at $H_1/R = 0.5$ to a minimum value of - 0.3 at $H_1/R = 2.2$, then increases to attain a value of - 0.1 at $H_1/R = 5.0$ (Insert Fig.12b). For this weir, at very large H_1/R, the limiting value of $(P/\gamma H_1)_{cr}$ is zero (atmospheric) and this weir shape denotes the flow over a ventilated sharp-crested plate weir. It should be noted that for standard spillways, the crest pressure is atmospheric on the entire surface of the crest, when the head over the spillway corresponds to the design head h_D.

As H_1/R increases from 0.55 to 1.38 (Fig.2c), the velocity component u at the free-surface maintains the value $0.52\sqrt{2g H_1}$. Its maximum value u_{max} at the edge of the crest boundary layer ($y = \delta$) continues to increase with H_1/R and attains a value close to $U = \sqrt{2g H_1}$. Since the elevation difference δ between the crest and the edge of the boundary layer is extremely small ($H_1 >> \delta$), the pressure recorded at the crest ($y = 0$) is representative of the pressure at $y = \delta$. Figs.12a, 12b and the insert of Fig.12b show that the increase of u_{max} with H_1/R occurs at the expense of the drop in the crest pressure with increasing H_1/R up to $H_1/R = 2.2$. As H_1/R continues to increase further to 4.40, u_{max} decreases with increasing H_1/R, while the pressure at $y = \delta$ and hence the crest pressure increases with H_1/R (Insert, Fig.12b). Fig.12c shows that the non-dimensional velocity profiles for $2.01 \leq H_1/R \leq 4.40$ collapse to a single curve when u is normalized by $U_1 = \sqrt{2g\left(H_1 - (P/\gamma)_{cr}\right)}$.

Fig.13a shows the variation of the area A* denoting the non-dimensional velocity profiles (Fig.2c). Fig.13b shows the variation of the weir discharge coefficient C_{dVel} with H_1/R. C_{dVel} was computed using the data of Fig.13a and Eq. 15. A* attains a maximum at H_1/R close to 2.2 which also corresponds to the value of H_1/R at which the minimum value of the crest pressure occurs for $2.01 \leq H_1/R \leq 4.40$ (Insert, Fig.12b). The value of Y_2/H_1 is essentially equal to a constant value of 0.715 for $H_1/R < 2.0$. For $2.01 \leq H_1/R \leq 4.40$, Y_2/H_1 continues to increase slightly (Fig.13a). However, the drop in the value of A* in this range of H_1/R is insignificant. Hence, the resulting variation of C_{dVel} with H_1/R causes the discharge coefficient to attain a relative maximum near $H_1/R = 2.5$. Fig.13b also shows the data points corresponding to C_{dVel} based on the velocity profile integration model (Eq. 15) which agree with the values of C_d (solid line- Fig.13b) obtained from direct discharge measurements.

4.4.2- Weir with $\alpha = 90°$ and $\beta = 45°$: Figs.14a and 14b show the non-dimensional velocity profiles for the second weir model with $\alpha = 90^o$ and a downstream slope $\beta = 45^o$. The insert of Fig.14b shows the non-dimensional crest pressure $(P/\gamma H_1)_{cr}$ and the non-dimensional minimum pressure $(P/\gamma H_1)_{min}$ on the weir crest surface for this weir. The recorded crest pressure continues to decrease with an increase in H_1/R and agrees very well with the relationship proposed by Bos (1978).

As H_1/R increases from 0.44 to 1.35 (Fig.14a), the velocity at the free-surface maintains the value $0.52\sqrt{2g H_1}$. Again, the value of u_{max} continues to increase with increasing H_1/R and attains a value close to $\sqrt{2g H_1}$ at $H_1/R = 1.35$. This increase in u_{max} comes at the expense of the crest pressure which continues to drop with an increase in H_1/R. The increase in u_{max} with an increase in H_1/R continues also in the range $2.29 \leq H_1/R \leq 4.78$. However, except for the narrow region $y/Y_2 < 0.1$, all the dimensionless velocity profiles collapse into a single curve, for $2.29 \leq H_1/R \leq 4.78$ (Fig.14b).

Figs.15a and 15b show the variation of the area A*, Y_2/H_1 and C_{dVel} with H_1/R. A* continues to increase from a low value of 0.57 at H_1/R =0.44 to the value of 0.74 at $H_1/R = 2.29$. In the range, $2.29 \leq H_1/R \leq 4.78$, A* increases slowly and attains a limiting value of 0.78. The value of Y_2/H_1 is essentially constant at 0.715 for $H_1/R \leq 1.35$ and increases gradually to the limiting value of 0.73 at $H_1/R = 4.78$. Using the data of Fig.15a and Eq. 15, C_{dVel} was determined. The resulting data points denoting C_{dVel} based on Eq. 15 agree very well with the values of C_d (solid line, Fig.15b) determined by present direct discharge measurements based on Eq. 5.

4.4.3- Weir with $\alpha = 60^o$ and $\beta = 45^o$: Although the upstream slope α of the third weir ($\alpha = 60^o$ and $\beta = 45^o$) is different from the second weir ($\alpha = 90^o$ and $\beta = 45^o$), the dependence of the various parameters such as $(P/\gamma H_1)_{cr}$, $(P/\gamma H_1)_{min}$, u_{max}/U, A*, Y_2/H_1, and C_{dVel} on H_1/R appear to be nearly identical (Figs.14, 15, 16 and 17) for $0.5 \leq H_1/R \leq 5.0$. The insert of Fig.17b shows the dependence of C_{dVel} on H_1/R for all the three weirs tested. Clearly, for $H_1/R < 2$, all the three weirs possess the same variation of C_{dVel} with H_1/R. This observation is consistent with the nearly identical variation of $(P/\gamma H_1)_{cr}$ with H_1/R (segments c'c) for all the three weirs in the lower H_1/R range (Inserts, Figs.12b, 14b and 16b). For all the weirs, it should be noted that the crest pressure $(P/\gamma H_1)_{cr} = 0$ at $H_1/R = 1.5$ (Inserts, Figs.12b, 14b, and 16b), which is close to the upper limit of the lower range of H_1/R (Fig.12a, 14a and 16a).

The variation of Y_2/H_1 with H_1/R is not very large for the range of H_1/R covered (Figs.18a, 18b and 18c). Hence, the variation of the velocity head $V_s^2/2gH_1$ at the surface with H_1/R is also not very large (Fig.18). On the other hand, the pressure at the crest and, hence, the pressure at the edge of the boundary layer decreases substantially with an increase in H_1/R. As such, for the two weirs with $\beta = 45°$, the maximum velocity head $V_\delta^2/2gH_1$ increases considerably with an increase in H_1/R (Figs.19b and 19c). For the weir with $\alpha = 90°$, with no downstream slope and a ventilated nappe, this velocity head increases with H_1/R, attains a maximum at $H_1/R = 2.2$ and then decreases with further increase in H_1/R (Fig.19a). For this weir, $(P/\gamma H_1)_{cr}$ attains a minimum (Fig.19a) and C_{dVel} attains a maximum (Fig.13b) near $H_1/R = 2.2$. The minimum pressure on the crest surface $(P/\gamma H_1)_{min}$ shown in inserts of Figs.12b, 14b and 16b are useful in determining the cavitation potential of the weirs.

The flow over the weir crest is treated as irrotational (assumption 5). Verification of this assumption will be discussed further in chapter 6.

4.5 - Summary: Non-intrusive LDV techniques enable one to obtain accurate velocity profiles in the curvilinear flow field above the weir crest. This, in turn, yields the weir discharge coefficient. The value of C_{dVel} determined on the basis of this procedure is found to agree very well with the previous results related to C_d obtained from direct discharge measurements and numerical studies (Cassidy, 1965). The data of the minimum pressure on the crest surface can be used to determine the cavitation potential of the weir.

The alternate method suggested in the present study to determine the discharge coefficient of circular-crested weirs can be adopted for the case of other weir types, since the determination of the velocity distribution over other weir crest sections using LDV technique is quite straight-forward. Lastly, the ability to measure the velocity field precisely in curvilinear flows enables one to determine the precise pressure distributions in those regions where the flow field is also irrotational, as in the case of flow over weirs.

CHAPTER V

MOMENTUM MODEL OF THE WEIR FLOW

CHAPTER V

MOMENTUM MODEL OF THE WEIR FLOW

5.1 - General remarks: A momentum balance model of the flow past the circular-crested weir is developed to determine the weir discharge coefficient, namely C_{dMom}. To this end, profiles of the water surface, pressure and velocity distributions at various locations of the control surface MNDBCA (Fig.2d) are determined. The experimental values of the weir discharge coefficient C_{dMom} are compared with previously published data based on direct discharge measurement methods and the ideal fluid flow models of Cassidy (1965).

5.2 - Theoretical considerations: The momentum balance model can be used to determine the characteristics of flow past a weir (Henderson, 1966 and Udoyara, 1986). Figs.2a and 2d show the flow past a circular-crested weir for which MNDBCA denotes a control volume. The following assumptions are made in the development of the model:

(1) The flow approaching the weir is steady, subcritical and two-dimensional,

(2) The frictional force at the solid boundary between sections 1 and 2 is negligible,

(3) The channel bed is horizontal,

(4) The weir crest is horizontal and perpendicular to the flow direction,

(5) For section 1, the pressure distribution is hydrostatic and the momentum coefficient β'_1 is unity,

(6) The boundary layer thickness δ at section 2 (crest C) is very small ($\delta/H_1 << 1$). The flow in the region above it ($y \geq \delta$) is irrotational and the total head is

constant.

Considering a discharge per unit length q for the weir which has a downstream slope, the momentum equation for the control volume between sections 1 and 2 (Fig.2d) can be written as follows:

$$Y_1^2 + \frac{2}{g} q V_1 = Y_2^2 K_2 + \frac{2}{g} q\, V_2 \beta'_2 + \left(2\, p\, Y_1 - p^2\right) K_w \text{ ----------- } (16)$$

where, Y = flow depth, V = average velocity, K = correction coefficient for pressure, p = weir height, β' = momentum coefficient, and subscripts 1, 2 and w denote the sections 1, 2 and the weir face (Fig.2d). For a weir having no downstream slope and ventilated nappe, the downstream section of the control volume is taken at the location where the lower nappe profile attains the maximum elevation. Noting that $q = VY$ and, using Eq. 5 in Eq. 16 and simplifying, one gets:

$$C_{dMom} = \left[\frac{27}{16} \left\{ \frac{\frac{Y_2}{H_1}\left(1 + \frac{p}{H_1}\right)}{\beta'_2\left(1 + \frac{p}{H_1}\right) - \frac{Y_2}{H_1}} \right\} \left\{ 1 - \left(\frac{Y_2}{H_1}\right)^2 K_2 + \frac{p}{H_1}\left(2 + \frac{p}{H_1}\right)\left(1 - K_w\right) \right\} \right]^{0.5} \text{ -- } (17)$$

From velocity and depth measurements at sections 2 and 1, β'_2 and Y_2/H_1 can be found. Based on assumption 6 and the measured velocity distribution, the static pressure distribution in the region above the boundary layer ($y \geq \delta$) at section 2 was obtained. Further, the pressure head at $y = \delta$ and the measured pressure head at the crest ($y = 0$) generally do not differ very much, since $\delta << H_1$. K_2 can be determined, using the pressure distribution derived from the measured velocity distribution. K_w can be obtained directly from the pressure distribution on the weir face.

5.3 - Experimental set-up and procedure: The set-up and equipments used are the same as described previously in chapters 3 and 4. The accuracies in measurement remain unchanged. On the upstream face of some weir models, additional pressure taps were provided at every 5 cm along the centre line to obtain the data to determine pressure force correction factors. Laser velocity measurement data of mainly three weir shapes were used to verify the application of the momentum analysis of the weir model. One of the weirs had a vertical upstream slope with no downstream slope. The two other weirs had a downstream slope of 45° and upstream slopes of 90° and 60°.

5.4 - Discussion of results:

5.4.1- Pressure correction coefficients: The static pressure distribution at the crest section is not hydrostatic. It was obtained indirectly from the measured velocity distribution. As stated earlier, this is possible, as the flow above the thin crest boundary layer ($y \geq \delta$) is irrotational (as will be shown in chapter 6). The elevation y above the weir crest and the corresponding pressure head (P/γ) are normalized by Y_2. The velocity component u is normalized by $U = \sqrt{2\,g\,H_1}$. For $0.44 \leq H_1/R \leq 4.88$, Figs.20a, 20b and 20c show the static pressure profiles at the crest section for the three weirs derived from experimental velocity data (Figs.12, 14 and 16). The inserts of Figs.20a, 20b and 20c indicate the experimental velocity profiles (Figs.12b, 14b and 16b) in the upper H_1/R range ($2.01 \leq H_1/R \leq 4.88$). In the lower H_1/R range ($0.44 \leq H_1/R \leq 1.38$), both the static pressure distributions (Fig.20) and the velocity distributions (Figs.12, 14 and 16) change with H_1/R. Further, in this H_1/R range, the value of $(P/\gamma Y_2)$ at $y = \delta$, which is nearly equal to $(P/\gamma Y_2)_{cr}$, decreases from a positive value of $\approx +0.7$ to 0.0 (atmospheric) as H_1/R increases from 0.44 to 1.38 (Figs.20a, 20b and 20c).

For the weir with $\alpha = 90^\circ$, no downstream slope and a ventilated nappe, Fig.20a also shows that $(P/\gamma Y_2)_{cr}$ decreases from 0.00 to -0.42 as H_1/R increases from 1.38 to 2.01. However, in the upper H_1/R range ($2.01 \le H_1/R \le 4.40$), at $y/Y_2 = 0$ (Fig.20a), $(P/\gamma Y_2)_{cr}$ increases from -0.42 to -0.12 as H_1/R increases from 2.01 to 4.40. Both the velocity (Insert Fig.20a) and the static pressure profiles (Fig.20a) of this weir do not merge into a single curve even in the upper range of H_1/R. For the other two weirs for which $\beta = 45^\circ$ and $\alpha = 60^\circ$ and 90°, a single curve denotes the velocity distribution (Inserts of Figs.20b and 20c) and hence, a single curve also denotes the pressure distribution (Figs.20b and 20c) for the upper range of H_1/R. Further, in this range of H_1/R, for the two weirs with $\beta = 45^\circ$, $(P/\gamma Y_2)_{cr}$ decreases continuously as H_1/R increases to 4.88 from 2.29 (Figs.20b and 20c, $y/Y_2 = 0$).

Figs.21 and 22 respectively show the variations of the pressure coefficient K_2 and K_w with H_1/R and the weir height parameter p/H_1 for all the three weirs in the complete H_1/R range ($0.44 \le H_1/R \le 4.88$). Insert of Fig.22 shows a typical pressure distribution on the upstream face of the weir with no downstream slope and $\alpha = 90^o$. In all the present tests, the weir height p is very large compared to H_1 and R. Hence, the pressure on the weir face is essentially hydrostatic and K_w is close to unity (Fig.22). The velocity and pressure distributions at the weir crest section and the pressure distributions on the upstream weir face yielded β'_2, K_2 and K_w of Eq. 17.

5.4.2- Water surface profiles and flow depth above the crest: The total head H_1 was used to normalize the distance variables x and y of the water surface profiles (Fig. 2a). For the lower H_1/R range ($0.44 \le H_1/R \le 1.38$), the water surface profiles essentially merge into a single curve for all the three weirs (Fig.23a). At the higher H_1/R range ($2.01 \le H_1/R \le 4.88$), the water surface profile of the weir with no downstream slope and $\alpha = 90^\circ$ is slightly higher than the water surface profiles of the weirs with

$\beta = 45^{o}$ (Fig.23b). Insert of Fig.23b shows the water surface profiles of all the weirs tested for the range $2.01 \leq H_1/R \leq 5.08$. For weirs with fixed downstream slopes, the upstream slope α has no significant effect on the water surface profile over the H_1/R range $0.44 \leq H_1/R \leq 4.88$ (Fig.23a: Curve 1 and Fig.23b: Curve 3). However, unlike the upstream slope α, the downstream slope β does influence the water surface profile (Insert Fig.23b: Curves 3 and 4). The experimental water surface profile for the weir with $\alpha = 90^{\circ}$ and $\beta = 60^{\circ}$ shown as Curve 4 in the Insert of Fig.23a is close to the theoretical water surface profile (Cassidy, 1965).

Fig.24 shows the variation of Y_2/H_1 with H_1/R for the three main weir types. Once again, the two weirs with fixed downstream slope ($\beta = 45^{\circ}$) behave similarly and have nearly identical values of Y_2/H_1 over the entire range of H_1/R (Fig.24). In the low H_1/R range ($0.44 \leq H_1/R \leq 1.38$), for all the three weirs shown, $Y_2/H_1 = 0.715$.

The water surface profile also enables one to determine the curvature and inclination of the surface streamline at the weir crest section C (Fig.2). Further information will be found in the analysis of curvilinear characteristics of the weir flow (chapter 6).

5.4.3- Discharge coefficient C_{dMom}: Fig.25 shows the relationship between C_{dMom} and H_1/R. Here, the solid curved lines LMT, LMS (present) and LMN (Bos,1978) of Fig.25 denote the mean trend of the relation between C_d and H_1/R derived from direct discharge measurements using Eq. 5. The segment LM is common to all weir types in the lower H_1/R range (Bos, 1978 and present). The segment MN refers to the weirs with $\alpha = 90^{\circ}$, $\beta = 45^{\circ}$ (Bos, 1978) while segment MT refers to the weir with $\beta = 45^{\circ}$ and $\alpha = 90^{\circ}$ & 60° (present). The segment MS refers to the weir with no downstream slope and $\alpha = 90^{\circ}$ (present).

The experimentally determined values of the parameters on the right hand side of Eq. 17 were used to relate C_{dMom} with H_1/R on the basis of the momentum equation. The data points pertaining to this relationship shown in Fig.25 agree very well with the corresponding solid lines denoting the results of direct discharge measurements. Insert of Fig.25 shows that the theoretical values of C_d (Cassidy, 1965) are slightly lower than the present data. For a qualitative comparison, the insert also contains the test data of Hager (1985) related to standard spillways. These data are adopted for comparison by using a scale factor of 1.5 to convert the scale h_1/h_D to H_1/R, based on the fact that the crest pressure is atmospheric for circular-crested weir at $H_1/R = 1.5$ and for standard spillways at $h_1/h_D = 1.0$.

5.5 - Summary: The experimentally determined velocity profiles in the region of curvilinear flow over the weir are shown to provide useful pressure distribution data needed for the momentum analysis of flow past a circular-crested weir. For the range $0.44 \leq H_1/R \leq 4.88$, the weir discharge coefficient C_{dMom} based on momentum analysis agree very well with C_d based on direct discharge measurement of past and present studies. The agreement of the present data with the earlier ideal flow model of Cassidy (1965) is also reasonable. The general procedure outlined in the momentum model can be used to analyse flow past other types of weirs.

CHAPTER VI

THEORETICAL CURVILINEAR FLOW MODEL

CHAPTER VI

THEORETICAL CURVILINEAR FLOW MODEL

6.1 - Application of Dressler theory to circular-crested weirs:

6.1.1- General remarks: In this section, Dressler equations are adapted to determine the weir flow characteristics such as the velocity distribution at the crest section C (Fig.2c) and the theoretical weir discharge coefficient, C_{dTh}. These results are verified using past and present test data for three types of circular-crested weirs in the range $H_1/R \leq 2.28$ or $-1.6 \leq kN$. The shallow depth model is applicable in these ranges of H_1/R.

6.1.2 - Theoretical considerations: The following assumptions are made in the development of the Dressler theory model for flow past a circular-crested weir (Figs.2a and 2c):

1) The approach flow is steady, two-dimensional and sub-critical,
2) The effects of fluid properties such as surface tension and viscosity on the weir flow characteristics are not significant,
3) For the accelerating flow on the crest surface upstream of C (Fig.2c), the crest boundary layer thickness δ is negligibly small compared to Y_2 and H_1. Typically, δ/H_1 is of the order of 0.02.

Following the procedures outlined by Dressler (1978) and Sivakumaran et al (1981, 1983), the equation for steady flow at a rate of q per unit crest length of the weir (Fig.2c) may be written as:

$$q = U_1 R \ln\left(1 + \frac{Y_2}{R}\right) \text{------------------------} (18)$$

where, $U_1 = \sqrt{2g\left(H_1 - (P/\gamma)_{cr}\right)}$ is the maximum velocity at the crest for the ideal flow. For this flow, the horizontal velocity u at a depth y over the crest C can be expressed as follows (Dressler, 1978):

$$u = \frac{U_1}{\left(1 + \frac{y}{R}\right)} \text{--------------------------} (19)$$

In real flows over a circular-crested weir, the maximum velocity U_1 is not at the crest but at the edge of the thin boundary layer (assumption 3). As such, for $\delta \le y \le Y_2$ the horizontal velocity component u (Fig.2c) is given by the following approximate relation:

$$u \cong \frac{U_1}{1 + \frac{(y - \delta)}{(R + \delta)}} \text{------------------------} (20)$$

Excluding the crest boundary layer, the converging flow over the weir in the region ($y \ge \delta$) is assumed to be irrotational. Hence, the total head is constant across the section AC'' (Fig.2c). At C'' where $y = \delta$, $u = U_1$, using assumption 3 and applying the energy equation between sections 1 and 2 (Fig.2a), one gets:

$$H_1 = \delta + \frac{U_1^2}{2g} + \left[\left(\frac{P}{\gamma}\right)_{cr} - \frac{dP}{\gamma dy}\delta\right] \approx \frac{U_1^2}{2g} + \left(\frac{P}{\gamma}\right)_{cr} \text{---------} (21)$$

Hence, rewriting Eq.21:

$$U_1 \approx \sqrt{2g\left(H_1-\left(\frac{P}{\gamma}\right)_{cr}\right)} \quad \text{------------------} \quad (22)$$

For the flow over the weir crest for which δ is extremely small ($\delta/H_1 << 1$, $\delta/R << 1$), the normalized velocity profile can be written as:

$$\frac{u}{U_1} = \frac{1}{\left(1 + \frac{y}{R}\right)} \quad \text{----------------------} \quad (23)$$

Alternatively, u can also be normalized by $U = \sqrt{2gH_1}$. Hence, using Eq. 22:

$$\frac{u}{U} = \frac{\left[1-\left(\frac{P}{\gamma H_1}\right)_{cr}\right]^{0.5}}{\left(1 + \frac{y}{R}\right)} \quad \text{----------------------} \quad (24)$$

Using Eqs. 18 and 22 in Eq. 5 and simplifying, C_{dTh} can be expressed as follows:

$$C_{dTh} = \frac{3\sqrt{3}}{2}\left[1-\left(\frac{P}{\gamma H_1}\right)_{cr}\right]^{0.5} \frac{\ln\left(1 + \frac{Y_2}{R}\right)}{\left[\frac{H_1}{R}\right]} \quad \text{--------} \quad (25)$$

Tests were mainly conducted to verify the above expression for C_{dTh} for $0<H_1/R\leq2.28$, which is in the practical range of application and where Dressler theory is applicable.

6.1.3 - Experimental set-up and procedure: The set-up and equipments used are the same as described previously (Ch.3 and Ch.4). The accuracies in measurement remain unchanged.

6.1.4 - Discussion of results:

- Flow characteristics: Figs.26a, 26b and 26c show the selected velocity profiles for the three weir models in the range $0.44 \leq H_1/R \leq 2.28$. Here, the depth y and the horizontal velocity u are normalized by R and $U_1 = \sqrt{2g\left(H_1 - (P/\gamma)_{cr}\right)}$, respectively. Experimental velocity distributions agree very well with the theoretical profiles (Eq.19) for the flow up to $Y_2/R \leq 1.0$. One can recall that Dressler (1978) recommended the use of his equations for $Y_2/R \leq 0.85$ for a convex bed. $Y_2/R = 1.0$ approximately corresponds to $H_1/R = 1.40$. Fig.27 shows the water surface profiles for the three weirs as in Fig.23a with additional data for the extended range $0.44 \leq H_1/R \leq 2.28$. The total head H_1 was used to normalize the depth h above the crest level and the horizontal distance x (Fig.2c). Fig.27 also shows that the water surface profiles for all the three weirs essentially merge into the same average curve, and the mean flow depth at the crest $Y_2 = 0.715\ H_1$.

- Range of applicability of Dressler equations: As H_1/R is increased from low values, the center of curvature of the segment of the surface profile above the crest C (Fig.2c) begins to drift away from the center of the circular crest surface. When H_1/R is large ($H_1/R > 1.4$), the center of curvature of the streamlines between C" and A (Fig.2c), will be very far from the center of the crest surface. Consequently, the formulation of Eq. 19 which implies that the crest surface and the streamlines above it are concentric (Fig.2c), begins to be strongly violated. Hence, the limit to obtain the accurate velocity distribution from Dressler theory appears to be $H_1/R \leq 1.4$, which is nearly the same as $Y_2/R \leq 1.0$. Fig.28 provides a comparison between the predicted maximum velocity U_1 (Eq. 22) and the measured maximum velocity u_{max} at the weir crest. At the crest, the variation of the dimensionless flow depth Y_2/R with H_1/R is given in Fig.29. This relationship is almost linear and identical for all the weirs up to $H_1/R = 1.4$. Beyond this value, data for the weir with $\alpha = 90°$ and with no downstream slope and a ventilated nappe show a slight deviation.

- **Nappe separation and minimum pressure:** Fig.30 shows the results of visual observation of the point of nappe separation from the crest surface for the weir with $\alpha = 90°$, no downstream slope and a ventilated nappe. The minimum pressure $(P/\gamma H_1)_{min}$ and its angular location recorded on the crest surface of all the three weirs are given in the upper and lower inserts of Fig.30 respectively. They indicate that the dependence of these parameters on H_1/R is essentially the same for the two weirs with the downstream slope $\beta = 45^o$. In this regard, their behaviour differs significantly from the weir with $\alpha = 90^o$ and with no downstream slope and a ventilated nappe. Further, the minimum pressure data needed for the determination of cavitation potential on the weir crest surface are important only for the two weirs with a downstream slope, since $(P/\gamma H_1)_{min}$ continues to drop as H_1/R increases. For these two weirs , the lower insert of Fig.30 shows that the angular locations of the points of minimum pressure occur downstream of the crest ($\theta = 90°$) for the entire recorded data range.

- **Discharge coefficient C_{dTh}:** Eq. 25 based on Dressler theory was used to compute C_{dTh} for the weirs. Fig.31 shows these data points plotted as a function of H_1/R. The solid line LM in this figure denotes the average relationship between C_d based on Eq. 5 (direct discharge measurement) of the present and existing (Seshadri, 1981 and Bos, 1978) studies. Insert of Fig.31 also provides a comparison of the present results with the existing ideal flow model of Cassidy (1965) for circular-crested weirs which, like Dressler's model, excludes effects due to boundary layer growth and flow separation. Hager (1985) has presented the values of C_d for standard spillways as a function of h_1/h_D (dashed line, Fig. 31). To qualitatively compare the present results with the results of Hager (1985), a scale factor of 1.5 was used to account for the fact that the cre·: pressure is atmospheric for standard spillways at $h_1/h_D = 1.0$ and for circular- crested weirs at $H_1/R = 1.5$.

In the range $H_1/R \leq 2.28$ or $Y_2/R \leq 1.6$, for all the weirs, the variations of C_{dTh} with

H_1/R based on Eq. 25 (Dressler theory) and Eq. 5 (direct discharge measurement) agree very well. Hence, the model based on Dressler theory appears to be valid in a larger range of H_1/R for C_{dTh} than for the velocity distribution. This, in part, can be traced to the fact that the velocity distribution refers to the detailed flow structure, while C_{dTh} refers to the gross flow characteristic.

6.1.5 - Summary: Dressler equations can be adapted to formulate the theoretical model for curvilinear flow past circular-crested weirs. For the prediction of the velocity distribution over the weir crest, the Y_2/R range of applicability of Dressler theory appears to be 1.0. However, the predicted values of C_{dTh} based on this model agree well with C_d determined from direct discharge measurements, in the range $H_1/R \leq 2.28$ or $Y_2/R \leq 1.6$. This corresponds to $-1.6 \leq kN$ (Convex bed).

6.2 - Examination of the basic assumptions in the theoretical curvilinear flow models:

6.2.1- General remarks: Theoretical curvilinear flow models are used to analyse the behaviour of the flow past various hydraulic structures. Among them, the commonly used model to study the characteristics of the flow past a circular-crested weir is considered and the validity of the main assumptions made in the development of the model are discussed in the following sections.

6.2.2- Basic theoretical assumptions: In the theoretical study of curvilinear flow past a weir, some of the basic assumptions related to the weir flow characteristics are listed as below:

(1) The flow upstream of the weir is steady, two-dimensional and sub-critical,

(2) The flow over the weir crest is irrotational ,

(3) The slope and radius of curvature of the streamline pattern vary linearly from the weir crest C (Fig.2b) to the free-surface.

As stated earlier (chapter 4), Fig.32 denotes the velocity distributions for the flow over the crest in the cross-sectional direction. The factors $U = \sqrt{2g H_1}$ and the depth Y_2 over the crest were used to normalize the velocity u and depth y above the crest. The velocity profiles were nearly identical. At section 1.5 cm away from the channel wall, the discrepancies in velocity near the boundary were generally within 1%, compared to other profiles in the mid-section. Only for the profile taken at 0.5 cm from the wall does one note a maximum deviation of 3% in the velocity component u. Further, besides the velocity profiles similarity, the deviation in the average velocity was of the order of 1%. These results support assumption (1) above.

6.2.3- Determination of streamline curvature parameters: For flow over the weir, defining x and y as the horizontal and vertical axis through the crest C (Fig.2b), the functional representation of the streamlines for the flow over the crest can be written as,

$$y = f(x) \qquad (26)$$

For any single streamline passing through a location y above the crest, knowing the form of f(x), the radius of curvature r and inclination ϕ can be found. Thus,

$$\tan \phi = f'(x) \qquad (27)$$

$$r = \frac{\left[1 + \left(f'(x)\right)^2\right]^{3/2}}{f''(x)} \qquad (28)$$

Where, $f'(x)$ and $f''(x)$ denote the first and second derivatives of $f(x)$, respectively for the streamline considered. It is easy to determine r at the free surface using the water surface profile. However, to obtain r at the interior points over the crest section, one needs to know the nature of $f(x)$. Hence, for a two-dimensional flow, the difference $\psi_2 - \psi_1 = udy$ between adjacent streamlines denotes the discharge passing between these streamlines. Determining the velocity distribution accurately at the vertical section over the crest and at a few other vertical sections in its neighbourhood (Insert, Fig.34), one can determine the general form of $f(x)$ which denotes the pattern of all streamlines for the flow passing over the crest. Following this, the parameters r and r_y related to the curvature of the streamlines above the crest can be determined easily, using Eqs.28 and 2.

- **Streamline geometry:** Fig.33 shows the locations of velocity measurement for the flow at a total head of $H_1 = 0.100$m. The velocity profiles shown in Fig.34 were taken along a vertical section through the weir crest and four other sections located at $\Delta x=\pm0.02$m and ±0.01m from the crest C and along the centre line. Here, Δx denotes the horizontal distance from the crest to the other four vertical sections. The dimensionless discharge $[u/\sqrt{(2gH1)} \times dy/Y]$ corresponding to the subsection dy/Y shown for curve 'a' in Fig.34 is denoted by the hatched area. Hence, the total computed area of the velocity distribution diagram related to curve 'a' denotes the total dimensionless discharge passing through x = -0.02m. Similar area computations were done for four other vertical sections over the crest surface BCE. Using these data, the actual discharges were computed for the five sections and they agreed among themselves within 2%. Fig.35 shows the incremental discharge passing through various vertical sub-sections. Using this, the streamline pattern was generated and plotted (Fig.36). Based on the streamline pattern, values of r, r_y and ϕ at the vertical section through the weir crest were determined with the help of Eqs. 28, 2 and 27 respectively. The specific data corresponding to the free-surface profiles included in Figs.36-39 were obtained from direct point gage measurement. Figs.37 and 38 indicate that the streamline radius r and the radius parameter r_y do not vary linearly with depth in a wide section close to the free-surface, although this deviation is not very large. The deviation from the linear model is restricted to the region $0.6Y_2 \leq y \leq Y_2$ for both r and r_y.

- **Streamline inclination ϕ :** Fig.39 shows that ϕ deviates slightly from the linear variation along the depth at the crest section C. A maximum deviation of the order of 10% in the ϕ value occurs at the mid-depth of the flow over the crest. Since ϕ has generally a low value (0.2 — 0.3 rad), the corresponding variation of $\cos\phi$ in Eq. 2 for the range of maximum deviation is of the order of 1%. Hence, the theoretical assumption of linear variation of ϕ with depth will not lead to erroneous results.

- **The parameter m:** As stated earlier (Ch.2), Jaeger (1956) assumed a linear variation of r_y across the flow depth and stated that $r_y = R + m\,Y_2$ with $m = 2$. For the tested weir with a downstream slope $\beta = 45^o$, Eq. 4 (Bos, 1978) gives m = 1.95, while Sarginson (1972) found m = 1.80 for circular-crested weirs ($0.1<H_1/R<10$) and 2.50 for sharp-crested weirs ($H_1/R \longrightarrow 0$). However, using the experimental data related to the present section (H_1 = 0.100m, Y_2 = 0.071m, $(P/\gamma)_{cr}$ = -0.105m and R = 0.025m), Eq.1 which does not consider H_1/R as a parameter yielded m =1.87. Fig.40 shows the variation of m with H_1/R for circular-crested weirs with α=90° and β=45° (Table 17).

6.2.4- Water surface profiles: Water surface profiles are outermost streamlines of flows past a weir crest, but precise data are required to determine experimentally the streamline pattern for the interior regions of the flow field. The free-surface profile data included in Fig.37 were obtained from direct point gage measurement, which are then fitted to a third degree curve (Ali, 1972). The values of r, r_y and ϕ at the free surface point A on the vertical section through the weir crest C were determined with the help of Eqs. 28, 2 and 27 respectively.

The characteristics of water surface profiles for the flow past circular-crested weirs and the flow depths above the weir crests were discussed previously in chapter 5.

6.2.5- Irrotationality of the flow: The flow over the weir crest is treated as irrotational in the theoretical models. To indirectly verify the validity of this assumption, the velocity profile data was analysed. For the accelerating flow over the crest, $\delta << Y_2$. In the present tests, δ/H_1 is of the order of 0.02. As such, one can assume $(P/\gamma)_\delta \approx (P/\gamma)_{cr}$, while computing the total head H_δ at the edge of the boundary layer C" (Fig.2c). In other words, H_δ can be expressed in terms of the measured quantities. Thus,

$$H_\delta = \frac{V_\delta^2}{2g} + \left[\left(\frac{P}{\gamma}\right)_{cr} - \frac{dP}{\gamma dy}\delta\right] + \delta \approx \frac{V_\delta^2}{2g} + \left(\frac{P}{\gamma}\right)_{cr} \quad \text{-------} (29)$$

At the location A (Fig.2c) of the free surface, setting v = vertical component of velocity and ϕ = inclination of the free surface, the resultant velocity head at A is $V_s^2/2g = (u^2+v^2)/2g = u^2(1+\tan^2\phi)/2g$. Hence, the total head H_s at the free surface can be expressed as:

$$H_s = \frac{V_s^2}{2g} + Y_2 \quad \text{--------------------------} (30)$$

The necessary condition for the flow to be irrotational in the region AC" (Fig.2c) is that $H_\delta/H_1 = H_s/H_1$. Figs.18 and 19 show that these ratios are in fact equal and hence indirectly confirm the irrotationality of the flow (assumption 2). For complete validation of irrotationality of the two dimensional flow in the region AC" (Fig.2c), one can independently obtain accurate static pressure and velocity distributions at many locations above the crest, compute the local total head values and compare them with the total heads at the free-surface and at C''.

Alternatively, one can experimentally determine the vorticity components at different locations in the region AC'' and show that their sum is equal to zero (Table 18f).

6.2.6- Summary: Laser Doppler velocimetry was used to obtain detailed velocity profiles for the flow over the weir crest. This information and the measured water surface profile data enables one to determine the curvature and inclination of the surface streamline at the weir crest section. In the existing theoretical models, the slope and curvature of the streamline pattern of the flow over the weir are assumed in general to vary linearly from the weir crest to the free-surface. The present results indicate that the linearity assumption of streamline slope and curvature appears to be quite valid over a wide range of depths, except in a narrow segment below the free-surface. The parameter m appears to be function of the flow parameter H_1/R. The region of crest flow above the boundary layer is verified to be irrotational. Hence, the basic assumption related to the development of existing theoretical weir models is validated. Lastly, the use of velocity profiles, taken along the channel axis and over the weir crest and its vicinity, to determine the geometry of streamlines in an two-dimensional flow field appears to be successful. Similar procedure can be applied to generate the corresponding potential lines.

CHAPTER VII

SUMMARY AND CONCLUSIONS

CHAPTER VII

SUMMARY AND CONCLUSIONS

The major conclusions of the present investigation related to the characteristics of curvilinear flow past circular-crested weirs are summarized below:

I.- 1) Circular-crested weirs will behave as a sharp-crested weir when the head causing flow is relatively very large compared to the crest radius.

2) For a circular-crested weir without the downstream slope and $\alpha = 90^o$, a ventilated nappe reduces C_d slightly for $2<H_1/R<18$, but improves flow stability and reduces the possibility of cavitation.

3) For all the combinations of weir slopes of the tested models, for a fixed downstream slope, the effect of upstream weir slope on C_d is marginal. For a fixed upstream weir slope, for $H_1/R > 3$, C_d improves when the downstream slope is increased.

4) The minimum pressure on the crest surface occurs at a location downstream of the crest for low H_1/R values and moves upstream towards the crest as H_1/R increases. This minimum pressure generally occurs very near the crest when C_d attains its maximum value. The variation of the crest pressure with H_1/R agrees very well with previous theoretical and experimental data.

5) Using an appropriate scale factor for h_1/h_D and H_1/R, some of the main characteristics of circular-crested weirs and standard spillways can be qualitatively compared.

II.- LDV techniques enable one to obtain accurate velocity profiles in the curvilinear flow field above the weir crest. This, in turn, yields the weir discharge coefficient. The value of C_{dVel} determined on the basis of this procedure is found to agree very well with the previous results related to C_d obtained from direct discharge measurements and numerical studies (Cassidy, 1965). The data of the minimum pressure on the crest surface can be used to determine the cavitation potential of the weir.

The alternate method suggested to determine the discharge coefficient of circular-crested weirs can be extended to the case of other weir types, since the determination of the velocity distribution in other weir crest section using LDV techniques is quite straight-forward.

III.- The experimentally determined velocity profiles in the region of curvilinear flow over the weir are shown to provide useful pressure distribution data needed for the momentum analysis of flow past a circular-crested weir. For the range of data analysed ($0.44 \leq H_1/R \leq 4.88$), the weir discharge coefficient C_{dMom} based on momentum analysis agree very well with C_d based on direct discharge measurement of past and present studies. The general procedure outlined in the momentum model can be used to analyse flow past other types of weirs.

IV.- Dressler equations can be adapted to formulate the model for curvilinear flow past circular-crested weirs. For the prediction of the velocity distribution over the weir crest, the Y_2/R range of applicability of Dressler theory appears to be 1.0. However, the predicted values of C_{dTh} based on this model agree well with C_d determined from direct discharge measurements, in the range $H_1/R \leq 2.28$ or $Y_2/R \leq 1.6$. This corresponds to $-1.6 \leq kN$ (Convex bed).

V.- Detailed velocity profiles for the flow over the weir crest and the measured water surface profile data enable one to determine the streamline pattern on the weir crest section.

In the existing theoretical models, the slope and curvature of the streamline pattern of the flow over the weir are assumed in general to vary linearly from the weir crest to the free-surface. The present results indicate that the linearity assumption of streamline slope and curvature appears to be quite valid over a wide range of depths, except in a narrow segment below the free-surface. The basic assumption related to the development of existing theoretical weir models is validated.

CHAPTER VIII

SCOPE FOR FUTURE INVESTIGATIONS

CHAPTER VIII

SCOPE FOR FUTURE INVESTIGATIONS

The present study on the hydraulic characteristics of circular-crested weirs can be extended to the following additional studies:

i) study the streamline pattern in detail over a wide range of H_1/R, to determine the dependence of dimensionless parameters r_y/R, ϕ and m on H_1/R,

ii) extend the range of applicability of Dressler theory to larger values of H_1/R,

iii) study the effect of air entrainment in the downstream section of the weir,

iv) determine the modular limit of the weir for submerged flow conditions and

v) incorporate information of field data to verify and improve the theoretical results.

vi) The use of LDV techniques described to obtain indirectly the pressure distribution in the region of irrotational flow on the basis of measured velocity distribution can be adopted to solve the problems related to end depth analysis of flows in circular pipes and trapezoidal channels using the momentum balance model.

APPENDIX I

REFERENCES

APPENDIX I: REFERENCES

1. Ackers, P. et al (1978): Weirs and flumes for flow measurement. John Wiley & Sons.

2. Ali, K.H.M. (1972): Flow over rounded spillways. Journal of the Hyd. Div., Proc. ASCE, vol. 98, No. HY2, pp. 365-380.

3. Balachandar, R. (1990): Characteristics of separated flows including cavitation effects, thesis presented at Concordia University, Montreal, Canada, in partial fulfillment of the requirements for the degree of Doctor of Philosophy.

4. Bos, M.G. (1978): Discharge measurement structures. Publ. 20, ILRI, The Netherlands.

5. Brater, E.F. and King, H.W. (1976): Handbook of hydraulics. 6th Edition (Weirs of triangular Section, Bazin (1890), pp. 5.24-5.43).

6. Cassidy, J.J. (1965): Irrotational flow over spillways of finite height. J. of the Engineering Mechanics Div., ASCE (82-12, paper 4591), Vol. 91, N. EM6, pp 155-173.

7. Cassidy, J.J. (1970): Designing spillway crests for high head operation. J. Hyd. Div., ASCE, Vol. 96, HY3, pp. 745-753.

8. Cassidy, J.J. and Elder, R.A. (1984): Spillways of high dams - Developments in Hydraulic Engineering - 2. Edited by P. Novak, Elsevier Applied Science Publishers Ltd. (Ch. 4, pp. 159-182).

9. Cassidy, J.J. (1990): Fluid mechanics and design of hydraulic structures. J. Hyd. Eng., ASCE, (Paper No. 24949), Vol. 116, No. 8, pp. 961-977.

10. Castro-Delgado, M., Celik, I. and Herrling, B. (1984): Computation of the potential flow over hinged-leaf gates. Computational methods and experimental measurements,

Proc. of the 2nd International Conference. Ed. C.A. Brebbia, G.A. Keramidas, pp. 3.15-3.27.

11. Chow, V.T. (1959): Open channel hydraulics. McGraw Hill.
12. Davidson, P.A. and Matthew, G.D. (1982): Potential flow over weirs of moderate curvature. J. of the Eng. Mech. Div., Proc. of the ASCE, Vol. 108, No. EM5, pp. 689-707.
13. Dressler, R.F. (1978): New nonlinear shallow flow equations with curvature. J. Hyd. Res., IAHR, Vol. 16, No. 3, pp. 205-222.
14. Dressler, R.F. and Yevjevick, V. (1984): Hydraulic resistance terms modified for the Dressler curved-flow equations. J. Hyd. Res., Vol. 22, No. 3, pp. 145-156.
15. Escande, L. and Sananes, F. (1959): "Etude des seuils deversants a fente aspiratrice (Weirs with suction slots). La Houille Blanche", Vol. 14, No. Special B, pp. 892-902.
16. Fox, R.W. and McDonald, A.T. (1985): Introduction to Fluid Mechanics, 3rd. Edition, John Wiley & Sons, Inc.
17. Hager, W.H. (1987): Continuous crest profile for standard spillway. J. Hyd. Eng., ASCE (Paper No. 21984-1), Vol. 113, No. 11, pp. 1453-1457.
18. Harrison, A.J.M. (1967): The streamlined broad-crested weir. Proc. Inst. of CE, Vol. 38, pp. 657-678.
19. Henderson, F.M. (1966): Open channel flow. MacMillan Co.
20. Jaeger, C. (1956): Engineering fluid mechanics. Blackie, London.
21. Kandaswamy, P.K. and Rouse, H. (1957): Characteristics of flow over terminal weirs and sills. Proc. paper 1345, J. Hyd. Div., Proc. ASCE, HY4, pp. 1345.1-13.
22. Keller, R.J. (1984): Cut-throat flume characteristics, J.Hyd. Div., (110,9), September 1984, pp. 1248-1263.
23. Matthew, G.D. (1963): On the influence of curvature, surface tension and viscosity on flow over round-crested weirs. Proc. of the Inst. of CE, ASCE, Vol.25, pp.511-

524.

24. Morris,H.M. and Wiggert, J.M. (1972): Applied hydraulics in engineering, 2nd. Edition, Ronald Press Company, N.Y..

25. Nasser, M.S., Venkataraman, P. and Ramamurthy, A.S. (1980): Curvature corrections in open channel flow. Can. J. Civ. Eng., vol. 7, pp. 421- 431.

26. Rajaratnam, N. and Muralidhar, D. (1971): Pressure and velocity distribution for sharp crested weirs, J. Hyd. Res., Vol. 9, No. 2, pp. 241-247.

27. Ramamurthy, A.S., Balachandar, R. and Vo, N.D.(1989): Blockage correction for sharp-edged Bluff bodies. J. of Engg. Mechs., ASCE, Vol. 115, No. 7 July 1989, pp.1569-1576.

28. Ramamurthy, A.S., Subramanya, K. and Pani, B.S. (1978): Sluice gate with high discharge coefficients. J. of the Irr. and Dr. Div., Proc. ASCE, Vol. 104, No. IR4, pp.437-441.

29. Ramamurthy, A.S., Carballada, L.B., Bergeron, D. and Vo, N.D. (1987): On the characteristics of circular-crested weirs. Conf. 11th Canadian Congress of Applied Mechanics, Alberta (CANCAM '87).

30. Ramamurthy, A.S., Rao, M.V.J., and Auckle, D. (1985): Free flow characteristics of throatless flumes. J. of the Irr. and Dr. Engg., ASCE, Vol. 111, No. 1, pp.65-75.

31. Ramamurthy, A.S., Tim, U.S. and Carballada, L.B. (1986): Lateral weirs in trapezoidal channels. J. of Irr. and Dr. Eng., ASCE, Vol. 112, No. 2, pp. 130-137.

32. Ramamurthy, A.S., Tim, U.S. and Rao, M.V.J. (1987): Flow over sharp-crested plate weirs. J.-of Irr. and Dr. Eng., ASCE, Vol. 113, No. 2, Paper No. 21460.

33. Ramamurthy, A.S., Vo, N.D., and Balachandar, R. (1988): Submerged flow characteristics of throatless flumes. J. of the Irr. and Dr. Engg., ASCE, Vol. 114, No. 1, pp. 186 - 194. Paper No. 22230.

34. Ramamurthy, A.S., Vo, N.D., and Balachandar, R. (1992a): LDV techniques applied to curvilinear flow. J. of Engg.Mechs., ASCE, (submitted).

35. Ramamurthy, A.S., Vo, N.D., and Vera, G. (1992b): Momentum model of flow past a weir. J. of the Irr. and Drain. Engg., ASCE, accepted Feb. 1992.

36. Ramamurthy, A.S., Vo, N.D.(1992c): Application of Dressler theory to weir flow. J. of App.Mechs., ASCE, accepted Jan. 1992.

37. Rouse, H. and Reid, L. (1935): Model research on spillway crests. Civil Eng., Vol. 5, No. I, pp. 10-14.

38. Sananes, M.F. (1957): "Etude des seuils deversants a fente aspiratrice". IAHR, 7th Gen. Meet. Tran., Lisbon, Vol. II, pp. D24.1-D24.23.

39. Sarginson, E.J. (1972): The influence of surface tension on weir flow. J. of Hyd. Res., Vol. 10, pp. 431-446.

40. Sarginson, E.J. (1984): Scale effects in model tests on weirs. IAHR, Symposium on scale effects, Germany, pp. 2.3-1-2.3-4.

41. Satish, M.G., Ramamurthy, A.S. and Vo,D.(1986): Characteristics of flow past a transverse floor slot in an open channel floor. CSCE, Annual Conf. May 1986, Toronto, Canada.

42. Schlichting, H. (1979): Boundary layer theory. 7th Ed., McGraw Hill.

43. Seshadri, S. (1981): Flow characteristics of hydrofoil weirs, hydrofoil topped weirs and streamlined triangular profiles weirs. Thesis presented to the Indian Institute of Science, November 1981, in partial fulfillment of the requirements for the degree of Doctor of Philosophy.

44. Sinniger, R. and Hager, W.H. (1985): Flood control by gated spillways. "Commission Internationale des Grands barrages, 15^{e} Congres des barrages", Lausanne, Q.59, R.9, pp. 121-149.

45. Sivakumaran, N.S., Hosking, R.J. and Tingsanchali, T. (1981): Steady shallow

flow over a spillway. J. of Fl. Mech., Vol. III, pp. 411-420.

46. Sivakumaran, N.S., Tingsanchali, T. and Hosking, R.J. (1983): Steady shallow flow over curved beds. J. of Fl. Mech., Vol. 128, pp. 469-487.

47. Sivakumaran, N.S. and Dressler, R.F. (1986): Distribution of resistive body-force in curved free-surface flow. Math. Meth. in the Appl. Sci. 8. pp. 492-501.

48. Sivakumaran, N.S. and Yevjevich, V. (1987): Experimental verification of the Dressler curved-flow equations. J. of Hyd. Res., Vol. 25, No. 3, pp. 373-391.

49. Sridharan, K., Rao, N.S.L. and Seshadri, S. (1984): Hydrofoil topped weirs for irrigation tanks. J. of the Inst. of Eng., CE (India), Vol. 65, pp. 27-32.

50. Udoyara, T.S. (1986): Characteristics of some hydraulic structures used for flow control and measurement in open channel. Thesis presented at Concordia University, Montreal, in September 1986, in partial fulfillment of the requirements for the degree of Doctor of Philosophy.

51. United States Bureau of Reclamation: Design of small dams. G.P.O. 1977, (A water resources technical publication.)

52. Vallentine, H.R. (1967): Applied hydrodynamics. Butterworths.

53. Verwoerd, A.L. (1941): "Calcul du debit de deversoirs denoyes et noyes a crete arrondie. L'Ingenieur des Indes Neerlandaises", Vol. 8, pp. 65-78.

APPENDIX II

FIGURES

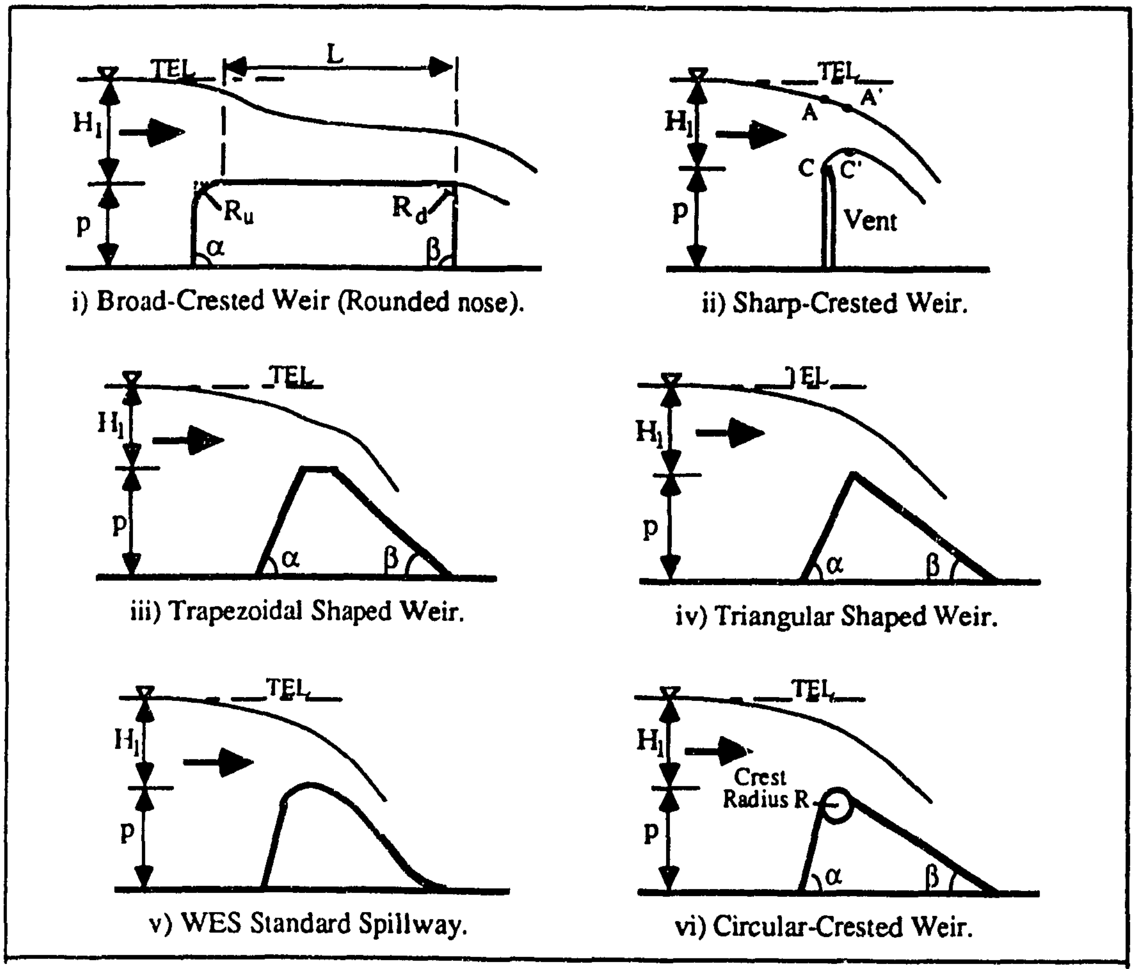

Fig.1a: Typical Hydraulic Structures for Measurement and Control of Open Channel Flow.

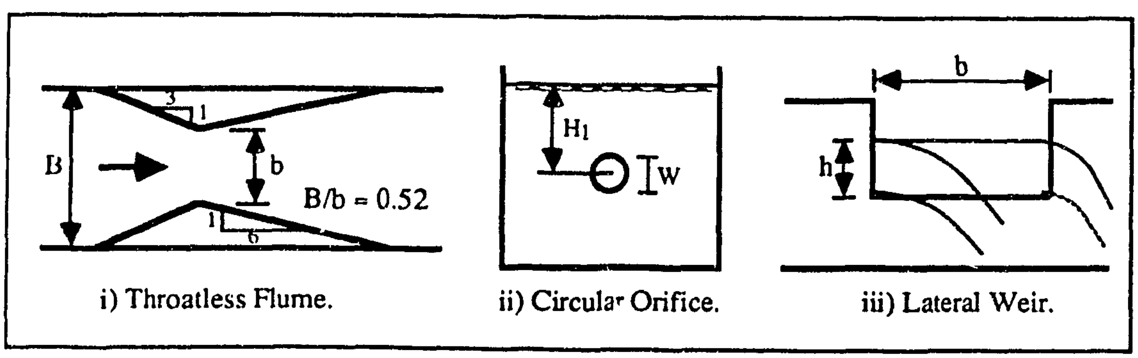

Fig.1b: Typical Hydraulic Structures for Measurement or Control of Open Channel Flow.

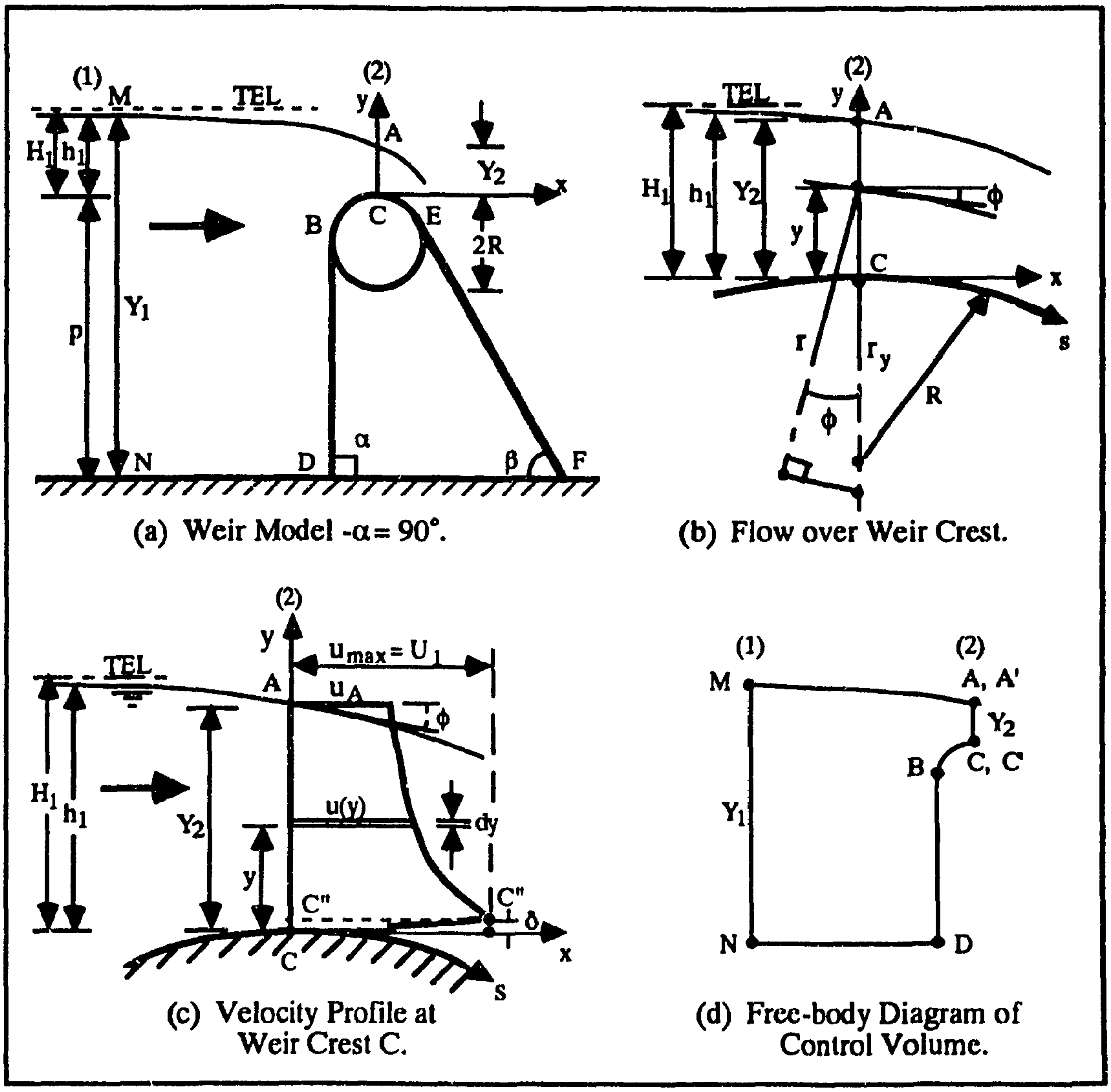

Fig.2: Flow Past a Circular-Crested Weir.

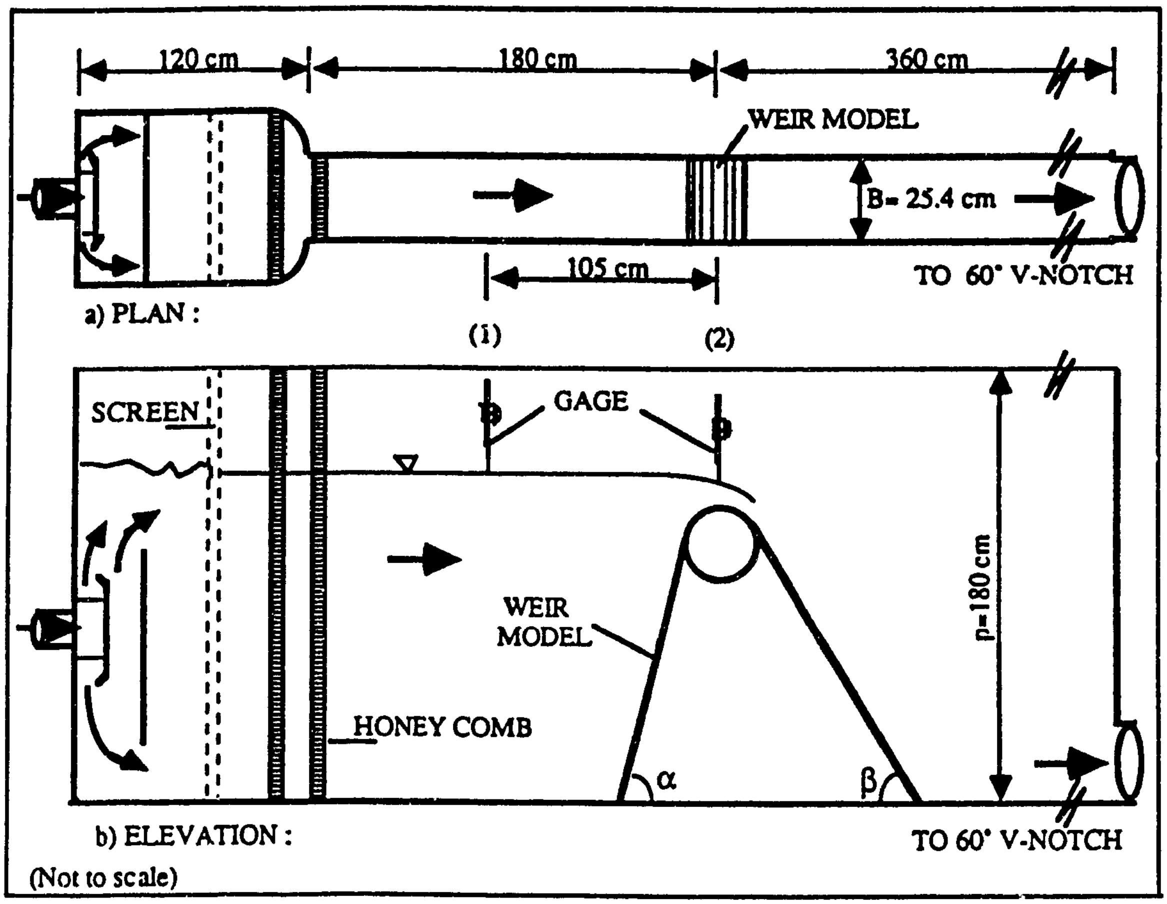

Fig.3: Test Set-up.

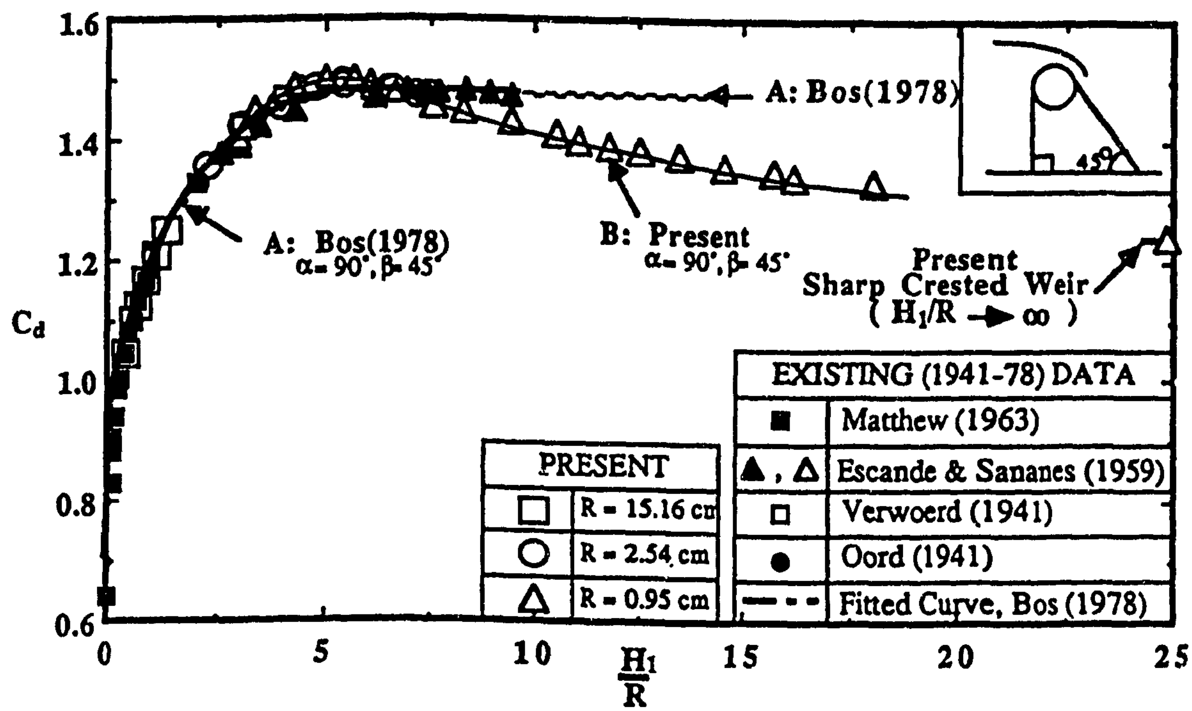

Fig.4a: Variation of C_d with H_1/R.

(a) Circular-crested weir: $0 < H_1/R < 25$ ($\alpha = 90°, \beta = 45°$).

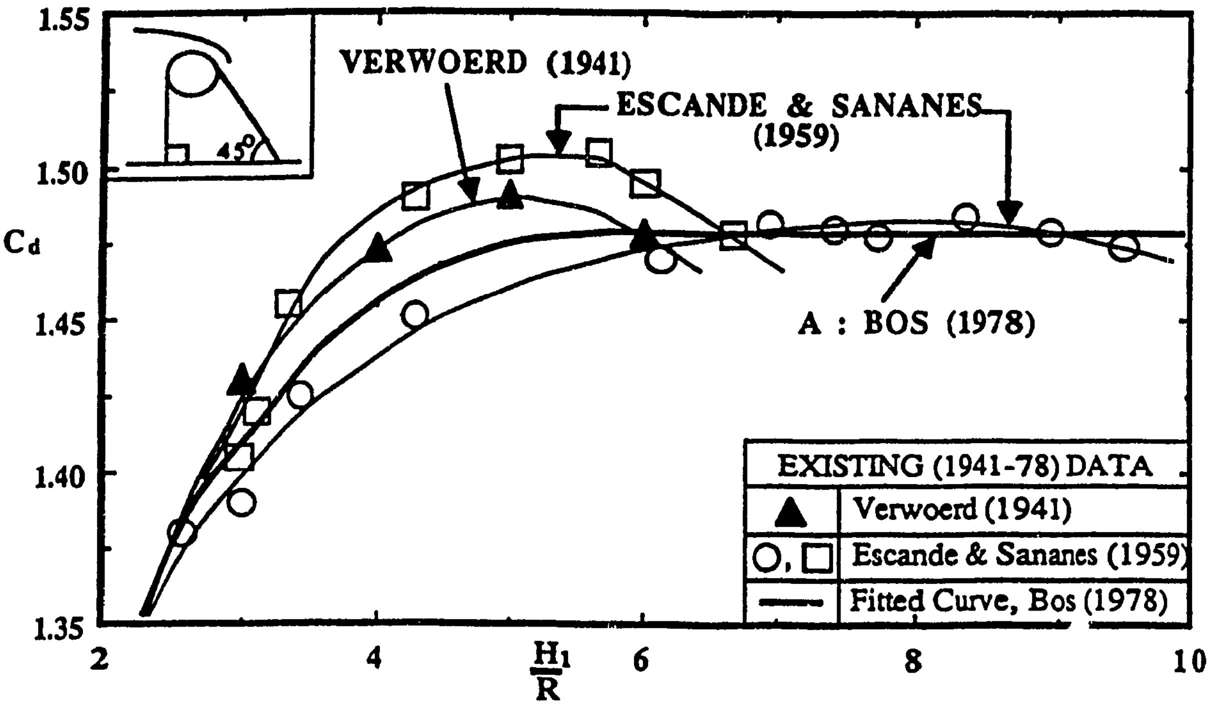

Fig.4b: Variation of C_d with H_1/R.

(b) Circular-crested weir: $2 \leq H_1/R \leq 10$ ($\alpha = 90°, \beta = 45°$).

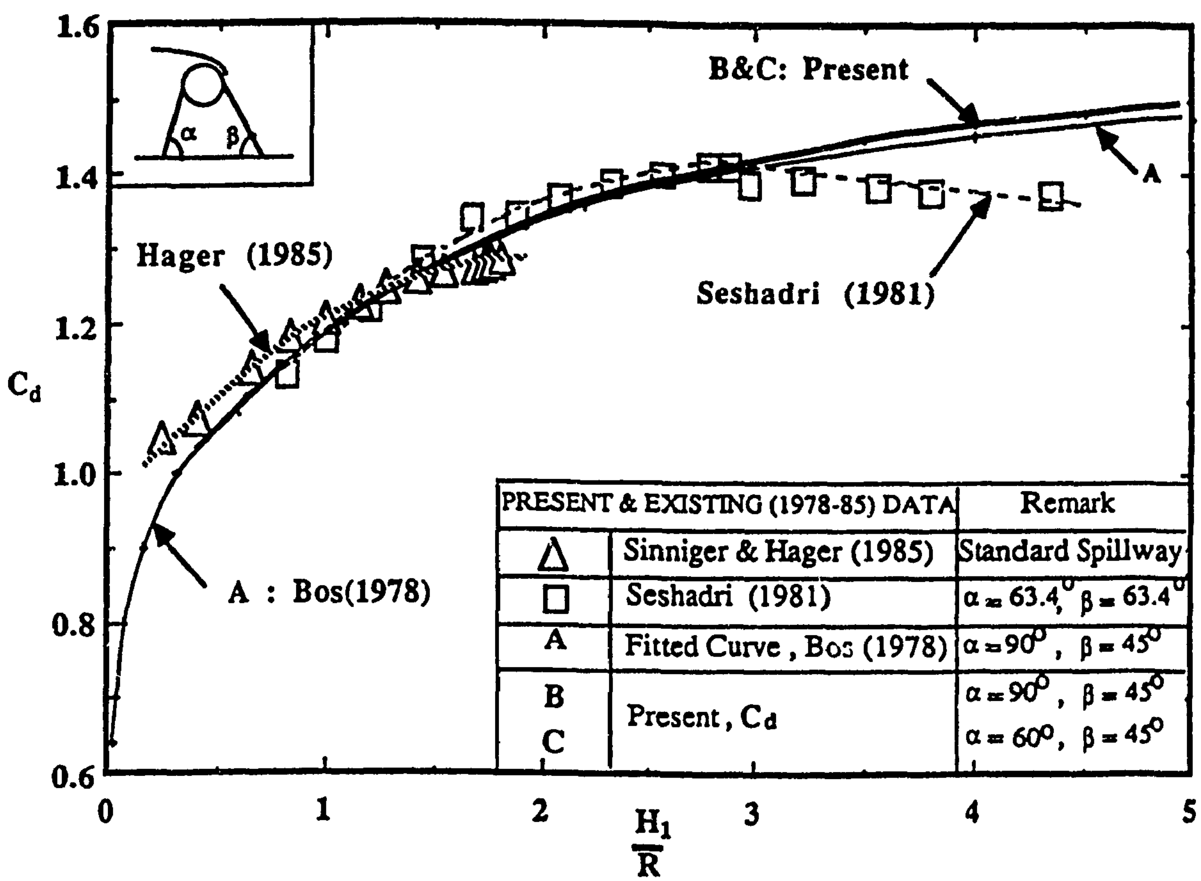

Fig.4c: Variation of C_d with H_1/R.

(c) Circular-crested weir and standard spillway: $0 < H_1/R \leq 5$.

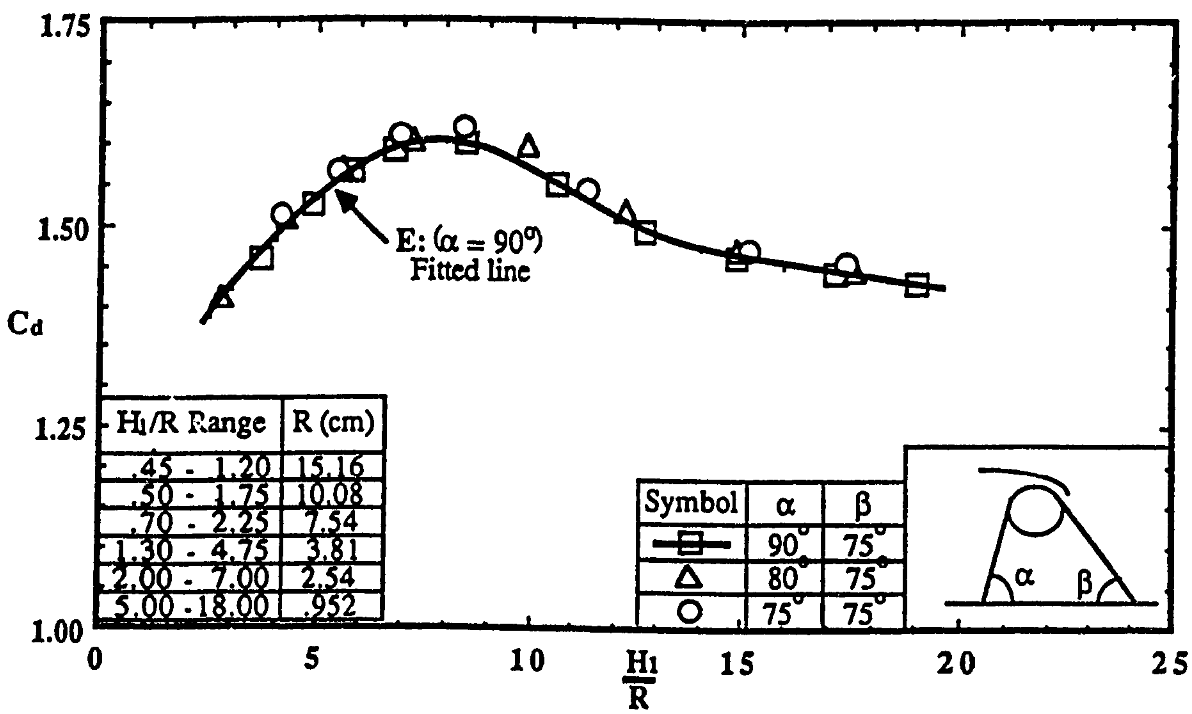

Fig.5a: Effects of Upstream Weir Slope on C_d- H_1/R Relationship.
$0 < H_1/R < 25$, $\beta = 75°$.

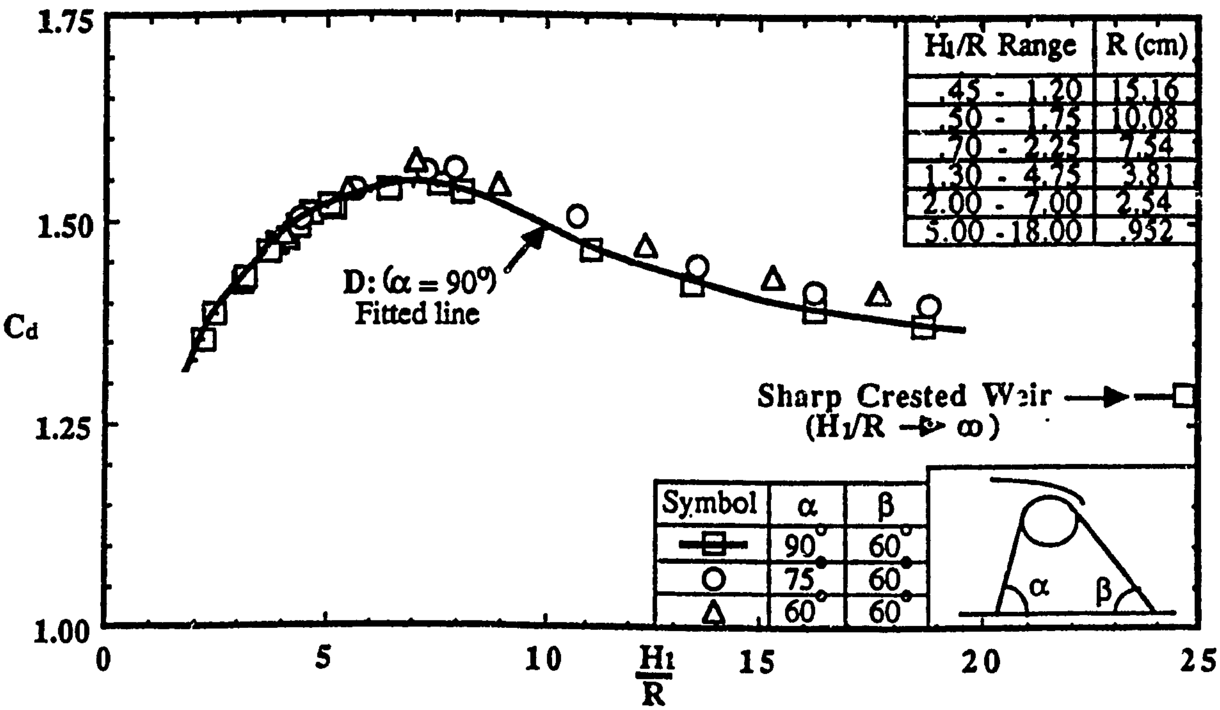

Fig.5b: Effects of Upstream Weir Slope on C_d- H_1/R Relationship.

$0 < H_1/R < 25, \beta = 60°$.

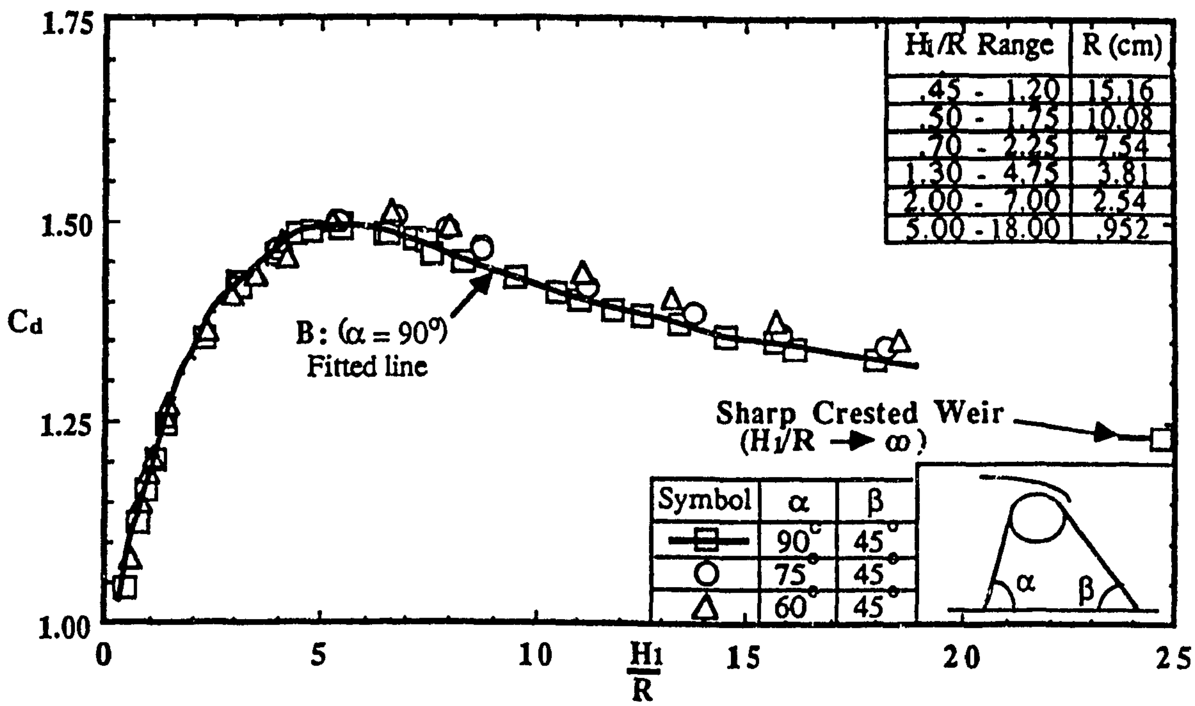

Fig.5c: Effects of Upstream Weir Slope on C_d- H_1/R Relationship. $0 < H_1/R < 25$, $\beta = 45°$.

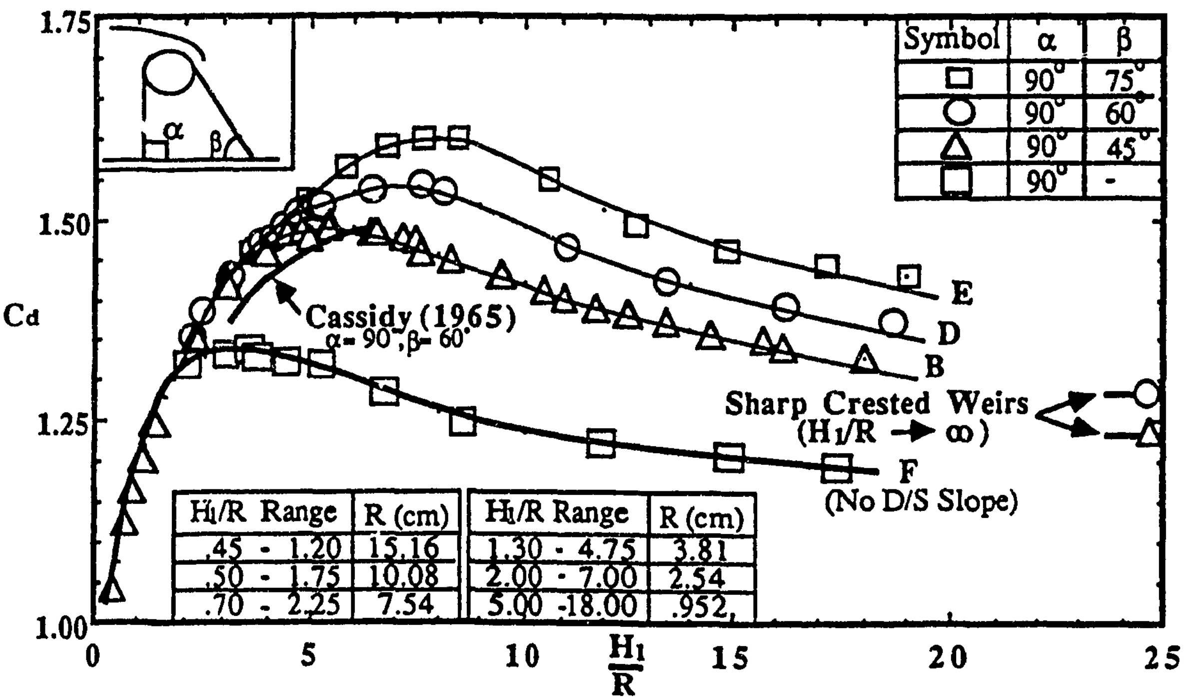

Fig.6: Effects of Downstream Weir Slope on C_d- H_1/R Relationship ($0 < H_1/R < 25, \alpha = 45^o$).

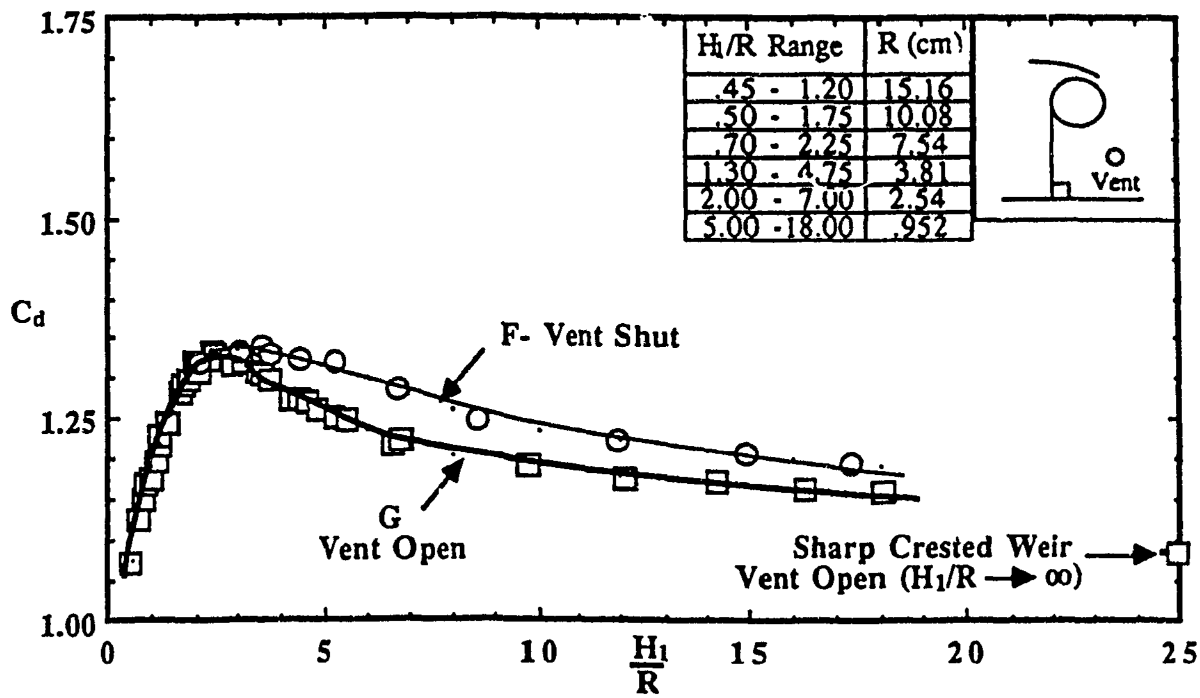

Fig.7: Effects of Nappe Ventilation on C_d- H_1/R Relationship, $0<H_1/R<25$, Weir with no downstream slope and $\alpha = 90°$.

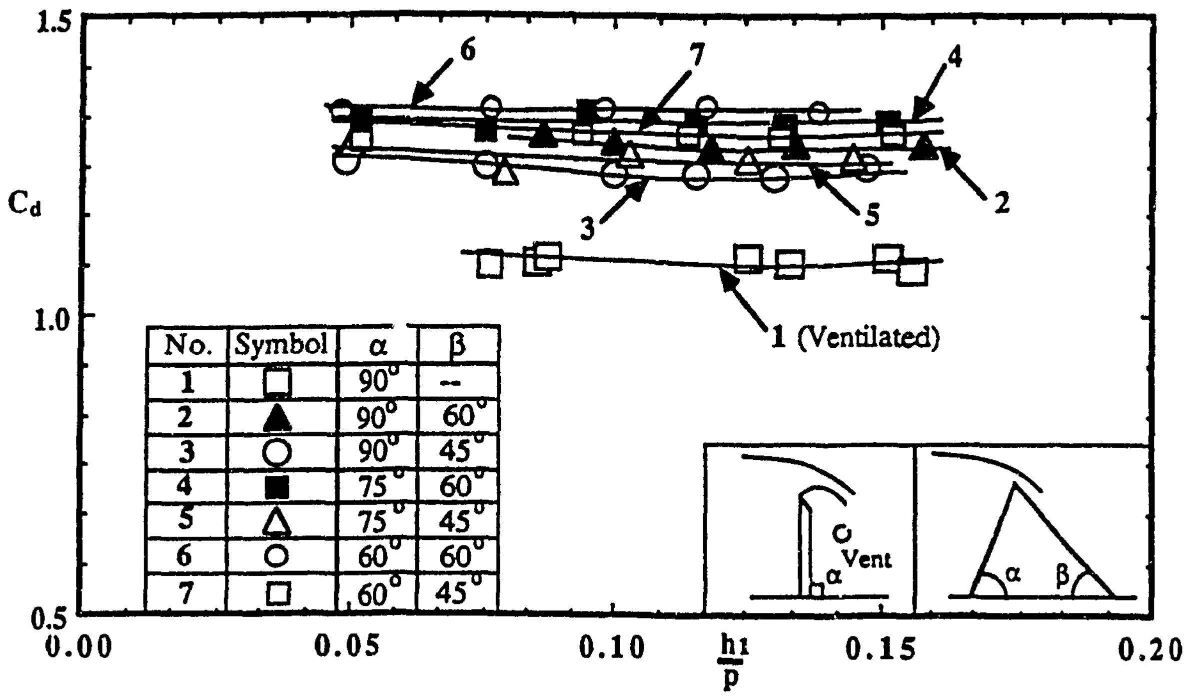

No.	Symbol	α	β
1	□	90°	--
2	▲	90°	60°
3	○	90°	45°
4	■	75°	60°
5	△	75°	45°
6	○	60°	60°
7	□	60°	45°

Fig.8: Variation of C_d with h_1/p: $0 < h_1/p < 0.2$, $H_1/R \rightarrow \infty$.

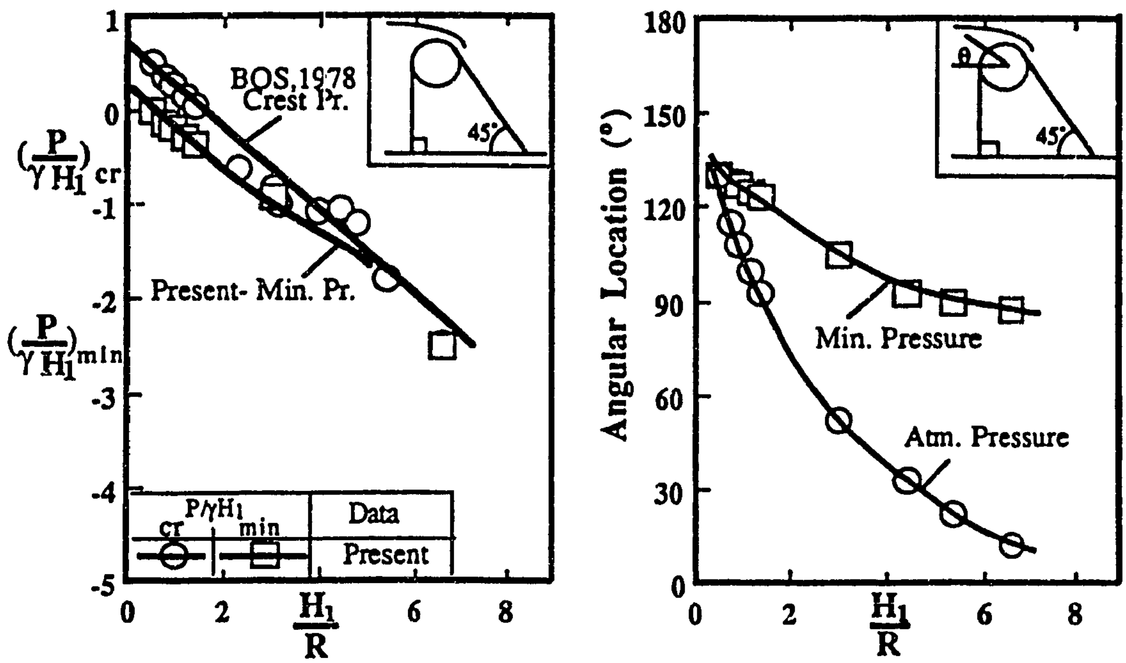

(a) Variation of $(P/\gamma H_1)_{cr}$ and $(P/\gamma H_1)_{min}$ with H_1/R-

(b) Location of minimum and atmospheric pressure on crest surface.

Fig.9: Pressure Distribution on the Crest Surface - (α = 90° , β = 45°).

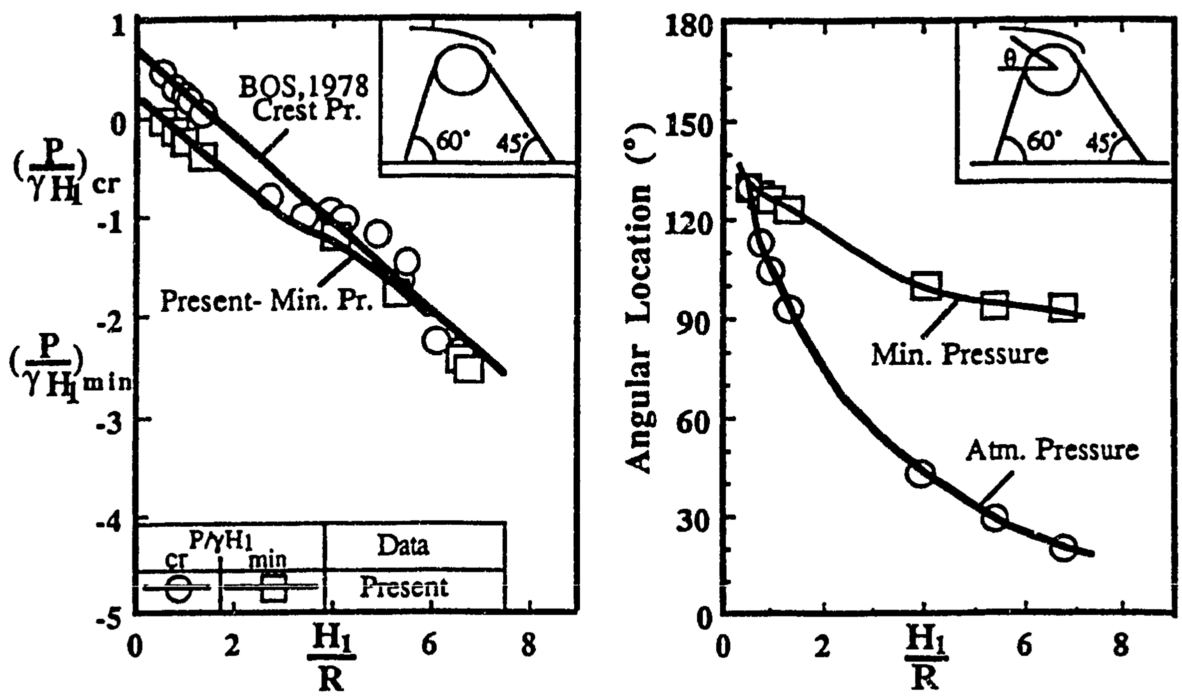

(a) Variation of $(P/\gamma H_1)_{cr}$ and $(P/\gamma H_1)_{min}$ with H_1/R-

(b) Location of minimum and atmospheric pressure on crest surface.

Fig.10: Pressure Distribution on the Crest Surface - ($\alpha = 60°$,$\beta = 45°$).

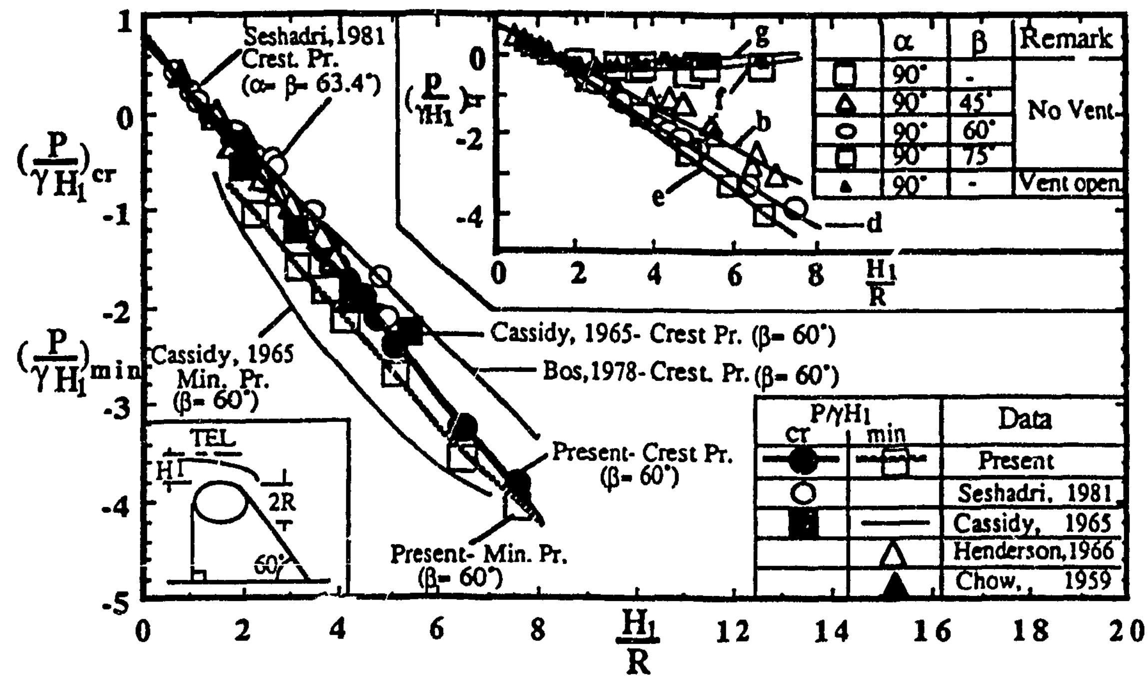

(a) Variation of $(P/\gamma H_1)_{cr}$ and $(P/\gamma H_1)_{min}$ with H_1/R.
Insert: Effects of β on $(P/\gamma H_1)_{cr}$.

Fig.11: Pressure Distribution on the Crest Surface - (α = 90° , β = 60°).

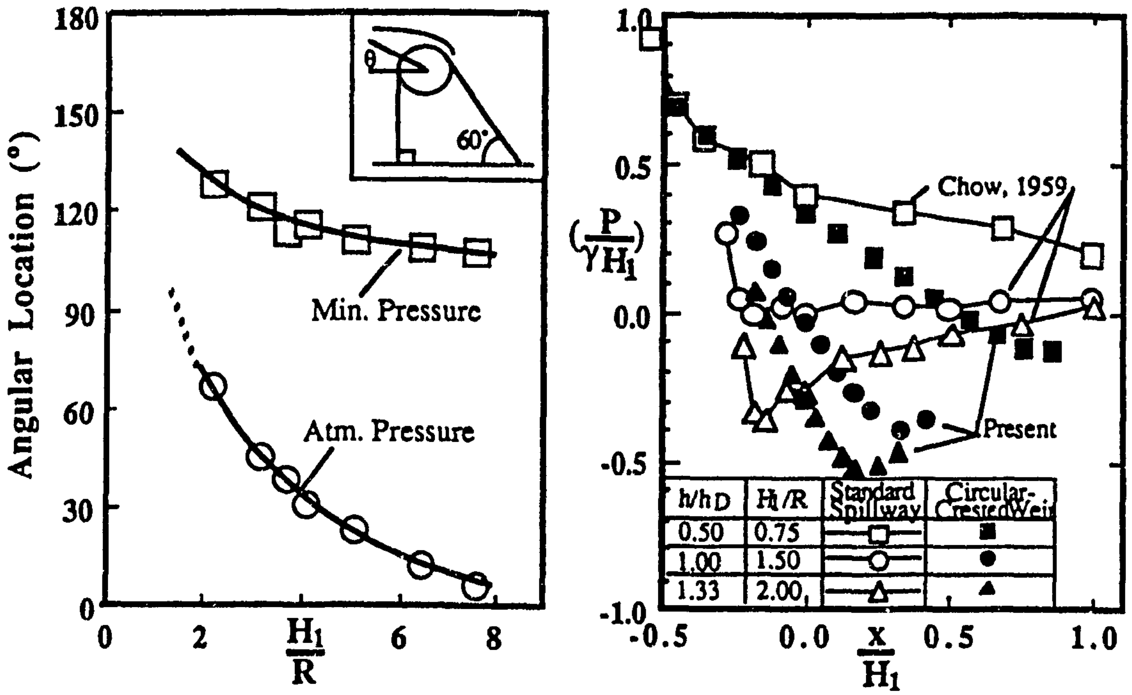

(b) Location of minimum and atmospheric pressure on crest surface.

(c) Typical pressure distribution for standard spillway.

Fig.11: Pressure Distribution on the Crest Surface - ($\alpha = 90°$, $\beta = 60°$).

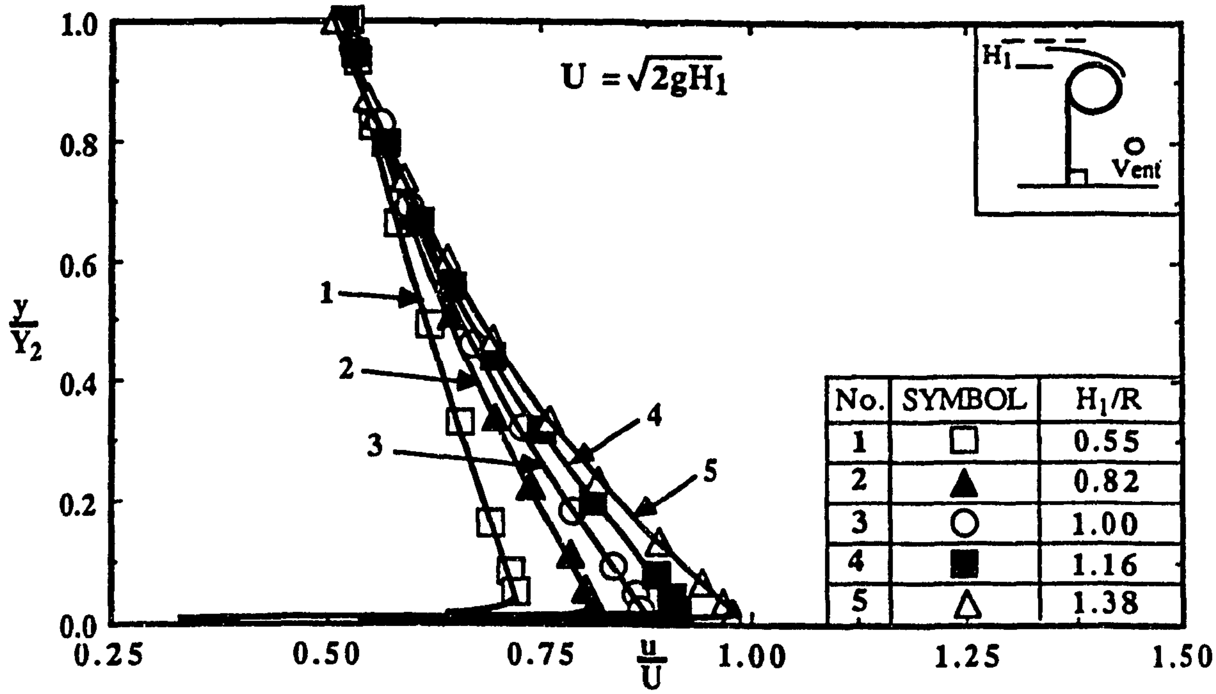

Fig.12a: Velocity Distribution for Circular-Crested Weir- with no D/S Slope, $\alpha = 90°$ (Ventilated).

(a) $0.55 \le H_1/R \le 1.38$: y/Y_2 versus u/U.

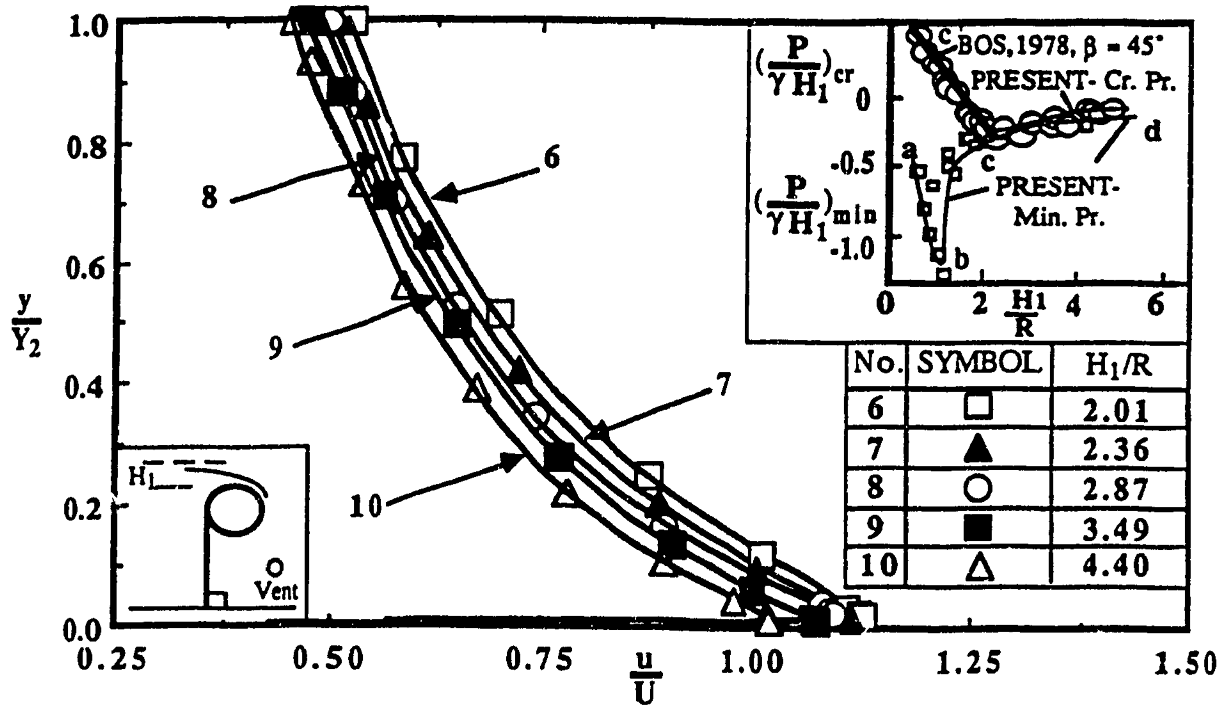

Fig.12b: Velocity Distribution for Circular-Crested Weir- with no D/S Slope, α = 90° (Ventilated).

(b) $2.01 \leq H_1/R \leq 4.40$: y/Y_2 versus u/U.

Insert: Variation of Crest Pressure and Minimum Pressure with H_1/R ($0.5 \leq H_1/R \leq 5.0$).

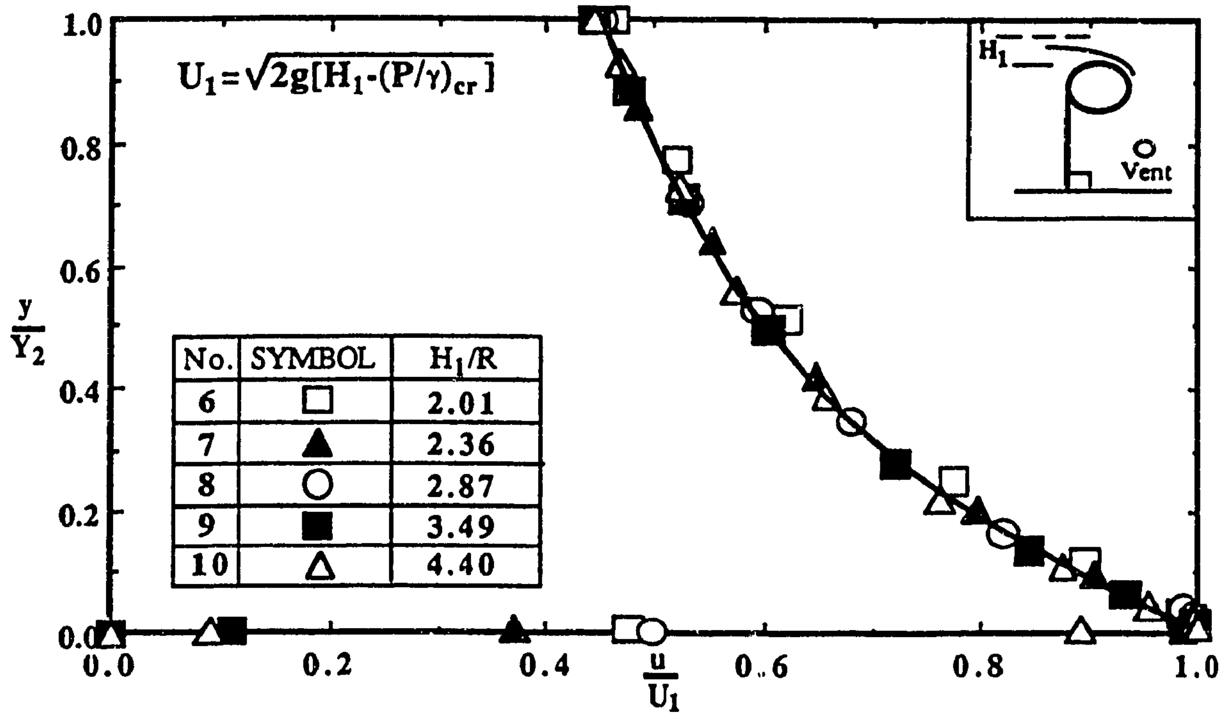

Fig.12c: Velocity Distribution for Circular-Crested Weir- with no D/S Slope, α = 90° (Ventilated).

(c) 2.01 ≤ H_1/R ≤ 4.40 : y/Y_2 versus u/U_1.

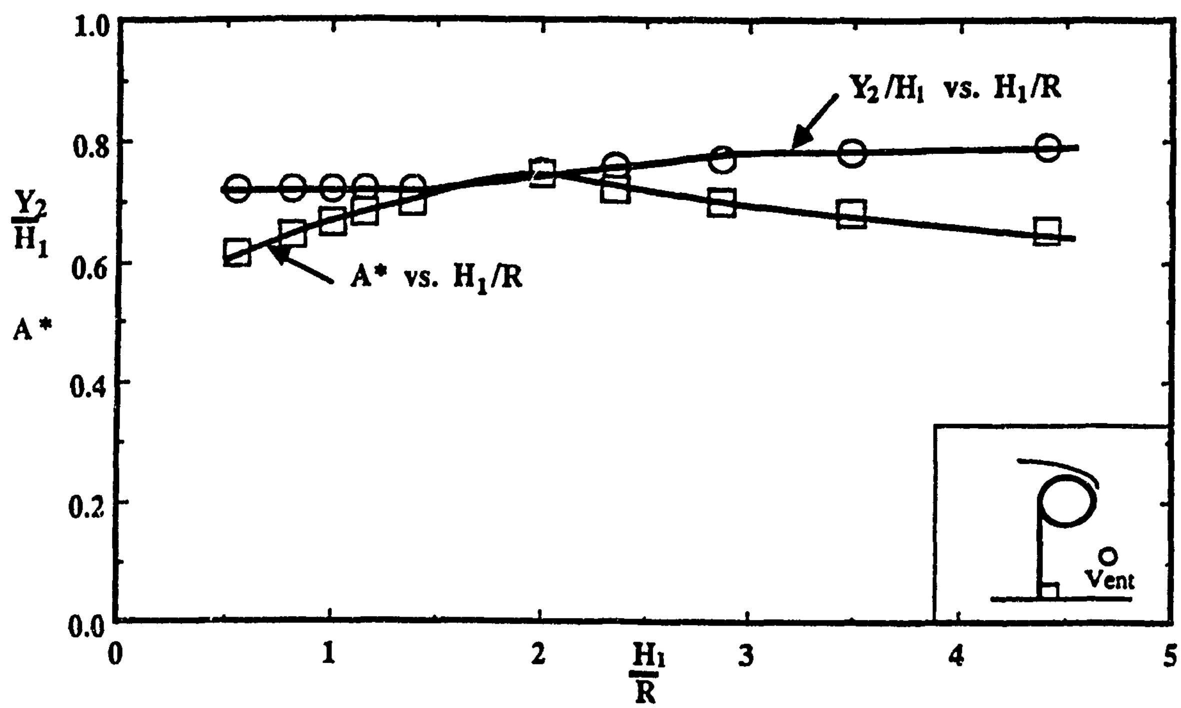

Fig.13a: Characteristics of Weirs with no D/S Slope (α = 90°) ($0.55 \leq H_1/R \leq 4.40$).

(a) Variation of Y_2/H_1 and A* with H_1/R, α =90°, ventilated.

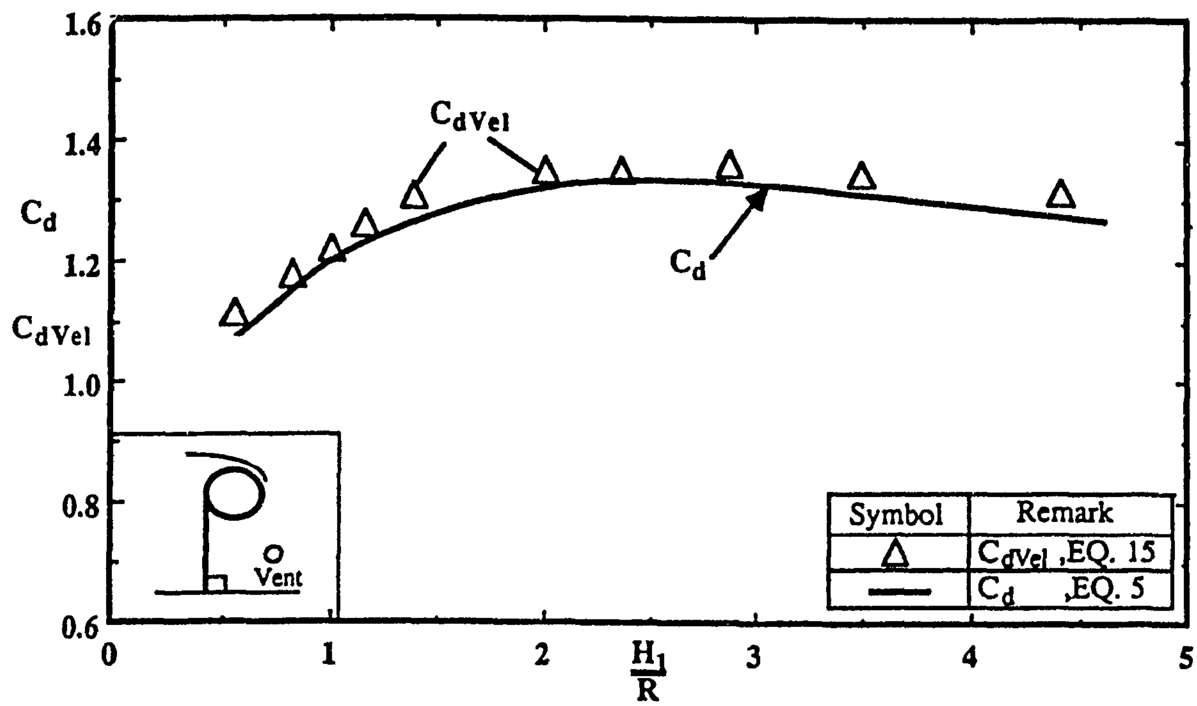

Fig.13b: Characteristics of Weirs with no D/S Slope (α = 90°) ($0.55 \leq H_1/R \leq 4.40$).

(b) Variation of C_d and C_{dVel} with $H_1/R, \alpha$ =90°, ventilated.

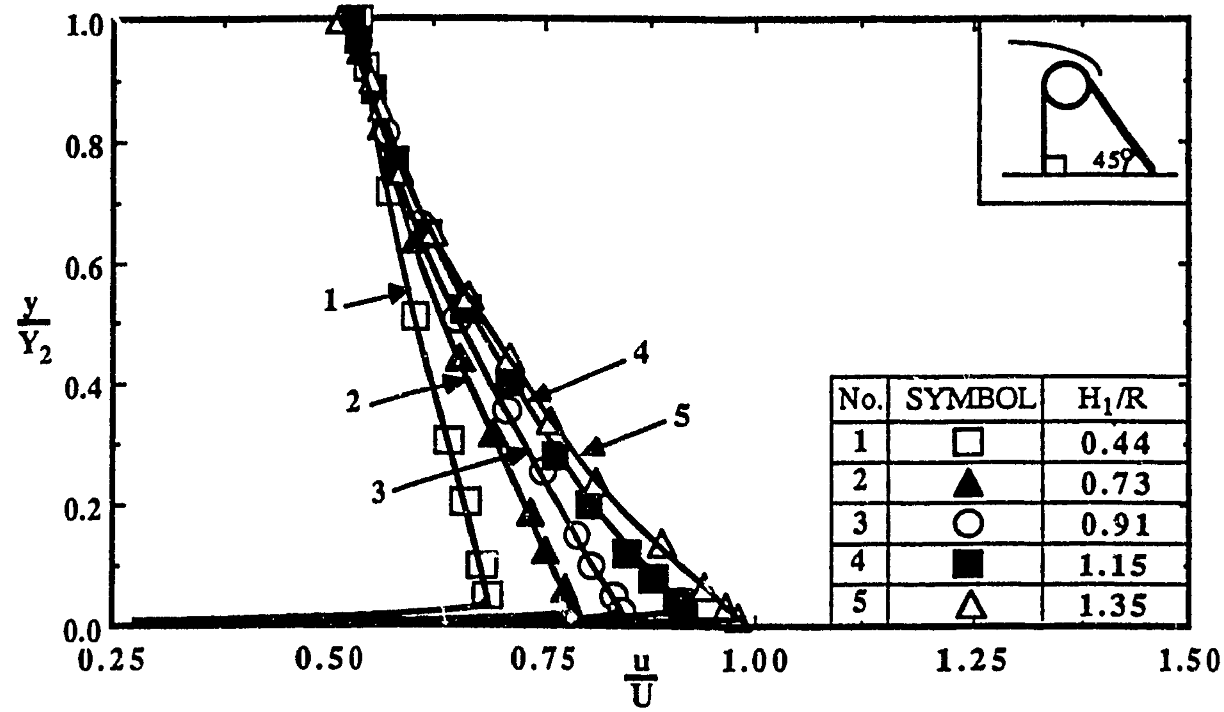

Fig.14a: Velocity Distribution for Circular-Crested Weir - (α = 90°,β = 45°).

(a) $0.44 \leq H_1/R \leq 1.35$: y/Y_2 versus u/U.

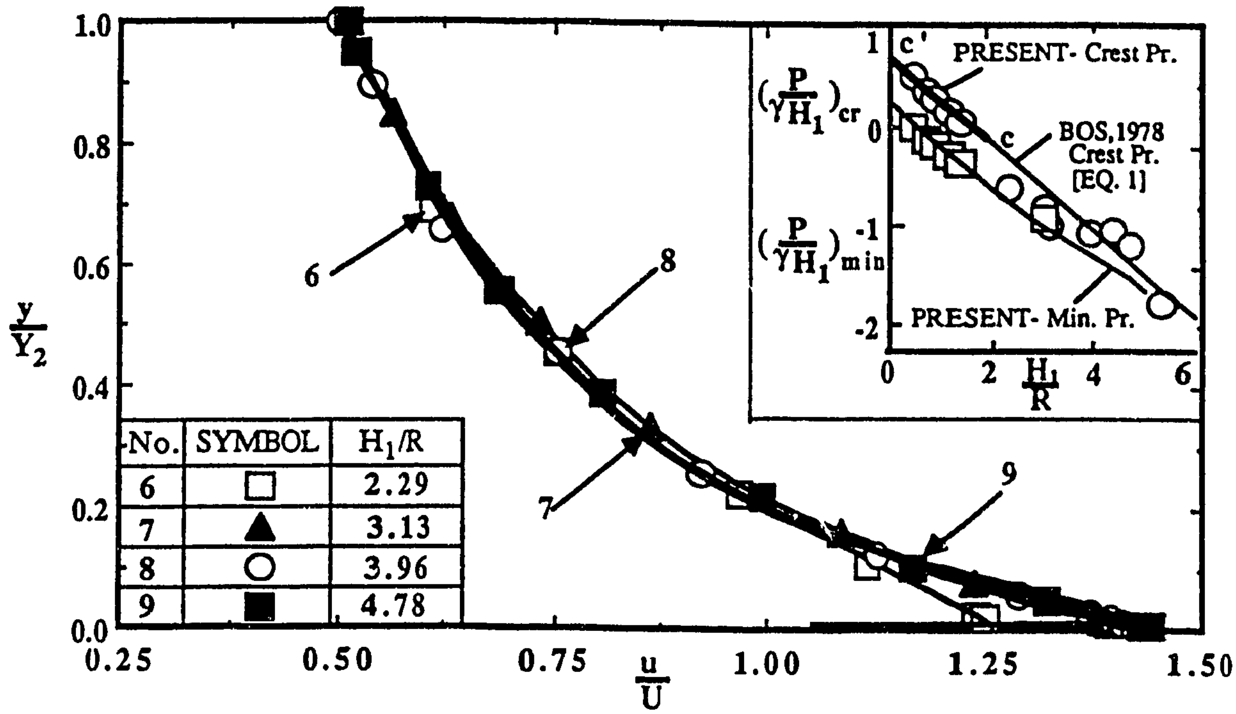

Fig.14b: Velocity Distribution for Circular-Crested Weir - (α = 90°,β = 45°).

(b) $2.29 \leq H_1/R \leq 4.78$: y/Y_2 versus u/U.

Insert: Pressure Distribution at the Crest ($0.50 \leq H_1/R \leq 5.50$).

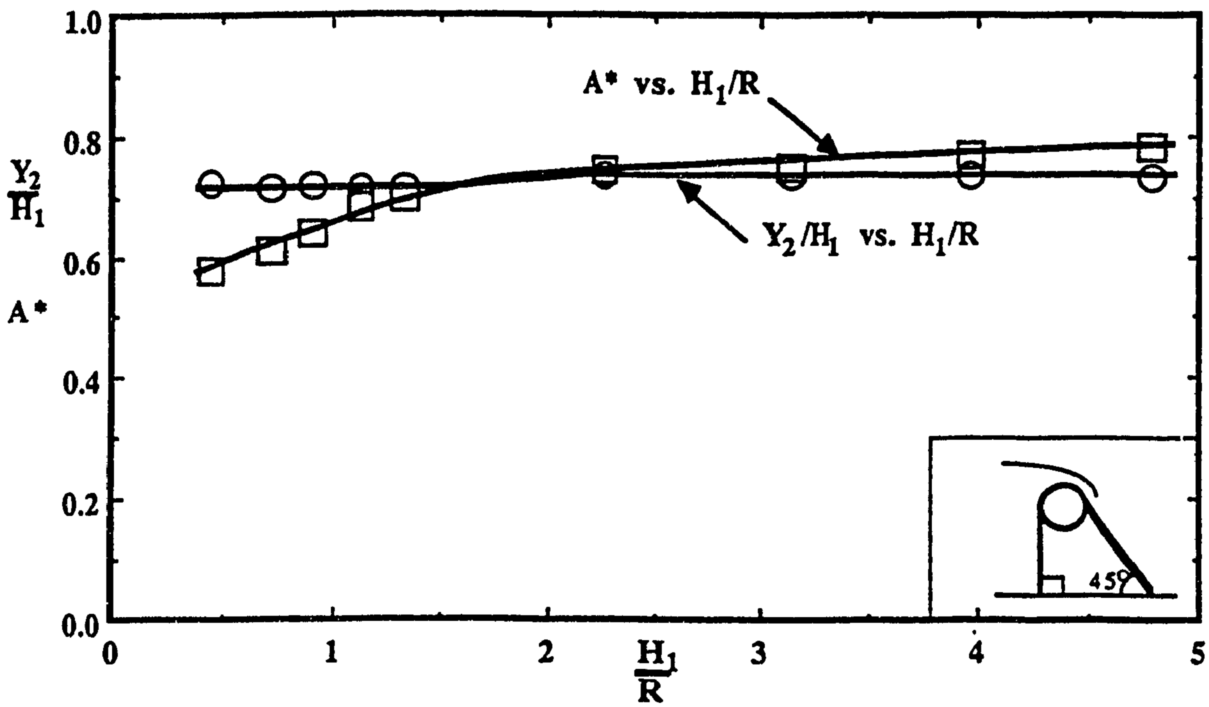

Fig.15a: Characteristics of Weirs with D/S Slope $\beta = 45°$ ($0.44 \le H_1/R \le 4.78$).

(a) Variation of Y_2/H_1 and A* with H_1/R- $\alpha = 90°$, $\beta = 45°$.

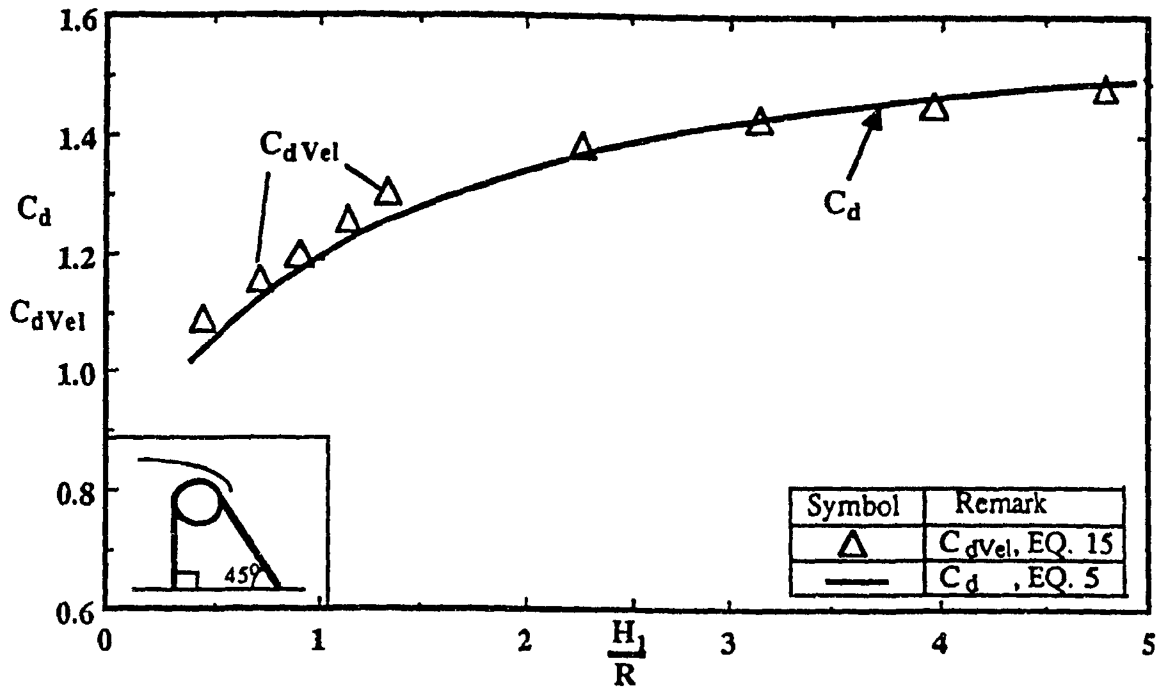

Fig.15b: Characteristics of Weirs with D/S Slope $\beta = 45°$ ($0.44 \le H_1/R \le 4.78$).

(b) Variation of C_d and C_{dVel} with H_1/R, ($\alpha = 90°$, $\beta = 45°$)

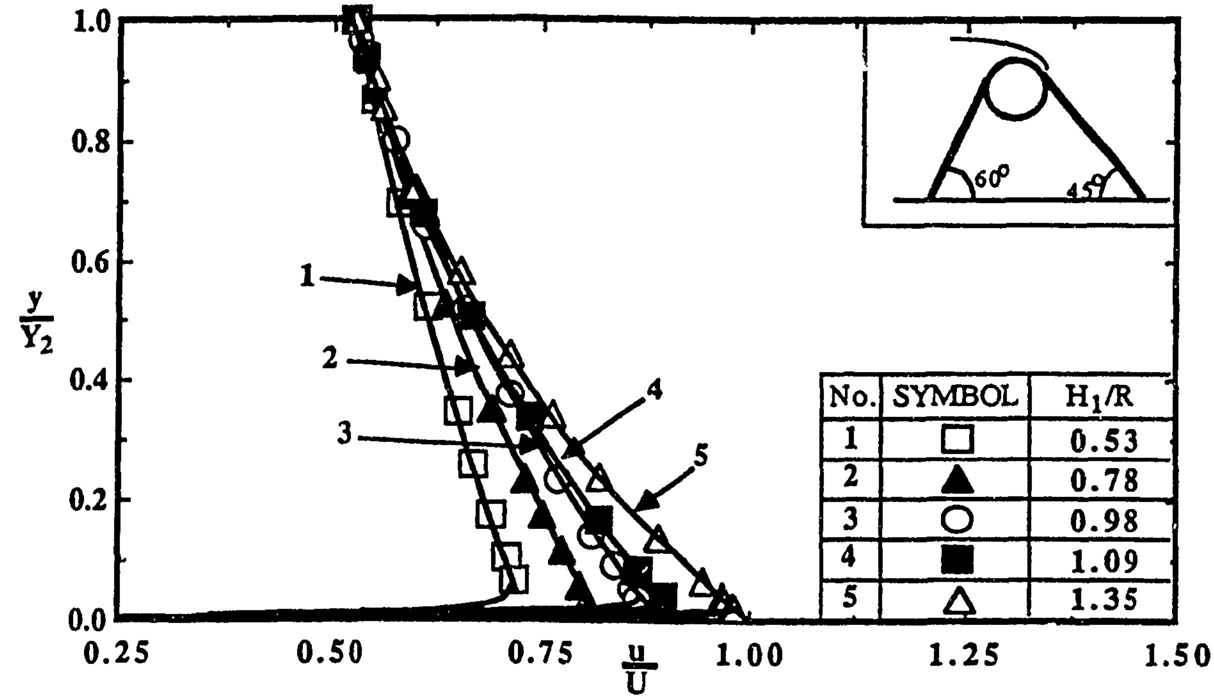

Fig.16a: Velocity Distribution for Circular-Crested Weir - ($\alpha = 60°$, $\beta = 45°$).

(a) $0.53 \le H_1/R \le 1.35$: y/Y_2 versus u/U.

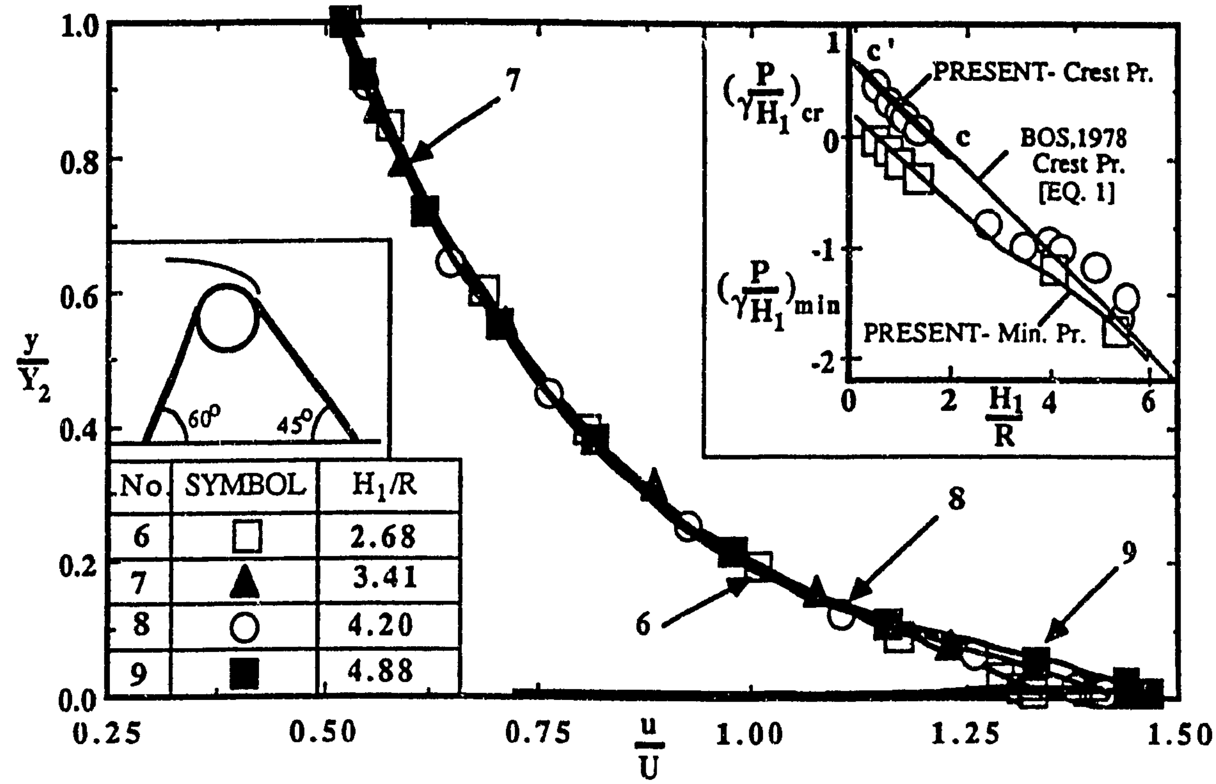

Fig.16b: Velocity Distribution for Circular-Crested Weir - ($\alpha = 60°$, $\beta = 45°$).

(b) $2.68 \le H_1/R \le 4.88$: y/Y_2 versus u/U.

Insert: Pressure Distribution at the Crest ($0.5 \le H_1/R \le 5.5$).

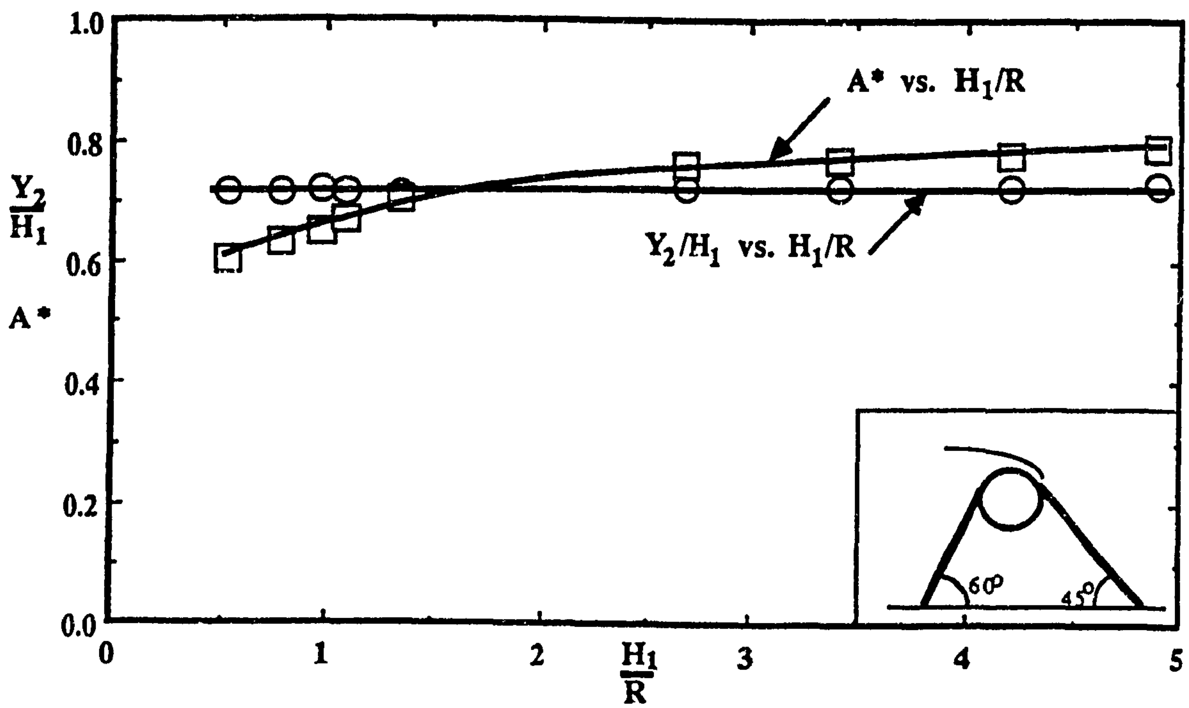

Fig.17a: Characteristics of Weirs with U/S and D/S Slopes ($0.53 \leq H_1/R \leq 4.88$).

(a) Variation of Y_2/H_1 and A* with $H_1/R, \alpha = 60°, \beta = 45°$.

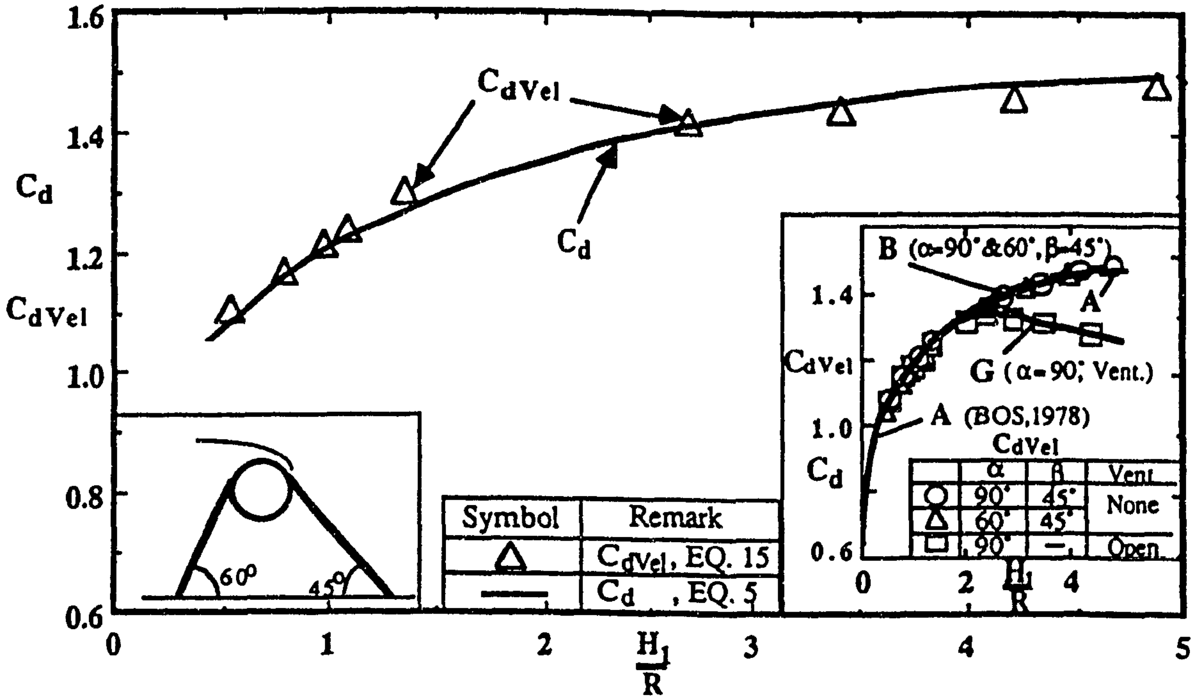

Fig.17b: Characteristics of Weirs with U/S and D/S Slopes ($0.53 \leq H_1/R \leq 4.88$).

(b) Variation of C_d and C_{dVel} with H_1/R, (α =60°, β =45°); Insert: C_{dVel} versus H_1/R for three types of weirs).

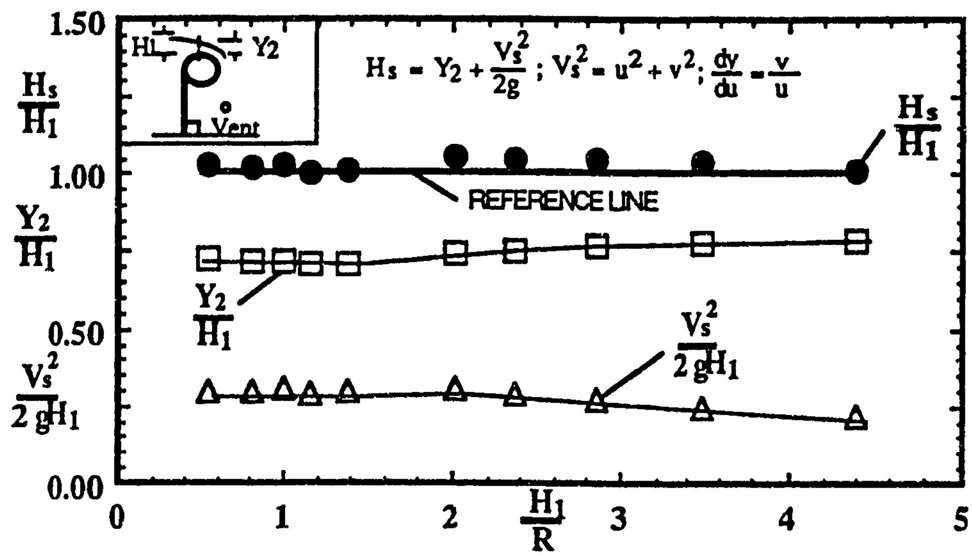

Fig.18a: Variation of Y_2/H_1, $V_s^2/2gH_1$ and H_s/H_1 with H_1/R.

(a) Weir with α =90°, no D/S Slope- Ventilated.

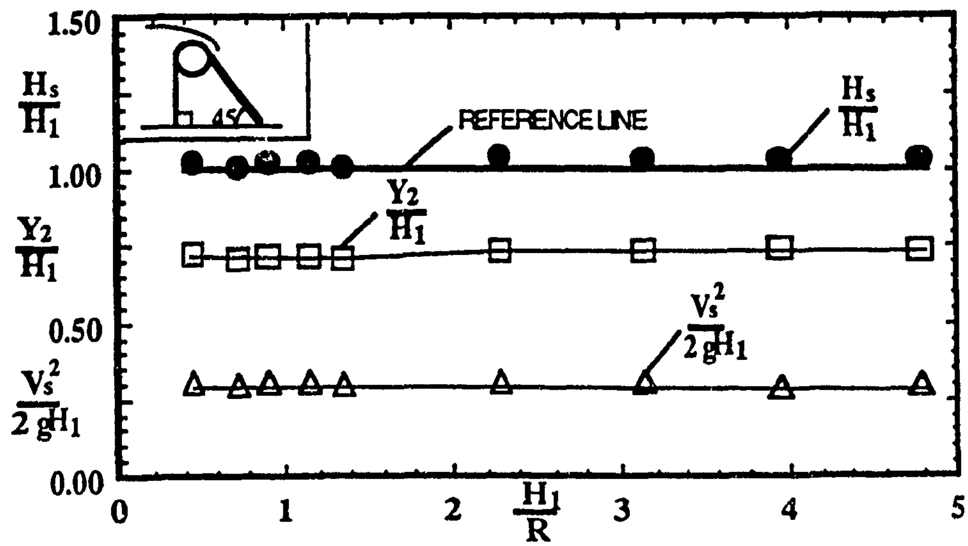

Fig.18b: Variation of Y_2/H_1, $V_s^2/2gH_1$ and H_s/H_1 with H_1/R.

(b) Weir with α =90°, β =45°.

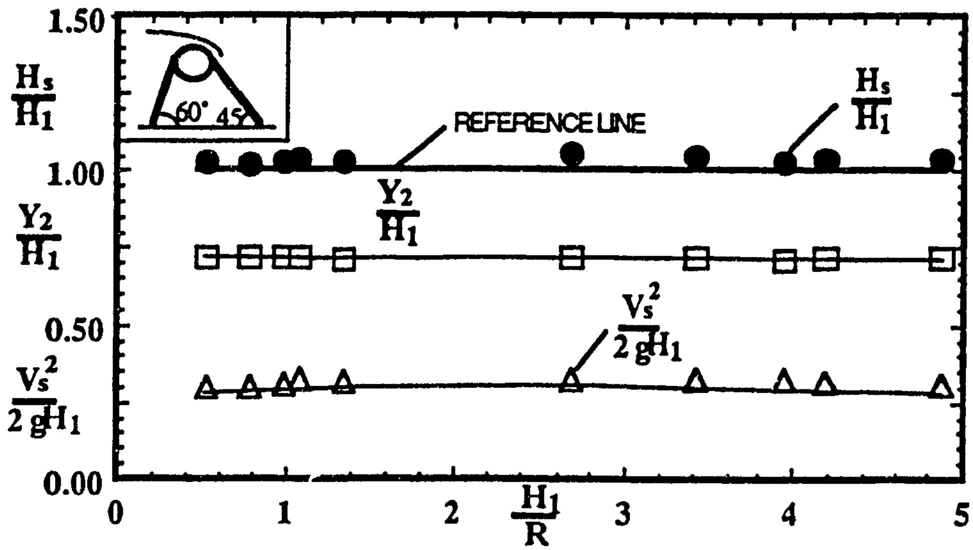

Fig.18c: Variation of Y_2/H_1, $V_s^2/2gH_1$ and H_s/H_1 with H_1/R.

(c) Weir with $\alpha = 60°$, $\beta = 45°$.

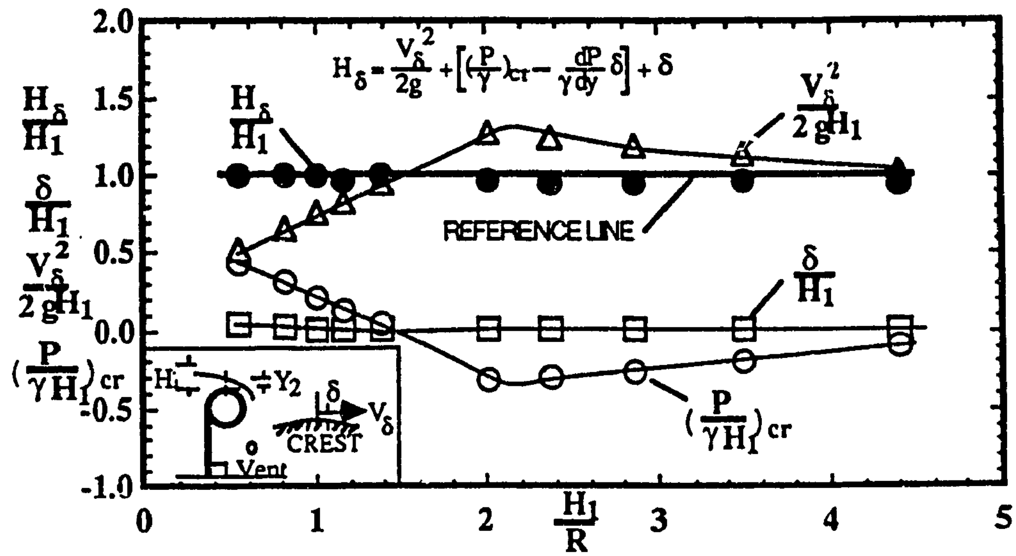

Fig.19a: Variation of δ/H_1, $V_\delta^2/2gH_1$, $(P/\gamma H_1)_{cr}$ and H_δ/H_1 with H_1/R.

(a) Weir with α =90°, no D/S Slope- Ventilated.

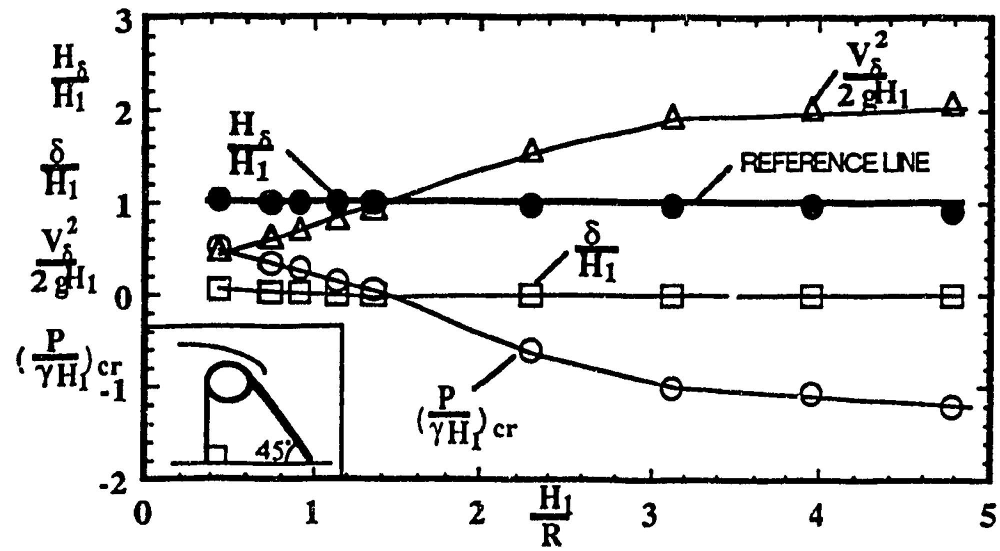

Fig.19b: Variation of δ/H_1, $V_\delta^2/2gH_1$, $(P/\gamma H_1)_{cr}$ and H_δ/H_1 with H_1/R.

(b) Weir with α =90°, β =45°.

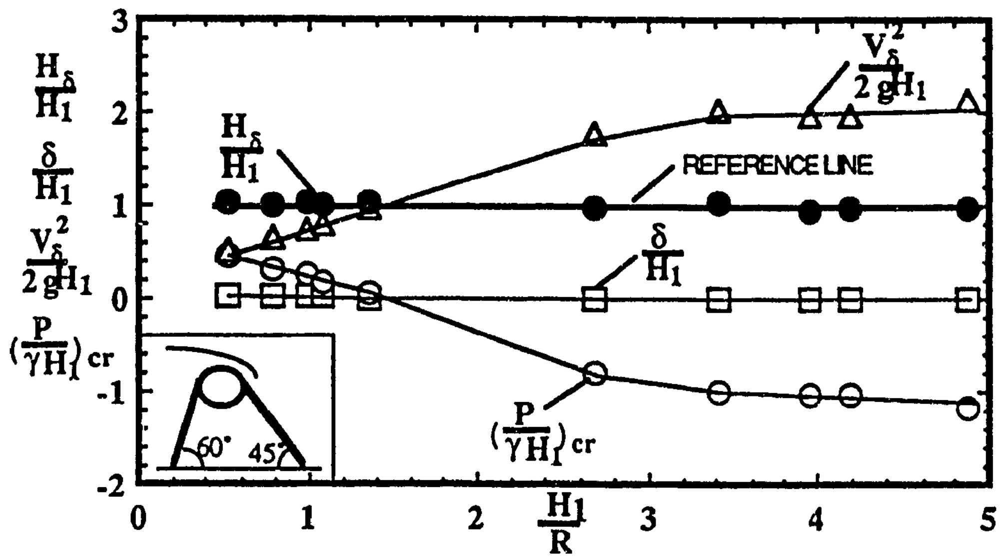

Fig.19c: Variation of δ/H_1, $V_\delta^2/2gH_1$, $(P/\gamma H_1)_{cr}$ and H_δ/H_1 with H_1/R.

(c) Weir with α =60°, β =45°.

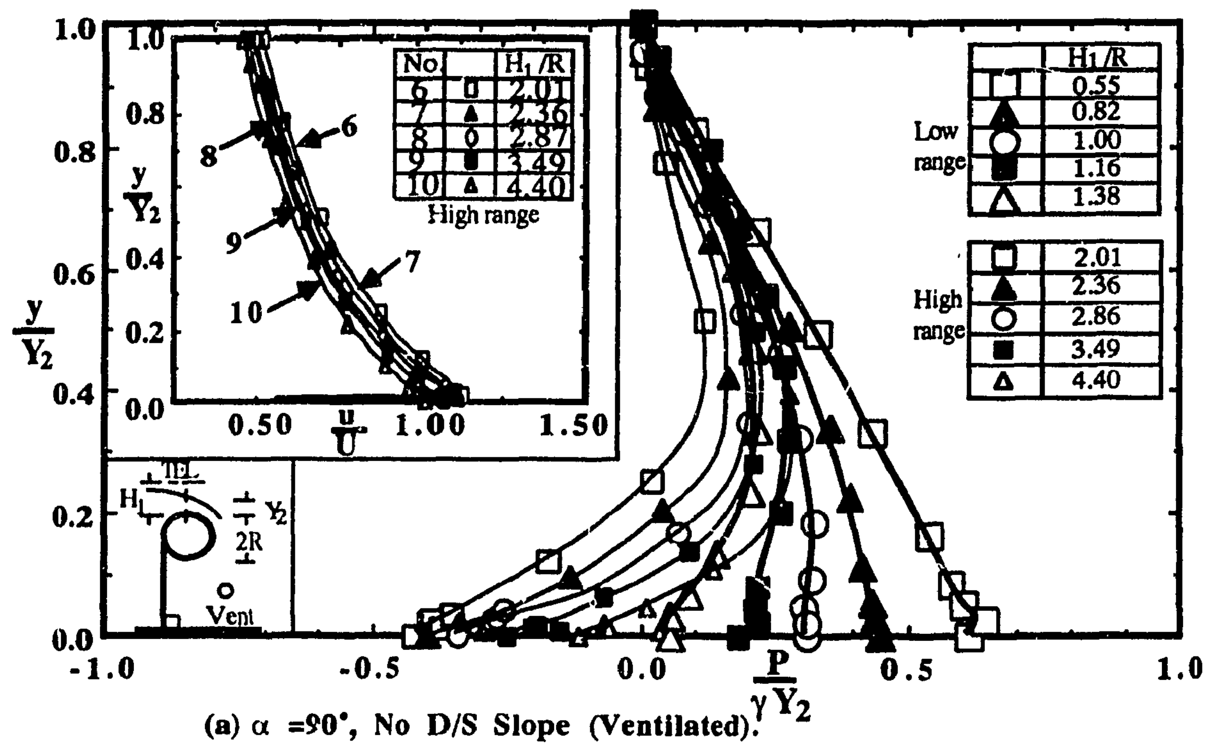

(a) α =90°, No D/S Slope (Ventilated).

Fig.20a: Static Pressure Distributions at the Crest Section-($0.44 \le H_1/R \le 4.88$).

Insert: Velocity Profiles at the Crest Section ($2.01 \le H_1/R \le 4.40$).

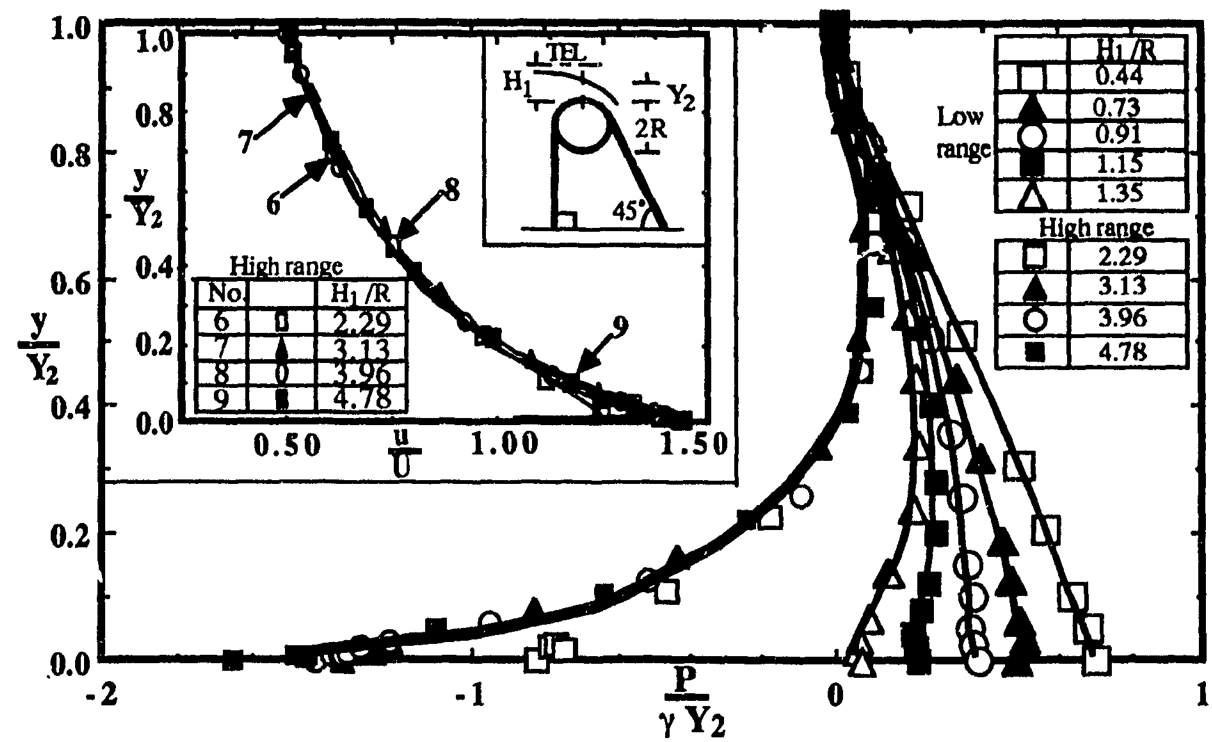

(b) α =90°, β =45°.

Fig.20b: Static Pressure Distributions at the Crest Section- (0.44≤H1 /R≤4.88).

Insert: Velocity Profiles at the Crest Section (2.29≤H_1/R≤4.78).

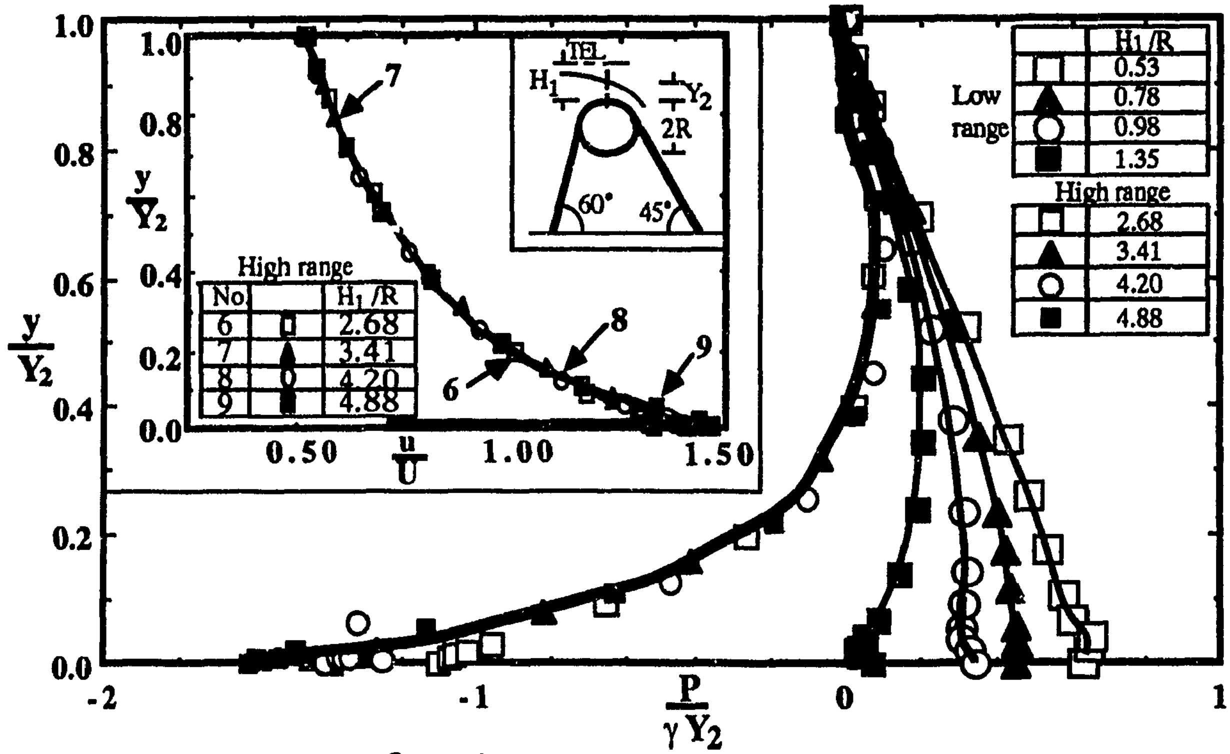

(c) α =60°, β =45°.

Fig.20c: Static Pressure Distributions at the Crest Section- ($0.44 \le H_1/R \le 4.88$).

Insert: Velocity Profiles at the Crest Section ($2.68 \le H_1/R \le 4.88$).

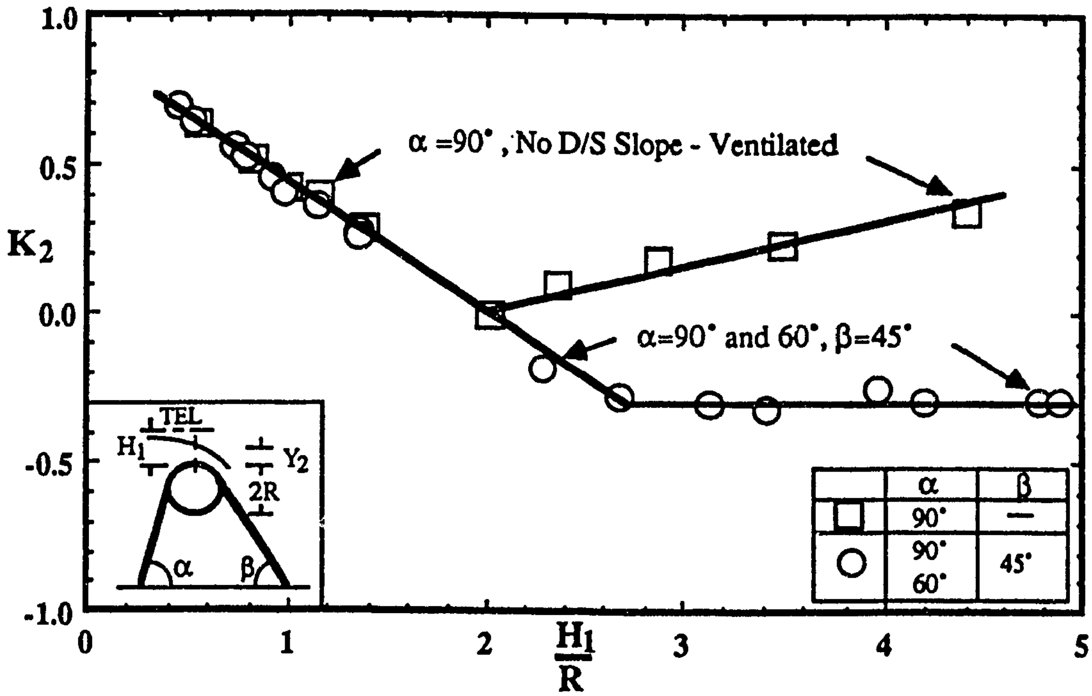

Fig.21: Variation of Pressure Coeffient K $_2$with H_1/R.
($0.44 \leq H_1/R \leq 4.88$).

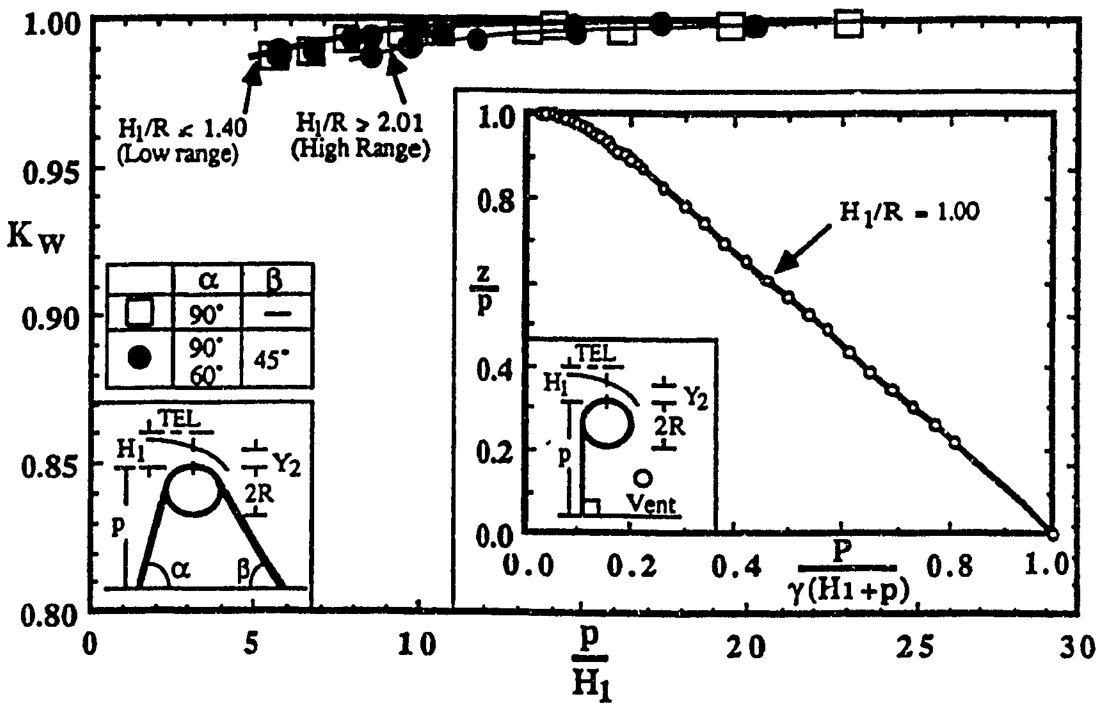

Fig.22: Variation of Pressure Coeffient K $_W$ with p/H_1.
(0.44≤H_1 /R≤4.88).

Insert: Typical Pressure Distribution on U/S Weir Face-
(α =90°, No D/S Slope- Ventilated).

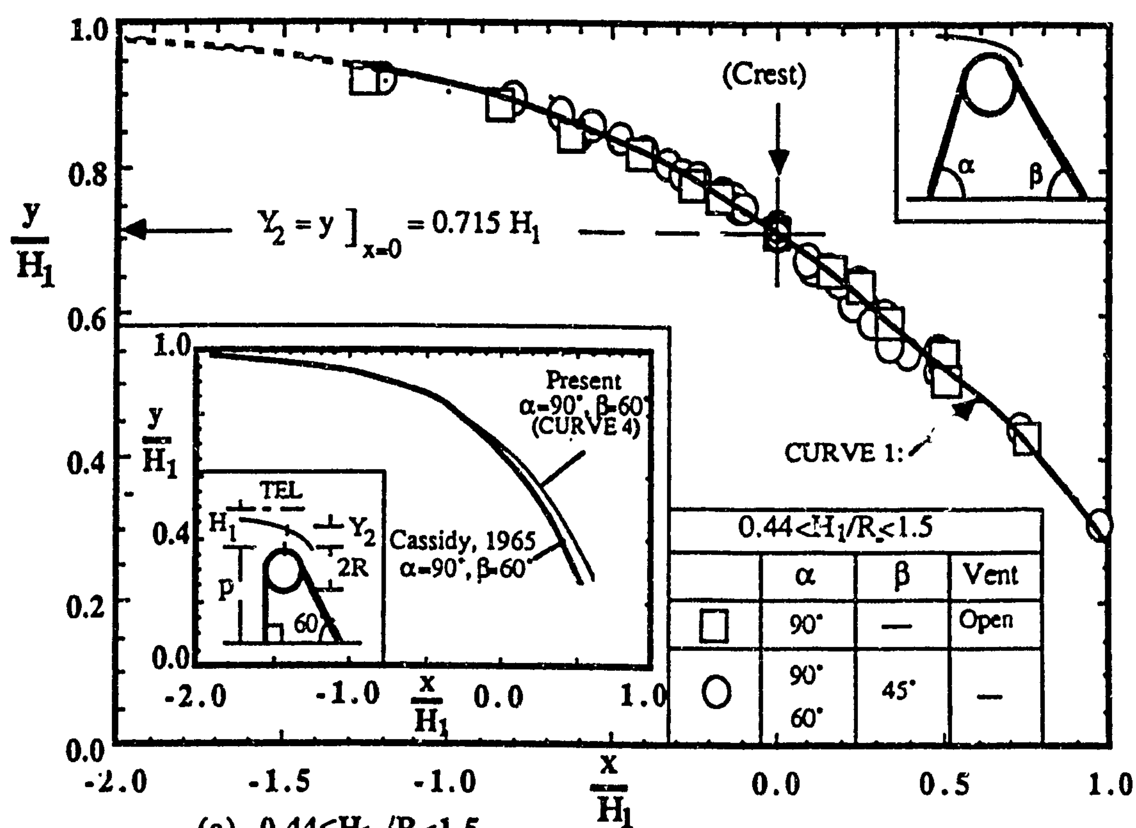

(a) $0.44 \le H_1/R < 1.5$.

Fig.23a: Water Surface Profiles over the Weir Crest.

Insert: Weire with $\alpha = 90°$, $\beta = 60°$ ($2.03 \le H_1/R \le 5.39$).

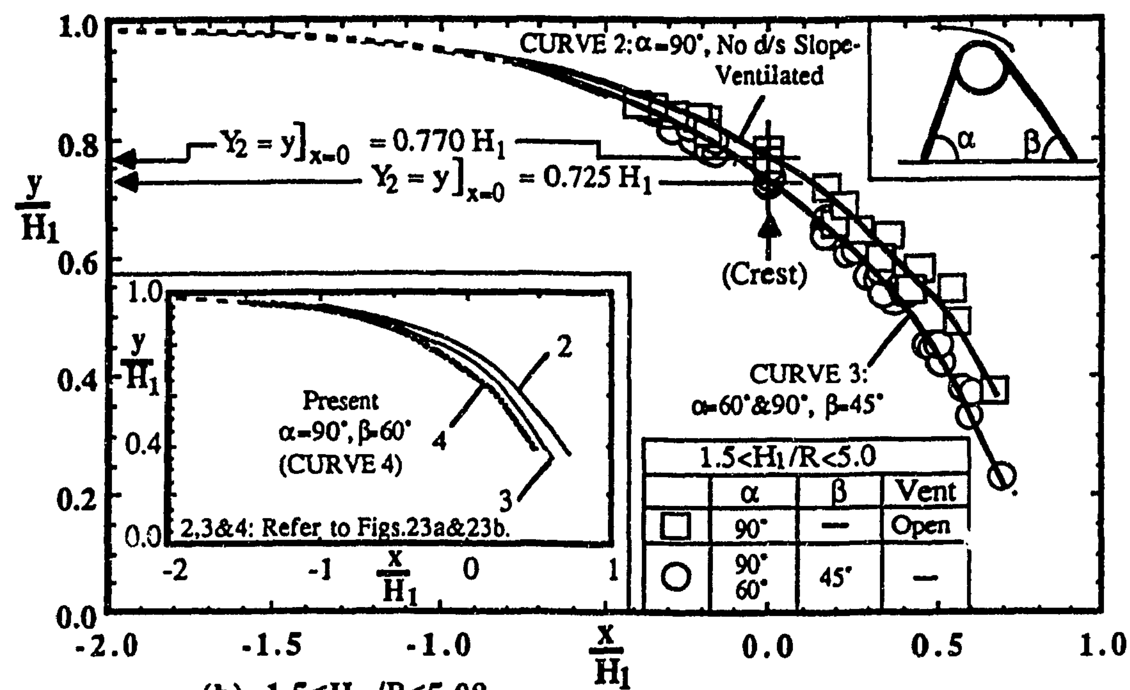

(b) $1.5 \leq H_1/R \leq 5.08$.

Fig.23b: Water Surface Profiles over the Weir Crest.

Insert: Weirs with α =90° & 60°, β =45° & 60° and α =90°, no D/S Slope, Ventilated ($0.44 \leq H_1/R \leq 5.08$).

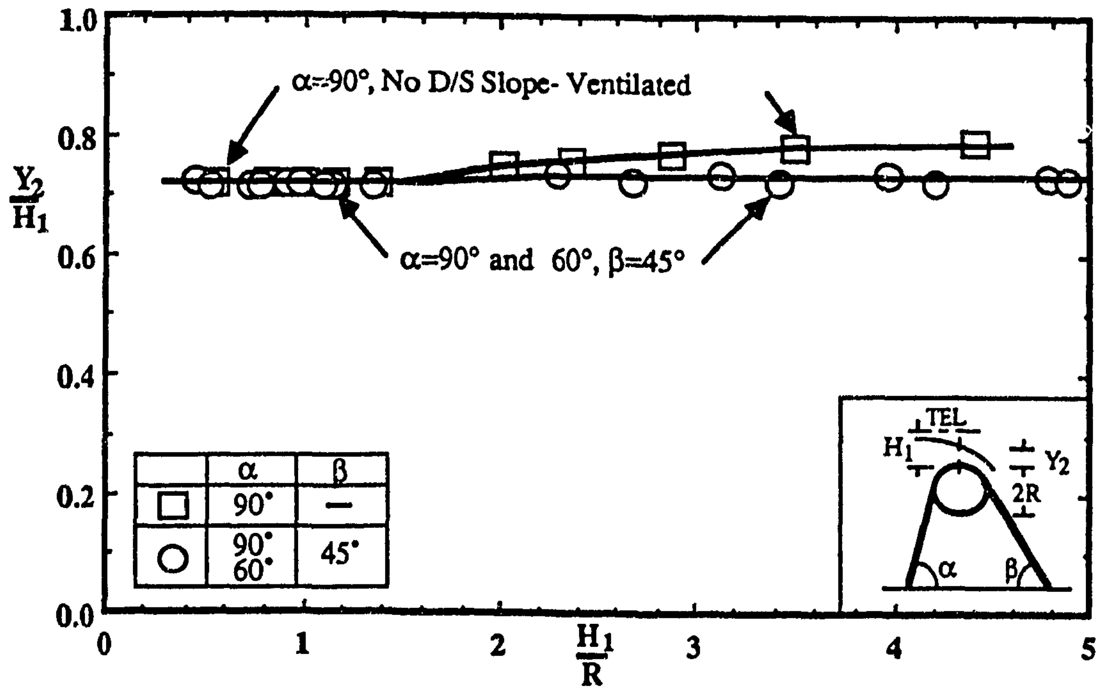

Fig.24: Crest Depth Y_2/H_1 versus H_1/R.

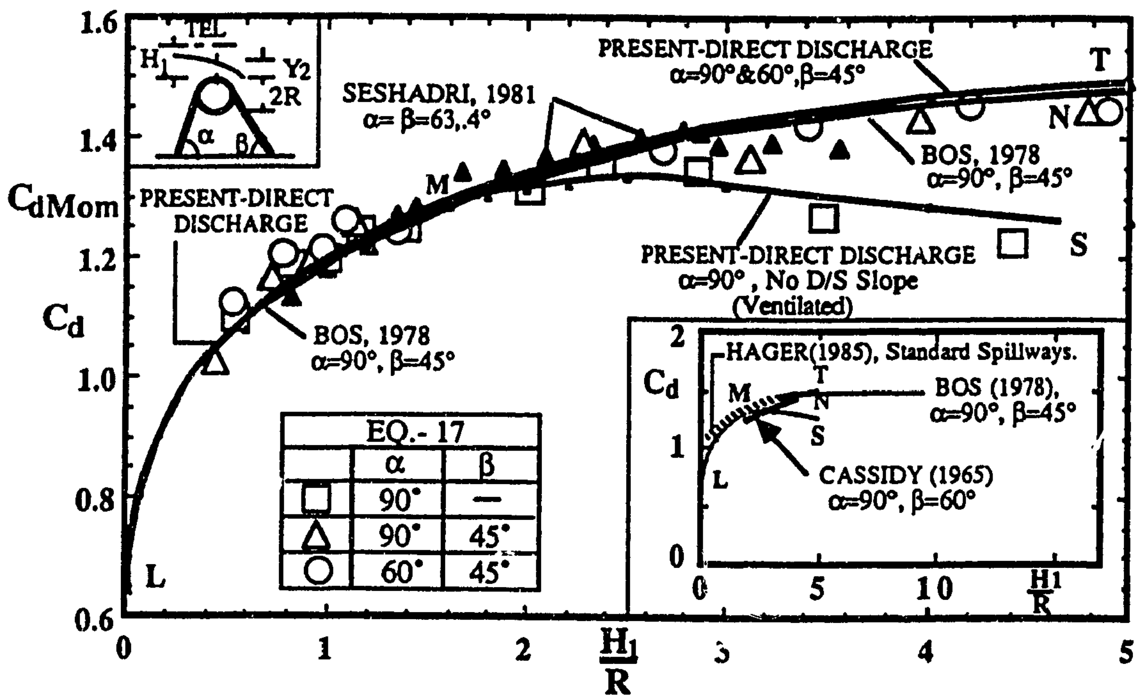

Fig.25: Weir Discharge Coefficient C_d and C_{dMom} versus H_1/R- ($0.44 \leq H_1/R \leq 4.88$).

Insert: C_d versus H_1/R for $0<H_1/R<10$).

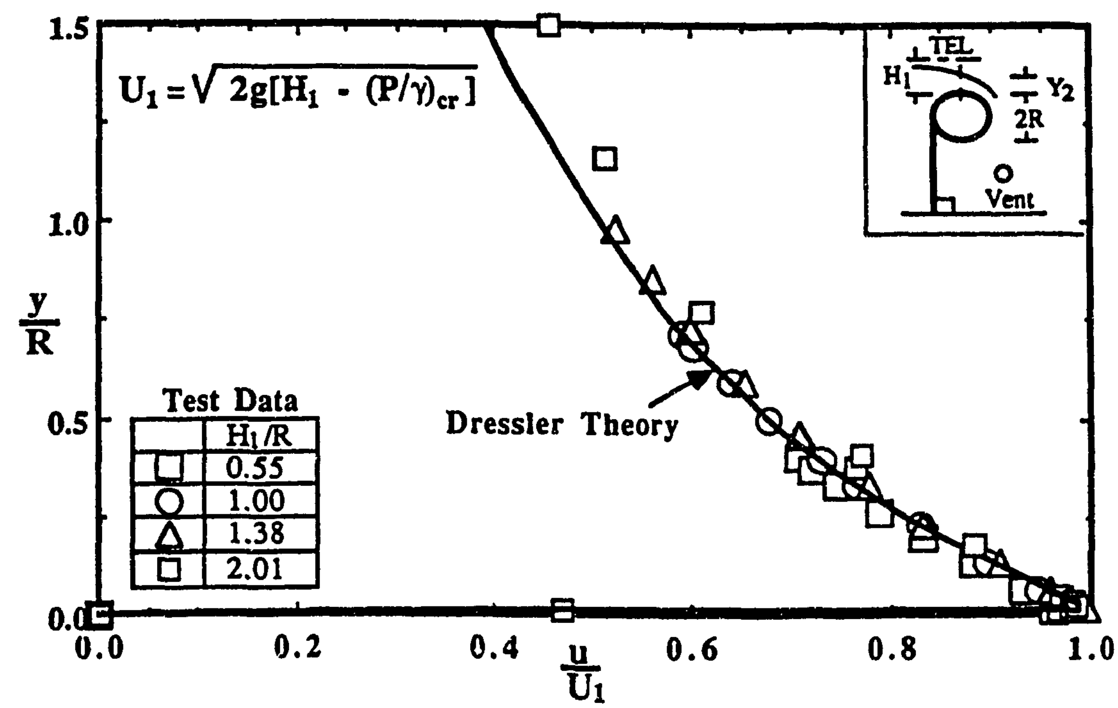

Fig.26a: Experimental Velocity Distribution at Crest Section- ($0.44 \leq H_1/R \leq 2.68$).

(a) Variation of y/R with u/U_1 -(α =90°, No D/S Slope- Ventilated).

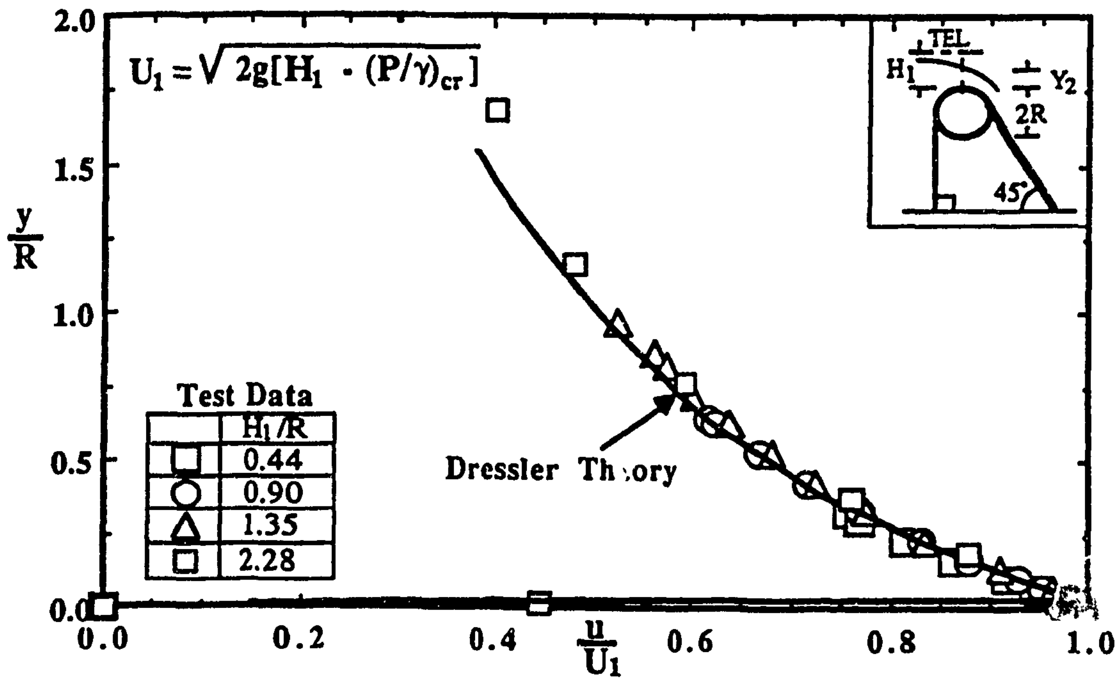

Fig.26b: Experimental Velocity Distribution at Crest Section-($0.44 \le H_1/R \le 2.68$).

(b) Variation of y/R with u/U_1-($\alpha = 90°, \beta = 45°$).

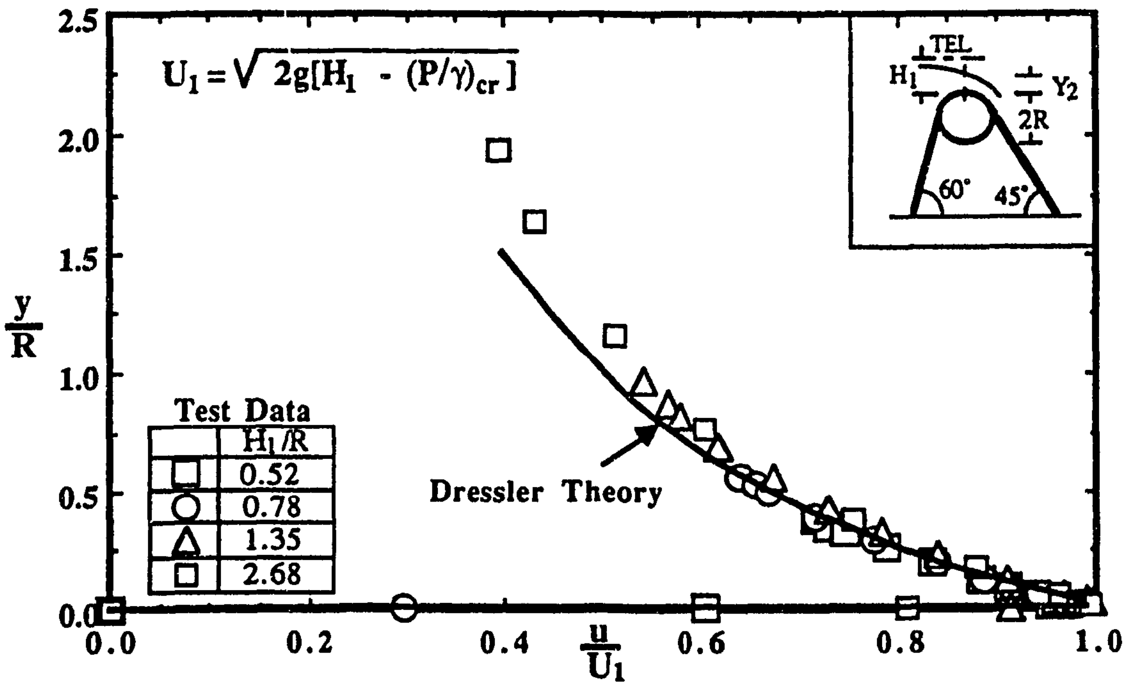

Fig.26c: Experimental Velocity Distribution at Crest Section- ($0.44 \leq H_1/R \leq 2.68$).

(c) Variation of y/R with u/U_1-(α =60°, β =45°).

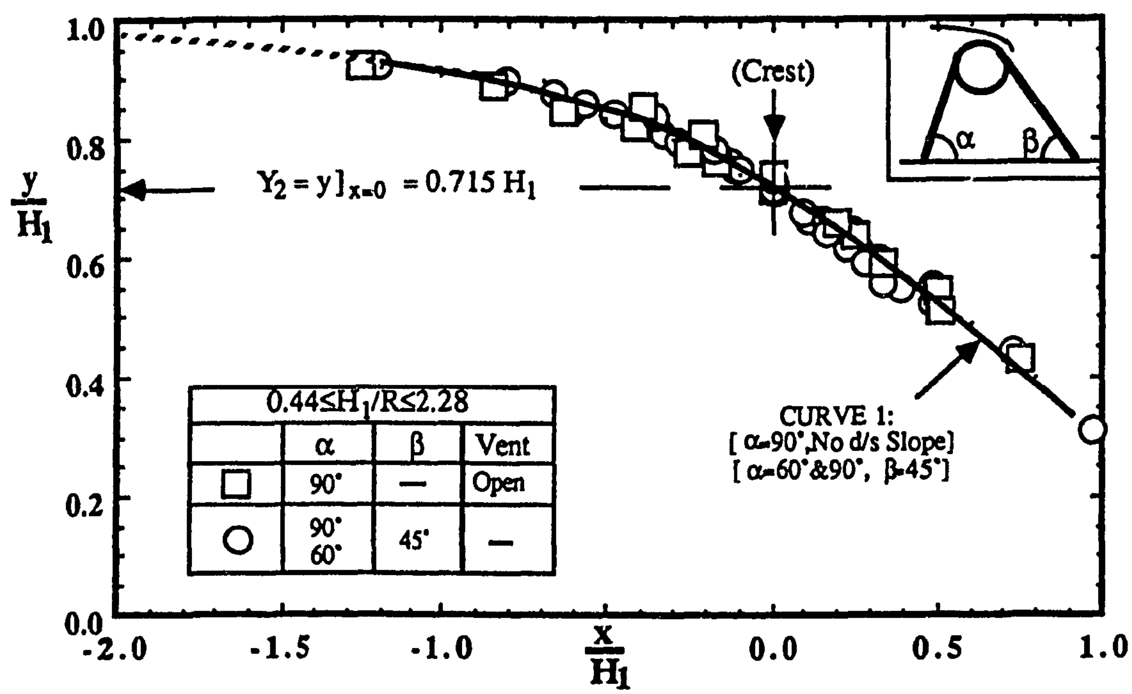

Fig.27: Water Surface Profiles over the Weir Crest
($0.44 \leq H_1/R \leq 2.28$).

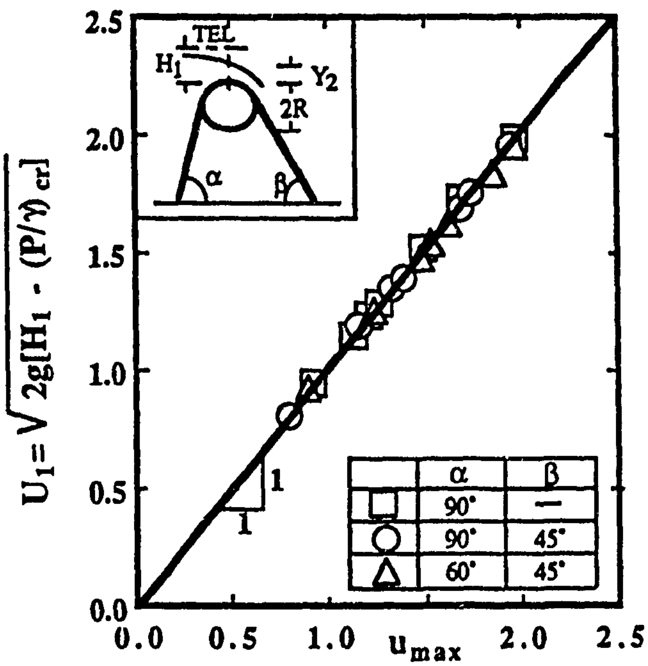

Fig.28: Predicted and Measured Values of Maximum Velocity.

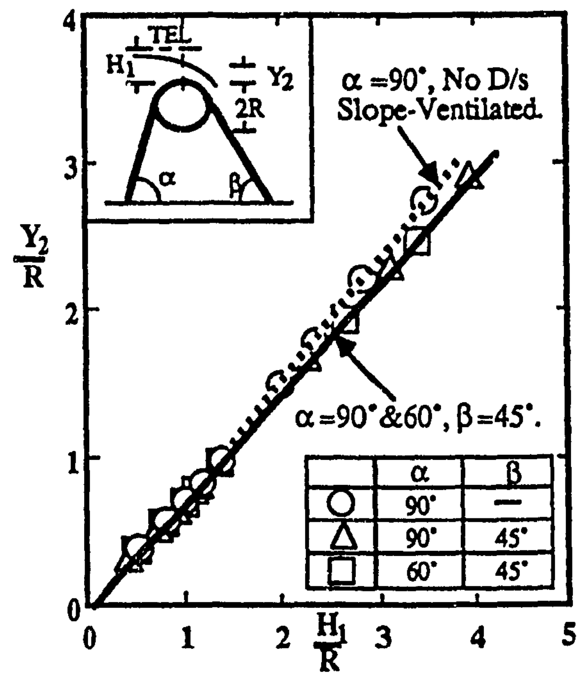

Fig.29: Variation of Y_2/R with H_1/R-
($0.44 \leq H_1/R \leq 4.00$).

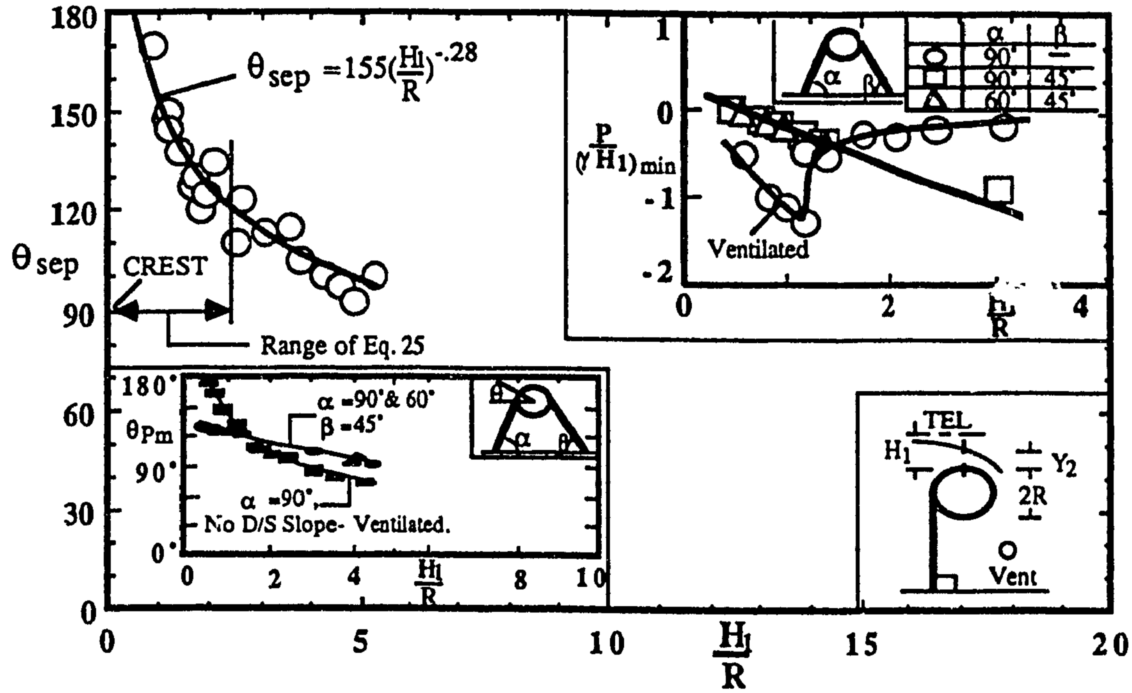

Fig.30: Point of Separation on Crest Surface (Visual Observation)- (α =90°, No D/S Slope- Ventilated).

Upper Insert: Variation of Minimum Pressures with H_1/R (All Weirs).
Lower Insert: Points of Minimum and Atmospheric Pressures over Crest Surface (All Weirs).

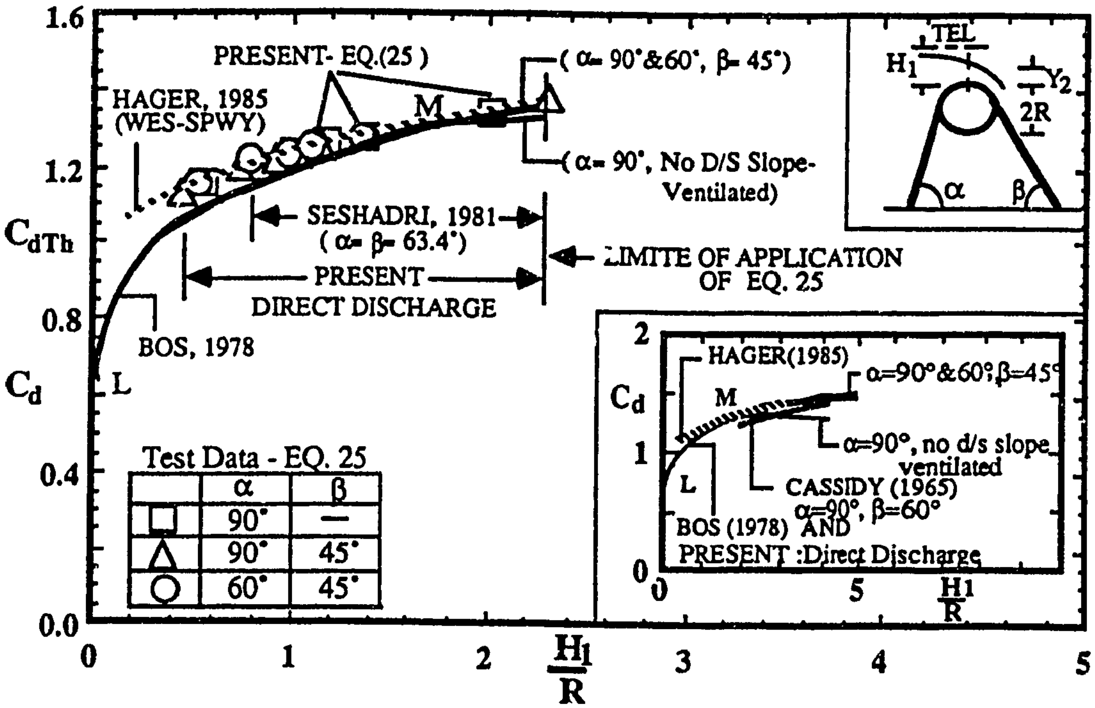

Fig.31: Variation of C_{dTh} with H_1/R - $(0.44 \leq H_1/R \leq 2.28)$.

Insert: C_d for Circular-Crested Weirs and C_d of WES-Standard Spillways.

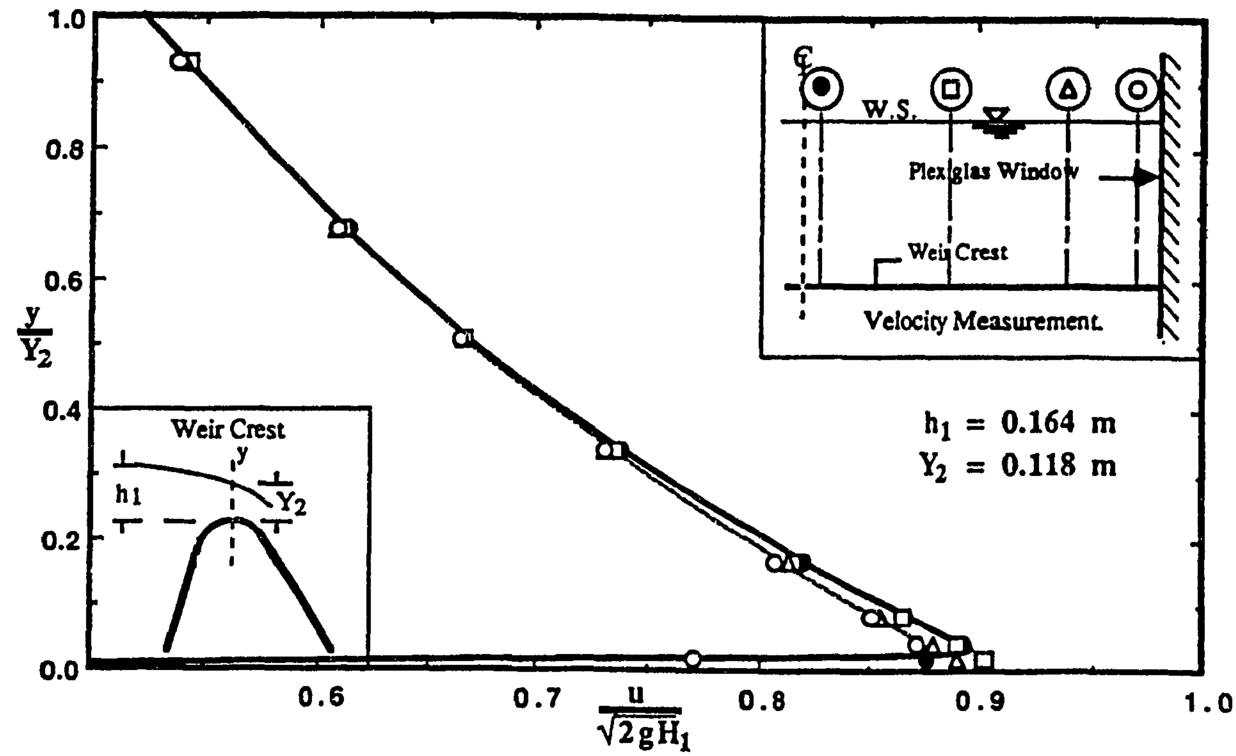

Fig.32: Velocity Profiles at Weir Crest - Cross Distribution.

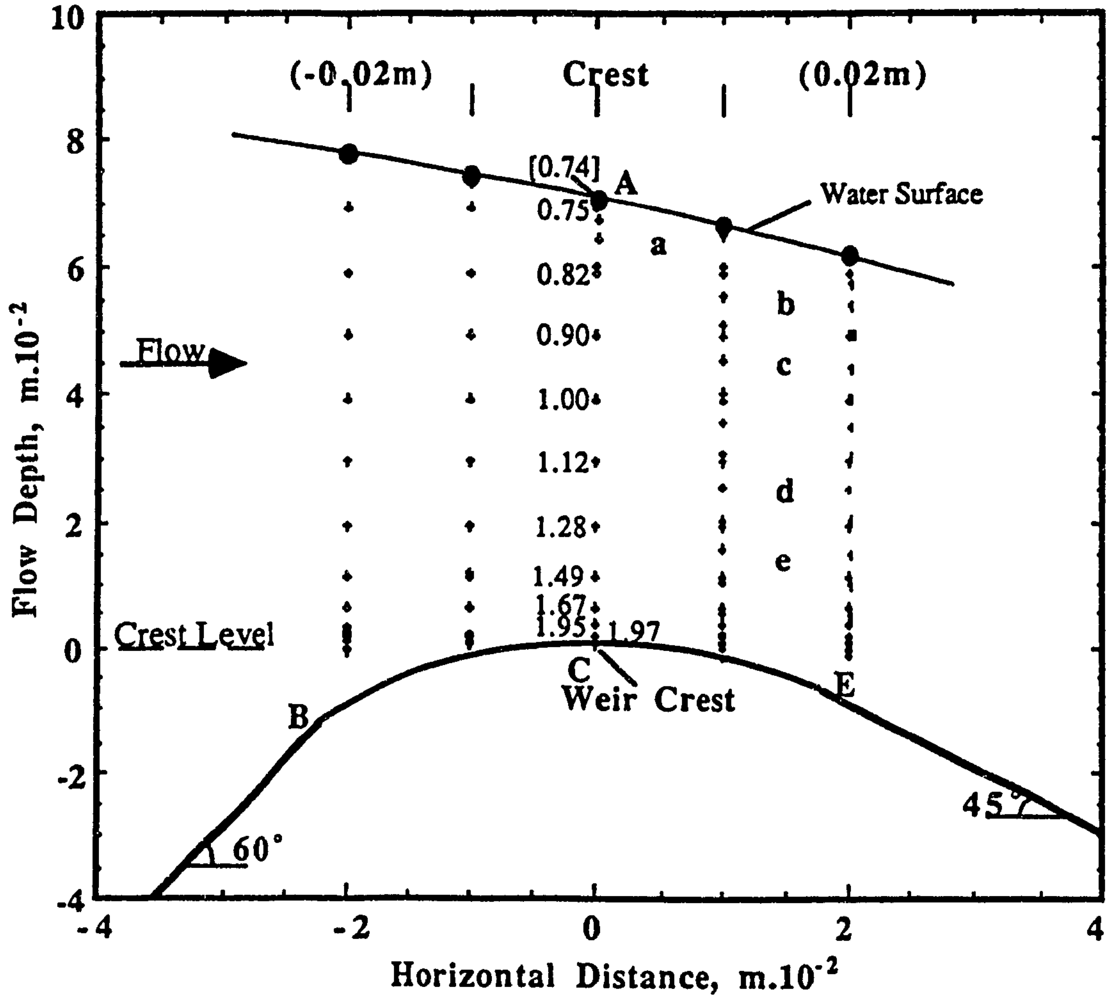

Fig.33: Velocity Measurement along Weir-Crest Center Line.
● – (x,y) locations for free surface profile measurement.
+ – (x,y) locations for velocity measurement (see Table 20f).
The values of u are shown only for the section above C.

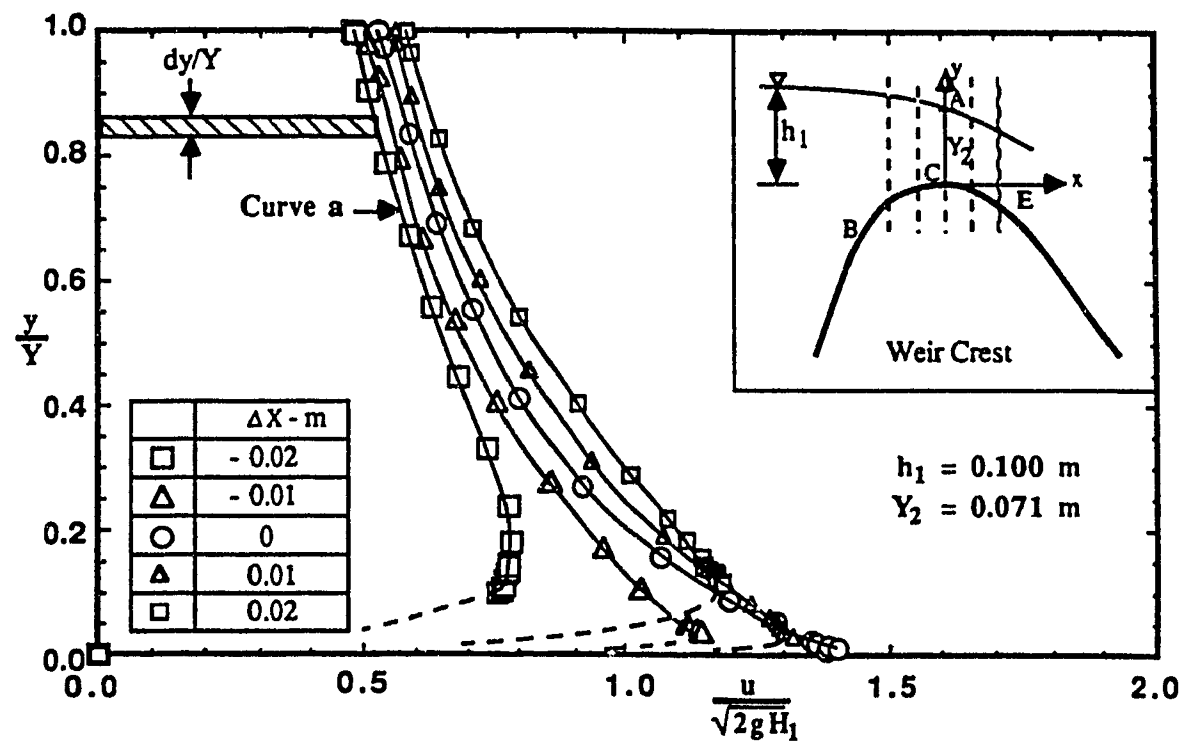

Fig.34: Experimental Velocity Profiles.

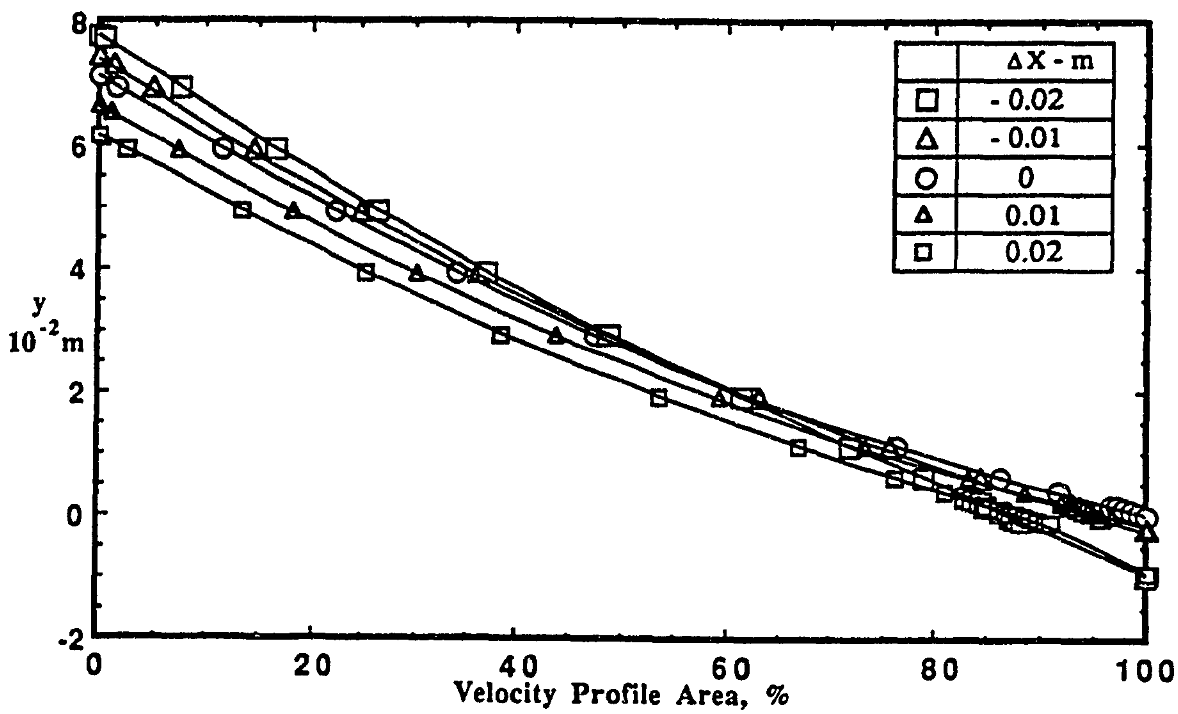

Fig.35: Distribution of Velocity Profile Area across Flow Depths.

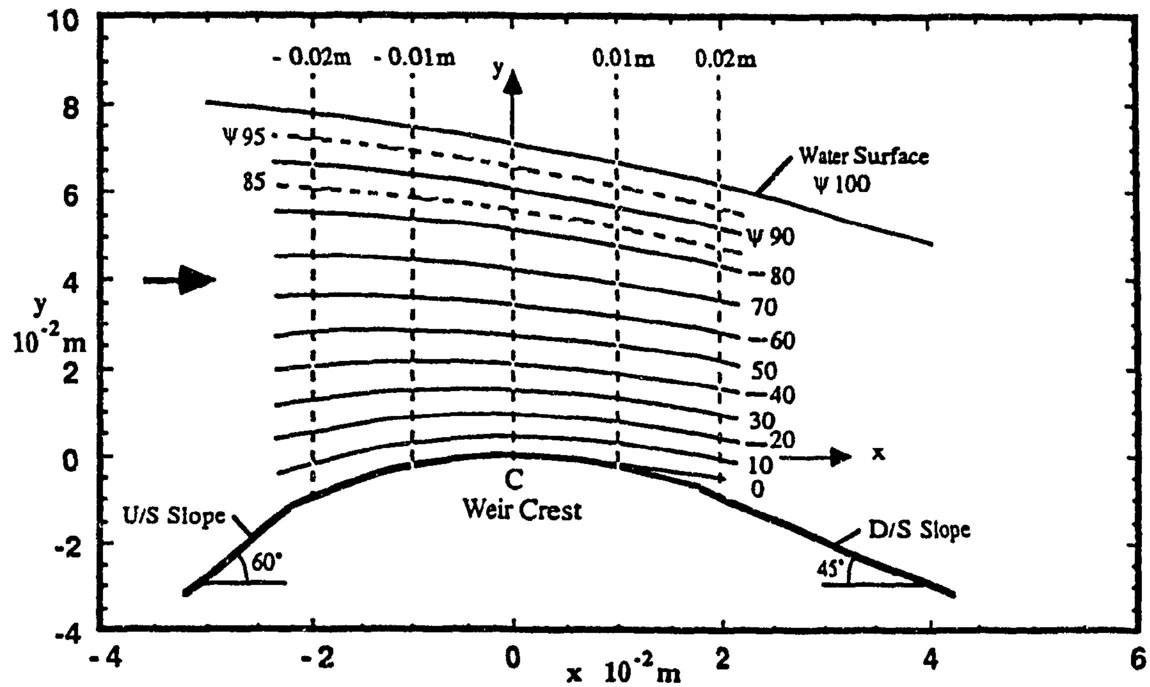

Fig.36: Water Surface and Streamline Pattern.

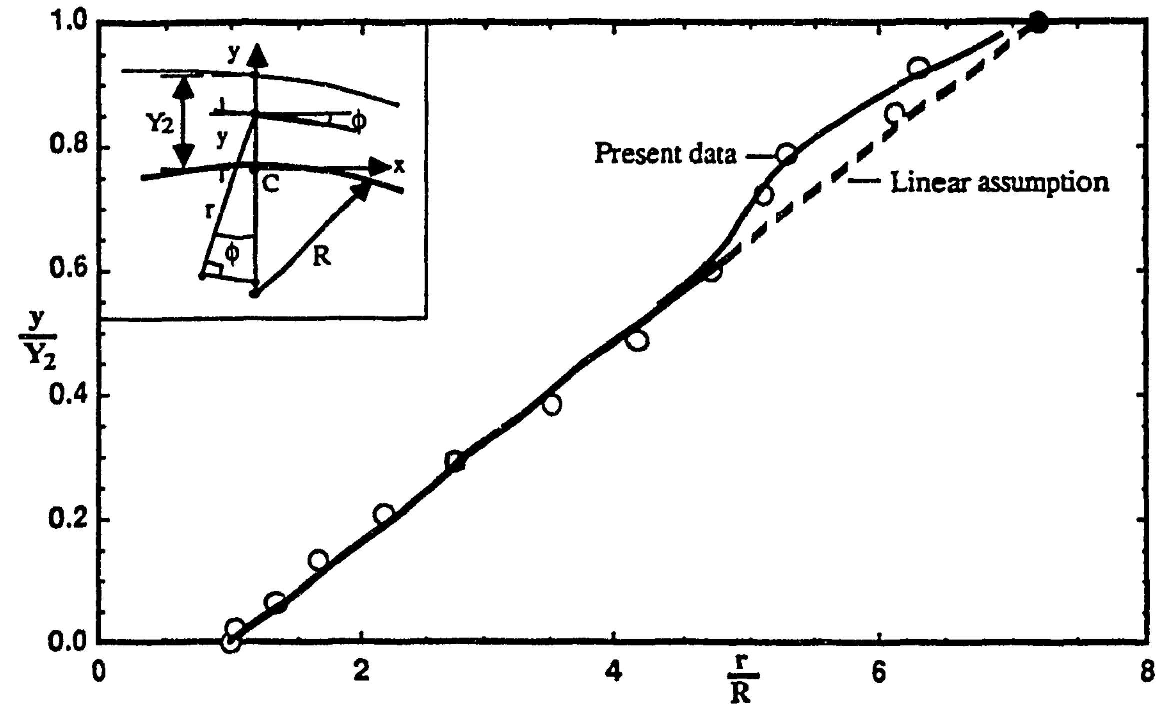

Fig.37: Variation of Streamline Radius r across Crest Depth Y_2.

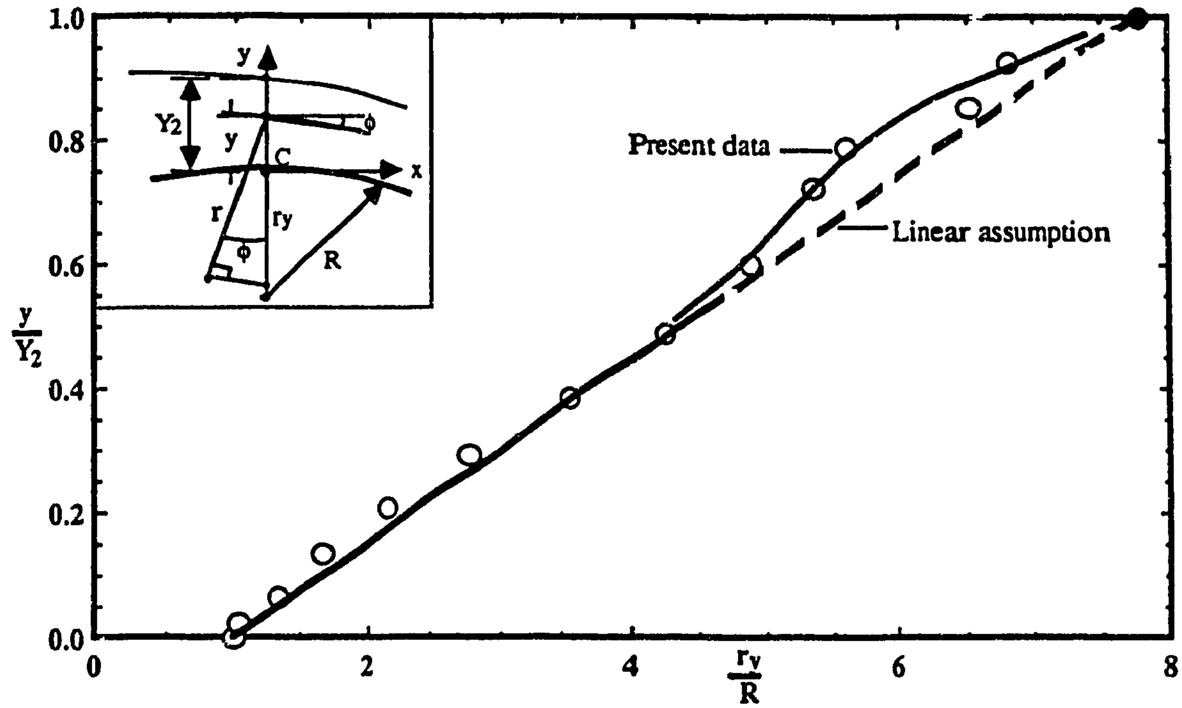

Fig.38: Variation of Streamline Radius Parameter r_y across Crest Depth Y_2.

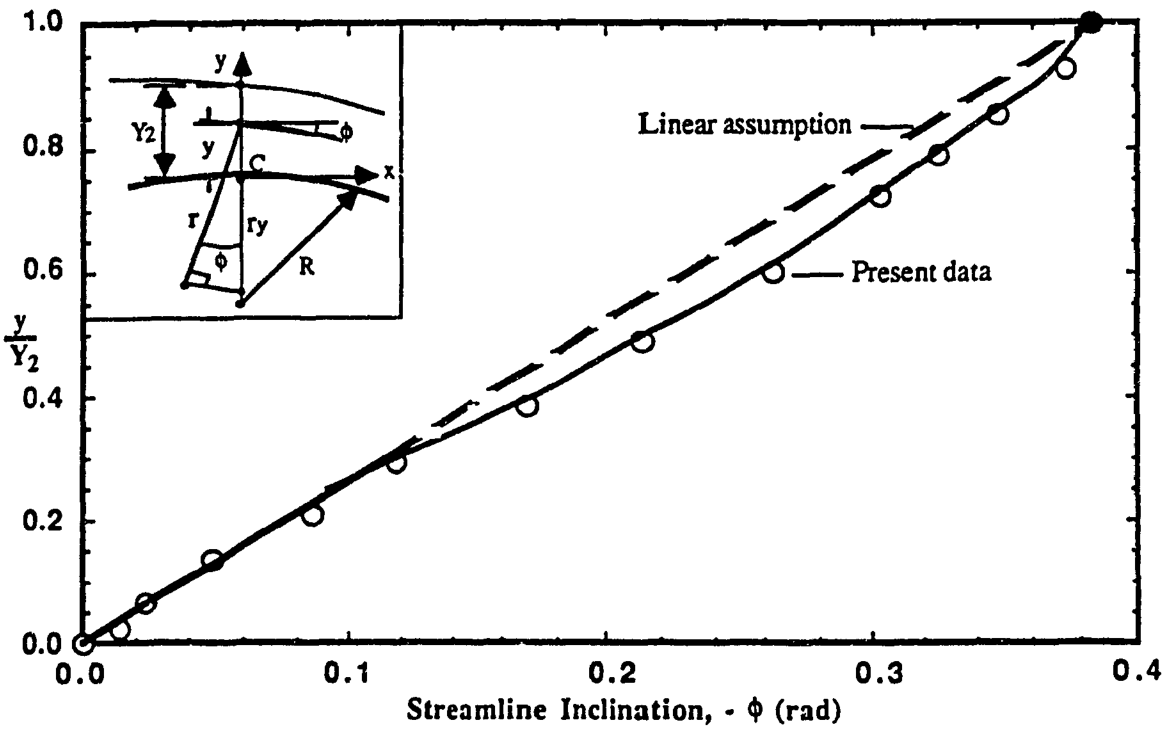

Fig.39: Variation of Streamline Inclination across Crest Depth Y_2.

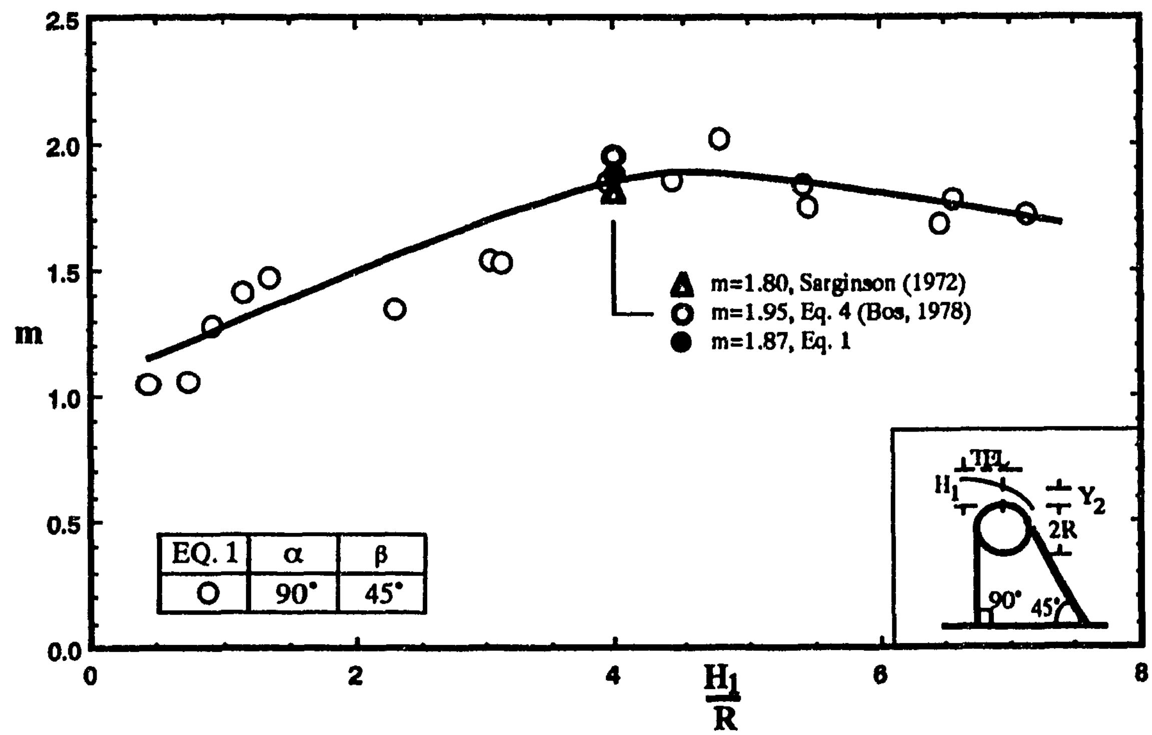

Fig.40: Variation of m with H_1/R for circular-crested weirs.

APPENDIX III

TABLES

Note: Some additional notations used in the tables are defined near the tabulations.

Table 1: -Range of test variables.

Overall ranges: $0.5 \leq \frac{H_1}{R} \leq 18.5$

to

$0.24 \leq Re \times 10^{-5} \leq 6.9$

$\left(Re = \frac{UD}{\nu},\ U = \sqrt{2gH_1}\right)$

Weir #	Radius (cm)	p (cm)	H_1/R	$Re \times 10^{-5}$
1	15.16	116.44	.50 - 1.4	3.9 - 6.9
2	10.08	116.92	.70 - 1.8	2.4 - 4.1
3	7.54	101.68	1.2 - 2.5	1.9 - 2.9
4	3.81	105.49	2.1 - 4.9	1.0 - 1.2
5	2.54	104.18	2.0 - 6.6	0.5 - 1.0
6	0.952	105.49	6.7 - 18.5	0.24 - 0.4
S.W.*	*	(114.30 (114.91	$0.05 < h_1/p < 0.20$	-

*Sharp-crested weirs. Actual edge thickness e=1.5mm.

Table 2a: -Experimental data: Discharge coefficient from direct discharge measurement:

(a) Weir models with R=15.16cm.

			P=3.82' 116.43cm, R=0.4974',15.16cm						
RUN#	Q cfs	Q (l)	h1 ft	H1 ft	H1/R	P/H1	Cd 1	Y2 ft	Y2/H1
9000FA									
407	0.392	11.10	0.272	0.272	0.54	14.04	1.07	0.196	0.719
408	0.766	21.69	0.405	0.406	0.81	9.40	1.15	0.292	0.719
409	1.062	30.07	0.496	0.497	0.99	7.68	1.17	0.357	0.718
410	1.365	38.65	0.576	0.578	1.16	6.60	1.19	0.415	0.718
411	1.825	51.67	0.683	0.687	1.38	5.56	1.24	0.493	0.718
9045									
413	0.279	7.90	0.221	0.221	0.44	17.28	1.04	0.158	0.715
414	0.629	17.81	0.361	0.362	0.72	10.55	1.12	0.259	0.715
415	0.905	25.62	0.449	0.450	0.90	8.48	1.16	0.324	0.720
416	1.334	37.77	0.568	0.570	1.14	6.70	1.20	0.408	0.716
417	1.776	50.29	0.670	0.673	1.35	5.67	1.24	0.481	0.715
6045									
419	0.371	10.50	0.261	0.261	0.52	14.63	1.08	0.187	0.717
420	0.718	20.33	0.388	0.389	0.78	9.82	1.15	0.279	0.717
421	1.038	29.39	0.485	0.486	0.97	7.86	1.18	0.349	0.718
422	1.784	50.51	0.669	0.673	1.35	5.67	1.25	0.480	0.713
423	1.231	34.85	0.538	0.540	1.08	7.07	1.20	0.387	0.717

Note: h1=h_1, H1=H_1, H1/R=H_1/R, P/H1=p/H_1, Cd 1=C_d (based on direct discharge measurement), Y2=Y_2 and Y2/H1=Y_2/H_1. 9000FA, 9045, 6045, - - -: Tests Nos. Q (l)= Q in liters.

Table 2b&c: -Experimental data: Discharge coefficient from direct discharge measurement:

(b) Weir models with R=10.08cm.

			P=3.836', 116.92cm, R=0.331', 10.08cm					
Run #	Q cfs	Q (l)	h1 ft	H1 ft	H1/R	Cd 1	Y2,(0)	Y2/H1
9000FA								
002	0.325	9.20	0.233	0.233	0.70	1.12	0.169	0.725
003	0.781	22.11	0.393	0.393	1.18	1.22	0.276	0.702
004	1.321	37.40	0.541	0.543	1.64	1.28	0.394	0.726
007	0.476	13.47	0.292	0.292	0.88	1.17	0.207	0.709
008	1.580	44.74	0.604	0.607	1.83	1.29	0.441	0.727

(c) Weir models with R=7.54cm.

			P=3.336', 101.68cm, R=0.2474', 7.54cm					
Run #	Q cfs	Q (l)	h1 ft	H1 ft	H1/R	Cd 1	Y2,(0)	Y2/H1
9000FA								
015	0.490	13.87	0.290	0.291	1.17	1.21	0.207	0.711
016	0.919	26.02	0.423	0.425	1.71	1.29	0.311	0.732
017	1.636	46.32	0.607	0.611	2.46	1.33	0.463	0.758
023b	1.132	32.05	0.479	0.481	1.94	1.31	0.356	0.740

Note: See notations of Table 2a.

Table 2d: -Experimental data: Discharge coefficient from direct discharge measurement:

(d) Weir models with R=3.81cm.

			P=3.461', 105.49cm, R=0.125', 3.81cm					
Run #	Q cfs	Q (l)	h1 ft	H1 ft	H1/R	Cd 1	Y2,(0)	Y2/H1
9000FA								
044a	0.622	17.61	0.322	0.322	2.57	1.32	0.244	0.758
045a	1.086	30.75	0.471	0.473	3.78	1.29	0.368	0.778
046a	1.422	40.26	0.571	0.574	4.58	1.27	0.451	0.786
048a	1.534	43.43	0.604	0.607	4.85	1.26	0.478	0.787
059	0.449	12.71	0.261	0.261	2.08	1.30	0.193	0.739
060	0.811	22.96	0.384	0.385	3.07	1.31	0.295	0.766
061	1.267	35.87	0.528	0.530	4.24	1.27	0.412	0.777
9000NA								
063	0.458	12.96	0.262	0.263	2.10	1.32	0.196	0.745
064	0.803	22.73	0.379	0.380	3.03	1.33	0.292	0.768
065	1.095	31.00	0.466	0.468	3.74	1.33	0.360	0.769
066	1.404	39.75	0.551	0.554	4.43	1.32	0.428	0.773
067	1.622	45.93	0.607	0.611	4.88	1.32	0.463	0.758
9060								
072	0.603	17.07	0.305	0.306	2.44	1.38	0.223	0.729
073	0.881	24.94	0.385	0.387	3.09	1.42	0.281	0.726
074	1.277	36.16	0.482	0.485	3.87	1.47	0.347	0.715
075	1.553	43.97	0.543	0.546	4.37	1.49	0.389	0.712
076	1.736	49.15	0.581	0.585	4.67	1.50	0.417	0.713
080	0.504	14.27	0.275	0.275	2.20	1.35	0.196	0.713
081	0.913	25.85	0.394	0.395	3.16	1.43	0.285	0.722
082	1.397	39.55	0.510	0.513	4.10	1.47	0.365	0.712

Note: See notations of Table 2a.

Table 2e: -Experimental data: Discharge coefficient from direct discharge measurement:

(c) Weir models with R=2.54cm.

P=3.418', 104.18cm, R=0.0833', 2.54cm

Run #	Q cfs	Q (l)	h1 ft	H1 ft	H1/R	Cd 1	Y2,(0)	Y2/H1
9000FA								
136	0.547	15.48	0.298	0.298	3.58	1.30	0.232	0.779
137	0.927	26.25	0.435	0.436	5.23	1.25	0.342	0.784
(A'C')	0.927	26.25	0.435	0.436	5.23	1.25	0.316	0.725
138	1.290	36.52	0.551	0.553	6.64	1.21	0.451	0.816
(A'C')	1.290	36.52	0.551	0.553	6.64	1.21	0.412	0.745
8000FA								
144	0.616	17.44	0.322	0.322	3.86	1.30	0.251	0.780
145	0.983	27.83	0.448	0.449	5.39	1.26	0.354	0.788
(A'C')	0.983	27.83	0.448	0.449	5.39	1.26	0.336	0.748
146	1.440	40.77	0.584	0.587	7.04	1.24	0.464	0.790
(A'C')	1.440	40.77	0.584	0.587	7.04	1.24	0.419	0.714
7000FA								
151	0.766	21.69	0.367	0.368	4.42	1.33	0.291	0.791
152	1.338	37.88	0.541	0.543	6.52	1.29	0.438	0.807
6000FA								
174	0.502	14.21	0.275	0.275	3.30	1.35	0.212	0.771
175	0.862	24.40	0.399	0.400	4.79	1.32	0.311	0.778
176	1.154	32.67	0.487	0.489	5.86	1.31	0.385	0.787
177	1.614	45.70	0.617	0.620	7.44	1.28	0.491	0.792
9000NA								
186	0.564	15.97	0.299	0.299	3.58	1.33	0.234	0.783
187	0.983	27.83	0.436	0.438	5.25	1.31	0.345	0.788
188	1.390	39.36	0.558	0.560	6.72	1.28	0.443	0.791
7000NA								
157	0.351	9.939	0.218	0.218	2.61	1.34	0.163	0.748
158	0.383	10.84	0.230	0.230	2.75	1.34	0.174	0.757
159	0.821	23.24	0.384	0.385	4.61	1.33	0.302	0.784
160	1.227	34.74	0.508	0.510	6.11	1.31	0.400	0.784
161	1.676	47.45	0.632	0.635	7.62	1.28	0.491	0.773
6000NA								
166	0.564	15.97	0.297	0.297	3.56	1.35	0.225	0.758
167	0.933	26.42	0.418	0.420	5.03	1.33	0.325	0.774
168	1.311	37.12	0.530	0.532	6.38	1.31	0.416	0.782
169	1.637	46.35	0.618	0.622	7.46	1.29	0.485	0.780
9075								
192	0.631	17.86	0.304	0.305	3.65	1.45	0.212	0.695
193	1.018	28.82	0.405	0.407	4.87	1.52	0.280	0.688
194	1.372	38.85	0.485	0.488	5.85	1.56	0.335	0.686
195	1.756	49.72	0.564	0.569	6.82	1.59	0.393	0.691
8075								
199	0.399	11.29	0.229	0.229	2.75	1.41	0.160	0.699
200	0.808	22.88	0.350	0.351	4.21	1.50	0.244	0.695
201	1.287	36.44	0.464	0.467	5.60	1.56	0.322	0.690
202	2.017	57.11	0.614	0.619	7.42	1.60	0.430	0.695
7575								
206	0.776	21.97	0.340	0.341	4.09	1.51	0.240	0.704
207	1.237	35.02	0.453	0.455	5.46	1.56	0.313	0.688
208	1.809	51.22	0.571	0.575	6.90	1.61	0.401	0.697

(Cont'd)

Note: See notations of Table 2a. (A'C') denotes data for section A'C', Figs.1&2.

Table 2e: (continued)

Run #	Q cfs	Q (1)	h1 ft	H1 ft	H1/R	Cd 1	Y2,(0)	Y2/H1
			P=3.418', 104.18cm, R=0.0833', 2.54cm					
9060								
218	0.647	18.32	0.308	0.309	3.70	1.46	0.222	0.718
219	1.077	30.49	0.422	0.423	5.08	1.51	0.300	0.709
220	1.553	43.97	0.533	0.537	6.43	1.53	0.375	0.698
221	1.987	56.26	0.625	0.630	7.56	1.54	0.444	0.705
7560								
212	0.865	24.49	0.367	0.369	4.42	1.50	0.262	0.710
213	1.280	36.24	0.469	0.472	5.65	1.53	0.328	0.695
214	1.888	53.46	0.600	0.605	7.26	1.55	0.421	0.696
6060								
226	0.754	21.35	0.338	0.339	4.06	1.48	0.238	0.702
227	1.221	34.57	0.454	0.457	5.47	1.53	0.319	0.698
228	1.809	51.22	0.581	0.585	7.02	1.57	0.409	0.699
9045								
245	0.463	13.11	0.252	0.252	3.02	1.42	0.186	0.738
246	0.855	24.21	0.367	0.369	4.42	1.48	0.279	0.756
247	1.163	32.93	0.448	0.450	5.40	1.49	0.334	0.742
248	1.550	43.89	0.545	0.548	6.57	1.48	0.396	0.723
7545								
238	0.708	20.04	0.327	0.328	3.93	1.46	0.244	0.744
239	1.157	32.76	0.446	0.448	5.37	1.49	0.329	0.734
240	1.629	46.12	0.558	0.561	6.73	1.50	0.401	0.715
6045								
232	0.749	21.20	0.338	0.339	4.06	1.47	0.247	0.729
233	1.126	31.88	0.438	0.440	5.27	1.49	0.320	0.727
234	1.587	44.93	0.546	0.550	6.59	1.51	0.391	0.711

(Cont'd)

Table 2e: (continued)

RUN#	Q cfs	Q (1)	h1 ft	H1 ft	H1/R	P/H1	Cd 1	Y2 ft	Y2/H1
			P=3.844', 117.2cm, R=0.0833', 2.54cm						
9000FA									
453	0.232	6.56	0.167	0.167	2.00	22.96	1.31	0.125	0.749
454	0.300	8.49	0.197	0.197	2.36	19.51	1.33	0.149	0.756
454a	0.396	11.21	0.239	0.239	2.86	16.10	1.31	0.184	0.770
455	0.527	14.92	0.290	0.291	3.48	13.22	1.30	0.228	0.784
456	0.727	20.58	0.366	0.366	4.39	10.48	1.27	0.289	0.790
9045									
459	0.290	8.21	0.190	0.190	2.28	20.18	1.35	0.140	0.737
460	0.485	13.73	0.260	0.260	3.12	14.75	1.41	0.191	0.735
461	0.710	20.10	0.329	0.330	3.95	11.65	1.45	0.247	0.748
462	0.960	27.18	0.397	0.398	4.77	9.65	1.48	0.292	0.734
6045									
467	0.378	10.70	0.223	0.223	2.68	17.21	1.39	0.161	0.722
468	0.557	15.77	0.284	0.284	3.41	13.52	1.42	0.205	0.722
469	0.780	22.08	0.349	0.350	4.19	10.99	1.46	0.253	0.723
470	0.989	28.00	0.405	0.406	4.87	9.45	1.48	0.295	0.727

Table 2f: -Experimental data: Discharge coefficient from direct discharge measurement:

(f) Weir models with R=0.95cm. Note: (A'C') denotes data for section A'C', Figs.1&2.

P=3.461', 105.49cm, R=0.03125', 0.9525cm

Run #	Q cfs	Q (l)	h1 ft	H1 ft	H1/R	Cd 1	Y2,(0)	Y2/H1
9000FA								
255	0.307	8.693	0.212	0.212	6.773	1.22	0.170	0.802
256	0.518	14.66	0.305	0.306	9.777	1.19	0.249	0.814
(A'C')	0.518	14.66	0.305	0.306	9.777	1.19	0.217	0.709
257	0.703	19.90	0.377	0.378	12.09	1.17	0.314	0.831
258	0.897	25.4	0.444	0.445	14.24	1.17	0.371	0.834
(A'C')	0.897	25.4	0.444	0.445	14.24	1.17	0.316	0.710
259	1.086	30.75	0.507	0.509	16.27	1.16	0.430	0.845
260	1.267	35.87	0.563	0.565	18.07	1.15	0.473	0.837
(A'C')	1.267	35.87	0.563	0.565	18.07	1.15	0.353	0.625
7500FA								
264	0.533	15.09	0.303	0.304	9.726	1.23	0.249	0.819
265	0.706	19.99	0.369	0.370	11.83	1.21	0.302	0.816
266	0.474	13.42	0.280	0.280	8.967	1.24	0.228	0.814
267	0.927	26.25	0.445	0.446	14.28	1.20	0.367	0.823
268	1.400	39.64	0.592	0.595	19.03	1.18	0.486	0.817
6000FA								
272	0.512	14.49	0.290	0.291	9.305	1.26	0.232	0.797
273	0.763	21.60	0.383	0.384	12.28	1.24	0.307	0.799
274	1.021	28.91	0.469	0.471	15.06	1.22	0.378	0.803
275	1.300	36.81	0.556	0.558	17.87	1.21	0.454	0.814
9000NA								
293	0.449	12.71	0.269	0.269	8.619	1.24	0.223	0.829
294	0.718	20.33	0.372	0.373	11.94	1.22	0.314	0.842
295	0.989	28.00	0.465	0.466	14.92	1.20	0.390	0.837
296	1.227	34.74	0.540	0.542	17.33	1.19	0.450	0.830
7500NA								
285	0.321	9.089	0.210	0.210	6.725	1.29	0.169	0.805
286	0.627	17.75	0.336	0.337	10.78	1.24	0.277	0.822
287	0.916	25.93	0.438	0.439	14.05	1.22	0.362	0.825
288	1.163	32.93	0.516	0.518	16.57	1.21	0.422	0.815
289	1.443	40.86	0.597	0.600	19.19	1.20	0.483	0.805
6000NA								
279	0.508	14.38	0.288	0.288	9.220	1.27	0.230	0.799
280	0.796	22.54	0.393	0.394	12.59	1.25	0.311	0.789
281	1.056	29.90	0.478	0.480	15.34	1.23	0.376	0.783
282	1.334	37.77	0.561	0.563	18.03	1.22	0.433	0.769
9075								
301	0.547	15.48	0.264	0.265	8.466	1.59	0.203	0.766
302	0.763	21.60	0.331	0.332	10.63	1.54	0.259	0.780
303	0.961	27.21	0.395	0.397	12.69	1.49	0.307	0.773
304	1.192	33.75	0.463	0.465	14.86	1.46	0.354	0.761
305	1.465	41.48	0.535	0.538	17.20	1.44	0.410	0.762
306	1.688	47.79	0.591	0.594	19.02	1.43	0.451	0.759
8075								
311	0.442	12.51	0.225	0.226	7.223	1.60	0.171	0.757
312	0.706	19.99	0.308	0.309	9.894	1.59	0.238	0.770
313	0.922	26.10	0.381	0.382	12.22	1.51	0.290	0.759
314	1.195	33.83	0.462	0.464	14.83	1.47	0.353	0.761
315	1.516	42.92	0.546	0.549	17.58	1.44	0.420	0.765
7575								
319	0.562	15.91	0.262	0.263	8.415	1.61	0.202	0.768
320	0.836	23.67	0.353	0.354	11.32	1.54	0.272	0.768
321	1.231	34.85	0.471	0.473	15.13	1.47	0.358	0.757
322	1.505	42.61	0.541	0.545	17.42	1.45	0.414	0.760

(Cont'd)

Table 2f: (continued)

			P=3.461', 105.49cm, R=0.03125', 0.9525cm					
Run #	Q cfs	Q (l)	h1 ft	H1 ft	H1/R	Cd 1	Y2,(0)	Y2/H1
9060								
334	0.502	14.21	0.253	0.253	8.097	1.53	0.197	0.779
335	0.773	21.88	0.347	0.348	11.12	1.46	0.269	0.773
336	0.998	28.26	0.418	0.420	13.43	1.42	0.325	0.774
337	1.297	36.72	0.505	0.508	16.24	1.39	0.393	0.774
338	1.576	44.62	0.581	0.584	18.69	1.37	0.450	0.771
7560								
326	0.497	14.07	0.248	0.248	7.939	1.56	0.197	0.794
327	0.754	21.35	0.335	0.336	10.73	1.50	0.261	0.777
328	1.024	28.99	0.422	0.423	13.54	1.44	0.328	0.775
329	1.317	37.29	0.505	0.508	16.24	1.41	0.390	0.768
330	1.622	45.93	0.584	0.588	18.80	1.39	0.448	0.762
6060								
343	0.586	16.59	0.279	0.279	8.941	1.54	0.211	0.756
344	0.905	25.62	0.384	0.385	12.32	1.47	0.291	0.756
345	1.218	34.49	0.476	0.478	15.29	1.43	0.358	0.749
346	1.494	42.30	0.550	0.553	17.68	1.41	0.411	0.743
9045								
361	0.732	20.72	0.344	0.345	11.05	1.40	0.281	0.814
362	0.961	27.21	0.418	0.420	13.43	1.37	0.336	0.800
363	1.195	33.83	0.489	0.491	15.70	1.35	0.392	0.798
364	1.450	41.05	0.561	0.564	18.04	1.33	0.449	0.796
378	0.431	12.20	0.236	0.237	7.569	1.45	0.185	0.781
379	0.493	13.96	0.259	0.260	8.307	1.44	0.205	0.788
380	0.593	16.79	0.295	0.296	9.467	1.43	0.235	0.794
381	0.685	19.39	0.328	0.329	10.52	1.41	0.263	0.799
382	0.806	22.82	0.369	0.370	11.84	1.39	0.296	0.800
383	0.873	24.72	0.390	0.392	12.53	1.38	0.313	0.798
384	1.065	30.15	0.451	0.453	14.48	1.35	0.361	0.797
385	1.241	35.14	0.503	0.505	16.16	1.34	0.402	0.796
7545								
369	0.537	15.20	0.272	0.273	8.729	1.46	0.216	0.791
370	0.756	21.40	0.349	0.350	11.20	1.41	0.277	0.791
371	1.006	28.48	0.429	0.430	13.77	1.38	0.337	0.784
372	1.224	34.66	0.494	0.496	15.86	1.36	0.392	0.790
373	1.494	42.30	0.568	0.571	18.26	1.34	0.447	0.783
6045								
351	0.480	13.59	0.249	0.250	7.991	1.49	0.193	0.772
352	0.754	21.35	0.345	0.346	11.08	1.43	0.268	0.775
353	0.966	27.35	0.413	0.415	13.27	1.40	0.322	0.776
354	1.224	34.66	0.490	0.493	15.76	1.37	0.381	0.773
355	1.538	43.55	0.576	0.579	18.52	1.35	0.446	0.770

Note: See notations of Table 2a.

Table 3a: -Experimental parameters:

(a) Weir models with $\alpha=90°$, no D/S slope and vent open.

90FA.Datf

H1/R	P/H1	C/R*1.5	F	CpCR	Cp Min	Teta	Teta Cpo	Y2/H1
0.55	14.04	4.04	0.47	0.45	-0.53	175	122	0.72
0.82	9.41	5.67	0.61	0.32	-0.99	180	110	0.72
1.00	7.69	6.71	0.68	0.22	-1.12	180	103	0.72
1.16	6.61	7.74	0.75	0.13	-1.29	180	97	0.72
1.38	5.51	9.11	0.83	0.04	-0.54	155	92	0.72
2.01*	22.96	12.63	1.02	-0.31				0.75
2.36	19.52	14.60	1.10	-0.30				0.76
2.87	16.10	16.95	1.19	-0.26				0.77
3.49	13.22	19.95	1.28	-0.19				0.78
4.40	10.49	24.23	1.40	-0.09				0.79
5.53	8.35	29.62	1.54	-0.08				0.80
0.70	16.46	4.96	0.55	0.33	-0.80	165	110	0.72
1.19	9.76	8.12	0.78	0.07	-0.41	127	94	0.70
1.64	7.06	10.62	0.92	-0.10	-0.29	111	84	0.73
0.88	13.14	6.17	0.65	0.24	-0.63	146	103	0.71
1.83	6.32	11.76	0.98	-0.17	-0.33	108	81	0.73
1.18	11.46	7.86	0.76	0.09	-0.48	134	95	0.71
1.72	7.85	11.01	0.94	-0.12	-0.29	108	83	0.73
2.47	5.46	15.12	1.12	-0.21	-0.23	99.	71	0.76
1.94*	6.94	12.38	1.01	-0.16				0.74
2.58	10.75	15.60	1.14	-0.33				0.76
3.78	7.32	21.49	1.33	-0.21				0.78
4.59	6.03	25.27	1.44	-0.11				0.79
4.86	5.70	26.47	1.46	-0.08				0.79
2.09	13.26	13.06	1.03	-0.21	-0.31	103	75	0.74
3.08	8.99	18.17	1.23	-0.19	-0.20	86	64	0.77
4.24	6.53	23.60	1.39	-0.09	-0.20	75	55	0.78
3.58	11.47	20.52	1.30	-0.14	-0.19	80	58	0.78
5.24	7.84	28.39	1.52	-0.07	-0.16	67	47	0.78
6.64	6.18	34.65	1.66	-0.07	-0.17	58	39	0.82
6.77	16.32	35.81	1.69	-0.11	-0.20	60	35	0.80
9.78	11.31	51.30	2.03	-0.08	-0.17	46	25	0.81
12.10	9.16	63.57	2.27	-0.06	-0.20	40	18	0.83
14.24	7.78	76.26	2.51	-0.05	-0.18	37	12	0.83
16.27*	6.80	87.64	2.70	-0.05	-0.17	30		0.84
18.08	6.13	98.97	2.90	-0.05	-0.18	30		0.84

Note: $H1/R=H_1/R$, $P/H1=p/H_1$, columns 3 and 4 are not used, $CpCR=(P/\gamma H_1)_{cr}$, pressure head at crest C (Fig.1a), Cp $Min=(P/\gamma H_1)_{min}$, minimum pressure head on crest surface, Teta= angular location of $(P/\gamma H_1)_{min}$, Teta Cp0= angular location where the pressure is atmospheric and $Y2/H1=Y_2/H_1$.
*Additional tests to check only specific parameters.

Table 3b-3e: -Experimental parameters:

(b) Weir models with α=90°, no D/S slope and vent shut.

H1/R	P/H1	C/R^1.5	F	Cp CR	Cp Min	Teta	Teta Cpo	Y2/H1
2.10*	13.16	13.19	1.04	-0.21				0.74
3.04	9.18	18.10	1.23	-0.27				0.77
3.74	7.39	21.93	1.36	-0.24	-0.29	80		0.77
4.43	6.25	25.66	1.48					0.77
4.88	5.66	28.44	1.57	-0.43	-0.45	70		0.76
3.59	11.43	21.05	1.34	-0.33	-0.35	83	56	0.78
5.25	7.80	29.97	1.60	-0.24	-0.24	73	46	0.79
6.72	6.10	37.64	1.79	-0.29	-0.41	63	30	0.79

(c) Weir models with α=90°, β=75°.

H1/R	P/H1	C/R^1.5	F	Cp CR	Cp Min	Teta	Teta Cpo	Y2/H1
3.66	11.21	24.89	1.55	-1.45	-2.14	120	37	0.69
4.88	8.40	34.51	1.89	-2.51	-3.15	120	22	0.69
5.85	7.00	42.45	2.14	-3.30	-3.99	122	17	0.69
6.82	6.01	50.28	2.36	-4.00	-4.69	122	12	0.69

(d) Weir models with α=90°, β=60°.

H1/R	P/H1	C/R^1.5	F	Cp CR	Cp Min	Teta	Teta Cpo	Y2/H1
2.45*	11.31	15.99	1.19	-0.69				0.73
3.09	8.94	20.31	1.37	-1.10				0.73
3.88	7.14	26.10	1.59	-1.58				0.71
4.37	6.34	29.82	1.73	-1.90				0.71
4.68	5.92	32.13	1.80	-2.11				0.71
2.20	12.59	14.51	1.12	-0.53	-1.04	128	67	0.71
3.16	8.76	20.87	1.39	-1.16	-1.58	121	45	0.72
4.10	6.75	27.77	1.65	-1.74	-2.13	116	31	0.71
3.71	11.06	24.87	1.55	-1.42	-1.81	113	38	0.72
5.08	8.08	35.23	1.90	-2.37	-2.70	111	23	0.71
6.44	6.37	45.47	2.19	-3.24	-3.55	109	12	0.70
7.56	5.42	53.76	2.40	-3.83	-4.05	107	6	0.70

(e) Weir models with α=90°, β=45°.

H1/R	P/H1	C/R^1.5	F	Cp CR	Cp Min	Teta	Teta Cpo	Y2/H1
0.44	17.29	3.46	0.42	0.51	0.00	130	130	0.71
0.73	10.55	5.14	0.56	0.35	-0.12	128	115	0.71
0.91	8.49	6.18	0.64	0.28	-0.18	127	108	0.72
1.15	6.70	7.61	0.74	0.15	-0.28	125	100	0.72
1.35	5.68	8.98	0.83	0.05	-0.36	123	93	0.71
2.29*	20.19	14.68	1.12	-0.60				0.74
3.13	14.76	20.31	1.36	-0.99				0.73
3.96	11.66	25.72	1.56	-1.06				0.73
4.78	9.65	31.82	1.77	-1.21				0.73
3.02	13.56	19.70	1.34	-0.82	-0.93	105	52	0.74
4.42	9 26	29.04	1.67	-1.05	-1.07	93	33	0.76
5.41	7.60	36.03	1.89	-1.78	-1.78	90	22	0.74
6.58	6.24	44.22	2.12	-2.47	-2.49	87	12	0.72

Note: See notations of Table 3a. *Additional tests to check only specific parameters.

Table 3f-3m: -Experimental parameters:

(f) Weir models with α=80°, no D/S slope and vent open.

H1/R	P/H1	C/R*1.5	F	CpCR	Cp Min	Teta	Teta Cpo	Y2/H1
3.87	10.62	22.13	1.36	-0.13	-0.20	78	57	0.78
5.39	7.61	29.60	1.56	-0.08	-0.17	67	48	0.79
7.04	5.82	38.19	1.77	-0.07	-0.19	58	42	0.79

(g) Weir models with α=75°, no D/S slope and vent open.

9.73	11.36	52.78	2.10	-0.12	-0.24	77	37	0.82
11.84	9.35	64.80	2.34	-0.09	-0.20	65	34	0.82
8.97	12.36	48.67	2.01	-0.12	-0.22	58	42	0.81
14.29	7.76	79.12	2.60	-0.06	-0.27	54	27	0.82
19.04	5.82	108.36	3.09					0.82

(h) Weir models with α=70°, no D/S slope and vent open.

4.42	9.29	25.45	1.47	-0.09	-0.17	73	56	0.79
6.52	6.29	36.42	1.75	-0.10	-0.20	67	46	0.81

(i) Weir models with α=60°, no D/S slope and vent open.

3.30	12.43	19.80	1.30	-0.26	-0.34	85	62	0.77
4.80	8.54	27.68	1.54	-0.14	-0.22	78	55	0.78
5.87	6.99	33.37	1.69	-0.11	-0.19	67	52	0.79
7.44	5.51	41.73	1.89	-0.10	-0.21	62	47	0.79
9.30	11.89	52.19	2.12	-0.11	-0.23	66	52	0.80
12.28	9.03	69.59	2.46	-0.13	-0.20	63	48	0.80
15.06	7.35	86.22	2.76	-0.10	-0.22	60	44	0.80
17.87	6.20	102.97	3.03	-0.09	-0.21	58	39	0.81

(j) Weir models with α=70°, no D/S slope and vent shut.

2.61	15.68	16.16	1.17	-0.30	-0.32	95	67	0.75
2.76	14.86	16.95	1.20	-0.31	-0.31	90	65	0.76
4.62	8.88	26.76	1.51	-0.14	-0.22	73	52	0.78
6.12	6.70	34.84	1.73	-0.28	-0.38	65	42	0.78
7.62	5.38	43.34	1.94	-0.32	-0.44	63	36	0.77

(k) Weir models with α=60°, no D/S slope and vent shut.

3.57	11.51	21.52	1.37	-0.23	-0.28	82	60	0.76
5.04	8.14	29.30	1.59	-0.14	-0.27	72	52	0.78
6.39	6.42	36.55	1.78	-0.26	-0.39	67	45	0.78
7.46	5.50	42.56	1.92	-0.18	-0.32	62	44	0.78

(l) Weir models with α=80°, β=75°.

2.75	14.93	18.59	1.31	-0.97	-1.72	130	54	0.70
4.22	9.74	29.48	1.73	-2.06	-2.73	124	30	0.69
5.60	7.32	40.61	2.09	-3.05	-3.70	118	22	0.69
7.43	5.52	55.38	2.50	-4.16	-4.60	115	12	0.69

(m) Weir models with α=β=75°.

4.09	10.02	28.57	1.70	-1.99	-2.70	124	30	0.70
5.46	7.51	39.59	2.06	-2.93	-3.67	120	22	0.69
6.90	5.94	51.31	2.40	-3.96	-4.51	118	13	0.70

Note: See notations of Table 3a.

Table 3n-3r: -Experimental parameters:

(n) Weir models with α=75°, β=60°.

H1/R	P/H1	C/R*1.5	F	CpCR	Cp Min	Teta	Teta Cpo	Y2/H1
4.42	9.26	30.37	1.74	-1.69	-2.19	112	32	0.71
5.66	7.24	40.02	2.05	-2.69	-3.04	110	23	0.69
7.26	5.65	52.34	2.39	-3.58	-3.89	108	14	0.70

(p) Weir models with α=β=60°.

4.07	10.08	27.89	1.66	-1.57	-2.03	117	44	0.70
5.48	7.48	38.71	2.01	-2.52	-2.95	113	33	0.70
7.02	5.84	50.83	2.35	-3.42	-3.81	110	29	0.70

(q) Weir models with α=75°, β=45°.

3.94	10.42			-0.95	-0.99	95	43	0.74
5.38	7.63			-1.64	-1.64	94	29	0.73
6.74	6.09			-2.50	-2.53	93	20	0.71

(r) Weir models with α=60°, β=45°.

0.53	14.64			0.45	-0.02	130	130	0.72
0.78	9.82			0.32	-0.13	128	113	0.72
0.98	7.86			0.24	-0.21	126	105	0.72
1.35*	5.68			0.05	-0.37	123	93	0.71
1.09	7.07			0.18				0.72
2.68*	17.21			-0.79				0.72
3.41	13.53			-1.00				0.72
4.20	11.00			-1.01				0.72
4.88	9.46			-1.17				0.73
4.07	10.08			-1.10	-1.21	100		0.73
5.28	7.77			-1.72	-1.76	105		0.73
6.60	6.21			-2.34	-2.43	100		0.71

Note: See notations of Table 3a. *Additional tests to check only specific parameters.

Table 4a-4b: -Variation of discharge coefficient based on direct discharge measurement with H_1/R for circular-crested weirs:

(a) Weir models with varied U/S slopes, no D/S slope and vent open.

Note: (H/R1, Cd1), (H/R2,Cd2), . . (H/R8, Cd8) refer to weir models with α=90° and R= 15.16cm, 10.08cm, 7.54cm, 3.81cm, 2.54cm and 0.95cm; numbers 80, 75, 70 and 60 following H/R and Cd refer to U/S slopes α=80°, 75°, 70° and 60° respectively.

H/R1	Cd1	H/R2	Cd2	H/R3	Cd3	H/R5	Cd5	H/R6	Cd6
0.55	1.07	0.70	1.12	1.18	1.22	2.58	1.32	3.59	1.30
0.82	1.15	1.19	1.23	1.72	1.29	3.78	1.30	5.24	1.25
1.00	1.18	1.64	1.28	2.47	1.33	4.59	1.27	6.64	1.22
1.16	1.20	0.88	1.17	1.94	1.32	4.86	1.26	2.01	1.32
1.38	1.25	1.83	1.30	2.78	1.32	2.09	1.31	2.36	1.33
						3.08	1.32	2.87	1.32
						4.24	1.27	3.49	1.31
								4.40	1.27

H/R8	Cd8	H/R80	Cd80	H/R75	Cd75	H/R70	Cd70	H/R60	Cd60
6.77	1.22	3.87	1.31	9.73	1.24	4.42	1.33	3.30	1.35
9.78	1.19	5.39	1.27	11.84	1.22	6.52	1.30	4.80	1.33
12.10	1.18	7.04	1.24	8.97	1.24	8.14	1.27	5.87	1.31
14.24	1.17	8.70	1.22	14.29	1.21	9.39	1.25	7.44	1.28
16.27	1.16	9.85	1.21	19.04	1.19			9.30	1.27
18.08	1.16							12.28	1.25
								15.06	1.23
								17.87	1.21

(b) Weir models with varied U/S slopes, no D/S slope and vent shut.

Note: See notations of Table 4a; numbers 75, 70 and 60 following (H/R, Cd) refer to U/S slopes α=75°, 70° and 60° respectively.

H/R5	Cd5	H/R6	Cd6	H/R8	Cd8	H/R75	Cd75	H/R70	Cd70
2.10	1.32	3.59	1.34	8.62	1.25	6.72	1.29	2.61	1.34
3.04	1.33	5.25	1.32	11.94	1.22	10.78	1.25	2.76	1.35
3.74	1.33	6.72	1.29	14.92	1.21	14.05	1.22	4.62	1.34
4.43	1.32			17.34	1.20	16.58	1.21	6.12	1.31
						19.20	1.21	7.62	1.29
								8.85	1.27

H/R60	Cd60
9.22	1.28
12.60	1.25
15.35	1.24
18.03	1.23
3.57	1.35
5.04	1.33
6.39	1.31
7.46	1.30
8.56	1.28

Table 4c-4d: -Variation of discharge coefficient based on direct discharge measurement with H_1/R for circular-crested weirs:

(c) Weir models with varied U/S slopes and constant D/S slope $\beta=75°$.

Note: See notations of Table 4a; numbers 80 and 75 following (H/R, Cd) refer to U/S slope $\alpha=80°$ and 75° respectively.

H/R6	Cd6	H/R8	Cd8	H/R80	Cd80	H/R75	Cd75
3.66	1.46	8.47	1.60	2.75	1.41	8.41	1.62
4.88	1.52	10.63	1.55	4.22	1.51	11.32	1.54
5.85	1.57	12.70	1.49	5.60	1.57	15.14	1.47
6.82	1.59	14.87	1.46	7.22	1.60	17.42	1.46
		17.21	1.44	9.89	1.59	4.09	1.51
		19.02	1.43	12.22	1.52	5.46	1.57
				14.84	1.47	6.90	1.61
				17.58	1.45		

(d) Weir models with varied U/S slopes and constant D/S slope $\beta=60°$.

Note: See notations of Table 4a; numbers 75 and 60 following (H/R, Cd) refer to U/S slope $\alpha=75°$ and 60° respectively.

H/R5	Cd5	H/R6	Cd6	H/R8	Cd8	H/R75	Cd75	H/R60	Cd60
2.45	1.39	3.71	1.46	8.10	1.53	4.42	1.50	4.07	1.48
3.09	1.42	5.08	1.52	11.13	1.47	5.66	1.54	5.48	1.54
3.88	1.47	6.44	1.54	13.43	1.43	7.26	1.56	7.02	1.57
4.37	1.49	7.56	1.54	16.25	1.39	7.94	1.56	8.94	1.54
4.68	1.51			18.69	1.37	10.74	1.51	12.32	1.47
2.20	1.35					13.54	1.45	15.29	1.43
3.16	1.43					16.25	1.42	17.68	1.41
4.10	1.48					18.80	1.40		
5.21	1.51								

(e) Weir models with varied U/S slopes and constant D/S slope $\beta=45°$.

Note: See notations of Table 4a; columns 7-8 refer to weir models with $\alpha=75°$, $\beta=45°$ and columns 9-10 refer to weir models with $\alpha=60°$, $\beta=45°$.

H/R1	Cd1	H/R6	Cd6	H/R8	Cd8	H/R 7545	Cd	H/R 6045	Cd
0.44	1.04	3.02	1.42	11.05	1.40	8.73	1.46	0.53	1.08
0.73	1.12	4.42	1.48	13.43	1.37	11.21	1.42	0.78	1.15
0.91	1.17	5.41	1.50	15.71	1.35	13.77	1.38	0.98	1.19
1.15	1.21	6.58	1.48	18.05	1.33	15.87	1.36	1.35	1.26
1.35	1.25	7.45	1.47	7.57	1.46	18.26	1.35	1.09	1.21
		2.29	1.36	8.31	1.45	3.94	1.46	4.07	1.47
		3.13	1.42	9.47	1.43	5.38	1.50	5.28	1.50
		3.96	1.46	10.52	1.41	6.74	1.50	6.60	1.51
		4.78	1.49	11.84	1.39			7.99	1.49
				12.53	1.38			11.08	1.44
				14.49	1.36			13.27	1.40
				16.16	1.34			15.76	1.38
								18.53	1.36
								2.68	1.39
								3.41	1.43
								4.20	1.47
								4.88	1.48

Table 5: -Peak C_d values of circular-crested weirs - Present study.

(Fitted values)

Slope Angles α degree (°)	Slope Angles β degree (°)	H_1/R	C_d (Peak)	Remarks
90	75	8.0	1.60	
90	60	7.0	1.54	
90	45	5.5	1.50	$C_{d\,max}$ = 1.48 (Bos, 1978)
90	(vent shut)	3.5	1.34	
90	(vent open)	2.5	1.33	(Nappe fully ventilated)
80	75	8.0	1.61	
80	(vent open)	2.7	1.34	(Nappe fully ventilated)
75	75	8.3	1.62	
75	60	7.5	1.56	
75	45	6.5	1.50	
75	(vent shut)	3.5	1.35	
75	(vent open)	3.0	1.34	(Nappe fully ventilated)
70	(vent shut)	3.5	1.35	
70	(vent open)	3.0	1.35	(Nappe fully ventilated)
60	60	7.0	1.57	
60	45	6.5	1.51	
60	(vent shut)	3.5	1.35	
60	(vent open)	3.5	1.35	(Nappe fully ventilated)

Table 6: -Variation of discharge coefficient based on direct discharge measurement for sharp-crested weirs.

Run#	Q (l)	h1 (m)	h1/P	P/h1	Cd Eq. 5	Cd (Bos)
90FA						
25	11.98	0.09	0.08	13.21	1.08	1.05
26	34.94	0.18	0.15	6.44	1.07	1.06
29	14.92	0.10	0.09	11.49	1.10	1.05
30	28.01	0.15	0.13	7.52	1.09	1.06
386	14.38	0.10	0.09	11.79	1.09	1.05
387	26.02	0.14	0.12	7.98	1.10	1.06
388	34.66	0.17	0.15	6.60	1.10	1.06
9060						
88	17.44	0.10	0.09	11.63	1.30	
89	21.83	0.11	0.10	9.96	1.29	
90	27.67	0.14	0.12	8.48	1.28	
91	33.84	0.15	0.13	7.43	1.29	
92	42.62	0.18	0.16	6.38	1.28	
9045						
126	7.31	0.06	0.05	20.27	1.26	
127	13.65	0.09	0.07	13.31	1.25	
128	20.64	0.11	0.10	10.04	1.24	
129	25.63	0.13	0.12	8.71	1.24	
130	30.75	0.15	0.13	7.70	1.23	
131	37.77	0.17	0.15	6.78	1.25	
7560						
94	8.33	0.06	0.05	19.24	1.32	
95	14.27	0.09	0.07	13.32	1.31	
96	20.93	0.11	0.10	10.51	1.34	
97	27.44	0.13	0.12	8.71	1.32	
98	33.67	0.15	0.13	7.56	1.32	
99	41.48	0.17	0.15	6.62	1.32	
7545						
118	7.67	0.06	0.05	19.91	1.28	
119	14.50	0.09	0.08	12.73	1.24	
120	22.17	0.12	0.10	9.74	1.27	
121	29.73	0.14	0.12	7.99	1.26	
122	37.41	0.17	0.14	6.88	1.26	
6060						
102	7.56	0.06	0.05	20.70	1.34	
103	14.84	0.09	0.08	13.24	1.34	
104	21.89	0.11	0.10	10.22	1.34	
105	28.66	0.13	0.12	8.56	1.35	
106	36.73	0.16	0.14	7.25	1.34	
6045						
110	8.01	0.06	0.05	19.41	1.29	
111	19.91	0.11	0.09	10.65	1.30	
112	26.73	0.13	0.11	8.77	1.30	
113	32.85	0.15	0.13	7.63	1.30	
114	41.06	0.17	0.15	6.60	1.30	

Note: Alpha-numerics 90FA, 9060, 9045, 7560,7545, 6060 and 6045 of column 1 refer to values of U/S (first two digits) and D/S (last two digits) slope angles in degrees of tested sharp-crested weirs having equivalent heights to the corresponding circular-crested weirs cited above: h1=h_1; h1/P=h_1/p; P/h1=p/h_1; Cd=C_d (Eq. 5) and Cd (Bos)=C_d (for rectangular sharp-crested weirs, Bos 1978).

Table 7: -Average C_d values of sharp-crested weirs - Present study ($0.05 \le h_1/p \le 0.20$). Results of preliminary tests calibration.

Slope Angles		C_d (Present) Eq. 5	C_d (Existing)
α	β		
degree (°)	degree (°)		
90	(Vent open)	1.08	1.06 (1),(2) 1.08(3)
90	60	1.28	
90	45	1.24	1.25(4)
75	60	1.32	
75	45	1.26	~ 1.27(4)
60	60	1.34	
60	45	1.30	~ 1.30(4)

[1] Ackers et al (1978), [2] Bos (1978), [3] Kandaswamy and Rouse (1957), (4) Brater and King (1976)

Table 8a: -Dimensionless velocity profiles and pressure distributions across the flow depth at weir crest C:

(a) Weir models with $\alpha=90^\circ$, no D/S slope andvent open.- R=15.16 cm.

Note: $Y/Y2=y/Y_2$, u/U, $P/g a Y2=P/\gamma Y_2$. Data are grouped in cluster of 3 columns.
*407, 408, . . 411: Run Nos. **Interpolated value.

Y/Y2 407*	u/U	P/gaY2	Y/Y2 408	u/U	P/gaY2	Y/Y2 409	u/U	P/gaY2
0.000	0.000	0.611	0.000	0.000	0.449	0.000	0.000	0.313
0.025	0.716	0.641	0.028	0.812	0.443	0.023	0.869	0.315
0.050	0.722	0.603	0.056	0.802	0.435	0.046	0.861	0.307
0.083	0.715	0.582	0.112	0.783	0.417	0.092	0.834	0.322
0.165	0.693	0.538	0.225	0.738	0.392	0.184	0.787	0.326
0.330	0.655	0.436	0.337	0.697	0.356	0.322	0.729	0.300
0.495	0.619	0.330	0.506	0.644	0.280	0.460	0.672	0.267
0.660	0.585	0.217	0.674	0.597	0.186	0.551	0.642	0.225
0.825	0.554	0.097	0.843	0.556	0.082	0.689	0.597	0.160
0.932	0.537	0.013	0.955	0.533	0.001	0.827	0.563	0.075
1.000	0.528	0.000	1.000	0.524	0.000	0.956	0.531	0.000
						1.000	0.522	0.000

Y/Y2 410	u/U	P/gaY2	Y/Y2 411	u/U	P/gaY2
0.000	0.000	0.183	0.000	0.000	0.054
0.020	0.910	0.221	0.017	0.977	0.045
0.040	0.903	0.218	0.033	0.966	0.055
0.080	0.884	0.220	0.067	0.939	0.087
0.199	0.812	0.267	0.134	0.889	0.141
0.318	0.750	0.280	0.234	0.816	0.206
0.438	0.694	0.270	0.335	0.761	0.220
0.557	0.647	0.238	0.469	0.696	0.211
0.667	0.608	0.185	0.602	0.641	0.177
0.796	0.570	0.129	0.736	0.589	0.131
0.947	0.534	0.032	0.870	0.549	0.058
1.000	0.522	0.000	1.000	0.511	0.000

(Cont'd)

Table 8a: (continued).- R=2.54 cm.

Note: See notations of Table 8a.
*453, 454, . . 457: Run Nos.

y/Y2 453*	u/U	P/gaY2	y/Y2 454	u/U	P/gaY2	y/Y2	u/U	P/gaY2
0.000	0.000	-0.420	0.000	0.000	-0.396	0.000	0.000	-0.339
0.008	0.536	-0.410**	0.007	0.415	-0.390**	0.005	0.540	-0.335**
0.013	1.124	-0.368	0.012	1.100	-0.290	0.024	1.091	-0.275
0.019	1.129	-0.390	0.016	1.114	-0.339	0.031	1.085	-0.267
0.024	1.125	-0.384	0.020	1.112	-0.336	0.041	1.075	-0.251
0.035	1.110	-0.352	0.097	1.006	-0.132	0.168	0.894	0.070
0.120	1.010	-0.170	0.205	0.889	0.042	0.348	0.744	0.201
0.251	0.876	0.022	0.423	0.724	0.166	0.527	0.650	0.187
0.513	0.699	0.117	0.643	0.618	0.128	0.705	0.579	0.119
0.776	0.586	0.044	0.863	0.539	0.025	0.883	0.520	0.024
1.000	0.520	0.000	1.000	0.502	0.000	1.000	0.494	0.000

y/Y2 455	u/U	P/gaY2	Y/Y2 456	u/U	P/gaY2
0.000	0.000	-0.245	0.000	0.000	-0.119
0.004	0.116	-0.240**	0.005	0.091	-0.110**
0.008	1.054	-0.150	0.007	0.910	-0.100**
0.012	1.070	-0.199	0.012	1.018	-0.059
0.015	1.066	-0.190	0.014	1.021	-0.070
0.064	0.998	-0.068	0.016	1.020	-0.068
0.136	0.902	0.087	0.023	1.017	-0.069
0.280	0.772	0.214	0.048	0.974	0.012
0.496	0.649	0.215	0.109	0.893	0.137
0.712	0.562	0.129	0.222	0.780	0.259
0.884	0.509	0.029	0.392	0.674	0.278
1.000	0.474	0.000	0.562	0.589	0.241
			0.733	0.534	0.148
			0.931	0.476	0.022
			1.000	0.453	0.000

Table 8b: -Dimensionless velocity profiles and pressure distributions across the flow depth at weir crest C:

(b) Weir models with α=90°, β=45°.- R=15.16 cm.

Y/Y2 413	u/U	P/gaY2
0.000	0.000	0.697
0.051	0.686	0.677
0.102	0.681	0.633
0.205	0.663	0.561
0.307	0.644	0.490
0.512	0.606	0.344
0.717	0.572	0.189
0.922	0.542	0.028
1.000	0.534	0.000

Y/Y2 414	u/U	P/gaY2
0.000	0.000	0.488
0.032	0.783	0.507
0.063	0.774	0.492
0.127	0.752	0.472
0.190	0.732	0.446
0.317	0.692	0.393
0.444	0.656	0.329
0.634	0.606	0.221
0.824	0.561	0.099
0.951	0.534	0.012
1.000	0.523	0.000

Y/Y2 415	u/U	P/gaY2
0.000	0.000	0.385
0.025	0.844	0.371
0.051	0.836	0.363
0.101	0.809	0.369
0.152	0.789	0.359
0.254	0.747	0.340
0.355	0.707	0.313
0.507	0.654	0.255
0.659	0.610	0.176
0.811	0.568	0.088
0.963	0.532	0.000
1.000	0.524	0.000

Y/Y2 416	u/U	P/gaY2
0.000	0.000	0.217
0.020	0.913	0.209
0.040	0.905	0.208
0.080	0.878	0.229
0.121	0.850	0.251
0.201	0.805	0.267
0.281	0.764	0.272
0.402	0.710	0.254
0.523	0.662	0.221
0.643	0.621	0.170
0.764	0.582	0.112
0.884	0.550	0.039
0.965	0.531	0.000
1.000	0.523	0.000

Y/Y2 417	u/U	P/gaY2
0.000	0.000	0.068
0.017	0.974	0.053
0.034	0.962	0.064
0.068	0.937	0.092
0.136	0.887	0.143
0.239	0.815	0.202
0.341	0.757	0.221
0.443	0.709	0.212
0.546	0.664	0.192
0.648	0.625	0.158
0.750	0.588	0.116
0.853	0.560	0.057
0.900	0.547	0.028
1.000	0.511	0.000

(Cont'd)

Note: See notations of Tabls 8a.
•413, 414, . . 417: Run Nos.

Table 8b: (continued).- R=2.54 cm.

y/Y2 459*	u/U	P/gaY2	y/Y2 460	u/U	P/gaY2	y/Y2 461	u/U	P/gaY2
0.000	0.000	-0.820	0.000	0.000	-1.349	0.000	0.000	-1.421
0.010	0.567	-0.800**	0.007	0.442	-1.340**	0.006	0.808	-1.410**
0.015	1.240	-0.750	0.010	0.919	-1.320**	0.007	1.417	-1.357
0.019	1.249	-0.784	0.012	1.385	-1.265	0.008	1.415	-1.351
0.024	1.241	-0.765	0.014	1.394	-1.305	0.010	1.421	-1.374
0.109	1.114	-0.465	0.016	1.385	-1.273	0.011	1.410	-1.336
0.224	0.965	-0.178	0.020	1.374	-1.237	0.014	1.409	-1.333
0.457	0.754	0.068	0.024	1.365	-1.210	0.022	1.396	-1.297
0.692	0.610	0.100	0.080	1.237	-0.827	0.031	1.372	-1.219
1.000	0.511	0.000	0.164	1.082	-0.438	0.057	1.287	-0.951
			0.336	0.865	-0.047	0.127	1.127	-0.517
			0.508	0.733	0.061	0.259	0.920	-0.093
			0.679	0.626	0.068	0.458	0.753	0.071
			0.851	0.561	0.019	0.657	0.624	0.108
			1.000	0.509	0.000	0.896	0.535	0.007
						1.000	0.502	0.000

y/Y2 462	u/U	P/gaY2
0.000	0.000	-1.646
0.004	1.435	-1.450
0.008	1.442	-1.480
0.010	1.430	-1.438
0.051	1.322	-1.089
0.104	1.171	-0.641
0.220	0.992	-0.243
0.389	0.807	0.032
0.558	0.688	0.103
0.726	0.604	0.081
0.951	0.519	0.010**
1.000	0.509	0.000

Note: See notations of Tabls 8a.
*459, 460, . . 465: Run Nos.

Table 8c: -Dimensionless velocity profiles and pressure distributions across the flow depth at weir crest C:

(c) Weir models with α=60°, β=45°.- R=15.16 cm.

Y/Y2 418*	u/U	P/gaY2	Y/Y2 419	u/U	P/gaY2	Y/Y2 420	u/U	P/gaY2
0.000	0.000	0.753	0.000	0.000	0.625	0.000	0.000	0.447
0.045	0.366	0.813	0.026	0.448	0.642	0.024	0.243	0.447
0.060	0.575	0.836	0.043	0.704	0.652	0.029	0.806	0.456
0.075	0.621	0.747	0.069	0.718	0.596	0.035	0.806	0.451
0.105	0.639	0.685	0.104	0.708	0.578	0.059	0.797	0.446
0.120	0.638	0.672	0.174	0.693	0.535	0.118	0.774	0.434
0.151	0.632	0.650	0.260	0.672	0.483	0.176	0.751	0.420
0.181	0.631	0.621	0.347	0.652	0.430	0.235	0.731	0.399
0.301	0.616	0.523	0.521	0.616	0.314	0.353	0.692	0.352
0.452	0.598	0.399	0.694	0.583	0.191	0.529	0.639	0.270
0.602	0.581	0.273	0.868	0.552	0.062	0.706	0.592	0.169
0.753	0.564	0.146	0.938	0.540	0.009	0.882	0.551	0.055
0.904	0.548	0.018	1.000	0.530	0.000	0.941	0.539	0.013
1.000	0.537	0.000				1.000	0.527	0.000

Y/Y2 421	u/U	P/gaY2	Y/Y2 422	u/U	P/gaY2
0.000	0.000	0.338	0.000	0.000	0.068
0.019	0.772	0.329	0.014	0.889	0.034
0.038	0.865	0.308	0.021	0.982	0.026
0.056	0.858	0.305	0.027	0.977	0.032
0.094	0.837	0.312	0.034	0.969	0.046
0.141	0.812	0.317	0.041	0.966	0.046
0.235	0.768	0.314	0.068	0.941	0.081
0.376	0.711	0.281	0.137	0.887	0.142
0.517	0.662	0.228	0.239	0.819	0.192
0.658	0.614	0.167	0.342	0.763	0.207
0.799	0.577	0.085	0.444	0.711	0.207
0.940	0.541	0.015**	0.581	0.656	0.171
0.968	0.534	0.005**	0.718	0.603	0.125
1.000	0.526	0.000	0.854	0.563	0.051
			0.902	0.553	0.018
			1.000	0.526	0.000

Note: See notations of Tabls 8a.

*418, 419, . . 422: Run Nos.

Table 8c: (continued).- R=2.54 cm.

y/Y2 467*	u/U	P/gaY2
0.000	0.000	-1.100
0.007	1.084	-1.100**
0.010	1.328	-1.072
0.014	1.323	-1.058
0.017	1.311	-1.018
0.031	1.288	-0.955
0.092	1.176	-0.650
0.197	1.009	-0.268
0.398	0.809	0.022
0.602	0.686	0.066
0.846	0.579	0.005
1.000	0.528	0.000

y/Y2 468	u/U	P/gaY2
0.000	0.000	-1.384
0.006	1.056	-1.385**
0.009	1.425	-1.440
0.011	1.401	-1.349
0.014	1.389	-1.309
0.021	1.374	-1.260
0.078	1.231	-0.818
0.158	1.078	-0.421
0.316	0.885	-0.069
0.556	0.710	0.069
0.796	0.592	0.039
0.876	0.562	0.007
1.000	0.529	0.000

y/Y2 469	u/U	P/gaY2
0.000	0.000	-1.404
0.004	0.684	-1.400**
0.006	1.378	-1.250
0.007	1.408	-1.369
0.009	1.403	-1.353
0.010	1.397	-1.331
0.017	1.376	-1.258
0.062	1.259	-1.313
0.124	1.110	-0.476
0.257	0.928	-0.103
0.452	0.764	0.070
0.646	0.650	0.095
0.906	0.549	0.003
1.000	0.522	0.000

y/Y2 470	u/U	P/gaY2
0.000	0.000	-1.605
0.004	0.360	-1.600**
0.006	1.462	-1.571
0.008	1.464	-1.582
0.010	1.449	-1.526
0.020	1.435	-1.485
0.054	1.331	-1.132
0.107	1.164	-0.622
0.219	0.978	-0.199
0.385	0.817	0.020
0.552	0.702	0.090
0.719	0.620	0.070
0.919	0.544	0.005**
1.000	0.520	0.000

Note: See notations of Tabls 8a.
*467, 468, . . 473: Run Nos.

Table 9a: -Samples of velocity distribution data for flow over the crest C (Fig.2a):

(a) Weir models with α=90°, no D/S slope and vent open.

Run #	y	u	y/yo	y/R	H1	y/H1	u/U	A*(4)	CulA*
407L	0.000	0.000	0.000	0.000	8.291	0.000	0.000	-	-
	0.150	0.913	0.025	0.010	8.291	0.018	0.716	0.009	0.009
	0.300	0.921	0.050	0.020	8.291	0.036	0.722	0.018	0.027
	0.500	0.912	0.083	0.033	8.291	0.060	0.715	0.024	0.050
	1.000	0.884	0.165	0.066	8.291	0.121	0.693	0.058	0.108
	2.000	0.836	0.330	0.132	8.291	0.241	0.655	0.111	0.220
	3.000	0.789	0.495	0.198	8.291	0.362	0.619	0.105	0.325
	4.000	0.746	0.660	0.264	8.291	0.482	0.585	0.099	0.424
	5.000	0.707	0.825	0.330	8.291	0.603	0.554	0.094	0.518
	5.650	0.685	0.932	0.373	8.291	0.681	0.537	0.059	0.577
	6.060	0.673	1.000	0.400	8.291	0.731	0.528	0.036	0.613
							SUM=	0.613	
408L	0.000	0.000	0.000	0.000	12.375	0.000	0.000	-	—
	0.250	1.265	0.028	0.016	12.375	0.020	0.812	0.011	0.011
	0.500	1.250	0.056	0.033	12.375	0.040	0.802	0.023	0.034
	1.000	1.220	0.112	0.066	12.375	0.081	0.783	0.045	0.079
	2.000	1.150	0.225	0.132	12.375	0.162	0.738	0.085	0.164
	3.000	1.086	0.337	0.198	12.375	0.242	0.697	0.081	0.245
	4.500	1.003	0.506	0.297	12.375	0.364	0.644	0.113	0.358
	6.000	0.931	0.674	0.396	12.375	0.485	0.597	0.105	0.462
	7.500	0.866	0.843	0.495	12.375	0.606	0.556	0.097	0.559
	8.500	0.831	0.955	0.561	12.375	0.687	0.533	0.061	0.621
	8.900	0.817	1.000	0.587	12.375	0.719	0.524	0.024	0.644
							SUM=	0.644	
409L	0.000	0.000	0.000	0.000	15.149	0.000	0.000	-	—
	0.250	1.498	0.023	0.016	15.149	0.017	0.869	0.010	0.010
	0.500	1.485	0.046	0.033	15.149	0.033	0.861	0.020	0.030
	1.000	1.437	0.092	0.066	15.149	0.066	0.834	0.039	0.069
	2.000	1.357	0.184	0.132	15.149	0.132	0.787	0.074	0.143
	3.500	1.257	0.322	0.231	15.149	0.231	0.729	0.105	0.248
	5.000	1.158	0.460	0.330	15.149	0.330	0.672	0.097	0.344
	6.000	1.107	0.551	0.396	15.149	0.396	0.642	0.060	0.405
	7.500	1.030	0.689	0.495	15.149	0.495	0.597	0.085	0.490
	9.000	0.970	0.827	0.594	15.149	0.594	0.563	0.080	0.570
	10.40	0.916	0.956	0.686	15.149	0.687	0.531	0.070	0.641
	10.88	0.900	1.000	0.718	15.149	0.718	0.522	0.023	0.664
							SUM=	0.664	

(Cont'd)

Note: Tables 9a, 9b and 9c consist of 26 columns to be read horizontally. y in cm, u in m/sec, y/yo=y/Y_2, H1=H_1, A* (4)= area of velocity diagram between two layers of thickness dy (Fig.2c), CulA*= Σ A*(4), %= % of A*(4), Umax=U_{max}, A*(5) and A*(7) are intermediate results (not relevant), UCR=U_1 (Eq.22), P/gaCR=P/γ at crest, Vt=V_t (tangential velocity u/sinϕ, Fig.2b), Vt2/2g=$V_t^2/2g$, Hc= computed total head, %AHc= % deviation between Hc and H_1, H1-Zi= H_1-Z (intermediate results), Pi/ga=P/γ, Pi/gah=P/γh, P/gaYo=P/γY_2, A(4)= area of elemental pressure diagram and K2=K_2. The sum (P/γ+z) for y$\leq\delta$ is assumed to be equal to measured wall pressure at the crest (Col.17). For other regions (y>δ) the pressure is computed using Bernoulli's equation (Col.23).

Table 9a: (continued)

%	u/Umax	A*(5)	A*(7)	u/UCR	A*(5)	P/gaCR	Vt	Vt2/2g
—	0.000	—	—	0.000	—	3.700	0.000	0.000
1.445	0.991	0.005	0.009	0.962	0.005		0.914	4.256
4.348	1.000	0.010	0.018	0.970	0.010		0.923	4.339
8.217	0.990	0.013	0.024	0.961	0.013		0.915	4.264
17.694	0.960	0.032	0.059	0.931	0.031		0.889	4.030
35.846	0.908	0.062	0.113	0.881	0.060		0.846	3.648
52.994	0.857	0.058	0.106	0.831	0.056		0.803	3.288
69.194	0.810	0.055	0.101	0.786	0.053		0.764	2.975
84.527	0.768	0.052	0.095	0.745	0.050		0.729	2.705
94.076	0.744	0.032	0.059	0.722	0.031		0.709	2.560
99.952	0.731	0.020	0.036	0.709	0.019	0.000	0.698	2.483
		0.339	0.620		0.329			
—	0.000	—	—	0.000	—	4.000	0.000	0.000
1.771	0.996	0.008	0.010	0.987	0.008		1.267	8.178
5.291	0.984	0.016	0.020	0.975	0.016		1.253	8.007
12.205	0.961	0.032	0.039	0.952	0.032		1.227	7.668
25.473	0.906	0.062	0.075	0.897	0.061		1.162	6.887
37.991	0.855	0.058	0.071	0.847	0.058		1.104	6.209
55.534	0.790	0.081	0.100	0.782	0.081		1.028	5.383
71.776	0.733	0.075	0.092	0.726	0.075		0.962	4.716
86.866	0.682	0.070	0.086	0.676	0.069		0.902	4.149
96.367	0.654	0.044	0.054	0.648	0.044		0.871	3.863
100.058	0.643	0.017	0.021	0.637	0.017	0.000	0.858	3.751
		0.464	0.569		0.460			
—	0.000	—	—	0.000	—	3.400	0.000	0.000
1.503	0.999	0.008	0.008	0.987	0.008		1.500	11.47
4.497	0.990	0.016	0.016	0.978	0.016		1.489	11.30
10.362	0.958	0.032	0.032	0.946	0.032		1.445	10.64
21.579	0.905	0.061	0.061	0.894	0.061		1.373	9.606
37.320	0.838	0.086	0.086	0.828	0.085		1.283	8.389
51.862	0.772	0.080	0.080	0.763	0.079		1.192	7.248
60.955	0.738	0.050	0.050	0.729	0.049		1.147	6.703
73.824	0.687	0.070	0.071	0.678	0.070		1.077	5.909
85.867	0.647	0.066	0.066	0.639	0.065		1.023	5.336
96.467	0.611	0.058	0.058	0.603	0.057		0.975	4.841
99.966	0.600	0.019	0.019	0.593	0.019	0.000	0.960	4.701
		0.547	0.548		0.541			

(Cont'd)

Table 9a: (continued)

Hc	%AHc	Hi-Zi	Pi/ga	Pi/gah	P/gaYo	A (4)
		8.291	3.700	0.611	0.611	–
		8.141	3.885	0.657	0.641	0.015
8.339	0.575	7.991	3.652	0.634	0.603	0.015
		7.791	3.527	0.634	0.582	0.020
		7.291	3.261	0.644	0.538	0.046
		6.291	2.643	0.651	0.436	0.080
		5.291	2.003	0.654	0.330	0.063
		4.291	1.316	0.639	0.217	0.045
		3.291	0.586	0.553	0.097	0.026
		2.641	0.081	0.199	0.013	0.006
8.543	3.041	2.231	0.000	0.000	0.000	0.000
					SUM=	0.318
					K2=	0.635
		12.37	4.000	0.449	0.449	–
12.428	0.428	12.12	3.947	0.456	0.443	0.013
		11.87	3.868	0.461	0.435	0.012
		11.37	3.707	0.469	0.417	0.024
		10.37	3.488	0.505	0.392	0.045
		9.375	3.166	0.537	0.356	0.042
		7.875	2.492	0.566	0.280	0.054
		6.375	1.659	0.572	0.186	0.039
		4.875	0.726	0.519	0.082	0.023
		3.875	0.012	0.030	0.001	0.005
12.651	2.227	3.475	0.000	0.000	0.000	0.000
					SUM=	0.256
					K2=	0.513
		15.14	3.400	0.313	0.313	–
15.120	-0.188	14.89	3.429	0.323	0.315	0.007
		14.64	3.344	0.322	0.307	0.007
		14.14	3.501	0.354	0.322	0.014
		13.14	3.543	0.399	0.326	0.030
		11.64	3.260	0.442	0.300	0.043
		10.14	2.901	0.493	0.267	0.039
		9.149	2.446	0.501	0.225	0.023
		7.649	1.740	0.515	0.160	0.027
		6.149	0.813	0.432	0.075	0.016
		4.749	0.000	0.000	0.000	0.005
15.581	2.853	4.269	0.000	0.000	0.000	0.000
					SUM=	0.211
					K2=	0.422

Table 9b: -Samples of velocity distribution data for flow over the crest C:
(b) Weir models with α=90°, β=45° (9045).

Note: See notations of Table 9a.

Run #	y	u	y/yo	y/R	H1	y/H1	u/U	A*(4)	u/Umax
416L	0.000	0.000	0.000	0.000	17.37	0.000	0.000	—	0.000
	0.250	1.686	0.020	0.016	17.37	0.014	0.913	0.009	0.998
	0.500	1.670	0.040	0.033	17.37	0.029	0.905	0.018	0.988
	1.000	1.621	0.080	0.066	17.37	0.058	0.878	0.036	0.959
	1.500	1.570	0.121	0.099	17.37	0.086	0.850	0.035	0.929
	2.500	1.487	0.201	0.165	17.37	0.144	0.805	0.067	0.880
	3.500	1.410	0.281	0.231	17.37	0.201	0.764	0.063	0.834
	5.000	1.311	0.402	0.330	17.37	0.288	0.710	0.089	0.776
	6.500	1.222	0.523	0.429	17.37	0.374	0.662	0.083	0.723
	8.000	1.146	0.643	0.528	17.37	0.460	0.621	0.077	0.678
	9.500	1.075	0.764	0.627	17.37	0.547	0.582	0.073	0.636
	11.00	1.016	0.884	0.726	17.37	0.633	0.550	0.068	0.601
	12.00	0.981	0.965	0.792	17.37	0.691	0.531	0.043	0.580
	12.44	0.965	1.000	0.821	17.37	0.716	0.523	0.019	0.571
							SUM=	0.679	
417L	0.000	0.000	0.000	0.000	20.51	0.000	0.000	—	0.000
	0.250	1.953	0.017	0.016	20.51	0.012	0.974	0.008	0.996
	0.500	1.9[illegible]	0.034	0.033	20.51	0.024	0.962	0.017	0.985
	1.000	1.880	0.068	0.066	20.51	0.049	0.937	0.032	0.959
	2.000	1.779	0.136	0.132	20.51	0.097	0.887	0.062	0.908
	3.500	1.635	0.239	0.231	20.51	0.171	0.815	0.087	0.834
	5.000	1.518	0.341	0.330	20.51	0.244	0.757	0.080	0.774
	6.500	1.422	0.443	0.429	20.51	0.317	0.709	0.075	0.726
	8.000	1.332	0.546	0.528	20.51	0.390	0.664	0.070	0.680
	9.500	1.253	0.648	0.627	20.51	0.463	0.625	0.066	0.639
	11.00	1.179	0.750	0.726	20.51	0.536	0.588	0.062	0.602
	12.50	1.123	0.853	0.824	20.51	0.609	0.560	0.059	0.573
	13.20	1.097	0.900	0.871	20.51	0.643	0.547	0.026	0.560
	14.66	1.025	1.000	0.967	20.51	0.715	0.511	0.053	0.523
							SUM=	0.698	

(Cont'd)

Table 9b: (continued)

A*(5)	A*(7)	u/UCR	A*(5)	P/gaCR	Vt	Vt2/2g	Hc	%AHc	H1-Zi
—	—	0.000	—	2.700	0.000	0.000			17.37
0.008	0.007	0.994	0.008		1.688	14.52	17.474	0.576	17.12
0.016	0.014	0.984	0.016		1.674	14.28			16.87
0.032	0.028	0.955	0.032		1.629	13.52			16.37
0.031	0.027	0.925	0.031		1.582	12.75			15.87
0.060	0.052	0.876	0.059		1.506	11.55			14.87
0.057	0.049	0.831	0.056		1.435	10.49			13.87
0.080	0.070	0.773	0.079		1.344	9.210			12.37
0.074	0.065	0.720	0.074		1.263	8.125			10.87
0.069	0.060	0.675	0.069		1.193	7.256			9.374
0.065	0.057	0.634	0.065		1.128	6.485			7.874
0.061	0.053	0.599	0.061		1.074	5.884			6.374
0.039	0.034	0.578	0.039		1.043	5.543			5.374
0.017	0.015	0.569	0.017	0.000	1.028	5.389	17.829	2.617	4.934
0.609	0.531		0.607						
—	—	0.000	—	1.000	0.000	0.000			20.51
0.008	0.006	1.123	0.009		1.955	19.48	20.732	1.070	20.26
0.016	0.012	1.110	0.018		1.934	19.06			20.01
0.032	0.024	1.081	0.036		1.888	18.17			19.51
0.062	0.046	1.023	0.069		1.794	16.41			18.51
0.086	0.064	0.940	0.097		1.660	14.04			17.01
0.080	0.059	0.873	0.090		1.551	12.26			15.51
0.074	0.055	0.818	0.084		1.463	10.91			14.01
0.070	0.051	0.766	0.078		1.380	9.702			12.51
0.065	0.048	0.720	0.074		1.307	8.701			11.01
0.061	0.045	0.678	0.069		1.238	7.809			9.513
0.058	0.043	0.646	0.065		1.187	7.182			8.013
0.026	0.019	0.631	0.029		1.163	6.897			7.313
0.052	0.039	0.589	0.059	0.000	1.094	6.103	20.763	1.219	5.853
0.691	0.510		0.778						

(Cont'd)

Table 9b: (continued)

Pi/ga	Pi/gah	P/gaYo	.A (4)
2.700	0.217	0.217	—
2.600	0.213	0.209	0.004
2.589	0.217	0.208	0.004
2.848	0.249	0.229	0.009
3.122	0.285	0.251	0.010
3.320	0.334	0.267	0.021
3.381	0.378	0.272	0.022
3.164	0.425	0.254	0.032
2.749	0.463	0.221	0.029
2.118	0.477	0.170	0.024
1.389	0.472	0.112	0.017
0.490	0.340	0.039	0.009
0.000	0.000	0.000	0.002
0.000	0.000	0.000	0.000
		SUM=	0.181
		K2=	0.362
1.000	0.068	0.068	—
0.781	0.054	0.053	0.001
0.946	0.067	0.064	0.001
1.342	0.098	0.092	0.003
2.100	0.166	0.143	0.008
2.967	0.266	0.202	0.018
3.244	0.336	0.221	0.022
3.103	0.380	0.212	0.022
2.811	0.422	0.192	0.021
2.312	0.448	0.158	0.018
1.704	0.466	0.116	0.014
0.831	0.385	0.057	0.009
0.416	0.285	0.028	0.002
0.000	0.000	0.000	0.001
		SUM=	0.139
		K2=	0.278

Table 9c: -Samples of velocity distribution data for flow over the crest C:
(c) Weir models with α=60°, β=45°.

Note: See notations of Table 9a.

Run #	y	u	y/yo	y/R	H1	y/H1	u/U	A*(4)	u/Umax
421L	0.000	0.000	0.000	0.000	14.81	0.000	0.000	—	0.000
	0.200	1.316	0.019	0.013	14.81	0.014	0.772	0.007	0.892
	0.400	1.475	0.038	0.026	14.81	0.027	0.865	0.015	1.000
	0.600	1.462	0.056	0.040	14.81	0.041	0.858	0.016	0.991
	1.000	1.427	0.094	0.066	14.81	0.068	0.837	0.032	0.967
	1.500	1.385	0.141	0.099	14.81	0.101	0.812	0.039	0.939
	2.500	1.309	0.235	0.165	14.81	0.169	0.768	0.074	0.887
	4.000	1.212	0.376	0.264	14.81	0.270	0.711	0.104	0.822
	5.500	1.128	0.517	0.363	14.81	0.371	0.662	0.097	0.765
	7.000	1.047	0.658	0.462	14.81	0.473	0.614	0.090	0.710
	8.500	0.983	0.799	0.561	14.81	0.574	0.577	0.084	0.666
	10.00	0.922	0.940	0.660	14.81	0.675	0.541	0.079	0.625
	10.30	0.910	0.968	0.679	14.81	0.695	0.534	0.015	0.617
	10.64	0.897	1.000	0.702	14.81	0.718	0.526	0.017	0.608
							SUM=	0.669	
422L	0.000	0.000	0.000	0.000	20.51	0.000	0.000	—	0.000
	0.200	1.784	0.014	0.013	20.51	0.010	0.889	0.006	0.906
	0.300	1.970	0.021	0.020	20.51	0.015	0.982	0.006	1.000
	0.400	1.960	0.027	0.026	20.51	0.019	0.977	0.007	0.995
	0.500	1.944	0.034	0.033	20.51	0.024	0.969	0.007	0.987
	0.600	1.938	0.041	0.040	20.51	0.029	0.966	0.007	0.984
	1.000	1.888	0.068	0.066	20.51	0.049	0.941	0.026	0.958
	2.000	1.780	0.137	0.132	20.51	0.097	0.887	0.062	0.904
	3.500	1.644	0.239	0.231	20.51	0.171	0.819	0.087	0.835
	5.000	1.531	0.342	0.330	20.51	0.244	0.763	0.081	0.777
	6.500	1.427	0.444	0.429	20.51	0.317	0.711	0.076	0.724
	8.500	1.316	0.581	0.561	20.51	0.414	0.656	0.093	0.668
	10.50	1.210	0.718	0.693	20.51	0.512	0.603	0.086	0.614
	12.50	1.130	0.854	0.824	20.51	0.609	0.563	0.080	0.574
	13.20	1.109	0.902	0.871	20.51	0.643	0.553	0.027	0.563
	14.63	1.056	1.000	0.965	20.51	0.713	0.526	0.053	0.536
							SUM=	0.704	

(Cont'd)

Table 9c: (continued)

A*(5)	A*(7)	u/UCR	A*(5)	P/gaCR	Vt	Vt2/2g	Hc	%AHc	H1-Zi
—	—	0.000	—	3.600	0.000	0.000			14.81
0.006	0.006	0.887	0.006		1.317	8.846			14.61
0.012	0.013	0.994	0.012		1.478	11.13	15.137	2.186	14.41
0.013	0.013	0.985	0.013		1.467	10.96			14.21
0.026	0.026	0.962	0.026		1.435	10.49			13.81
0.031	0.032	0.934	0.031		1.396	9.937			13.31
0.060	0.062	0.883	0.060		1.327	8.974			12.31
0.085	0.087	0.817	0.084		1.239	7.821			10.81
0.078	0.080	0.760	0.078		1.162	6.888			9.313
0.073	0.075	0.706	0.073		1.088	6.034			7.813
0.068	0.070	0.663	0.068		1.030	5.410			6.313
0.064	0.065	0.622	0.064		0.975	4.841			4.813
0.012	0.013	0.614	0.012		0.964	4.732			4.513
0.014	0.014	0.605	0.014	0.000	0.952	4.616	15.256	2.988	4.173
0.543	0.556		0.540						
—	—	0.000	—	1.000	0.000	0.000			20.51
0.006	0.004	0.912	0.006		1.786	16.25			20.31
0.006	0.005	1.007	0.006		1.973	19.83	21.132	3.017	20.21
0.007	0.005	1.002	0.007		1.963	19.64			20.11
0.007	0.005	0.994	0.007		1.948	19.34			20.01
0.006	0.005	0.990	0.007		1.943	19.24			19.91
0.026	0.019	0.965	0.026		1.896	18.32			19.51
0.061	0.045	0.910	0.062		1.796	16.43			18.51
0.086	0.064	0.840	0.087		1.669	14.20			17.01
0.080	0.059	0.782	0.080		1.565	12.48			15.51
0.074	0.055	0.729	0.075		1.468	10.98			14.01
0.092	0.068	0.673	0.092		1.366	9.514			12.01
0.085	0.063	0.618	0.085		1.268	8.189			10.01
0.078	0.058	0.578	0.079		1.195	7.274			8.013
0.026	0.019	0.567	0.026		1.176	7.051			7.313
0.052	0.038	0.540	0.052	0.000	1.127	6.478	21.108	2.900	5.883
0.692	0.511		0.696						

(Cont'd)

Table 9c: (continued)

Pi/ga	Pi/gah	P/gaYo	A (4)
3.600	0.338	0.338	—
3.500	0.335	0.329	0.006
3.276	0.320	0.308	0.006
3.248	0.323	0.305	0.006
3.321	0.345	0.312	0.012
3.376	0.369	0.317	0.015
3.339	0.410	0.314	0.030
2.992	0.451	0.281	0.042
2.425	0.472	0.228	0.036
1.779	0.489	0.167	0.028
0.903	0.422	0.085	0.018
0.000	0.000	0.000	0.006
0.000	0.000	0.000	0.000
0.000	0.000	0.000	0.000
		SUM=	0.204
		K2=	0.407
1.000	0.068	0.068	—
0.500	0.035	0.034	0.001
0.381	0.027	0.026	0.000
0.465	0.033	0.032	0.000
0.668	0.047	0.046	0.000
0.670	0.048	0.046	0.000
1.187	0.087	0.081	0.002
2.081	0.165	0.142	0.008
2.811	0.253	0.192	0.017
3.032	0.315	0.207	0.020
3.025	0.372	0.207	0.021
2.499	0.408	0.171	0.026
1.824	0.442	0.125	0.020
0.739	0.347	0.051	0.012
0.262	0.183	0.018	0.002
0.000	0.000	0.000	0.001
		SUM=	0.130
		K2=	0.261

Table 10: -Variation with H_1/R of experimental parameters related to tests with measured velocity profiles.

Run#	H1/R	P/H1	Y2/H1	A* (4)	K2 (4)	m	Kw
407	0.547	14.04	0.719	0.613	0.635	0.786	0.998
408	0.816	9.40	0.719	0.644	0.513	1.250	0.995
409	0.999	7.68	0.718	0.664	0.422	1.312	0.993
410	1.162	6.60	0.718	0.680	0.399	1.313	0.989
411	1.381	5.56	0.718	0.697	0.284	1.460	0.987
453	2.009	22.96	0.749	0.744	-0.003	1.406	0.999
454	2.364	19.51	0.756	0.720	0.095	1.689	0.998
454a	2.865	16.10	0.770	0.699	0.183	2.000	0.997
455	3.489	13.22	0.784	0.683	0.231	2.528	0.997
456	4.359	10.48	0.790	0.653	0.341	2.980	0.996
413	0.444	17.28	0.724	0.593	0.694	1.051	0.999
414	0.728	10.55	0.715	0.634	0.561	1.061	0.996
415	0.905	8.48	0.720	0.658	0.454	1.280	0.994
416	1.146	6.70	0.716	0.679	0.362	1.418	0.989
417	1.353	5.67	0.715	0.698	0.278	1.467	0.987
459	2.285	20.18	0.737	0.777	-0.183	1.346	0.998
460	3.126	14.75	0.735	0.797	-0.300	1.528	0.996
461	3.957	11.65	0.735	0.787	-0.254	1.847	0.993
462	4.778	9.65	0.734	0.797	-0.297	2.018	0.991
419	0.525	14.63	0.717	0.609	0.640	0.786	0.998
420	0.782	9.82	0.717	0.638	0.523	1.090	0.996
421	0.977	7.86	0.718	0.669	0.407	1.346	0.993
422	1.353	5.67	0.713	0.704	0.261	1.480	0.989
423	1.086	7.07	0.717	0.682	0.405**	1.333	
467	2.680	17.21	0.722	0.799	-0.274	1.439	
468	3.411	13.52	0.722	0.807	-0.319	1.665	
469	4.195	10.99	0.723	0.801	-0.290	1.979	
470	4.877	9.45	0.727	0.802	-0.297	2.082	

Note: Run#= identification codes of tests, H1/R=H_1/R, P/H1=p/H_1, Y2/H1=Y_2/H_1, A*(4)=total A*, K2(4)=K_2 (correction factor for pressure distribution across flow depth at crest), m= computed m using Eq.1 and Kw=K_w (correction factor for wall pressure force). **Interpolated value.

Table 11a*: -Variation with H_1/R of H_δ/H_1, H_S/H_1, Y_2/H_1, δ/H_1 and $(P/\gamma H_1)_{cr}$ -Verification of irrotationality of flow over the weir crest.

(a) Weir models with α=90°, no D/S slope and vent open.

Run #	H1/R	H1	Y2	d	P/ga)cr	u max	u fs	Pi	v^2/2g
407	0.55	8.29	6.06	0.34	3.70	0.92	0.67	0.28	4.34
408	0.82	12.36	8 90	0.29	4.00	1.26	0.82	0.31	8.16
409	1.00	15.15	10.88	0.27	3.40	1.50	0.90	0.33	11.47
410	1.16	17.62	12.56	0.25	2.30	1.69	0.97	0.35	14.59
411	1.38	20.94	14.94	0.23	0.80	1.98	1.03	0.36	20.02
453	2.01	5.09	3.81	0.07	-1.60	1.13	0.52	0.39	6.50
454	2.36	6.00	4.54	0.07	-1.80	1.21	0.55	0.37	7.47
451	2 87	7.28	5.61	0.13	-1.90	1.30	0.59	0.35	8.69
455	3.49	8.87	6.95	0.08	-1.70	1.41	0.62	0.32	10.17
456	4.40	11.16	8.81	0.12	-1.05	1.51	0.67	0.30	11.65

(Cont'd)

(Table 11a - continued)

v^2/2g fs	H d	H fs	Hd/Hfs	Hd/H1	Hfs/H1	Y2/H1	d/H1	P/gacrH1
2.48	8.34	8.54	0.98	1.01	1.03	0.73	0.04	0.45
3.75	12.43	12.65	0.98	1.00	1.02	0.72	0.02	0.32
4.70	15.12	15.58	0.97	1.00	1.03	0.72	0.02	0.22
5.10	17.14	17.66	0.97	0.97	1.00	0.71	0.01	0.13
6.23	21.07	21.17	1.00	1.01	1.01	0.71	0.01	0.04
1.58	4.97	5.39	0.92	0 98	1.06	0.75	0.01	-0.31
1.74	5.74	6.28	0.91	0.96	1.05	0.76	0.01	-0.30
2.00	6.92	7.61	0.91	0.95	1.05	0.77	0.02	-0.26
2.21	8.55	9.16	0.93	0.96	1.03	0.78	0.01	-0.19
2.51	10.72	11.32	0.95	0.96	1.01	0.79	0.01	-0.09

(Cont'd)

(Table 11a - continued)

Vd/H1	Vf/H1
0.52	0.30
0.66	0.30
0.76	0.31
0.83	0.29
0.96	0.30
1.28	0.31
1.24	0.29
1.19	0 28
1.15	0.25
1.04	0.22

*Note: Tables 11a, 11b and 11c consist of 21 columns to be read horizontally. H1/R=H_1/R, H1=H_1 in cm, Y2=Y_2 in cm, d=δ in cm, P/ga)cr=$(P/\gamma)_{cr}$ in cm, u max= u_{max} in m/sec, u fs=u_S at free surface in m/sec, Pi=ϕ at free surface in radian, v^2/2g=$V_\delta^2/2g$ in cm, v^2/2g=$V_S^2/2g$ in cm, Hd=H_δ in cm, H fs=H_S in cm, P/gacrH1=$P/\gamma H_1$ at crest, P/gaminH=$P/\gamma H_1$ at minimum pressure location, Vd/H1=normalized velocity head at y=δ and Vf/H1=normalized velocity head at free surface.

Table 11b: -Variation with H_1/R of $H_\delta/H_1, H_S/H_1, Y_2/H_1, \delta/H_1$ and $(P/\gamma H_1)_{cr}$ -Verification of irrotationality of flow over the weir crest.

(b) Weir models with $\alpha=90°$, $\beta=45°$.

Note: See notations of Table 11a.

Run #	H1/R	H1	Y2	d	P/ga)cr	u max	u fs	Pi	v^2/2g	v^2/2g fs
413	0.44	6.74	4.88	0.36	3.40	0 79	0.61	0.26	3.18	2 05
414	0.73	11.03	7.89	0.30	3.85	1.15	0.77	0.30	6.78	3.31
415	0.91	13.72	9.86	0.27	3.80	1.39	0 86	0.32	9.80	4 22
416	1.15	17.37	12.44	0.25	2.70	1.69	0.96	0.35	14.52	5.39
417	1.35	20.51	14.66	0.23	1.00	1.95	1.02	0.37	19.48	6.10
459	2.29	5.79	4.27	0.08	-3.50	1.33	0.55	0.41	9.06	1.79
460	3.13	7.92	5.82	0.08	-7.85	1.74	0.64	0.40	15.43	2.41
461	3.96	10.06	7.53	0.07	-10.70	2.00	0.70	0.37	20 33	2.92
462	4.78	12.13	8.90	0.07	-14.40	2.22	0.79	0.39	25.33	3.67

(Cont'd)

(Table 11b - continued)

Hd	H fs	Hd/Hfs	Hd/H1	Hfs/H1	Y2/H1	d/H1	P/gacrH1	Vd/H1	Vf/H1
6.83	6.93	0.99	1.01	1.03	0.72	0.05	0.50	0.47	0.30
10.88	11.20	0.97	0.99	1.02	0.72	0.03	0.35	0.61	0.30
13.85	14.08	0.98	1.01	1.03	0.72	0.02	0.28	0.71	0 31
17.47	17.83	0.98	1.01	1.03	0.72	0.01	0.16	0.84	0.31
20.73	20.76	1.00	1.01	1.01	0.71	0.01	0.05	0.95	0.30
5.64	6.06	0.93	0.97	1.05	0.74	0.01	-0.60	1.56	0.31
7.66	8.23	0.93	0.97	1.04	0.73	0.01	-0.99	1.95	0 30
9.71	10.45	0.93	0.96	1.04	0.75	0.01	-1.06	2.02	0 29
10.99	12.57	0.87	0.91	1.04	0.73	0.01	-1.19	2.09	0.30

Table 11c: -Variation with H_1/R of $H_\delta/H_1, H_S/H_1, Y_2/H_1, \delta/H_1$ and $(P/\gamma H_1)_{cr}$ -Verification of irrotationality of flow over the weir crest.

(c) Weir models with $\alpha=60°$, $\beta=45°$.

Note: See notations of Table 11a.

Run #	H1/R	H1	Y2	d	P/ga)cr	u max	u fs	PI	v^2/2g
419	0.53	7.96	5.76	0.34	3.60	0.90	0.66	0.27	4.12
420	0.78	11.86	8.50	0.29	3.80	1.23	0.80	0.30	7.73
421	0.98	14.81	10.64	0.26	3.60	1.48	0.90	0.33	11.14
422	1.35	20.51	14.63	0.23	1.00	1.97	1.06	0.37	19.83
423	1.09	16.48	11.80	0.25	2.90	1.62	0.96	0.34	13 38
467	2.68	6.80	4.91	0.05	-5.40	1.53	0.61	0.40	12.01
468	3.41	8.66	6.25	0.06	-8.65	1.86	0.69	0.39	17.60
469	4.20	10.67	7.71	0.06	-10.82	2.04	0.76	0.38	21.17
470	4.88	12.37	8.90	0.07	-14.43	2.28	0.81	0.38	26.52
474	3.94	10.03	7.10	0.08	-10.45	1.97	0.74	0.38	19.78

(Cont'd)

(Table 11c - continued)

v^2/2g fs	Hd	H fs	Hd/Hfs	Hd/H1	Hfs/H1	Y2/H1	d/H1	P/gacrH1
2.42	8.12	8.18	0.99	1.02	1.03	0.72	0.04	0.45
3.60	11.78	12.10	0.97	0.99	1.02	0.72	0.02	0.32
4.62	15.14	15.26	0.99	1.02	1.03	0.72	0.02	0.24
6.48	21.13	21.11	1.00	1.03	1.03	0.71	0.01	0.05
5.32	16.58	17.12	0.97	1.01	1.04	0.72	0.02	0.18
2.23	6.66	7.14	0.93	0.98	1.05	0.72	0.01	-0.79
2.84	9.01	9.09	0.99	1.04	1.05	0.72	0.01	-1.00
3.36	10.40	11.07	0.94	0.97	1.04	0.72	0.01	-1.01
3.87	12.17	12.86	0.95	0.98	1.04	0.72	0.01	-1.17
3 24	9.41	10.34	0.91	0.94	1.03	0.71	0.01	-1.04

(Cont'd)

(Table 11c - continued)

Vd/H1	Vf/H1
0.52	0.30
0.65	0.30
0.75	0.31
0.97	0.32
0.81	0.32
1.77	0.33
2.03	0.33
1.98	0.31
2.14	0.31
1.97	0.32

Table 12a: -Pressure distribution measured on U/S vertical walls:
(a) Weir model with R=15.16 cm.

Z CW1	P/ga407	408	409	410	411	413	414	415	416
0.00	124.72	128.80	131.58	134.05	137.37	123.17	127.46	130 15	133.80
25.08	99.24	103 34	106.19	108.74	112.04	97.94	102.04	104.79	108 54
30.16	94.15	98.25	101.10	103.65	106 95	92.85	96.95	99 70	103.45
35.24	89.10	93.20	96.05	98.60	101.90	87.80	91.90	94 65	98.40
40.32	84.00	88.10	90.95	93.50	96.80	82 70	86.80	89.55	93.30
45.40	78.91	83.01	85.86	88 41	91.71	77.61	81.71	84 46	88 21
50.48	73.68	77.96	80.81	83 36	86 66	72.56	76.66	79.41	83.16
56.56	68.76	72.86	75 71	78 26	81.56	67.46	71.56	74 31	78.06
60.64	63.07	67.77	70.62	73.17	76.47	62 37	66 47	69 22	72 97
65.72	58.62	62.72	65.57	68.12	71.42	57.32	61.42	64 17	67 92
70.80	53 52	57 62	60 47	63.02	66.27	52 22	56 32	59 07	62 82
75.88	48.43	52.53	55.38	57 83	61.13	47.08	51 18	53.93	57.73
80.96	43.38	47 48	50.28	52.68	56.08	42.03	46 13	48.88	52 68
86.04	38.28	42.38	45.18	47.48	50.88	36.88	40.98	43 78	47 48
91.12	33.14	37.19	39 99	42.29	45.69	31.79	35 79	38 59	42 29
96.20	28.09	32.04	34.74	37.14	40.24	26 74	30 74	33 44	37.04
101.28	22.97	26.84	29.49	31 64	34.54	21.59	25.59	28 14	31 54
102.60	21.63	25.43	27.98	29.93	32 63	20.26	24.23	26 63	29 83
103.91	20.22	24.02	26.42	28 32	30.82	18 92	22.82	25.12	28 17
105.22	18.86	22.61	24.91	26 61	29 01	17.61	21 41	23 61	26 51
106.47	17.56	21.06	23.31	24 96	27.16	16 31	19 96	22 06	24 86
107.69	16 24	19.74	21.89	23.44	25 34	15.04	18.64	20 69	23 24
108.87	14.96	18.21	20.26	21.76	23.56	13.86	17.16	19.21	21.56
109.97	13.81	16.86	18 86	20.16	21.66	12 76	15 86	17 86	20.06
111.04	12.59	15 59	17.39	18 54	19.79	11.64	14.59	16 49	18.39
112.01	11.42	14.32	15.82	16.92	17.82	10 52	13.42	15 02	16 82
112.90	10.38	13.13	14.43	15 43	15 93	9.53	12.18	13 73	15 13
113 69	9 54	11.84	13.04	13 64	13.94	8.54	11 14	12 39	13 54
114.42	8.61	10.66	11 56	11.96	12.01	7 61	9.91	11.01	12 01
115.03	7.60	9.55	10.20	10.64	10.20	6.80	8.90	9 80	10 40
115.52	6 71	8 36	8.76	8 71	8 21	6 11	7.81	8 51	8 71
115.92	5.91	7.21	7.46	7.21	6.41	5 31	6.71	7 21	7 31
116.22	5.11	6.21	6.16	5 61	4.51	4 61	5 81	6 11	5 81
116.37	4.46	5.06	4.76	3 96	2.56	3.96	4.86	4.86	4.16
116.43	3.70	4.00	3.40	2 30	0 80	3.40	3.85	3 80	2 70

Additional columns - continued in subsequent two pages.

Note: Table 12a consists of 22 columns to be read horizontally. Z CW1= elevation z in cm from channel bed, Col.2-11=P/γ values and the three-digit numbers (408, 409,..) are identification codes of tests, Col. 12 (y=z/p): normalized distance from channel bed, other coordinates x () columns denote normalized pressure head; the number in () such as .547, .816,..denote values of corresponding H_1/R.

Table 12a: (continued)

417	y=z/P	x(.547/	x(.816)	x(.999)	x(1.16)	x(1.38)	x(.444/	x(.728)	x(.905)
136.94	0.00	1.00	1.00	1.00	1.00	1.00	1.00	1.00	1.00
111.74	0.22	0.80	0.80	0.81	0.81	0.82	0.80	0.80	0.81
106.65	0.26	0.75	0.76	0.77	0.77	0.78	0.75	0.76	0.77
101.60	0.30	0.71	0.72	0.73	0.74	0.74	0.71	0.72	0.73
96.50	0.35	0.67	0.68	0.69	0.70	0.70	0.67	0.68	0.69
91.41	0.39	0.63	0.64	0.65	0.66	0.67	0.63	0.64	0.65
86.36	0.43	0.59	0.61	0.61	0.62	0.63	0.59	0.60	0.61
81.21	0.49	0.55	0.57	0.58	0.58	0.59	0.55	0.56	0.57
76.07	0.52	0.51	0.53	0.54	0.55	0.56	0.51	0.52	0.53
71.02	0.56	0.47	0.49	0.50	0.51	0.52	0.47	0.48	0.49
65.92	0.61	0.43	0.45	0.46	0.47	0.48	0.42	0.44	0.45
60.78	0.65	0 39	0.41	0.42	0.43	0.45	0.38	0.40	0.41
55.68	0.70	0.35	0.37	0.38	0.39	0.41	0.34	0.36	0.38
50.48	0.74	0.31	0.33	0.34	0.35	0.37	0.30	0.32	0.34
45.28	0.78	0.27	0.29	0.30	0.32	0.33	0.26	0.28	0.30
39.94	0.83	0.23	0.25	0.26	0.28	0.29	0.22	0.24	0.26
34.14	0.87	0.18	0.21	0.22	0.24	0.25	0.18	0.20	0.22
32.23	0.88	0.17	0.20	0.21	0.22	0.24	0.16	0.19	0.20
30.57	0.89	0.16	0.19	0.20	0.21	0.22	0.15	0.18	0.19
28.66	0.90	0.15	0.18	0.19	0.20	0.21	0.14	0.17	0.18
26.96	0.91	0.14	0.16	0.18	0.19	0.20	0.13	0.16	0.17
25.14	0.92	0.13	0.15	0.17	0.17	0.18	0.12	0.15	0.16
23.26	0.94	0.12	0.14	0.15	0.16	0.17	0.11	0.13	0.15
21.46	0.94	0.11	0.13	0.14	0.15	0.16	0.10	0.12	0.14
19.59	0.95	0.10	0.12	0.13	0.14	0.14	0.09	0.11	0.13
17.82	0.96	0.09	0.11	0.12	0.13	0.13	0.09	0 11	0.12
16.73	0.97	0.08	0.10	0.11	0.12	0.12	0.08	0.10	0.11
13.84	0.98	0.08	0.09	0.10	0.10	0.10	0.07	0.09	0.10
12.01	0.98	0.07	0.08	0.09	0.09	0.09	0.06	0.08	0.08
10.30	0.99	0.06	0.07	0.08	0.08	0.07	0.06	0.07	0.08
8.31	0.99	0.05	0.06	0.07	0.06	0.06	0.05	0.06	0.07
6.51	1.00	0.05	0.06	0.06	0.05	0.05	0.04	0.05	0.06
4.71	1.00	0.04	0.05	0.05	0.04	0.03	0.04	0.05	0.05
2.71	1.00	0.04	0.04	0.04	0.03	0.02	0.03	0.04	0.04
1.00	1.00	0.03	0.03	0.03	0.02	0.01	0.03	0.03	0.03

(Cont'd)

Table 12a: (continued)

x(1.15)	x(1.35)
1.00	1.00
0.81	0.82
0.77	0.78
0.74	0.74
0.70	0.70
0.66	0.67
0.62	0.63
0.58	0.59
0.55	0.56
0.51	0.52
0.47	0.48
0.43	0.44
0.39	0.41
0.35	0.37
0.32	0.33
0.28	0.29
0.24	0.25
0.22	0.24
0.21	0.22
0.20	0.21
0.19	0.20
0.17	0.18
0.16	0.17
0.15	0.16
0.14	0.14
0.13	0.13
0.11	0.12
0.10	0.10
0.09	0.09
0.08	0.08
0.07	0.06
0.05	0.05
0.04	0.03
0.03	0.02
0.02	0.01

Note: See Table 12a for notations.

Table 12b: -Pressure distribution measured on U/S vertical walls:
(b) Weir model with R=10.08 cm.

z (cm)	y=z/P	H/R=.704	x(.704)	H/R=1.19	x(1.19)	H/R=1.64	x(1.64)	H/R=.883	x(.883)
0.00	0.00	124.02	1.00	128.90	1.00	133.47	1.00	125.82	1.00
28.01	0.24	95.89	0.77	100.69	0.78	105.34	0.79	97.59	0.78
33.18	0.28	90.71	0.73	95.61	0.74	100.26	0.75	92.51	0.74
38.26	0.33	85.73	0.69	90.53	0.70	95.18	0.71	87.43	0.69
43.34	0.37	80.55	0.65	85.42	0.66	90.10	0.68	82.35	0.65
48.42	0.41	75.47	0.61	80.37	0.62	85.02	0.64	77.27	0.61
53.50	0.46	70.39	0.57	75.26	0.58	79.94	0.60	72.19	0.57
58.58	0.50	65.31	0.53	70.16	0.54	74.81	0.56	67.11	0.53
63.66	0.54	60.23	0.49	65 08	0.50	69.73	0.52	62.03	0.49
68.74	0.59	55.15	0.44	60.00	0.47	64.65	0.48	56.95	0.45
73.82	0.63	50.07	0.40	54.92	0.43	59.57	0.45	51.87	0.41
78.90	0.67	44.99	0.36	49.82	0.39	54.46	0.41	46.79	0.37
83.98	0.72	39.91	0.32	44.74	0.35	49.31	0.37	41.71	0.33
89.06	0.76	34.83	0.28	39.63	0.31	44.13	0.33	36.63	0.29
94.14	0.81	29.75	0.24	34.55	0.27	38.95	0.29	31.55	0.25
99.22	0.85	24.57	0.20	29.32	0.23	33.67	0.25	26.44	0.21
104.30	0.89	19.59	0.16	24.09	0.19	28.24	0.21	21.29	0.17
106.84	0.91	16.85	0.14	21.25	0.16	24.95	0.19	18.55	0.15
107.72	0.92	15.87	0.13	20.04	0.16	23.57	0.18	17.57	0.14
108.59	0.93	15.00	0.12	18.90	0.15	22.10	0.17	16.65	0.13
109.45	0.94	14.04	0.11	17.89	0.14	20.74	0.16	15.74	0.13
110.29	0.94	13.20	0.11	16.80	0.13	19.45	0.15	14.67	0.12
111.10	0.95	12.29	0.10	15.49	0.12	17.84	0.13	13.79	0.11
111.88	0.96	11.41	0.09	14.41	0.11	16 44	0.12	12.78	0.10
112.62	0.96	10.57	0.09	13.34	0.10	15.04	0.11	11.77	0.09
113.32	0.97	9.67	0.08	11.97	0.09	13.37	0.10	10.87	0.09
113.97	0.97	8.72	0.07	10.92	0.08	11.87	0.09	9.92	0.08
114.56	0.98	8.03	0.06	9.88	0.08	10.38	0.08	9.03	0.07
115.10	0.98	7.19	0.06	8.62	0.07	8.74	0.07	7.99	0.06
115.57	0.99	6.42	0.05	7.49	0.06	7.32	0.05	7.22	0.06
115.98	0.99	5.81	0.05	6.34	0.05	5.91	0.04	6.41	0.05
116.31	0.99	5 08	0.04	5.18	0.04	4.28	0.03	5.38	0.04
116.58	1.00	4.31	0.03	4.24	0.03	2.71	0.02	4.56	0.04
116.77	1.00	3.72	0.03	3.17	0.02	1.32	0.01	3.79	0.03
116.88	1.00	3.01	0.02	1.96	0.02	-0.29	-0.00	2.94	0.02
116.92	1.00	2.37	0.02	0.87	0.01	-1.63	-0.01	2.14	0.02

(Cont'd)

Note: See Table 12a for notations.

Table 12b: (continued)

H/R=1.83	x(1.83)
135.42	1.00
107.39	0.79
102.31	0.76
97.23	0.72
92.15	0.68
87.07	0.64
81.99	0.61
76.88	0.57
71.78	0.53
66.65	0.49
61.52	0.45
56.39	0.42
51.28	0.38
46.08	0.34
40.95	0.30
35.57	0.26
29.89	0.22
26.55	0.20
24.97	0.18
23.50	0.17
22.01	0.16
20.50	0.15
18.79	0.14
17.21	0.13
15.77	0.12
13.62	0.10
11.92	0.09
10.38	0.08
8.49	0.06
6.82	0.05
5.21	0.04
3.28	0.02
1.71	0.01
0.22	0.00
-1.69	-0.01
-3.13	-0.02

Note: See Table 12a for notations.

Table 12c: -Pressure distribution measured on U/S vertical walls:
(c) Weir model with R=7.54 cm.

z (cm)	y=z/P	H/R=1.18	x(1.18)	H/R=1.72	x(1.72)	H/R=2.47	x(2.47)
0.00	0.00	110.55	1.00	114.63	1.00	120.30	1.00
17.95	0.18	92.73	0.84	96.78	0.84	102.73	0.85
23.01	0.23	87.67	0.79	91.72	0.80	97.67	0.81
28.10	0.28	82.58	0.75	86.63	0.76	92.58	0.77
33.19	0.33	77.49	0.70	81.54	0.71	87.49	0.73
38.25	0.38	72.38	0.65	76.48	0.67	82.43	0.69
43.34	0.43	67.29	0.61	71.34	0.62	77.24	0.64
48.43	0.48	62.20	0.56	66.25	0.58	72.15	0.60
53.49	0.53	57.09	0.52	61.19	0.53	67.09	0.56
58.58	0.58	52.00	0.47	56.10	0.49	61.95	0.51
63.67	0.63	46.91	0.42	51.01	0.44	56.86	0.47
68.73	0.68	41.80	0.38	45.85	0.40	51.70	0.43
73.82	0.73	36.71	0.33	40.71	0.36	46.51	0.39
78.91	0.78	31.62	0.29	35.62	0.31	41.37	0.34
83.97	0.83	26.54	0.24	30.51	0.27	36.11	0.30
89.06	0.88	21.34	0.19	25.22	0.22	30.42	0.25
91.59	0.90	18.56	0.17	22.49	0.20	27.44	0.23
94.15	0.93	15.88	0.14	19.28	0.17	23.43	0.19
94.79	0.93						
95.46	0.94	14.22	0.13	16.97	0.15	20.02	0.17
96.10	0.95	13.38	0.12	15.93	0.14	18.58	0.15
96.71	0.95	12.57	0.11	14.97	0.13	17.07	0.14
97.32	0.96	11.76	0.11	13.66	0.12	15.26	0.13
97.90	0.96	10.83	0.10	12.58	0.11	13.68	0.11
98.45	0.97	10.03	0.09	11.43	0.10	12.03	0.10
99.00	0.97	9.08	0.08	10.08	0.09	10.08	0.08
99.46	0.98	8.22	0.07	9.02	0.08	8.52	0.07
99.91	0.98	7.57	0.07	7.97	0.07	6.97	0.06
100.31	0.99	6.57	0.06	6.57	0.06	5.02	0.04
100.68	0.99	5.80	0.05	5.40	0.05	3.40	0.03
100.98	0.99	4.95	0.04	4.20	0.04	1.90	0.02
101.22	1.00	4.06	0.04	2.96	0.03	0.16	0.00
101.44	1.00	3.24	0.03	1.84	0.02	-1.21	-0.01
101.56	1.00	2.62	0.02	0.72	0.01	-2.38	-0.02
101.65	1.00	1.63	0.01	-0.47	-0.00	-3.47	-0.03
101.68	1.00	0.80	0.01	-1.50	-0.01	-4.00	-0.03

Note: See Table 12a for notations.

Table 12d: -Pressure distribution measured on U/S vertical walls:
(d) Weir model with R=3.81 cm.

z (cm)	y=z/P	H/R=2.09	x(2.09)	H/R=3.08	x(3.08)	H/R=4.24	x(4.24)	HR=2.20/	x(2.20)
0.00	0.00	113.45	1.00	117.22	1.00	121.64	1.00	113.87	1.00
28.01	0.27	85.68	0.76	89.48	0.76	93.83	0.77	85.83	0.75
33.10	0.31	80.59	0.71	84.39	0.72	88.74	0.73	80.74	0.71
38.19	0.36	75.50	0.67	79.30	0.68	83.65	0.69	75.65	0.66
43.25	0.41	70.44	0.62	74.24	0.63	78.59	0.65	70.59	0.62
48.34	0.46	65.35	0.58	69.12	0.59	73.45	0.60	65.55	0.58
53.43	0.51	60.26	0.53	64.03	0.55	68.36	0.56	60.46	0.53
58.49	0.55	55.17	0.49	58.97	0.50	63.25	0.52	55.35	0.49
63.58	0.60	50.06	0.44	53.86	0.46	58.16	0.48	50.21	0.44
68.67	0.65	44.92	0.40	48.77	0.42	53.02	0.44	45.07	0.40
73.73	0.70	39.86	0.35	43.66	0.37	47.96	0.39	40 01	0.35
78.82	0.75	34.74	0.31	38.54	0.33	42.67	0.35	34.92	0.31
83.91	0.80	29.65	0.26	33.43	0.29	37.48	0.31	29.83	0.26
88.97	0.84	24.57	0.22	28.32	0.24	32.32	0.27	24.72	0.22
94.06	0.89	19.43	0.17	.23.08	0.20	27.03	0.22	19.63	0.17
96.59	0.92	16.80	0.15	20.30	0.17	24.10	0.20	16.95	0.15
99.15	0.94	14.14	0.12	17.44	0.15	20.74	0.17	14.14	0.12
100.40	0.95	12.69	0.11	15.69	0.13	18.84	0.15	12.69	0.11
101.68	0.96	10.81	0.10	13.11	0.11	15.31	0.13	10.81	0.09
102.35	0.97	9.54	0.08	11.04	0.09	12.24	0.10	9.34	0.08
102.99	0.98	8.20	0.07	8 90	0.08	9.20	0.08	7.80	0.07
103.60	0.98	6.69	0.06	6.99	0.06	6.49	0.05	6.29	0.06
104.12	0.99	5.27	0.05	4.82	0.04	3.67	0.03	4.57	0.04
104.61	0.99	3.68	0.03	2.68	0.02	1.08	0.01	2.88	0.03
104.97	1.00	2.22	0.02	0.72	0.01	-1.08	-0.01	1.12	0.01
105.25	1.00	0.79	0.01	-0.96	-0.01	-2.76	-0.02	-0.76	-0.01
105.37	1.00	0.07	0.00	-1.58	-0.01	-3.18	-0.03	-1.68	-0.01
105.43	1.00	-0.54	-0.00	-2.04	-0.02	-2.54	-0.02	-2.64	-0.02
105.48	1.00	-1.19	-0.01	-2.29	-0.02	-1.59	-0.01	-3.59	-0 03
105.49	1.00	-1.70	-0.01	-2.20	-0.02	-1.40	-0.01	-4.40	-0.04

(Cont'd)

Note: See Table 12a for notations.

Table 12d: (continued)

H/R=3.16	x(3.16)	H/R=4.10	x(4.10)
117.53	1.00	121.13	1.00
89.68	0.76	93.28	0.77
84.59	0.72	88.22	0.73
79.50	0.68	83.13	0.69
74.44	0.63	78.07	0.64
69.35	0.59	72.98	0.60
64.26	0.55	67.86	0.56
59.20	0.50	62.80	0.52
54.11	0.46	57.66	0.48
48.99	0.42	52.52	0.43
43.91	0.37	47.41	0.39
38.72	0.33	42.17	0.35
33.58	0.29	36.93	0.30
28.42	0.24	31.72	0.26
23.13	0.20	26.23	0.22
20.30	0.17	23.10	0.19
17.19	0.15	19.54	0.16
15.39	0.13	17.29	0.14
12.41	0.11	12.81	0.11
9.74	0.08	8.74	0.07
7.10	0.06	4.70	0.04
4.59	0.04	0.49	0.00
1.57	0.01	-4.08	-0.03
-1.32	-0.01	-8.72	-0.07
-4.43	-0.04	-13.58	-0.11
-7.76	-0.07	-18.36	-0.15
-9.28	-0.08	-20.78	-0.17
-11.04	-0.09	-23.14	-0.19
-12.34	-0.10	-25.09	-0.21
-13.90	-0.12	-27.20	-0.22

Note: See Table 12a for notations.

Table 12e: -Pressure distribution measured on U/S vertical walls:
(c) Weir model with R=2.54 cm.

z (cm)	y=z/P	HR=3.58/	x(3.58)90	H/R=5.24	x(5.24)	H/R=6.64	x(6.64)	HR=3.59/	x(3.59)90
0.00	0.00	113.26	1.00	117.47	1.00	121.04	1.00	113.29	1.00
22.90	0.22	90.39	0.80	94.49	0.80	98.49	0.81	90.49	0.80
27.98	0.27	85.30	0.75	89.40	0.76	93.40	0.77	85.40	0.75
33.07	0.32	80.21	0.71	84.31	0.72	88.31	0.73	80.31	0.71
38.13	0.37	75.15	0.66	79.25	0.67	83.25	0.69	75.25	0.66
43.22	0.41	70.06	0.62	74.16	0.63	78.16	0.65	70.16	0.62
48.31	0.46	64.97	0.57	69.07	0.59	73.07	0.60	65.07	0.57
53.37	0.51	59.86	0.53	63.96	0.54	68.01	0.56	60.01	0.53
58.46	0.56	54.72	0.48	58.87	0.50	62.87	0.52	54.92	0.48
63.55	0.61	49.63	0.44	53.78	0.46	57.78	0.48	49.83	0.44
68.61	0.66	44.57	0.39	48.72	0.41	52.67	0.44	44.77	0.40
73.70	0.71	39.48	0.35	43.58	0.37	47.48	0.39	39.68	0.35
78.79	0.76	34.39	0.30	38.49	0.33	42.34	0.35	34.54	0.30
83.85	0.80	29.33	0.26	33.38	0.28	37.23	0.31	29.48	0.26
88.94	0.85	24.19	0.21	28.24	0.24	32.04	0.26	24.34	0.21
94.03	0.90	19.05	0.17	22.80	0.19	26.55	0.22	19.15	0.17
96.56	0.93	16.32	0.14	20.02	0.17	23.42	0.19	16.47	0.15
99.09	0.95	13.49	0.12	16.89	0.14	19.89	0.16	13.54	0.12
100.37	0.96	11.86	0.10	14.81	0.13	17.51	0.14	11.81	0.10
101.65	0.98	9.33	0.08	11.43	0.10	13.03	0.11	9.33	0.08
102.08	0.98	7.60	0.07	8.40	0.07	8.90	0.07	7.50	0.07
102.50	0.98	5.58	0.05	5.78	0.05	5.18	0.04	5.88	0.05
102.90	0.99	4.28	0.04	3.43	0.03	2.18	0.02	4.18	0.04
103.27	0.99	2.81	0.02	1.41	0.01	-0.19	-0.00	2.61	0.02
103.57	0.99	1.21	0.01	-0.49	-0.00	-2.09	-0.02	0.91	0.01
103.85	1.00	-0.32	-0.00	-1.97	-0.02	-2.87	-0.02	-0.67	-0.01
104.03	1.00	-1.30	-0.01	-2.15	-0.02	-1.65	-0.01	-1.75	-0.02
104.09	1.00	-1.56	-0.01	-1.61	-0.01	-1.31	-0.01	-1.91	-0.02
104.14	1.00	-1.76	-0.02	-1.16	-0.01	-1.26	-0.01	-3.16	-0.03
104.17	1.00	-1.64	-0.01	-0.94	-0.01	-1.19	-0.01	-3.19	-0.03
104.18	1.00	-1.30	-0.01	-1.00	-0.01	-1.10	-0.01	-3.00	-0.03

(Cont'd)

Note: See Table 12a for notations.

Table 12e: (continued)

H/R=5.25	x(5.25)	H/R=6.73	x(6.73)	HR=3.71/	x(3.71)90	H/R=5.08	x(5.08)	H/R=6.44	x(6.44)
117.53	1.00	121.25	1.00	113.60	1.00	117.07	1.00	120.55	1.00
94.79	0.81	98.49	0.81	90.74	0.80	94.29	0.81	97.59	0.81
89.70	0.76	93.40	0.77	85.65	0.75	89.20	0.76	92.50	0.77
84.61	0.72	88.31	0.73	80.56	0.71	84.11	0.72	87.41	0.73
79.55	0.68	83.25	0.69	75.50	0.66	79.05	0.68	82.35	0.68
74.46	0.63	78.16	0.64	70.41	0.62	73.86	0.63	77.16	0.64
69.37	0.59	73.07	0.60	65.27	0.57	68.77	0.59	72.07	0 60
64.31	0.55	68.01	0.56	60.21	0.53	63.71	0.54	67.01	0.56
59.22	0.50	62.92	0.52	55.12	0.49	58.52	0.50	61.82	0 51
54.03	0.46	57.73	0.48	50.03	0.44	53.43	0 46	56.73	0.47
48.97	0.42	52.67	0.43	44.97	0.40	48.37	0.41	51.67	0.43
43.88	0.37	47.48	0.39	39.78	0.35	43.28	0.37	46.58	0.39
38.69	0.33	42.29	0.35	34.69	0.31	38.09	0.33	41.39	0 34
33.53	0.29	37.13	0.31	29.63	0.26	33.03	0.28	36.13	0.30
28.39	0.24	31.94	0.26	24.44	0.22	27.84	0.24	30.74	0.25
22.95	0.20	26.35	0.22	19.25	0.17	22.15	0.19	24.95	0.21
20.12	0.17	23.22	0.19	16.52	0.15	19.22	0.16	21.62	0.18
16.99	0.14	19.69	0.16	13.69	0.12	15.69	0.13	17.39	0.14
14.91	0.13	17.11	0.14	11.61	0.10	13.21	0.11	14 01	0.12
11.33	0.10	12.23	0.10	8.93	0.08	8.43	0.07	8.93	0.07
8.40	0.07	7.40	0.06	6.50	0.06	4.10	0 04	0.20	0.00
5.68	0.05	3.28	0.03	3.88	0.03	-0.62	-0.01	-8 12	-0.07
3.08	0.03	0.08	0.00	1.48	0.01	-4.72	-0 04	-14 22	-0 12
0.91	0.01	-2.99	-0.02	-0.79	-0.01	-8.99	-0.08	-20 79	-0.17
-1.19	-0.01	-5.39	-0.04	-3.59	-0.03	-13.89	-0.12	-28.39	-0.24
-2.97	-0.03	-7.07	-0.06	-6.47	-0.06	-19.17	-0.16	-36 27	-0.30
-2.55	-0.02	-6.05	-0.05	-8.45	-0.07	-22.55	-0.19	-41.85	-0 35
-2.81	-0.02	-5.31	-0.04	-10.21	-0.09	-25.31	-0.22	-45 31	-0.38
-3.26	-0.03	-4.86	-0.04	-11.76	-0.10	-27.26	-0.23	-47.86	-0.40
-3.09	-0.03	-4.79	-0.04	-12.19	-0.11	-28.39	-0.24	-50.59	-0.42
-3.20	-0.03	-4.90	-0.04	-13.40	-0.12	-30.60	-0.26	-53.10	-0.44

(Cont'd)

Note: See Table 12a for notations.

Table 12e: (continued)

H/R=7.56	x(7.56)	HR=3.02/	x(3.02)90	H/R=4.42	x(4.42)	H/R=5.41	x(5.41)	H/R=6.58	x(6.58)
123.38	1.00	111.86	1.00	115.43	1.00	117.90	1.00	120.88	1.00
100.49	0.81	89.24	0.80	92.74	0.80	95.29	0.81	97.99	0.81
95.40	0.77	84.15	0.75	87.65	0.76	90.20	0.77	92.90	0.77
* 90.31	0.73	79.06	0.71	82.56	0.72				
85.25	0.69	73.95	0.66	77.50	0.67	80.05	0.68	82.75	0.68
80.06	0.65	68.86	0.62	72.41	0.63				
74.97	0.61	63.77	0.57	67.27	0.58	69.77	0.59	72.57	0.60
69.91	0.57	58.71	0.52	62.21	0.54				
64.72	0.52	53.52	0.48	57.12	0.49	59.62	0.51	62.42	0.52
59.63	0.48	48.43	0.43	52.03	0.45				
54.57	0.44	43.32	0.39	46.92	0.41	49.37	0.42	52.17	0.43
49.38	0.40	38.23	0.34	41.83	0.36				
44.29	0.36	33.09	0.30	36.69	0.32	39.09	0.33	41.89	0.35
38.83	0.31	28.03	0.25	31.58	0.27				
33.34	0.27	22.94	0.21	26.44	0.23	28.74	0.24	31.24	0.26
27.25	0.22	17.75	0.16	21.05	0.18				
23.52	0.19	15.02	0.13	18.22	0.16	20.12	0.17	22.12	0.18
18.49	0.15	12.29	0 11	15.19	0.13				
14.31	0.12	10.61	0.09	13.01	0.11	14.01	0.12	14.81	0.12
9.93	0.08	8.33	0.07	9.53	0.08	9.03	0.08	7.93	0.07
-4.10	-0.03	6.60	0.06	6.40	0.06	4.50	0.04	1.10	0.01
-15.42	-0.12	5.18	0.05	3.58	0.03	-0.42	-0.00	-6.12	-0.05
-23.72	-0.19	3.48	0.03	0.78	0.01	-4.12	-0.03	-11.72	-0.10
-32.69	-0.26	1.91	0.02	-1.89	-0.02	-7.79	-0.07	-17.59	-0.15
-41.19	-0.33	0.21	0.00	-4.59	-0.04	-12.69	-0.11	-23.79	-0.20
-52.97	-0.43	-1.77	-0.02	-7.47	-0.06	-17.07	-0.14	-30.57	-0.25
-59.35	-0.48	-3.35	-0.03	-9.75	-0.08	-19.65	-0.17	-34.85	-0.29
-64.01	-0.52	-4.21	-0.04	-10.51	-0.09	-21.51	-0.18	-37.01	-0.31
-66.76	-0.54	-4.96	-0 04	-10.96	-0.09	-21.96	-0.19	-38.76	-0.32
-70.39	-0.57	-5.69	-0.05	-11.99	-0.10	-23.79	-0.20	-39.99	-0.33
-73.60	-0.60	-6.30	-0.06	-11.80	-0.10	-24.40	-0.21	-41.30	-0.34

Note: See Table 12a for notations. *Additional information obtained for more detail.

Table 12f: -Pressure distribution measured on U/S vertical walls:
(f) Weir model with R=0.95 cm.

z (cm)	y=z/P	HR=6.77/	x(6.77)	H/R=9.7	x(9.78)	H/R=12.	x(12.10)	H/R=14.	x(14.24)	H/R=16.
0.00	0.00	111.95	1.00	114.82	1.00	117.01	1.00	119.05	1.00	121.00
21.34	0.20	90.50	0.81	93.45	0.81	95.65	0.82	97.70	0.82	99.85
31.52	0.30	80.32	0.72	83.27	0.73	85.47	0.73	87.52	0.74	89.67
41.67	0.40	70.17	0.63	73.12	0.64	75.32	0.64	77.37	0.65	79.52
56.91	0.54	54.93	0.49	57.88	0.50	59.98	0.51	62.08	0.52	64.23
67.06	0.64	44.78	0.40	47.73	0.42	49.83	0.43	51.93	0.44	54.08
77.24	0.73	34.60	0.31	37.35	0.33	39.65	0.34	41.75	0.35	43.85
87.39	0.83	24.30	0.22	27.10	0.24	29.40	0.25	31.50	0.26	33.50
97.54	0.92	14.05	0.13	16.75	0.15	18.85	0.16	20.65	0.17	22.65
102.63	0.97	8.56	0.08	10.96	0.10	12.66	0.11	14.26	0.12	15.66
103.91	0.99	6.68	0.06	8.48	0.07	9.78	0.08	10.98	0 09	12.18
104.55	0.99	4.34	0.04	4.84	0.04	5.24	0.04	5.44	0.05	5.64
104.70	0.99	2.89	0.03	2.69	0.02	2.39	0.02	2.09	0.02	1.49
104.88	0.99	1.71	0.02	0.81	0.01	0.11	0.00	-0.59	-0.00	-1.29
105.03	1.00	0.56	0.01	-0.64	-0.01	-1.44	-0.01	-2.14	-0.02	-2.69
105.16	1.00	-0.57	-0.01	-1.57	-0.01	-2.27	-0.02	-2.47	-0.02	-1.57
105.28	1.00	-1.09	-0.01	-1.59	-0.01	-1.49	-0.01	-1.29	-0.01	-1.29
105.37	1.00	-1.28	-0.01	-0.98	-0.01	-0.98	-0.01	-1.08	-0.01	-1.18
105.43	1.00	-0.94	-0.01	-0.64	-0.01	-0.84	-0.01	-0.94	-0.01	-0.94
105.48	1.00	-0.69	-0.01	-0.80	-0.01	-0.99	-0.01	-1.09	-0.01	-1.09
105.49	1.00	-0.71	-0.01	-0.71	-0.01	-0.71	-0.01	-0 71	-0.01	-0.76

(Cont'd)

(Table 12f - continued)

x(16.27	H/R=18.	x(18.08)
1.00	122.71	1.00
0.83	101.65	0.83
0.74	91.37	0.74
0.66	81.22	0.66
0.53	65.93	0.54
0.45	55.78	0.45
0.36	45.55	0.37
0.28	35.20	0.29
0.19	24.25	0.20
0.13	16.96	0.14
0.10	13.08	0.11
0.05	5.64	0.05
0.01	1.09	0.01
-0.01	-1.89	-0.02
-0.02	-3.09	-0.03
-0 01	-2.37	-0 02
-0.01	-1.29	-0.01
-0.01	-1.28	-0.01
-0.01	-1.04	-0.01
-0.01	-1.09	-0.01
-0.01	-0.81	-0.01

Note: See Table 12a for notations.

Table 13a: -Pressure distribution measured on weir crest surfaces.
(a) Weir models with $\alpha=90^{\circ}$, no D/S slope and vent open.

TETA #1	H/R=.54	H/R=.816	H/R=.999	H/R=1.16	H/R=1.38	TETA #2	H/R=.70	H/R=1.19	H/R=1.64
30	14.96	18.21	20.26	21.76	23.56	30.00	11.41	14.41	16.44
35	13.81	16.86	18.86	20.16	21.66	35.00	10.57	13.34	15.04
40	12.59	15.59	17.39	18.54	19.79	40.00	9.67	11.97	13.37
45	11.42	14.32	15.82	16.92	17.82	45.00	8.72	10.92	11.87
50	10.39	13.13	14.43	15.43	15.93	50.00	8.03	9.88	10.38
55	9.54	11.84	13.04	13.64	13.94	55.00	7.19	8.62	8.74
60	8.61	10.66	11.56	11.96	12.01	60.00	6.42	7.49	7.32
65	7.60	9.55	10.20	10.40	10.20	65.00	5.81	6.34	5.91
70	6.71	8.36	8.76	8.71	8.21	70.00	5.08	5.18	4.28
75	5.91	7.21	7.46	7.21	6.41	75.00	4.31	4.24	2.71
80	5.11	6.21	6.16	5.61	4.51	80.00	3.72	3.17	1.32
85	4.46	5.06	4.76	3.96	2.56	85.00	3.01	1.96	-0.29
90	3.70	4.00	3.40	2.30	0.80	90.00	2.37	0.87	-1.63
95	3.06	3.01	2.06	0.76	-1.04	95.00	1.81	-0.24	-2.59
100	2.21	1.91	0.71	-0.99	-2.69	100.00	1.12	-1.43	-3.88
105	1.71	0.91	-0.59	-2.59	-4.29	105.00	0.51	-2.29	-4.49
110	1.01	-0.09	-1.89	-4.09	-5.49	110.00	-0.02	-3.19	-4.82
115	0.60	-1.10	-3.30	-5.70	-6.00	115.00	-0.79	-4.14	-4.39
120	0.11	-2.09	-4.69	-7.39	-6.79	120.00	-1.18	-4.73	-3.48
125	-0.46	-2.96	-5.76	-8.76	-7.86	125.00	-1.91	-4.96	-2.21
130	-1.07	-4.07	-7.07	-10.57	-8.27	130.00	-2.37	-4.87	-4.27
135	-1.58	-4.88	-8.28	-12.08	-3.28	135.00	-2.98	-3.68	-2.78
140	-2.01	-5.81	-9.51	-13.51	-7.81	140.00	-3.53	-2.28	
145	-2.69	-6.64	-10.64	-14.94	-5.74	145.00	-4.03	-1.48	
150	-2.94	-7.64	-11.64	-16 34	-8.34	150.00	-4.39	-0.82	
155	-3.16	-8.36	-12.56	-17.56	-11.26	155.00	-4.81	-0.88	
160	-3.84	-9.34	-13.64	-18.84	-9.74	160.00	-5.30	-1.13	

(Cont'd)

Note: Table13a consists of 30 columns to read horizontally. Cols. 1, 7, 13, 17, 21 and 29 are angular locations θ°. Other cols. denote the values of (P/γ) in cm for various values of H_1/R.

Table 13a: (continued)

H/R=.883	H/R=1.83	TETA #3	H/R=1.1	H/R=1.72	H/R=2.47	TETA #5	H/R=2.09	H/R=3.08	H/R=4.2
12.78	17.21	30	10.83	12.58	13.68	30	6.69	6.99	6.49
11.77	15.77	35	10.03	11.43	12.03	40	5.27	4.82	3.67
10.87	13.62	40	9.08	10.08	10.08	50	3.68	2.68	1.08
9.92	11.92	45	8.22	9.02	8.52	60	2.22	0.72	-1.08
9.03	10.38	50	7.57	7.97	6.97	70	0.79	-0.96	-2.76
7.99	8.49	55	6.57	6.57	5.02	75	0.07	-1.58	-3.18
7.22	6.82	60	5.80	5.40	3.40	80	-0.54	-2.04	-2.54
6.41	5.21	65	4.95	4.20	1.90	85	-1.19	-2.29	-1.59
5.38	3.28	70	4.06	2.96	0.16	90	-1.70	-2.20	-1.40
4.56	1.71	75	3.24	1.84	-1.21	95	-2.19	-1.69	-1.29
3.79	0.22	80	2.62	0.72	-2.38	100	-2.44	-1.24	-1.14
2.94	-1.69	85	1.63	-0.47	-3.47	105	-2.48	-0.88	-0 78
2.14	-3.13	90	0.80	-1.50	-4.00	110	-2.26	-0.66	-0.26
1.41	-4.19	95	0.03	-2.37	-4.27	115	-1.74	-0.84	-0.94
0.32	-5.38	100	-0.78	-3.08	-4.28	120	-1.28	-0.33	-0.02
-0.19	-5.89	105	-1.61	-3.66	-2.16	125	-1.05	-0 80	
-1.02	-6.12	110	-2.24	-3.74	-1.94				
-1.89	-4.99	115	-3.10	-3.40	-1.70				
-2.61	-4.68	120	-3.50	-2.40	-1.40				
-3.26	-3.21	125	-4.03	-1.73	-1.03				
-4.02	-2.17	130	-4.23	-1.23	-0.63				
-4.63	-1.58	135	-4.28	-0.58	-0.18				
-5.13		140	-3.62	-0.92	-0.28				
-5.53		145	-1.97						
-5.59		150	-1.52						
-5.06		155	-0.94						
-3.50		160							

(Cont'd)

Table 13a: (continued)

TETA #6	H/R=3.58	H/R=5 24	H/R=6.64	TETA#8	H/R=6.77	H/R=9 78	H/R=12.1	H/R=14.2	H/R=16 2
30	4.28	3.43	2.18	30	0 56	-0.64	-1.44	-2.14	-2 69
40	2.81	1.41	-0 19	40	-0.57	-1.57	-2 27	-2 47	-1.57
50	1.21	-0.49	-2.09	50	-1.09	-1.59	-1.49	-1.29	-1.29
60	-0.32	-1.97	-2.87	60	-1.28	-0.98	-0.98	-1.08	-1.18
70	-1.30	-2.15	-1.65	70	-0.94	-0.64	-0.84	-0.94	-0.94
75	-1.56	-1.61	-1.31	80	-0.69	-0.80	-0.99	-1.09	-1.09
80	-1.76	-1.16	-1.26	90	-0.71	-0 71	-0.71	-0.71	-0 76
85	-1.64	-0.94	-1.19	100	-0.59	-0.65	-0.65	-0 65	-0 69
90	-1.30	-1.00	-1.10	110	-2 04	-1.94	-1.94	-2 04	-2.04
95	-0.99	-0.89	-2.19	120	-1.78	-1.83	-1.88	-1.88	-1 88
100	-0.86	-0.96	-0.06	130	-0 69	-0 79	-0.89	-0.89	-0 89
105	-0.71	-0.81	-0 31	140	-0.47	-0 47	-0 47	-0 47	-0 47
110	-0.75	-0.85	-0 85						
120	-0.77	-0.17	-0.07						
130	-1.19	-0.99							
140	-0.99	-1.19							

Table 13b: -Pressure distribution measured on weir crest surfaces.

(b) Weir models with $\alpha=90^{\circ}$, $\beta=45^{\circ}$ (9045).

TETA #1	H/R=.444	y(444)	H/R=.728	y(.728)	H/R=.90	y(.905)	H/R=1.15	y(1.15)	H/R=1.35	y(1.35)
30	13.86	2.06	17.16	1.56	19.21	1.40	21.56	1.24	23.26	1.13
35	12.76	1.89	15.86	1.44	17.86	1.30	20.06	1.15	21.46	1.05
40	11.64	1.73	14.59	1.32	16 49	1.20	18.39	1.06	19.59	0.96
45	10.52	1.56	13.42	1.22	15.02	1.09	16.82	0.97	17.82	0.87
50	9.53	1.41	12.18	1.10	13.73	1.00	15.13	0.87	16.73	0.82
55	8.54	1.27	11.14	1.01	12.39	0.90	13.54	0.78	13.84	0.67
60	7.61	1.13	9.91	0.90	11.01	0 80	12.01	0.69	12.01	0.59
65	6.80	1.01	8.90	0.81	9.80	0.71	10.40	0.60	10 30	0.50
70	6.11	0.91	7.81	0.71	8.51	0.62	8.71	0 50	8.31	0.41
75	5.31	0 79	6.71	0 61	7.21	0.53	7.31	0.42	6.51	0.32
80	4.61	0.68	5.81	0 53	6.11	0.45	5.81	0.33	4.71	0.23
85	3.96	0.59	4.86	0.44	4.86	0.35	4.16	0.24	2.71	0.13
90	3.40	0.50	3.85	0.35	3.80	0.28	2.70	0.16	1.00	0.05
95	2.86	0.42	3.06	0.28	2.76	0.20	1.26	0.07	-0.79	-0.04
100	2.21	0.33	2.21	0.20	1.61	0.12	-0.29	-0.02	-2.59	-0.13
105	1.81	0.27	1.51	0.14	0.51	0.04	-1.54	-0.09	-4.19	-0.20
110	1.31	0.19	0.71	0.06	-0.49	-0.04	-2.79	-0.16	-5.49	-0.27
115	1.00	0.15	-0.10	-0.01	-1.40	-0.10	-3.90	-0.22	-6.70	-0.33
120	0.51	0.08	-0.69	-0.06	-2.09	-0.15	-4.79	-0.28	-7.39	-0.36
125	0.24	0.04	-1.16	-0.11	-2.46	-0.18	-4.86	-0.28	-7.46	-0.36
130	0 03	0.00	-1.27	-0.12	-2.47	-0 18	-4.57	-0.26	-6.87	-0.33
135	0.12	0.02	-0.58	-0.05	-1.38	-0.10	-2.88	-0.17	-4.68	-0.23

(Cont'd)

(Table 13b - continued)

TETA #6	H/R=3.0	y(3.02)	H/R=4.42	y(4.42)	H/R=5.41	y(5.41)	H/R=6 58	y(6.58)
30	3.48	0.45	0.78	0.07	-4.12	-0 30	-11.72	-0.70
40	1.91	0 25	-1.89	-0.17	-7.79	-0 57	-17.59	-1.05
50	0.21	0.03	-4.59	-0.41	-12.69	-0.92	-23.79	-1.42
60	-1.77	-0.23	-7.47	-0.66	-17.07	-1.24	-30.57	-1.83
70	-3.35	-0.44	-9.75	-0.87	-19.65	-1.43	-34.85	-2.09
75	-4.21	-0 55	-10 51	-0.93	-21.51	-1.57	-37.01	-2 22
80	-4.96	-0 65	-10.96	-0.97	-21.96	-1.60	-38.76	-2 32
85	-5.69	-0 74	-11.99	-1.07	-23.79	-1.73	-39.99	-2.39
90	-6.30	-0.82	-11 80	-1.05	-24 40	-1.78	-41.30	-2.47
95	-6.59	-0.86	-11.39	-1.01	-22.59	-1.65	-41.59	-2.49
100	-6 96	-0.91	-11.26	-1.00	-23 36	-1.70	-41.46	-2.48
105	-7.11	-0.93	-10.91	-0.97	-22.71	-1.66	-40 81	-2.44
110	-6.95	-0.90	-10 05	-0.89	-21 65	-1.58	-39 35	-2.36
120	-5.77	-0.75	-10.67	-0.95	-21.87	-1.59	-36 57	-2.19
130	-5.19	-0.68	-10 39	-0.92	-20.99	-1.53	-34 09	-2 04
140								

Note: Table13b consists of 20 columns to read horizontally. Cols. 1 and 12 are angular locations θ°. Other cols. denote the values of (P/γ) in cm for various values of H_1/R.

Table 13c: -Pressure distribution measured on weir crest surfaces.
(c) Weir models with α=60°, β=45° (6045).

TETA#1	H/R=.525	y(.525)	H/R=.78	y(.782)	H/R=.977	y(.977)	H/R=1 35	y(1.35)
35	13.81	1.73	16.86	1.42	19.18	1.29	22.66	1.10
40	12.49	1.57	15.49	1.31	17.59	1.19	20 39	0 99
45	11.32	1.42	1[illegible].22	1.20	16.02	1.08	18.42	0.90
50	10.23	1.29	12.83	1.08	14 43	0 97	16.33	0.80
55	9.34	1.17	11.64	0.98	13.04	0.88	14.34	0.70
60	8.31	1.04	10.41	0.88	11.61	0.78	12.41	0.61
65	7.40	0.93	9.30	0.78	10 20	0 69	10.45	0.51
70	6.51	0 82	8.11	0.68	8.71	0.59	8.56	0.42
75	5.71	0.72	6.91	0 58	7.36	0.50	6.71	0.33
80	5.01	0.63	5.91	0.50	6.06	0.41	4.81	0 23
85	4.26	0.54	4.86	0.41	4.81	0.32	2.76	0.13
90	3.60	0.45	3.80	0.32	3.60	0.24	1.00	0.05
95	2.86	0.36	2.96	0.25	2.36	0.16	-0.84	-0.04
100	2.11	0.27	2.11	0.18	1.11	0.07	-2.59	-0 13
105	1.61	0.20	1.31	0 11	-0.09	-0.01	-4.29	-0.21
110	1.11	0.14	0.41	0.03	-1.19	-0.08	-5.59	-0 27
115	0.70	0.09	-0.50	-0.04	-2.20	-0.15	-6.80	-0 33
120	0.31	0.04	-1.09	-0.09	-2.79	-0.19	-7.49	-0.37
125	-0.06	-0.01	-1.46	-0.12	-3 16	-0.21	-7.56	-0 37
130	-0.17	-0.02	-1.57	-0.13	-3.07	-0 21	-6.87	-0.33
135	-0.03	-0.00	-0.78	-0.07	-1.88	-0 13	-4.68	-0 23

(Cont'd)

(Table 13c - continued)

TETA #6	H/R=4.0	y(4.07)	H/R=5.28	y(5.28)	H/R=6.60	y(6 60)
40	2.51	0.24	-0 39	-0.03	-6 49	-0 39
50	-1.09	-0.11	-6.49	-0.48	-15.79	-0.94
60	-4.87	-0.47	-12.17	-0.91	-24 47	-1.46
70	-7.45	-0.72	-15.95	-1.19	-29.75	-1.78
75	-8.61	-0.83	-18.51	-1.38	-33.11	-1.98
80	-9.86	-0.95	-20.56	-1.53	-35 86	-2 14
85	-10.99	-1.06	-21.59	-1.61	-37.39	-2.23
90	-11.40	-1.10	-23.00	-1.72	-39 30	-2 34
95	-12.29	-1.19	-22.79	-1.70	-39 89	-2 38
100	-12.46	-1.21	-22.86	-1.70	-40 76	-2.43
105	-11.71	-1.13	-23.61	-1.76	-40 61	-2.42
110	-11.45	-1.11	-22.85	-1.70	-39 65	-2 37
120	-11.07	-1.07	-20.47	-1.53	-36 47	-2 18
130	-10 59	-1.03	[illegible].79	-1.48	-33 69	-2 01

Note: Table 13c consists of 16 columns to read horizontally. Cols. 1and 10 are angular locations θ°. Other cols. denote the values of (P/γ) in cm for various values of H_1/R.

Table 14a: -Normalized water surface profiles of flow over the crest section:

(a) Weir models with α=90°, no D/S slope and vent open.

x 407	y 407	x 408	y 408	x 409	y 409	x 410	y 410	x 411	y 411
-1.21	0.92	-0.81	0.90	-0.66	0.88	-0.57	0.86	-0.48	0.84
-0.60	0.85	-0.40	0.83	-0.33	0.81	-0.28	0.80	-0.24	0.79
-0.24	0.78	-0.16	0.77	-0.13	0.76	-0.11	0.75	-0.10	0.75
0.00	0.72	0.00	0.72	0.00	0.72	0.00	0.71	0.00	0.71
0.24	0.65	0.16	0.67	0.13	0.66	0.11	0.67	0.10	0.68
0.48	0.55	0.32	0.60	0.26	0.61	0.23	0.62	0.19	0.64
0.72	0.44	0.49	0.52	0.40	0.55	0.34	0.56	0.29	0.59
0.97	0.31								

(Cont'd)

(Table 14a - continued)

x 002	y 002	x 003	y 003	x 004	y 004	x 007	y 007	x 008	y 008
-1.41	0.97	-0.75	0.89	-0.54	0.87	-1.12	0.93	-0.54	0.87
-0.85	0.91	-0.50	0.85	-0.36	0.84	-0.67	0.88	-0.43	0.85
-0.56	0.86	-0.33	0.81	-0.24	0.80	-0.45	0.83	-0.32	0.82
-0.28	0.80	-0.17	0.76	-0.12	0.77	-0.22	0.78	-0.22	0.80
-0.14	0.76	0.00	0.70	0.00	0.72	0.00	0.71	-0.11	0.77
0.00	0.73	0.17	0.64	0.12	0.68	0.22	0.62	0.00	0.73
0.14	0.67	0.33	0.55	0.24	0.62	0.45	0.51	0.11	0.69
0.28	0.62	0.42	0.50	0.30	0.57			0.22	0.64
0.42	0.58			0.42	0.52			0.32	0.58
0.56	0.48							0.43	0.52
0.70	0.40								

(Cont'd)

(Table 14a - continued)

x 23b	y 23b	x 059	y 059	x 060	y 060	x 061	y 061	x 136	y 136
-0.48	0.87	-1.26	0.96	-0.85	0.94	-0.62	0.90	-1.10	0.96
-0.27	0.83	-0.63	0.90	-0.68	0.92	-0.49	0.88	-0.66	0.92
-0.14	0.79	-0.38	0.85	-0.51	0.89	-0.37	0.87	-0.44	0.88
0.00	0.74	-0.25	0.82	-0.34	0.86	-0.25	0.84	-0.22	0.84
0.14	0.68	-0.13	0.78	-0.17	0.82	-0.12	0.81	0.00	0.78
0.27	0.62	0.00	0.74	-0.09	0.80	-0.06	0.79	0.22	0.69
0.41	0.54	0.13	0.69	0.00	0.77	0.00	0.78	0.44	0.59
0.55	0.46	0.25	0.63	0.09	0.74	0.06	0.75	0.66	0.45
		0.38	0.57	0.17	0.71	0.12	0.73		
		0.50	0.49	0.26	0.67	0.19	0.71		
		0.63	0.39	0.34	0.63	0.25	0.69		
		0.75	0.27	0.51	0.54	0.31	0.66		
						0.37	0.63		

(Cont'd)

(Table 14a - continued)

x 137	y 137	x 138	y 138	x 255	y 255	x 256	y 256	x 257	y 257
-0.75	0.93	-0.59	0.93	-1.55	0.98	-1.07	0.96	-0.87	0.95
-0.45	0.89	-0.30	0.89	-0.78	0.94	-0.54	0.92	-0.43	0.91
-0.30	0.86	-0.12	0.84	-0.47	0.91	-0.32	0.88	-0.26	0.89
-0.15	0.83	0.00	0.82	-0.31	0.88	-0.21	0.85	-0.17	0.87
0.00	0.78	0.12	0.78	-0.16	0.85	-0.11	0.84	-0.09	0.85
0.15	0.74	0.24	0.73	0.00	0.80	0.00	0.82	0.00	0.83
0.30	0.67	0.36	0.68	0.16	0.76	0.11	0.79	0.09	0.80
0.45	0.60			0.31	0.70	0.21	0.75	0.17	0.78
				0.62	0.53	0.43	0.66	0.35	0.71
						0.64	0.55	0.52	0.63
								0.69	0.53

(Cont'd)

Note: Grouped every two columns per profile with x=horizontal distances and y= vertical distances above crest. The origin of coordinates is at crest C (Fig.2a) and H_1 is used to normalized x and y. The three-digit numbers are identification codes of tests.

Table 14a: (continued)

(Table 14a - continued)

x 258	y 258	x 259	y 259	x 260	y 260	x 453	y 453	x 454	y 454
-0.74	0.95	-0.65	0.95	-0.58	0.94	-0.39	0.87	-0.33	0.86
-0.37	0.90	-0.32	0.91	-0.29	0.90	-0.20	0.82	0.00	0.76
-0.22	0.88	-0.13	0.87	-0.12	0.86	0.00	0.75	0.33	0.60
-0.07	0.85	0.00	0.85	0.00	0.84	0.20	0.66	0.67	0.38
0.00	0.83	0.13	0.81	0.12	0.81	0.39	0.55		
0.15	0.79	0.26	0.76	0.23	0.77				
0.29	0.74	0.39	0.71	0.35	0.73				
0.44	0.67	0.52	0.65	0.46	0.68				
0.59	0.60	0.65	0.58	0.58	0.62				

(Cont'd)

(Table 14a - continued)

x 454a	y 454a	x 455	y 455	x 456	y 456
-0.27	0.85	-0.23	0.85	-0.18	0.84
0.00	0.77	0.00	0.78	0.00	0.79
0.27	0.65	0.23	0.70	0.18	0.72
0.55	0.49	0.45	0.59	0.36	0.64
				0.54	0.55

Table 14b: -Normalized water surface profiles of flow over the crest section:
(b) Weir models with α=90°, β=45° (9045).

x 245	y 245	x 246	y 246	x 247	y 247	x 248	y 248	x 459	y 459
-1.30	0.98	-0.89	0.94	-0.73	0.91	-0.60	0.88	-0.34	0.85
-0.65	0.91	-0.45	0.88	-0.36	0.85	-0.30	0.82	-0.17	0.79
-0.26	0.83	-0.18	0.81	-0.15	0.79	-0.12	0.77	0.00	0.74
0.00	0.74	0.00	0.76	0.00	0.74	0.00	0.72	0.17	0.65
0.26	0.61	0.18	0.68	0.15	0.67	0.12	0.67	0.34	0.54
0.52	0.44	0.36	0.58	0.29	0.59	0.24	0.60	0.69	0.23
		0.53	0.44	0.44	0.49	0.36	0.53		
		0.80	0.21	0.66	0.30	0.54	0.37		

(Cont'd)

(Table 14b - continued)

x 460	y 460	x 461	y 461	x 462	y 462
-0.25	0.82	-0.20	0.82	-0.16	0.80
0.00	0.73	0.00	0.75	0.00	0.73
0.25	0.61	0.20	0.66	0.16	0.67
0.50	0.43	0.40	0.54	0.33	0.57
		0.60	0.37	0.49	0.45

Note: See Table 14a for notations.

Table 14c: -Normalized water surface profiles of flow over the crest section:

(c) Weir models with $\alpha=90^{\circ}$, $\beta=60^{\circ}$ (9060).

x`#80	y`#80	x`	y`#218	y`#219	y`#220	y`#221	x`/H1/2.2	y`/H1/2.2	x`/H1/3.7
-20.00	8.17	-20.00	9.30	12.74	15.18	17.65	-2.39	0.97	-2.12
-10.00	7.83	-15.00	9.14	12.04	14.78	17.10	-1.19	0.93	-1.59
-8.00	7.65	-10.00	8.87	11.58	12.65	16.43	-0.95	0.91	-1.08
-6.00	7.41	-5.00	8.20	10.67	13.20	15.30	-0.72	0.88	-0.53
-4.00	7.07	-2.00	7.44	9.88	12.25	14.20	-0.48	0.84	-0.21
-2.00	6.61	0.00	6.77	9.14	11.43	13.53	-0.24	0.79	0.00
-1.00	6.28	2.00	5.73	8.08	10.52	12.59	-0.12	0.73	0.21
0.00	5.97	4.00	4.36	6.83	9.33	11.46	0.00	0.71	0.42
1.00	5.52	6.00	2.26	5.09	7.89	10.18	0.12	0.66	0.64
2.00	5.03	9.00			4.79	7.56	0.24	0.60	0.96
4.00	3.69						0.48	0.44	
6.00	1.68						0.72	0.20	

(Cont'd)

(Table 14c - continued)

y`/H1/3.7	x`/H1/5.0	y`/H1/5.	x`/H1/6.4	y`/H1/6.4	x`/H1/7.5	y`/H1/7.5
0.99	-1.55	0.99	-1.22	0.93	-7.04	0.92
0.97	-1.16	0.93	-0.92	0.90	-0.78	0.89
0.94	-0.78	0.90	-0.61	0.77	-0.52	0.86
0.87	-0.39	0.83	-0.31	0.81	-0.26	0.80
0.79	-0.16	0.77	-0.12	0.75	-0.10	0.74
0.72	0.00	0.71	0.00	0.70	0.00	0.70
0.61	0.16	0.63	0.12	0.64	0.10	0.66
0.46	0.31	0.53	0.24	0.57	0.21	0.60
0.24	0.47	0.39	0.37	0.48	0.31	0.53
			0.55	0.29	0.47	0.39

Note: Table 14c consists of 17 columns. The first seven columns are horizontal distances (x` in cm) and vertical distances above the weir crest (y` in cm), the remaining columns are corresponding normalized values $x=x`/H_1$ and $y=y`/H_1$ for various values of H_1/R.

Table 15: -Variation of K_w with p/H_1.

p/H_1	K_w
14.04	0.993
9.41	0.992
7.69	0.991
6.61	0.989
5.56	0.986
20.51	0.998
16.46	0.997
9.76	0.994
7.06	0.991
5.05	0.985
24.91	0.999
13.14	0.996
6.32	0.990
4.96	0.985
26.42	0.999
13.26	0.999
8.99	0.998
6.53	0.993
5.33	0.988
5.33	0.988
11.47	0.996
7.84	0.992
7.84	0.992
6.18	0.995
6.18	0.995
4.75	0.987
4.75	0.987
1[illegible].32	0.996
11.31	0.996
11.31	0.995
7.78	0.996
6.13	0.995

Table 16: -Variation of K_w and K_2 with H_1/R.

H_1/R	K_w	K_2
0.999	0.991	0.506
1.162	0.989	0.412
1.381	0.986	0.413
1.189	0.994	0.410
0.466	0.999	0.780
0.882	0.996	0.522
1.050	0.999	0.324
5.201	0.988	0.231
5.201	0.988	0.139
3.582	0.996	0.291
5.235	0.992	0.302
5.235	0.992	0.235
6.640	0.995	0.168
8.638	0.987	0.330
6.773	0.996	0.364
9.777	0.996	0.412
9.777	0.995	0.306
14.242	0.996	0.321
18.076	0.995	0.300

Table 17: -Variation of Y_2/H_1 and m with H_1/R ($\alpha=90°$, $\beta=45°$)

H_1/R	Y_2/H_1	m
3.02	0.74	1.53
4.42	0.76	1.86
5.41	0.74	1.84
6.58	0.72	1.78
0.44	0.71	1.05
0.73	0.71	1.06
0.91	0.72	1.28
1.15	0.72	1.42
1.35	0.71	1.47
2.29	0.74	1.35
3.13	0.73	1.53
3.96	0.73	1.85
4.78	0.73	2.02
5.45	0.72	1.75
6.47	0.72	1.68
7.14	0.72	1.72

Table 18a: -Streamline pattern of flow over the weir crest (Fig.33):

(a) Normalized velocity profiles and their area distributions.

y CR	y/Y	u (m/s)	u/(2gH1	%A Cum	y -1cm	y/Y (-1)	u (m/s)	u/(2gH1	%A Cum-1
7.10	1.00	0.74	0.53	0.00	7.47	1.00	0.70	0.50	0.00
6.92	0.97	0.75	0.53	1.68	7.32	0.98	0.71	0.51	1.32
5.92	0.83	0.82	0.58	11.52	6.92	0.93	0.74	0.53	4.96
4.92	0.69	0.90	0.64	22.29	5.92	0.80	0.80	0.57	14.61
3.92	0.55	1.00	0.71	34.20	4.92	0.67	0.86	0.61	25.01
2.92	0.41	1.12	0.80	47.48	3.92	0.54	0.95	0.68	36.35
1.92	0.27	1.28	0.92	62.55	2.92	0.41	1.06	0.76	48.94
1.12	0.16	1.49	1.06	76.46	1.92	0.28	1.20	0.86	63.10
0.62	0.09	1.67	1.19	86.36	1.12	0.17	1.34	0.96	75.83
0.37	0.05	1.80	1.28	91.79	0.62	0.11	1.44	1.03	84.54
0.17	0.02	1.90	1.35	96.43	0.22	0.06	1.56	1.11	92.06
0.14	0.02	1.91	1.36	97.14	0.18	0.05	1.56	1.11	92.84
0.11	0.02	1.95	1.39	97.87	0.15	0.05	1.57	1.12	93.43
0.08	0.01	1.97	1.40	98.61	0.12	0.04	1.59	1.13	94.02
0.05	0.01	1.94	1.38	99.34	0.09	0.04	1.60	1.14	94.62
0.00	0.00	0.00	0.00	99.95	0.00	0.03	–	–	95.53
					-0.20	0.00	0.00	0.00	100.00

(Cont'd)

(Table 18a - continued)

y -2cm	y/Y (-2)	u (m/s)	u/(2gH1)^.	%A Cum-2	y +1cm	y/Y(+1)	u (m/s)	u/(2gH1)^.	%A
7.77	1.00	0.68	0.48	0.00	6.64	1.00	0.79	0.56	0.00
7.72	0.99	0.68	0.48	0.42	6.52	0.98	0.79	0.56	1.18
6.92	0.90	0.71	0 51	7.39	5.92	0 89	0.83	0.59	7.27
5.92	0.79	0.76	0.54	16.60	4.92	0.75	0.91	0.65	18.18
4.92	0.67	0.82	0.58	26.50	3.92	0.60	1.02	0.73	30.27
3.92	0.56	0.89	0.63	37.22	2.92	0.46	1.15	0.82	43.86
2.92	0.45	0.96	0.68	48.81	1.92	0.31	1.31	0.93	59.28
1.92	0.33	1.04	0.74	61 34	1.12	0.19	1.50	1.07	73.36
1.12	0 24	1.09	0.78	72.03	0 62	0.12	1.66	1.18	83.26
0.62	0.18	1.10	0.79	78.92	0.37	0.08	1.73	1.23	88.57
0.32	0.15	1.09	0.78	83.05	0.22	0.06	1.78	1.27	91.87
0.27	0.14	1.09	0.78	83.73	0.17	0.05	1.80	1.28	92.99
0.22	0.14	1.09	0.78	84.42	0.11	0.05	1.81	1.29	94 35
0.17	0.13	1.09	0.78	85.10	0.08	0.04	1.82	1.30	95.03
0.07	0 12	1.08	0.77	86.46	0.05	0.04	1.82	1.30	95.71
0.01	0.11	1.08	0 77	87.27	0 00	0.03	1 85	1.32	96.86
-0.02	0.11	1.07	0.77	87.68	-0.20	0.00	0.00	0.00	100.00
-0.05	0.11	1.07	0.76	88.08					
-0.08	0.10	1.06	0.76	88.48					
-0.97	0.00	0.00	0.00	100 00					

(Cont'd)

Note: Table 18a consists of 25 columns to be read horizontally. y CR= vertical above crest C (Fig.33 provides grid location for velocity survey), Y= total depth above crest surface, u/(2gH1)^.5=u/U, %A Cum=Σ area of velocity distribution. -1cm, -2cm, +1cm and +2cm are horizontal distances with respect to crest C as origin of coordinates.

Table 18a: (continued)

y +2cm	y/Y	u (m/s)	u/(2gH1	%A
6.16	1.00	0.82	0.58	0.00
5.92	0.97	0.83	0.59	2.48
4.92	0.83	0.91	0.65	13.38
3.92	0.68	1.00	0.71	25.34
2.92	0.54	1.12	0.80	38.63
1.92	0.40	1.27	0.91	53.60
1.12	0.29	1.41	1.00	67.03
0.62	0.22	1.51	1.08	76.18
0.37	0.18	1.56	1.11	80.99
0.17	0.16	1.60	1.14	84.95
0.11	0.15	1.61	1.15	86.16
0.08	0.14	1.61	1.15	86.76
0.05	0.14	1.62	1.15	87.37
0.02	0.14	1.63	1.16	87.98
-0.01	0.13	1.64	1.17	88.59
-0.04	0.13	1.64	1.17	89.21
-0.07	0.12	1.64	1.17	89.83
-0.10	0.12	1.65	1.18	90.45
-0.13	0.11	1.65	1.18	91.07
-0.94	0.00	0.00	0.00	100.00

Table 18b-18c: -Streamline pattern of flow over the weir crest:

(b) Cordinates of water surface and streamlines.

Note: Table 18b consists of 16 columns to be read horizontally. WS(SL0)=y of ψ=0, SL10= y of ψ=10, ..., xCR and yCR are coordinates of crest surface.

x	WS(SL0)	SL5	SL10	SL15	SL20	SL30	SL40	SL50	SL60
-2.00	7.77	7.18	6.62	6.07	5.55	4.58	3.68	2.84	2.04
-1.00	7.47	6.92	6.38	5.87	5.38	4.47	3.62	2.85	2.13
0.00	7.10	6.57	6.07	5.59	5.13	4.26	3.47	2.74	2.08
1.00	6.64	6.14	5.66	5.20	4.76	3.94	3.19	2.51	1.89
2.00	6.16	5.65	5.20	4.75	4.34	3.56	2.84	2.17	1.54
3.00	5.55] From water surface profile.								
4.00	4.88] From water surface profile.								

(Cont'd)

(Table 18b - continued)

SL70	SL80	SL90	SL100	xCR	yCR
1.28	0.54	-0.20	-0.99	-2.83	-2.54
1.48	0.88	0.32	-0.20	-2.20	-1.27
1.48	0.94	0.45	0.02	-1.00	-0.20
1.31	0.79	0.30	-0.15	0.00	0.00
0.95	0.40	-0.07	-0.50	1.00	-0.20
	Data from crest surface [			1.80	-0.74
	Data from crest surface [			3.60	-2.54

(c) Streamline inclinations.

Note: Table 18c consists of 16 columns to be read horizontally. Col.1, STL=ψ (474=test code). For Col.2-11, y in cm, -Pi=-ϕ in rad. (-2, -1, cr, +1 and +2 are horizontal distances in cm). For col. 12-16, y=y/Y.

STL 474	y -2	-PI -2	y -1	-Pi -1	y cr	-Pi cr	y +1	-PI +1	y +2	-PI +2
0	7.78	0.27	7.47	0.33	7.10	0.38	6.64	0.44	6.16	0.50
5	7.18	0.21	6.92	0.30	6.57	0.37	6.14	0.43	5.65	0.48
10	6.62	0.18	6.38	0.27	6.07	0.35	5.66	0.41	5.20	0.46
15	6.07	0.14	5.87	0.24	5.59	0.33	5.20	0.40	4.75	0.46
20	5.55	0.10	5.38	0.21	5.13	0.30	4.76	0.38	4.34	0.43
30	4.58	0.04	4.47	0.16	4.26	0.26	3.94	0.34	3.56	0.39
40	3.68	-0.01	3.62	0.11	3.47	0.21	3.19	0.30	2.84	0.38
50	2.84	-0.07	2.85	0.05	2.74	0.17	2.51	0.29	2.17	0.38
60	2.04	-0.15	2.13	-0.02	2.08	0.12	1.89	0.26	1.54	0.41
70	1.28	-0.28	1.48	-0.10	1.48	0.09	1.31	0.26	0.95	0.42
80	0.54	-0.44	0.88	-0.20	0.94	0.05	0.79	0.27	0.40	0.45
90	-0.20	-0.63	0.32	-0.30	0.45	0.02	0.30	0.27	-0.07	0.42
100	-0.99	-0.86	-0.20	-0.44	0.02	0.01	-0.15	0.28	-0.50	0.35

(Cont'd)

(Table 18c - continued)

y (-2)	y (-1)	y(cr)	y(+1)	y(+2)
1.00	1.00	1.00	1.00	1.00
0.93	0.93	0.93	0.93	0.92
0.87	0.86	0.85	0.86	0.86
0.81	0.79	0.79	0.79	0.79
0.75	0.73	0.72	0.72	0.73
0.64	0.61	0.60	0.60	0.61
0.53	0.50	0.49	0.49	0.50
0.44	0.40	0.39	0.39	0.40
0.35	0.30	0.29	0.30	0.31
0.26	0.22	0.21	0.22	0.22
0.17	0.14	0.13	0.14	0.14
0.09	0.07	0.06	0.07	0.06
0.00	0.00	0.00	0.00	0.00

Table 18d: -Streamline pattern of flow over the weir crest:

(d) Computation of streamline inclination and curvature parameters.

Note: Table 18d consists of 12 columns to be read horizontally. Col.1 , SL=ψ (474=test code). Col. 3-6 are constants of fitted cubics of streamlines (Eq.25), Pi=-ϕ in rad. (Eq.27), K=r (Eq.28), Kz=r_y (Eq.2).

Run #	R cm	Ao	A1	A2	A3	Pi rad	COS Pi	K cm	Kz cm	K/R	Kz/R
6045											
474 WS	2.54	7.095	-0.403	-0.034	-0.0008	-0.383	0.9274	-18.29	-19.72	7.198	7.762
SL 5	2.54	6.569	-0.393	-0.038	0.002	-0.374	0.9309	-16.07	-17.26	6.327	6.797
SL 10	2.54	6.063	-0.362	-0.038	0.00166	-0.347	0.9404	-15.59	-16.58	6.13	6.526
SL 15	2.54	5.583	-0.337	-0.043	0.00166	-0.325	0.9477	-13.48	-14.22	5.307	5.600
SL 20	2.54	5.120	-0.313	-0.044	0.002	-0.303	0.9545	-12.98	-13.6	5.111	5.355
SL 30	2.54	4.254	-0.268	-0.046	0.00333	-0.262	0.9658	-11.95	-12.38	4.705	4.872
SL 40	2.54	3.461	-0.217	-0.050	0.00166	-0.213	0.9773	-10.56	-10.81	4.158	4.254
SL 50	2.54	2.739	-0.171	-0.058	0.00083	-0.169	0.9857	-8.913	-9.042	3.509	3.559
SL 60	2.54	2.081	-0.118	-0.072	-0.0016	-0.118	0.9931	-7.007	-7.056	2.758	2.778
SL 70	2.54	1.484	-0.086	-0.092	0.00083	-0.086	0.9963	-5.486	-5.507	2.1	2.16
SL 80	2.54	0.948	-0.048	-0.119	0.00333	-0.048	0.9988	-4.206	-4.211	1.65	1.657
SL 90	2.54	0.454	-0.024	-0.147	0.01416	-0.024	0.9997	-3.401	-3.402	1.33	1.339
SL 100	2.54	0.016	-0.015	-0.190	0.034	-0.014	0.9999	-2.621	-2.621	1.031	1.031

(Cont'd)

(Table 18d - continued)

Table 18e: -Streamline pattern of flow over the weir crest:

(e) Variation of streamline inclination, radius of curvature r and ry from crest C to the water surface.

Pt.#	y2	y/Y CR	-PI rad	-K cm	-Kz cm	K/R	Kz/R
WS	7.10	1.00	0.38	18.29	19.72	7.20	7.76
SL 05	6.57	0.93	0.37	16.07	17.26	6.33	6.80
SL 10	6.06	0.85	0.35	15.59	16.58	6.14	6.53
SL 15	5.58	0.79	0.33	13.48	14.22	5.31	5.60
SL 20	5.12	0.72	0.30	12.98	13.60	5.11	5.36
SL 30	4.25	0.60	0.26	11.95	12.38	4.71	4.87
SL 40	3.46	0.49	0.21	10.56	10.81	4.16	4.25
SL 50	2.74	0.39	0.17	8.91	9.04	3.51	3.56
SL 60	2.08	0.29	0.12	7.01	7.06	2.76	2.78
SL 70	1.48	0.21	0.09	5.49	5.51	2.16	2.17
SL 80	0.95	0.13	0.05	4.21	4.21	1.66	1.66
SL 90	0.45	0.06	0.02	3.40	3.40	1.34	1.34
SL 100	0.02	0.02	0.01	2.62	2.62	1.03	1.03
Crest	0.00	0.00	0.00	2.54	2.54	1.00	1.00

Note: SL=ψ , y2=Y_2, CR= at crest C (Fig.2a), Pi=ϕ, K=r and Kz=r_y.

Table 18f: -Velocity distribution over the weir crest surface:

1) u-components in m/sec and coordinates x,y in $m x 10^{-2}$.

x = -2		x = -1		x = 0 (Crest C)		x = 1		x = 2	
y	u	y	u	y	u	y	u	y	u
7.77	0.68	7.47	0.70	7.10	0.74	6.64	0.78	6.16	0.82
7.72	0.68	7.32	0.71	6.92	0.75	6.52	0.79	5.92	0.83
6.92	0.71	6.92	0.74	5.92	0.82	5.92	0.83	4.92	0.91
5.92	0.76	5.92	0.80	4.92	0.90	4.92	0.91	3.92	1.00
4.92	0.82	4.92	0.86	3.92	1.00	3.92	1.02	2.92	1.12
3.92	0.89	3.92	0.95	2.92	1.12	2.92	1.15	1.92	1.27
2.92	0.96	2.92	1.06	1.92	1.28	1.92	1.31	1.12	1.41
1.92	1.04	1.92	1.20	1.12	1.49	1.12	1.50	0.62	1.51
1.12	1.09	1.12	1.34	0.62	1.67	0.62	1.66	0.37	1.56
0.62	1.10	0.62	1.44	0.37	1.80	0.37	1.73	0.17	1.60
0.32	1.09	0.22	1.56	0.17	1.90	0.22	1.78	0.11	1.61
0.27	1.09	0.18	1.56	0.14	1.91	0.17	1.80	0.08	1.61
0.22	1.09	0.15	1.57	0.11	1.94	0.11	1.81	0.05	1.62
0.17	1.09	0.12	1.59	0.08	1.97	0.08	1.82	0.02	1.63
0.07	1.08	0.09	1.60	0.05	1.94	0.05	1.82	-0.01	1.64
0.01	1.08	0.00		0.00	0.00	0.00	1.85	-0.04	1.64
-0.02	1.07	-0.20	0.00			-0.20	0.00	-0.07	1.64
-0.05	1.07							-0.10	1.65
-0.08	1.06			*				-0.13	1.65
-0.97	0.00							-0.94	0.00

*Crest geometry allows only part of table to be filled.

2) Typical v-components in m/sec and coordinates x, y in $m x 10^{-2}$.

x = 1		x = 2	
y	v	y	v
6.04	-0.37	5.74	-0.45
5.54	-0.38	5.44	-0.46
5.04	-0.38	4.94	-0.47
4.54	-0.40	4.44	-0.49
4.04	-0.41	3.94	-0.51
3.54	-0.41	3.51	-0.53
3.04	-0.41	3.01	-0.56
2.54	-0.43	2.51	-0.58
2.04	-0.44	2.01	-0.61
1.54	-0.45	1.51	-0.66
1.04	-0.51	1.01	-0.74
0.54	-0.56	0.51	-0.77

3) Check for irrotationality of flow; x,and y in $m x 10^{-2}$; u and v in m/sec; du/dy and dv/dx in sec^{-1}.

Check points	y	x = 0		x = 1		x = 0.5	
		u	v	u	v	du/dy	dv/dx
a	6.92	0.75		0.78			
	6.50		-0.30		-0.37	-7	-7
	5.92	0.82		0.83			
		x = 1		x = 2		x = 1.5	
b	5.92	0.83		0.83			
	5.50		-0.38		-0.46	-8	-8
	4.92	0.91		0.91			
c	4.92	0.91		0.91			
	4.50		-0.40		-0.49	-10	-9
	3.92	1.02		1.00			
d	2.92	1.15		1.12			
	2.50		-0.43		-0.58	-15.5	-15
	1.92	1.31		1.27			
e	1.92	1.31		1.27			
	1.50		-0.45		-0.66	-21	-21
	1.12	1.50		1.41			

Locations a, b, c, d and e are shown in Fig.33.

Table 19: -Samples of computation of weir coefficient C_d and C_{dVel}.

Note: h1=h_1, H1=H_1, P/H1=p/H_1, Cd 1=C_d (Eq.5), Y2=Y_2, A*=velocity diagram area, Cd 2.1=C_{dVel} (Eq.15), %Dev=deviation between C_d and C_{dVel} in %.

RUN#	Q cfs	h1 ft	H1 ft	H1/R	P/H1	C_d	Y2 ft	Y2/R	Fitted A*	Fitted Y2/H1	C_{dVel}	%Dev
9000FA												
407	0.392	0.272	0.272	0.547	14.044	1.073	0.196	0.393	0.599	0.715	1.114	3.780
408	0.766	0.405	0.406	0.816	9.409	1.151	0.292	0.587	0.634	0.715	1.177	2.260
409	1.062	0.496	0.497	0.999	7.686	1.176	0.357	0.718	0.657	0.715	1.220	3.757
410	1.365	0.576	0.578	1.162	6.609	1.198	0.412	0.828	0.678	0.715	1.259	5.062
411	1.825	0.683	0.687	1.381	5.560	1.246	0.490	0.985	0.705	0.715	1.310	5.161
9045												
413	0.279	0.221	0.221	0.444	17.285	1.043	0.158	0.318	0.586	0.715	1.089	4.435
414	0.629	0.361	0.362	0.728	10.552	1.124	0.259	0.520	0.622	0.715	1.156	2.870
415	0.905	0.449	0.450	0.905	8.489	1.165	0.324	0.650	0.645	0.715	1.198	2.834
416	1.334	0.568	0.570	1.146	6.702	1.205	0.408	0.821	0.676	0.715	1.255	4.138
417	1.776	0.670	0.673	1.353	5.676	1.248	0.481	0.967	0.702	0.715	1.304	4.463
6045												
419	0.371	0.261	0.261	0.525	14.636	1.081	0.187	0.376	0.597	0.715	1.108	2.532
420	0.718	0.388	0.389	0.782	9.820	1.151	0.279	0.561	0.629	0.715	1.169	1.563
421	1.038	0.485	0.486	0.977	7.860	1.189	0.349	0.702	0.654	0.715	1.215	2.187
422	1.784	0.669	0.673	1.353	5.676	1.257	0.480	0.965	0.702	0.715	1.304	3.715
423	1.231	0.538	0.540	1.086	7.074	1.206	0.387	0.778	0.668	0.715	1.241	2.878

(Cont'd)

(Table 19 - continued)

Table 19a: -Samples of computation of weir coefficient C_d and C_{dVel}.

Note: See Table 19 for notations.

RUN#	Q cfs	h1 ft	H1 ft	H1/R	P/H1	C_d	Y2 ft	Y2/R	Fitted A*	Fitted Y2/H1	C_{dVel}	%Dev
9000FA												
453	0.232	0.167	0.167	2.009	22.963	1.317	0.125	1.500	0.703	0.734	1.341	1.802
454	0.300	0.197	0.197	2.364	19.515	1.332	0.149	1.788	0.694	0.747	1.347	1.111
454a	0.396	0.239	0.239	2.865	16.102	1.318	0.184	2.208	0.681	0.766	1.354	2.752
455	0.527	0.290	0.291	3.489	13.222	1.307	0.228	2.736	0.664	0.775	1.338	2.384
456	0.727	0.366	0.366	4.398	10.489	1.273	0.289	3.468	0.641	0.785	1.307	2.686
9045												
459	0.290	0.190	0.190	2.285	20.189	1.356	0.140	1.680	0.739	0.715	1.372	1.214
460	0.485	0.260	0.260	3.126	14.757	1.418	0.191	2.292	0.753	0.715	1.399	-1.339
461	0.710	0.329	0.330	3.957	11.659	1.458	0.247	2.964	0.767	0.715	1.425	-2.246
462	0.960	0.397	0.398	4.778	9.655	1.485	0.292	3.504	0.781	0.715	1.451	-2.277
6045												
467	0.378	0.223	0.223	2.680	17.215	1.391	0.161	1.932	0.758	0.715	1.408	1.209
468	0.557	0.284	0.284	3.411	13.526	1.429	0.205	2.460	0.770	0.715	1.430	0.038
469	0.780	0.349	0.350	4.195	10.998	1.467	0.253	3.036	0.782	0.715	1.453	-0.965
470	0.989	0.405	0.406	4.877	9.459	1.483	0.295	3.540	0.793	0.715	1.473	-0.667

(Cont'd)

(Table 19a - continued)

Table 20: -Samples of computation of weir coefficient C_d and C_{dMom}.

RUN#	Q cfs	h1 ft	H1 ft	H1/R	P/H1	C_d	Y2 ft	Y2/R	Y2/H1
9000FA									
407	0.392	0.272	0.272	0.547	14.044	1.073	0.196	0.393	0.719
408	0.766	0.405	0.406	0.816	9.409	1.151	0.292	0.587	0.719
409	1.062	0.496	0.497	0.999	7.686	1.176	0.357	0.718	0.718
410	1.365	0.576	0.578	1.162	6.609	1.198	0.415	0.828	0.718
411	1.825	0.683	0.687	1.381	5.560	1.246	0.493	0.985	0.718
9045									
413	0.279	0.221	0.221	0.444	17.285	1.043	0.158	0.318	0.715
414	0.629	0.361	0.362	0.728	10.552	1.124	0.259	0.520	0.715
415	0.905	0.449	0.450	0.905	8.489	1.165	0.324	0.650	0.720
416	1.334	0.568	0.570	1.146	6.702	1.205	0.408	0.821	0.716
417	1.776	0.670	0.673	1.353	5.676	1.248	0.481	0.967	0.715
6045									
419	0.371	0.261	0.261	0.525	14.636	1.081	0.187	0.376	0.717
420	0.718	0.388	0.389	0.782	9.820	1.151	0.279	0.561	0.717
421	1.038	0.485	0.486	0.977	7.860	1.189	0.349	0.702	0.718
422	1.784	0.669	0.673	1.353	5.676	1.257	0.480	0.965	0.713
423	1.231	0.538	0.540	1.086	7.074	1.206	0.387	0.778	0.717

(Cont'd)

(Table 20 - continue)

Uo	h CR	2gH^.5	Beta2	K2	Kf	X1	X2	C_{dMom}	%Dev
m/s	cm	m/s							
0.921	3.700	1.275	1.178	0.635	0.998	0.636	1.122	1.098	2.300
1.265	4.000	1.558	1.161	0.513	0.995	0.659	1.271	1.189	3.281
1.498	3.400	1.724	1.189	0.422	0.993	0.649	1.303	1.195	1.618
1.691	2.300	1.859	1.204	0.399	0.989	0.647	1.415	1.243	3.755
1.980	0.800	2.027	1.208	0.284	0.987	0.653	1.412	1.248	0.134
0.798	3.400	1.150	1.162	0.694	0.999	0.637	0.979	1.025	-1.687
1.152	3.850	1.471	1.163	0.561	0.996	0.650	1.243	1.167	3.852
1.385	3.800	1.640	1.191	0.454	0.994	0.646	1.299	1.190	2.115
1.686	2.700	1.846	1.196	0.362	0.989	0.649	1.441	1.256	4.247
1.953	1.000	2.006	1.191	0.278	0.987	0.659	1.423	1.258	0.832
0.897	3.600	1.249	1.152	0.640	0.998	0.648	1.158	1.125	4.111
1.230	3.800	1.525	1.158	0.523	0.995	0.657	1.311	1.206	4.755
1.475	3.600	1.705	1.180	0.407	0.993	0.653	1.333	1.212	1.953
1.970	1.000	2.006	1.194	0.261	0.987	0.656	1.432	1.259	0.181
1.620	2.900	1.797	1.190	0.334	0.991	0.651	1.406	1.243	3.041

Note: Table 20 consists of 20 columns to be read horizontally. h1=h_1, H1=H_1, P/H1=p/H_1, Cd 1=C_d (Eq.5), Y2=Y_2, Uo=u_{max}, CR=at crest, 2gH^.5=U, Beta2=β_2, K2=K_2, Kf=K_w, X1&X2=intermediate results, Cd 3=C_{dMom} (Eq.17), %Dev=deviation between C_d and C_{dMom} in %.

Table 20a: -Samples of computation of weir coefficient C_d and C_{dMom}.

Note: See Table 20 for notations.

RUN#	Q cfs	h1 ft	H1 ft	H1/R	P/H1	C_d	Y2 ft	Y2/R	Y2/H1
9000FA									
453	0.232	0.167	0.167	2.009	22.963	1.317	0.125	1.500	0.749
454	0.300	0.197	0.197	2.364	19.515	1.332	0.149	1.788	0.756
454a	0.396	0.239	0.239	2.865	16.102	1.318	0.184	2.208	0.770
455	0.527	0.290	0.291	3.489	13.222	1.307	0.228	2.736	0.784
456	0.727	0.366	0.366	4.398	10.489	1.273	0.289	3.468	0.790
9045									
459	0.290	0.190	0.190	2.285	20.189	1.356	0.140	1.680	0.737
460	0.485	0.260	0.260	3.126	14.757	1.418	0.191	2.292	0.735
461	0.710	0.329	0.330	3.957	11.659	1.458	0.247	2.964	0.748
462	0.960	0.397	0.398	4.778	9.655	1.485	0.292	3.504	0.734
6045									
467	0.378	0.223	0.223	2.680	17.215	1.391	0.161	1.932	0.722
468	0.557	0.284	0.284	3.411	13.526	1.429	0.205	2.460	0.722
469	0.780	0.349	0.350	4.195	10.998	1.467	0.253	3.036	0.723
470	0.989	0.405	0.406	4.877	9.459	1.483	0.295	3.540	0.727

(Cont'd)

(Table 20a - continued)

Uo	h CR	2gH^.5	Beta2	K2	Kf	X1	X2	C_{dMom}	%Dev
m/s	cm	m/s							
1.128	-1.600	0.999	1.399	0.000	0.999	0.547	1.860	1.311	-0.490
1.209	-1.800	1.085	1.325	0.095	0.998	0.587	1.851	1.354	1.664
1.304	-1.900	1.196	1.317	0.183	0.997	0.605	1.766	1.343	1.898
1.412	-1.700	1.319	1.336	0.231	0.997	0.612	1.563	1.270	-2.829
1.511	-1.050	1.479	1.289	0.341	0.996	0.647	1.377	1.226	-3.679
1.331	-3.500	1.066	1.457	-0.183	0.998	0.518	2.219	1.393	2.724
1.738	-7.850	1.247	1.471	-0.300	0.996	0.516	2.151	1.368	-3.509
1.996	-10.700	1.405	1.441	-0.254	0.993	0.542	2.257	1.436	-1.487
2.225	-14.650	1.543	1.362	-0.297	0.991	0.567	2.190	1.448	-2.487
1.534	-5.400	1.155	1.421	-0.274	0.997	0.523	2.159	1.380	-0.796
1.856	-8.650	1.303	1.409	-0.319	0.995	0.531	2.257	1.422	-0.489
2.037	-10.825	1.447	1.336	-0.290	0.993	0.567	2.219	1.457	-0.714
2.280	-14.425	1.558	1.345	-0.297	0.991	0.570	2.180	1.448	-2.378

Table 21: -Sample of computation of weir coefficient C_d and C_{dTh}.

RUN#	Q cfs	h1 ft	H1 ft	H1/R	P/H1	C_d	Y2 ft	C10*C5 Y2/R	Fitted Y2/H1	Uo	d	h CR	S	C_{dTh}	%Dev
										m/s	cm	cm			
9000FA															
407	0.392	0.272	0.272	0.547	14.044	1.073	0.196	0.391	0.715	0.921	0.300	3.700	1.391	1.167	8.727
408	0.766	0.405	0.406	0.816	9.409	1.151	0.292	0.583	0.715	1.265	0.250	4.000	1.583	1.204	4.586
409	1.062	0.496	0.497	0.999	7.686	1.176	0.357	0.714	0.715	1.498	0.250	3.400	1.714	1.234	4.968
410	1.365	0.576	0.578	1.162	6.609	1.198	0.415	0.831	0.715	1.691	0.250	2.300	1.831	1.261	5.242
411	1.825	0.683	0.687	1.381	5.560	1.246	0.493	0.987	0.715	1.980	0.250	0.800	1.987	1.267	1.700
453	0.232	0.167	0.167	2.009	22.963	1.317	0.125	1.475	0.734	1.128	0.072	-1.600	2.475	1.344	2.029
454	0.300	0.197	0.197	2.364	19.515	1.332	0.149	1.767	0.747	1.209	0.074	-1.800	2.767	1.275	-4.265
9045															
413	0.279	0.221	0.221	0.444	17.285	1.043	0.158	0.317	0.715	0.798	0.250	3.400	1.317	1.135	8.851
414	0.629	0.361	0.362	0.728	10.552	1.124	0.259	0.521	0.715	1.152	0.250	3.850	1.521	1.207	7.355
415	0.905	0.449	0.450	0.905	8.489	1.165	0.324	0.647	0.715	1.385	0.250	3.800	1.647	1.218	4.549
416	1.334	0.568	0.570	1.146	6.702	1.205	0.408	0.819	0.715	1.686	0.250	2.700	1.819	1.247	3.480
417	1.776	0.670	0.673	1.353	5.676	1.248	0.481	0.967	0.715	1.953	0.250	1.000	1.967	1.267	1.549
459	0.290	0.190	0.190	2.285	20.18[illegible]	1.356	0.140	1.634	0.715	1.331	0.082	-3.500	2.634	1.395	2.851
460	0.485	0.260	0.260	3.126	14.757	1.418	0.191	2.235	0.715	1.738	0.083	-7.850	3.235	1.377	-2.915
6045															
419	0.371	0.261	0.261	0.525	14.636	1.081	0.187	0.375	0.715	0.897	0.400	3.600	1.375	1.167	7.957
420	0.718	0.388	0.389	0.782	9.820	1.151	0.279	0.559	0.715	1.230	0.250	3.800	1.559	1.216	5.673
421	1.038	0.485	0.486	0.977	7.860	1.189	0.349	0.699	0.715	1.475	0.400	3.600	1.699	1.226	3.085
422	1.784	0.669	0.673	1.353	5.676	1.257	0.480	0.967	0.715	1.970	0.300	1.000	1.967	1.267	0.822
423	1.231	0.538	0.540	1.086	7.074	1.206	0.387	0.776	0.715	1.620	0.300	2.900	1.776	1.248	3.459
467	0.378	0.223	0.223	2.680	17.215	1.391	0.161	1.916	0.715	1.534	0.050	-5.400	2.916	1.390	-0.082
468	0.557	0.284	0.284	3.411	13.526	1.429	0.205	2.439	0.715	1.856	0.057	-8.650	3.439	1.330	-6.915

(Cont'd)

(Table 21 - continue)

Note: Table 21 consists of 16 columns to be read horizontally. h1=h_1, H1=H_1, P/H1=p/H_1, Cd 1=C_d (Eq.5), Y2=Y_2, Uo=u_{max}, d=δ, h CR=$P/\gamma)_{cr}$, S=intermediate results, Cd (a)=C_{dTh} (Eq.25), %Dev=deviation between C_d and C_{dTh} in %.

APPENDIX IV

EXPERIMENTAL UNCERTAINTY

APPENDIX IV

EXPERIMENTAL UNCERTAINTIES

A.IV.1.- Uncertainty in the measurands: The uncertainties in the measurands for the present study are listed below:

1. Model sizes: Radius $= R \pm 0.02$ mm
   Height $= p \pm 0.5$ mm
   Width $= B \pm 0.3$ mm
2. Depth, using point gauge: $y \pm 0.3$ mm
   dial gauge: ± 0.01 mm (LDV-linear , x and y)
3. Pressure head: $P/g \pm 0.5$ mm (water column)
4. LDV measurements:
   Average velocity (typical value) $V \pm 0.5$ %
5. Discharge, using standard (ASME)
   V-notch: $Q \pm 3\%$

A.IV.2.- Uncertainty in computed results: The uncertainties in the computed results were obtained by the method given by Fox and McDonald (1985). The **maximum uncertainties** in the computed results for the present study are listed as the following:

1. Dimensionless parameters: $Y_2/R \pm 1.2\%$ max.
   $H_1/R \pm 1.2\%$ max.
   $Y_2/H_1 \pm 1.7\%$ max.
   $u/U \pm 5\%$ max.
   $P/\gamma H_1 \pm 5\%$ max.
2. Average velocity: $V \pm 3\%$ max.

3. Discharge coefficient: $C_d \pm 3\%$ max.

A.IV.3.- Example of uncertainty estimation : The following is an example of uncertainty estimation for the discharge coefficient of circular-crested weir based on direct discharge measurement (Eq.5):

$$q = C_d \frac{2}{3} \sqrt{\frac{2}{3} g}\, H_1^{1.5} \text{ ----------- ----------- } (5)$$

Here, $q = Q/B$.

For the test data set:	Q =	0.0111 m^3
	H_1 =	0.0829 m
	B =	0.254 m
Uncertainty in discharge:	± 3%	
Uncertainty in head:	± 0.4%	
Uncertainty in flume width:	± 0.12%	

The uncertainty in C_d can be estimated as below:

$$u_{Cd} = \pm \{[(1)(\pm 0.03)]^2 + [(1.5)(-1)(\pm 0.004)]^2 + [(-1)(\pm 0.0012)]^2\}^{0.5}$$

$$= \pm 0.0306$$

i.e. uncertainty of C_d is close to 3%.

APPENDIX V

MISCELLANEOUS DATA

A.V.1: -Sample of LDV measurement output (#460).

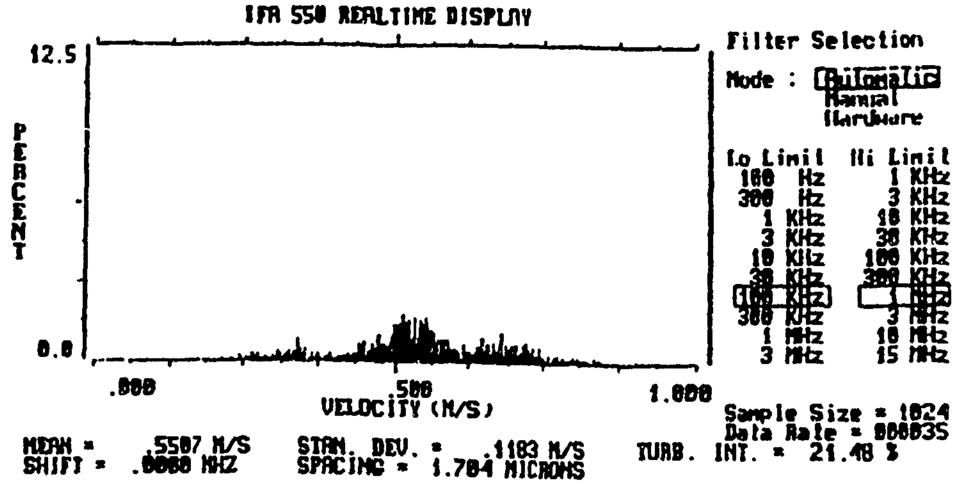

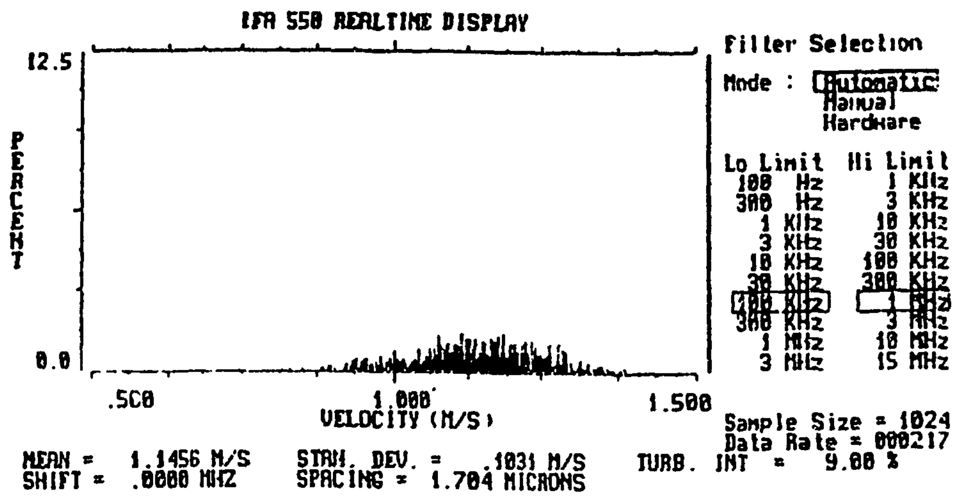

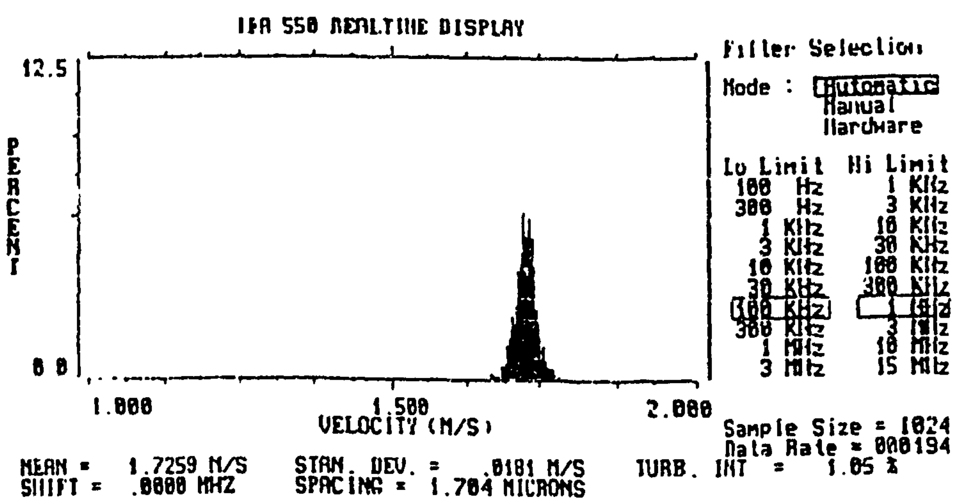

A.V.1: (continued).

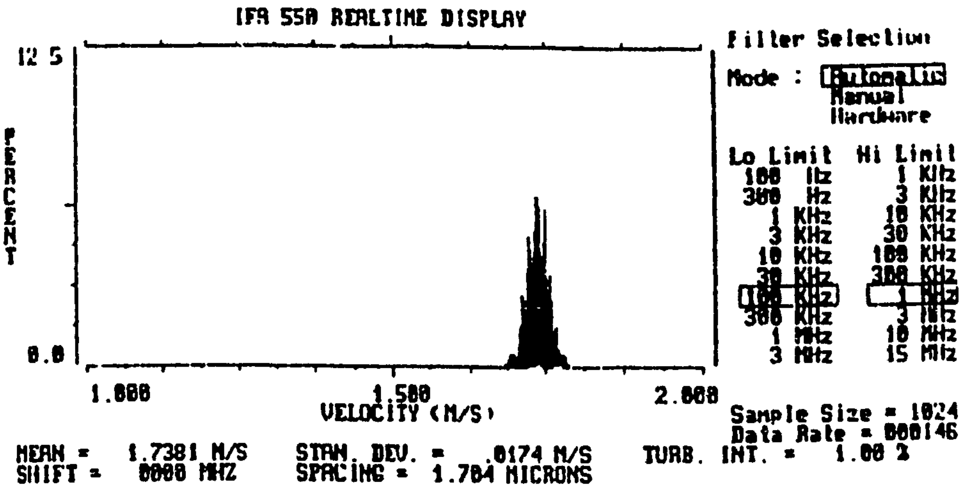

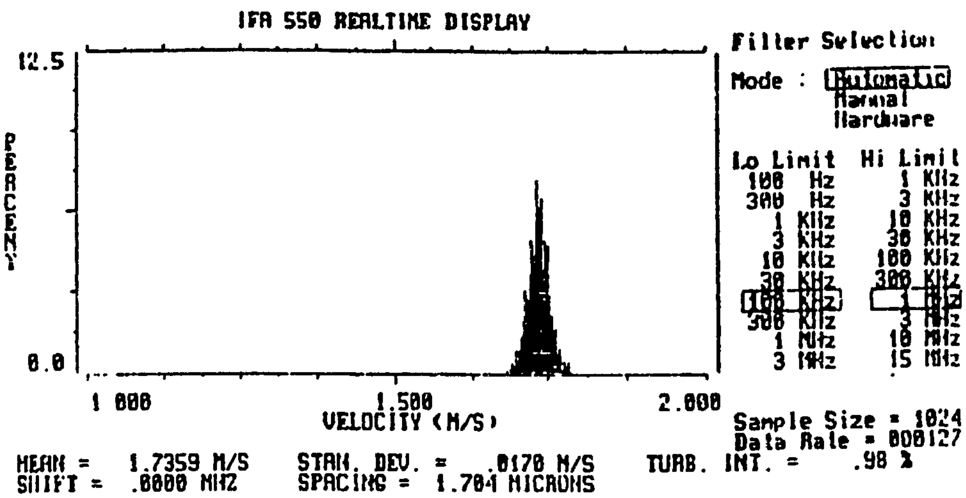

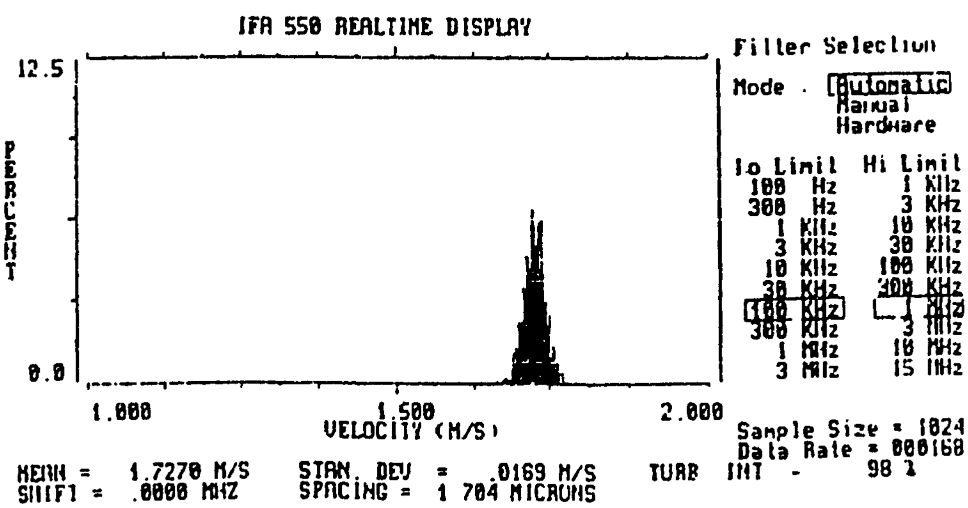

A.V.1: (continued).

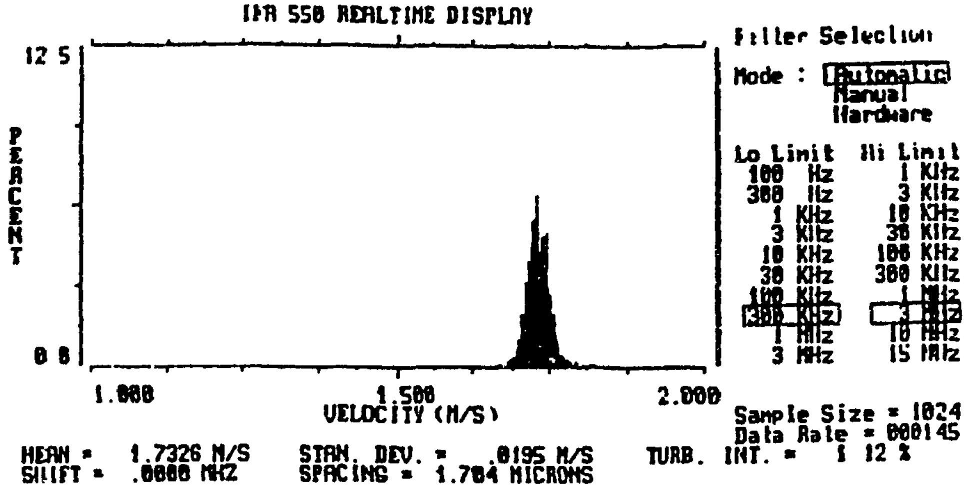

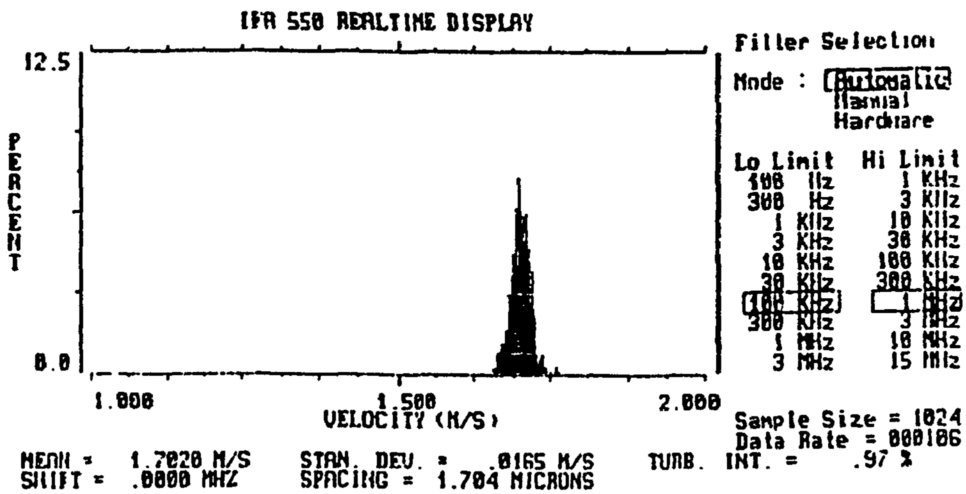

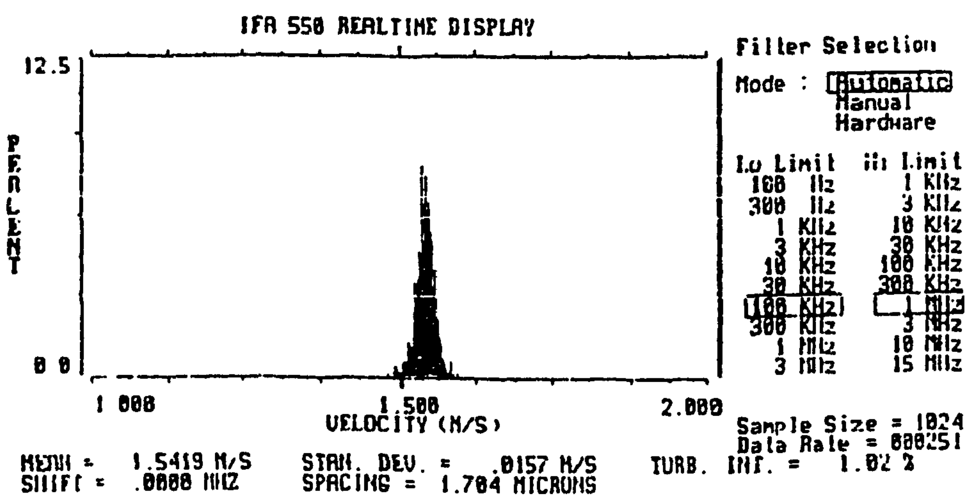

A.V.1: (continued).

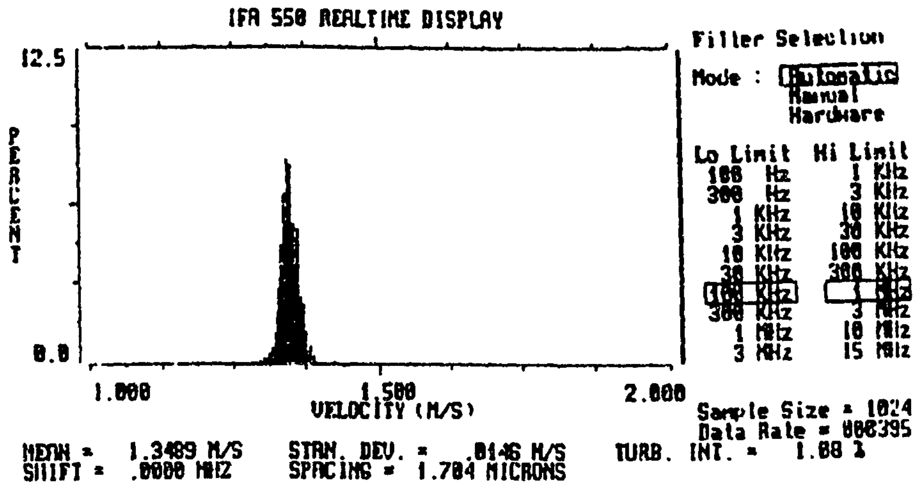

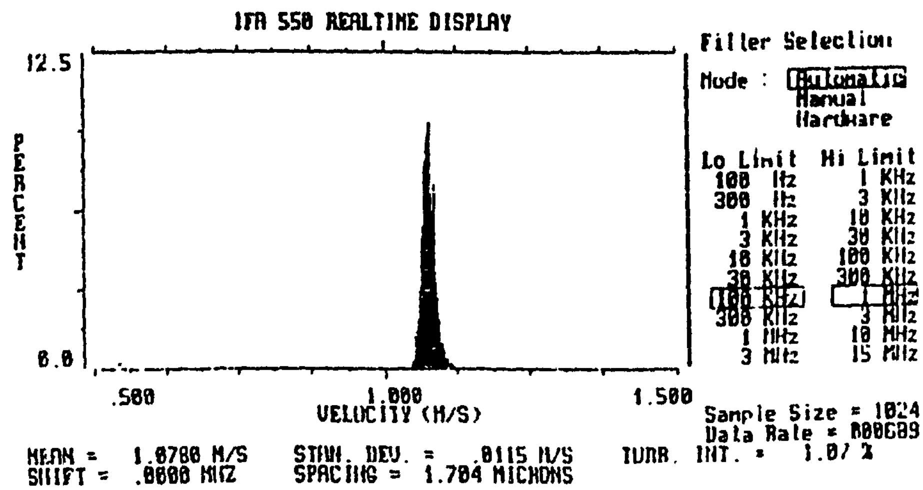

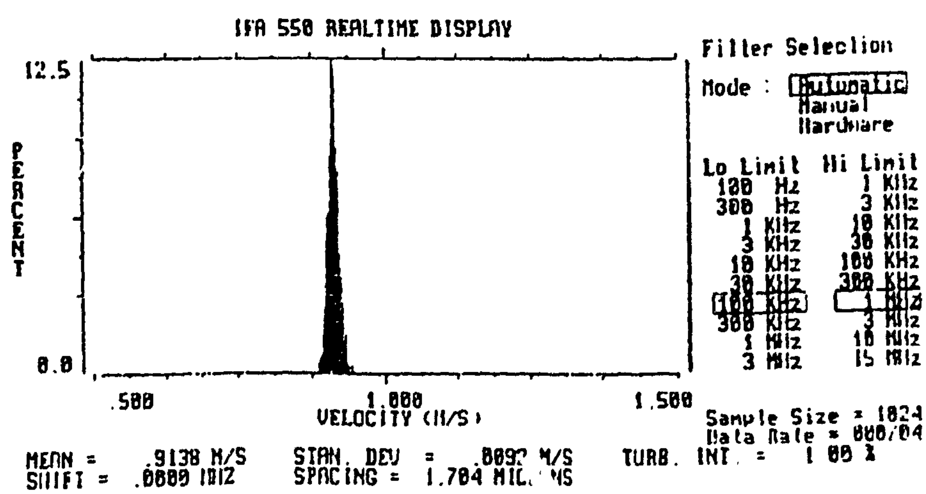

A.V.1: (continued).

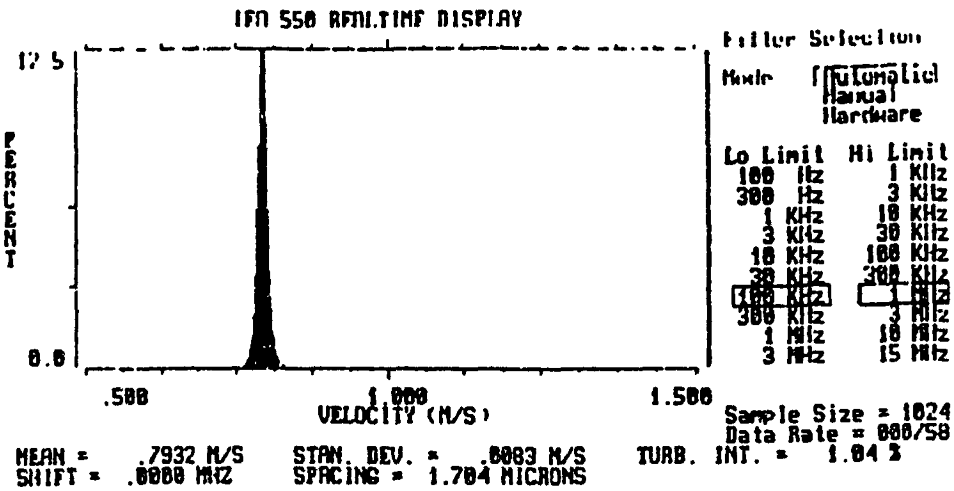

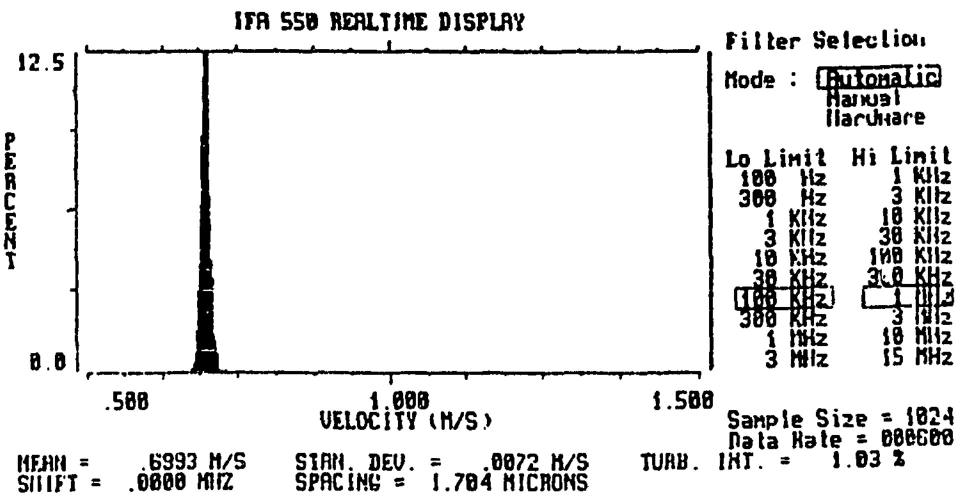

A.V.2: BOUNDARY LAYER THICKNESS AT WEIR CREST.

For a limited range of H_1/R, the experimentally determined values of the boundary layer thickness δ_{exp} were compared with the theoretical values δ_{Th} computed from Pohlhausen method (Schlichting). The computation of δ_{Th} was initiated from the tangent point (θ=0°) of the weir. The stagnation point itself was always slightly below the tangent point and it was not clearly determined. The use of the tangent point (θ=0°) as the starting point for computation provide only approximate values of the boundary layer thickness δ and underestimate it.

Fig. A.V.2.1 show the values of δ based on theory and experiment for a limited range of data. When H_1/R was very small ($H_1/R<1.5$), the velocity $U_{max}(x)$ at the edge of the boundary layer along the crest was such that $U'(x)>0$. This prevents one to compute δ using the available standard tables of the shape factors of the boundary layer profile. Partly due to this reason, the computations based on theory were limited to higher ranges of H_1/R. Further more, for the weir with no downstream slope, the flow was generally not very stable near the maximum discharge coefficient, in the range of H_1/R close to 2.25 as such Fig. A.V.2.1 shows the result of boundary layer computations for the weir with downstream slope, the corresponding maximum value of C_d was at very much larger H_1/R.

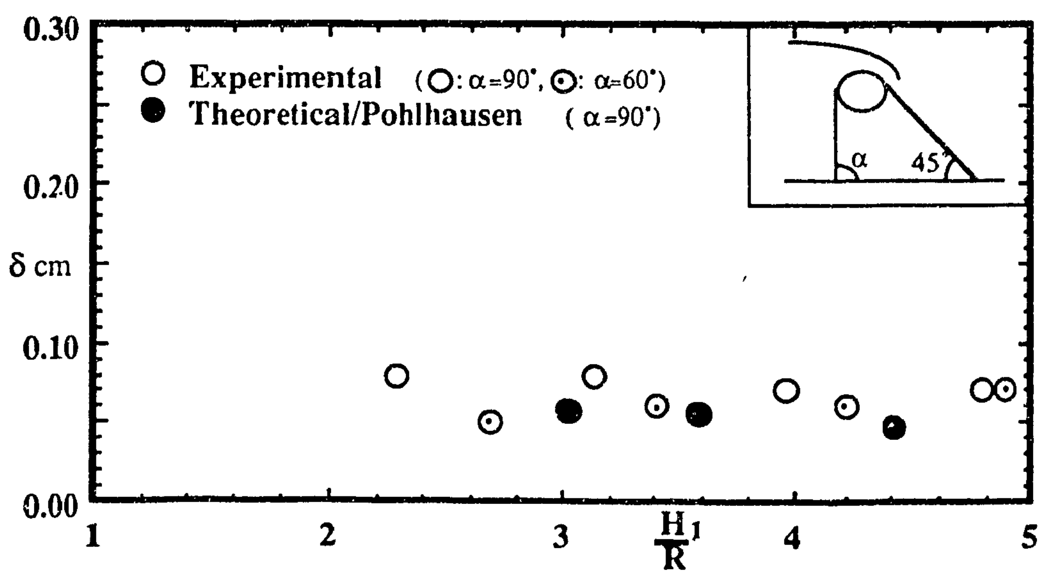

Fig. A.V.2.1: Theoretical and experimental boundary layer thickness.